9-2013

Designing Novel Emulsion Performance by Controlled Hetero-Aggregation of Mixed Biopolymer Systems

Yingyi Mao
University of Massachusetts Amherst, ericamao@gmail.com

DESIGNING NOVEL EMULSION PERFORMANCE BY CONTROLLED HETERO-AGGREGATION OF MIXED BIOPOLYMER SYSTEMS

A Dissertation Presented

by

YINGYI MAO

Submitted to the Graduate School of the
University of Massachusetts Amherst in partial fulfillment
of the requirements for the degree of

DOCTOR OF PHILOSOPHY

September 2013

The Department of Food Science

DESIGNING NOVEL EMULSION PERFORMANCE BY CONTROLLED HETERO-AGGREGATION OF MIXED BIOPOLYMER SYSTEMS

A Dissertation Presented

by

YINGYI MAO

Approved as to style and content by:

_____
D. Julian Mcclements, Chair

_____
Paul Dubin, Member

_____
Hang Xiao, Member

_____
Eric A. Decker, Department Head
Department of Food Science

DEDICATION

To my supportive family

ACKNOWLEGEMENT

First and Foremost, I acknowledge, with gratitude, my debt of thanks to my advisor, Dr. Julian McClements, for his academic guidance and assistant in the past four years. His attitude and passion for research really help me to understand the meaning of being a scientist and also encourage me to pursue my academic goal in the future. I would also like to thank my committee members: Dr. Xiao and Dr. Dubin, for serving on my committee and their academic suggestion and foresight for my research.

All special thanks go to all Julian Lab members. This thesis would not have been possible without your help. In particular, I would like to than Jean Alamed for her support and friendship in the past four years. She was the one person I would always go for help and advice. I would also thank Cheryl, Alison, Cheng, Jiajia, Ying, Yan, Mingru, Tanu for helping me for my research and my life. To Fang, thanks to your patience for listening my complaints and encouraging me all the time.

Lastly, I would express my deepest appreciation to my family. To my parents, thank you for all your sacrifices to help me to achieve so many goals and dreams in my life. I feel so blessed for having you. To my husband Dingqiang Li, whenever I am confused and in difficulties, you always know how to make things become easy and never stop supporting me. I am so lucky to have you. Thank you for all the people helped me in my life.

ABSTRACT

DESIGNING NOVEL EMULSION PERFORMANCE BY CONTROLLED HETERO-AGGREGATION OF MIXED BIOPOLYMER SYSTEMS

SEPTEMBER 2013

YINGYI MAO, B.S., NORTHWEST AGRICULTURE AND FORESTRY UNIVERSITY

M.S., SICHUAN UNIVERSITY

Ph.D., UNIVERSITY OF MASSACHUSETTS AMHERST

Directed by: Professor D. Julian McClements

The increase in obesity and overweight in many countries has led to an upsurge of interest in the development of reduced fat food products. However, the development of these products is challenging because of the many roles that fat droplets normally plays in these food products, including contributing to flavor, texture, appearance, and bioactivity. The goal of this research was to develop novel reduced-fat emulsions based on hetero-aggregation of oppositely charged food-grade colloidal particles or polymers.

Initially, lactoferrin (LF) and β-lactoglobulin (β-Lg) were selected as emulsifiers to form protein-coated fat droplets ($d_{43} \approx 0.38$ μm) with opposite charges at neutral pH: $pK_{a\beta\text{-}Lg} \approx 5 <$ pH 7 $< pK_{aLF} \approx 8.5$. Droplet aggregation occurred when these two emulsions were mixed together due to electrostatic attraction. The structural organization of the droplets in these mixed emulsions depended on the positive-to-negative particle ratio, particle concentration, pH, ionic strength, and temperature. The nature of the structures formed influenced the rheology, stability, and appearance of the mixed emulsions, which enabled some control over emulsion functionality. The largest microclusters were formed at particle ratios of 40% LF-coated and 60% β-Lg-coated fat

droplets, which led to mixed emulsions with the highest apparent viscosity or gel strength. At low total particle concentrations (0.1%), there was a relatively large distance between microclusters and the mixed emulsions were fluid. At high particle concentrations (>20%), a three-dimensional network of aggregated droplets formed that led to gel-like or paste-like properties. The influence of environmental stresses on the physicochemical stability of the microclusters formed by hetero-aggregation was investigated: pH (2-9); ionic strength (0-400 mM NaCl); and temperature (30-90 ºC). Large microclusters were obtained at pH 7 ($d_{43} \approx 10$ μm) with the absence of salt at room temperature. More acidic (< pH 6) or alkaline (> pH 8.5) solutions resulted in smaller aggregates by minimizing the electrostatic attraction between the protein-coated fat droplets. Microclusters dissociated upon addition of intermediate levels of salt, which was attributed to screening of attractive electrostatic interactions. Heating the microclusters above the thermal denaturation temperature of the proteins led to an increase in gel-strength, which was attributed to increased hydrophobic attraction.

The influence of hetero-aggregation of lipid droplets on their potential biological fate was studied using a simulated gastrointestinal tract (GIT). Results showed that the mixed emulsions had high viscosity in the simulated oral environment but exhibited similar rheological properties and particle characteristics as single-protein emulsions in the simulated gastric and small intestinal tract regions. The mixed emulsions also had similar lipid digestion rates in the simulated small intestine as single-protein emulsions suggesting that they could be used as delivery systems for bioactive lipophilic compounds in reduced fat food products.

The possibility of using more practical food ingredients to promote hetero-aggregation system was also examined. Whey protein isolate (positive) and modified starch (negative) were selected as building blocks due to their opposite charges at pH 3.5. The largest aggregates and highest viscosities occurred at a particle ratio of 70% MS and 30% WPI, which was attributed to strong electrostatic attraction between the oppositely charged droplets. Particle aggregation and viscosity decreased when the pH was changed to reduce the electrostatic attraction between the droplets.

Finally, the influence of interfacial properties on the chemical stability of bioactive components in emulsion-based delivery systems containing mixed proteins was studied. Lactoferrin (LF: pI ≈ 8) and β-lactoglobulin (β-Lg: pI ≈ 5) were selected to engineer the interfacial properties. Interfaces with different structures were formed: LF only; β-Lg only; LF-β-Lg (laminated); β-Lg -LF (laminated); β-Lg /LF (mixed). The influence of pH, ionic strength, and temperature on the physical stability of β-carotene-enriched emulsions was then investigated. LF- emulsions were stable to the pH change from 2 to 9 but the aggregation was occurred in intermediate pH for other emulsions. β-Lg- emulsions aggregated at low salt concentration (≥ 50mM NaCl), however other emulsions were stable (0 - 300mM NaCl). β-Lg /LF (mixed) emulsions were unstable to heating (≥ 60 ºC), but all other emulsions were stable (30 to 90 ºC). Color fading due to β-carotene degradation occurred relatively quickly in β-Lg-emulsions (37 ºC), but was considerably lower in all other emulsions, which was attributed to the ability of LF to bind iron or interact with β-carotene.

Overall, this study shows that hetero-aggregation may be a viable method of creating novel structures and rheological properties that could be used in the food industry.

TABLE OF CONTENTS

LIST OF TABLES

LIST OF FIGURES

CHAPTER 1

INTRODUCTION

The recent increase in the number of overweight or obese individuals in many populations has become a major health and economic issue, due to the increase in chronic diseases and associated health care costs [1, 2]. In response to this problem the food industry is developing reduced-calorie versions of many of its products. Dietary fat has the highest energy density of all the major macronutrients found in foods (*i.e.* fat, protein, and carbohydrates). Consequently, the removal of fat from food products has been a major target of the food industry. However, the development of high quality reduced fat products has proved to be challenging because fats play complex roles in determining the overall appearance, flavor profile, texture, and biological response (such as satiety) of foods [3, 4]. These desirable attributes of a product may be lost once the fats are removed, which leads to rejection by consumers. Therefore, there is a need to develop new strategies to create reduced fat foods that maintain their desirable characteristic sensory attributes, such as creaminess, richness, or smoothness.

In this article, we focus on the development of reduced fat emulsion-based foods. Emulsions consist of the two of immiscible liquids (usually oil and water) and are formed by application of vigorous stirring or more intense mechanical forces [5]. The most common emulsions used in the food industry are oil-in-water (O/W) and water-in-oil (W/O) emulsions: O/W emulsions consist of oil droplets dispersed in water (*e.g.,* milk, cream, dressings, sauces and desserts), whereas W/O emulsions consist of water droplets dispersed in oil (*e.g.,* butter and margarine). The optical properties, rheology, and stability of these products depend on the concentration, size, and interactions of the

droplets they contain. Typically, the lightness, viscosity, and stability of emulsions increases as their fat content increases [6]. Consequently, removing some or all of the fat droplets from a product (such as a dressing or sauce) will alter its desirable sensory properties [7, 8]. For this reason, fat replacers are typically added to reduced-fat foods to replace the physicochemical and sensory attributes normally provided by the fat droplets. For example, food-grade polymers or particles may be added to the aqueous phase of reduced-fat O/W emulsions to increase their texture or provide opacity.

Recently, there has been a trend toward the application of techniques from other areas into the food science field. In this research, the focus is on the adaption of structural design principles based on controlled *hetero-aggregation* of colloidal particles within emulsion-based systems. Hetero-aggregation is defined as the aggregation of mixed particle systems where the colloidal particles may differ in their charge, size, and/or chemical composition. For ionized particles with opposite charges the main driving force for hetero-aggregation is electrostatic attraction [9] and the performance of emulsions can be persicely controlled by modulating the electrostatic attraction between oppositecly charged particles.

Therefore, it is necessary to understand the physical principles of hetero-aggregation, the factors that affect the formation and physicochemical properties of hetero-aggregates, the potential behavior of hetero-aggregates within the gastrointestinal tract, the alternative food grade ingredients to form hydrocolloidal hetero-aggregation and encapsulation of bioactive lipophilic compound using the engneering of interfacial properties. This information should be useful for the development of novel food products, as well as other emulsion-based commercial products, such as cosmetics and

health care products. Thus, the overall goal of this project is to rationalize the fabrication of emulsion-based hetero-aggregates with specific structures, physicochemical and biophysical properties. The objective of these experiments is to identify the applicability of hetero-aggregates as a potential technique to apply in reduced fat foods, delivery bioactive food compounds and promote food quality.

CHAPTER 2

LITERATURE REVIEW

2.1 Principles of Hetero-aggregation

In general, hetero-aggregation is defined as the aggregation of dissimilar particles, which may differ in their size, shape, charge, chemical composition, and other properties [10, 11]. Hetero-aggregation has been widely used in non-food science applications for a variety of reasons, such as controlling the rheological properties of ceramics [12], creating ion exchange columns [13], removing colloidal particles from aqueous solutions [14], and encapsulating and targeting biomolecules [15-18]. Hetero-aggregation of oppositely charged particles through electrostatic attraction is the most commonly used method for most applications, and therefore this method will be the focus of this review.

There can be considered to be two different stages in the hetero-aggregation of oppositely charged particles. First, the particles are attracted to each other through electrostatic attraction, which leads to the formation of aggregates. Second, the continued growth of aggregates is inhibited due to electrostatic repulsion.

2.1.1 Colloidal Interactions

One of the most widely utilized models for describing the interactions between charged colloidal is taken to particles is the extended DLVO theory. In this theory, the overall interaction between colloidal particles be the sum of three contributions: $V_T = V_V + V_E + V_S$ where V_T is the total interaction energy, V_V is the energy resulting from van der Waals attractive forces, V_E is the energy associated with electrostatic interactions, and V_S is the energy associated with steric repulsion forces [19]. The

electrostatic interactions may either be attractive (oppositely charged particles) or repulsive (similarly charged particles), which leads to different colloidal interaction profiles (**Figure 2.1**). In addition, their sign, magnitude, and range may change appreciably if solution conditions (such as pH and ionic strength) are changed[20, 21]. In particular, the strength of the electrostatic interactions tends to decrease appreciably when the ionic strength of the aqueous phase increases.

(a)

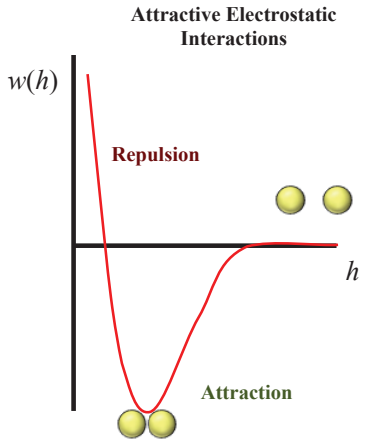

(b)

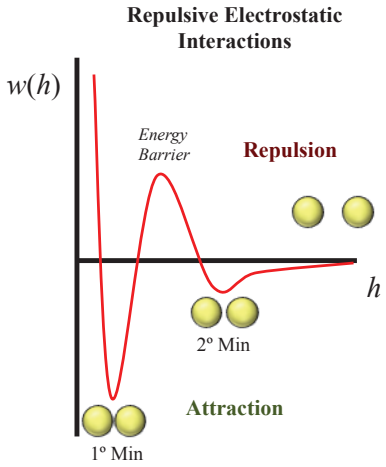

Figure 2.1 Schematic representation of the interaction potential between two emulsion droplets: Left – extended DLVO theory with van der Waals attraction,

electrostatic *attraction*, and steric repulsion; Right – extended DLVO theory with van der Waals attraction, electrostatic *repulsion*, and steric repulsion.

At large separations between the colloidal particles all of the interactions are relatively weak. However, as the particles get closer together the various types of attractive and repulsion interactions become stronger. The Van der Waals attractive force tends to be strong and relatively long-range, whereas the steric repulsive force tends to be very strong and short range. As already mentioned, the electrostatic force may be attractive or repulsive, and its magnitude and range depend strongly on ionic composition. Mathematical models are available to predict the distance dependence of the different colloidal interactions between two spherical particles [22]:

$$U(h) = U_V(h) + U_E(h) + U_S(h) \tag{2.1}$$

where $U(h)$, $U_V(h)$, and $U_E(h)$ are the overall, van der Waals, electrostatic and interaction potentials at a surface-to-surface separation of h. Expressions for the interactions between two spherical particles of similar size but different charge are available in the literature [23, 24]:

$$U_V(h) = -\frac{Ar}{12h} \tag{2.2}$$

$$U_E(h) = \frac{\pi\varepsilon_0\varepsilon_R r}{2}\left(\psi_A^2 + \psi_B^2\right)\times\left[\frac{2\psi_1\psi_2}{\psi_A^2 + \psi_B^2}\ln\left(\frac{1+e^{-\kappa' h}}{1-e^{-\kappa' h}}\right) + \ln(1-e^{-2\kappa' h})\right] \tag{2.3}$$

$$U_S(h) = \left(\frac{2\delta}{D}\right)^{12} \tag{2.4}$$

where r is the droplet radius, A is the Hamaker function, ε_0 is the permittivity of free space, ε_R is the relative dielectric constant of the aqueous phase, Ψ is the surface potential of the particles (in V), and $1/\kappa'$ is the Debye screening length (m), and the

subscripts *A* and *B* refer to the two different kinds of droplets. For aqueous solutions at room temperature: $1/\kappa' \approx 0.304/\sqrt{I}$ nm, where *I* is the ionic strength expressed in moles per liter.

In computer simulations, it is often more convenient to use a simpler mathematical theory to model the colloidal interactions between two colloidal particles rather than the more complex DLVO so as to speed up the many calculations involved [25, 26]. For example, the sticky hard-sphere model has been utilized [25]:

$$U_{AB}(h) = \infty \qquad \text{(for } h \leq 2\delta\text{)} \qquad (2.5a)$$

$$U_{AB}(h) = -\varepsilon \frac{d}{h+d} \exp\left(\frac{Kh}{d}\right) \qquad \text{(for } h > 2\delta\text{)} \qquad (2.5b)$$

Here ε is a measure of the *magnitude* of the attraction and 1/K is a measure of the range of the attractive interaction [25].

2.1.2 Modeling Aggregate Formation

Ideally, one would like to predict the structural organization of the particles within any aggregates formed when a suspension of positive and negative particles are mixed together. A number of different approaches have been developed to provide insights into the structure of the aggregates formed.

Recently, a statistical thermodynamic theory has been developed to model aggregate formation when two types of equal-sized particles (A and B) are mixed together [25]. This theory relates the number of particles per aggregate to the total particle concentration, the mass ratio of the two particle types, and the strength of the attractive forces between the different particle types. It is assumed that the interactions between similar particle types (*i.e.,* A-A or B-B) can be described by a hard shell model,

while interactions between different particle types (*i.e.,* A-B) can be described by the "sticky" hard shell model mentioned above. The development of this statistical thermodynamic approach have been described in a recent paper by Dickinson [25]. We provide an overview of some of the equations here so as to highlight the important features involved. The average aggregate size (S) is given by the following expression:

$$S = \frac{\left[x_A(1+\phi_B\lambda_{AB})^2 + x_B(1+\phi_A\lambda_{AB})^2\right]}{\left[1-\phi_A\phi_B\lambda_{AB}^2\right]^2} \tag{2.6}$$

Here, x_A and x_B are the mole fractions of type A and type B particles, ϕ_A and ϕ_B are the volume fractions, and λ_{AB} is the interaction coefficient:

$$\lambda_{AB} = \frac{K_1}{\tau_{AB} + K_2} \tag{2.7}$$

Where:

$$K_1 = \frac{1}{(1-\phi)} + \frac{3\phi}{2(1-\phi)^2} \qquad K_2 = \frac{\phi}{2(1-\phi)}$$

Here ϕ is the total volume fraction of particles present ($\phi_A + \phi_B$), and $1/\tau_{AB}$ provides a measure of the "stickiness" of the attractive interaction between the different particle types: the larger $1/\tau_{AB}$, the stronger the attraction between different particle types. For a sticky hard shell system, the stickiness parameter can be calculated from the colloidal interaction potential (U_{AB}) between the particles (Equation 2.5):

$$\frac{1}{\tau_{AB}} = \frac{12}{d^3}\int_d^\infty x^2\left\{\exp\left[\frac{U_{AB}(x)}{kT}\right] - 1\right\}dx \tag{2.8}$$

Here, d is the particle diameter, x is the center-to-center particle separation ($x = h + d$), k is Boltzmann's constant, and T is the absolute temperature [25]. It should be noted

that this model is based on the assumption that the system is in thermodynamic equilibrium, but in practice there will be kinetic energy barriers that lead to the formation of metastable structures.

The above model is based on the assumption that the system is in thermodynamic equilibrium, but in practice there will be kinetic energy barriers that lead to the formation of metastable structures. In addition, the above model does not provide information about the structural organization of the different kinds of colloidal particles within the aggregates. More sophisticated approaches are therefore required to take into account non-equilibrium effects and structural organization, such as those based on computer simulations [10, 24, 27]. For example, hetero-aggregation can be modeled using diffusion-limited cluster-cluster aggregation simulations [28]. These simulation methods have been used to examine the influence of various factors on the structural organization of mixed colloidal systems, such as total particle concentration, positive-to-negative particle ratio, particle size ratio, and interaction strength. These computational studies have shown that various kinds of aggregates with different structures can be formed depending on the initial characteristics of the system (**Figure 2.2**). When one kind of particle dominates, then small hetero-aggregates tend to be formed that consist of one kind of particle surrounded by the other kind of particle. On the other hand, when the two types of particles are present in similar concentrations, then large hetero-aggregates are formed that contain a mixture of both particles. At relatively high total particle concentration, hetero-aggregation may lead to the formation of a three-dimension network of particles that give the system gel-like or paste-like characteristics.

(a)

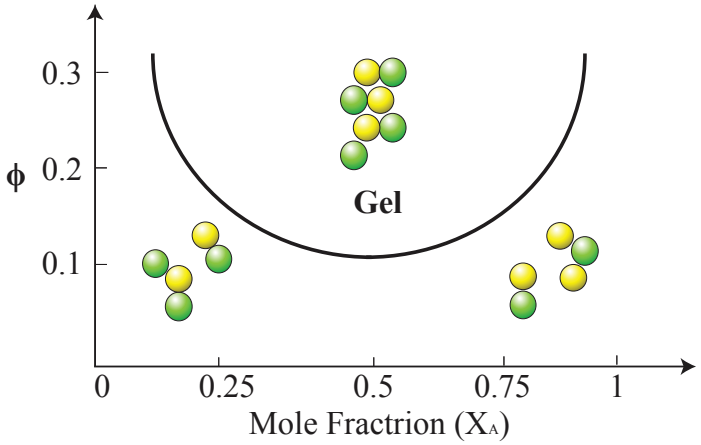

(b)

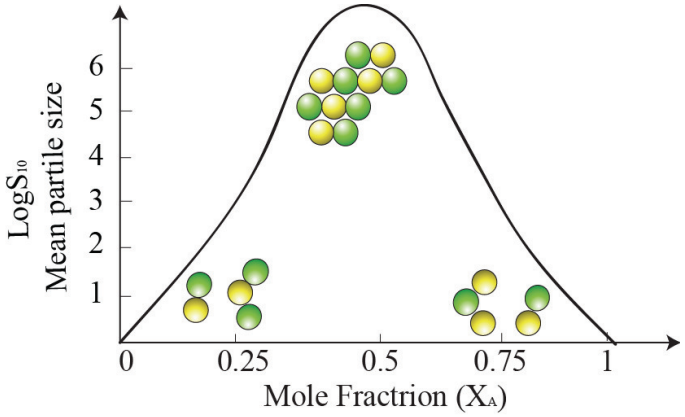

Figure 2.2 Schematic representation of a phase diagram (a) and average cluster size, (b) for a hetero-aggregated system containing particles that are attracted to each other.

2.2 Conventional Emulsions

Initially, we consider the formation and properties of conventional emulsions so as to contrast their behavior with mixed emulsions in which hetero-aggregation has been induced. A conventional O/W emulsion consists of fat droplets dispersed within an aqueous medium (**Figure 2.3**). Each fat droplet is coated by a thin layer of emulsifier molecules that normally protects the droplets from aggregation. There are many different methods available for preparing oil-in-water emulsions, including various low-

energy and high-energy methods, which have been reviewed elsewhere [29, 30]. In the food industry, the most common method of making fine emulsions is to use high pressure homogenization. In this method, an oil phase is blended with an aqueous phase that contains a water-soluble emulsifier. The resulting coarse emulsion is then passed through the high pressure homogenizer to further reduce the particle size. The size of the droplets present within an emulsion can be controlled by varying the homogenizer type or operating conditions, as well as sample composition, such as the type and amount of emulsifiers present [31].

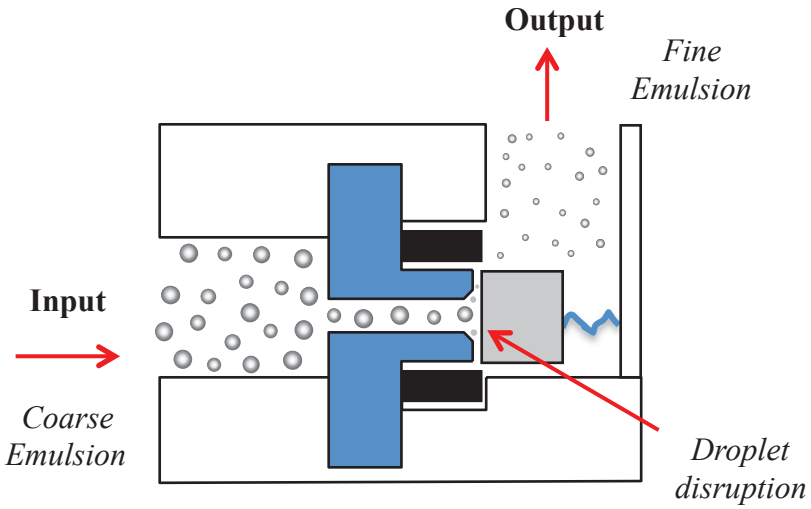

Figure 2.3 Schematic representation of mechanical devices that can be used to produce conventional emulsions using a high pressure valve homogenizer.

The long-term stability of the emulsions can be controlled by selecting different types of emulsifiers to coat the fat droplets. The nature of the emulsifier selected determines interfacial characteristics such as thickness, polarity, charge, and chemical reactivity. In turn, these interfacial characteristics influence the physiochemical properties, sensory attributes, and biological fate of emulsions [32, 33].

The tendency for fat droplets to aggregate with each other, or to remain as individual entities, depends on the balance of attractive and repulsive interactions operating between them. When the attractive interactions dominate, then the droplets will tend to associate with each other and form aggregates. In the case of conventional emulsions, this process can be referred to as *homoaggregation* since there is only one type of fat droplet involved. The size, shape, and deformability of the aggregates formed depend on the strength of the attractive interactions between droplets.

The aggregation state of the droplets within an emulsion plays a major role in determining the overall texture and stability. In dilute emulsions, droplet aggregation tends to lead to an increase in the creaming rate due to an increase in effective particle size. Conversely, in concentrated emulsions, droplet aggregation may decrease the creaming rate because the droplets are trapped within a three-dimensional network that inhibits droplet movement. The textural characteristics of emulsions are also strongly dependent on the droplet aggregation state. Droplet aggregation leads to an increase in shear viscosity in relatively dilute systems and to gel formation in relatively concentrated systems.

2.3 Hetero-aggregated Emulsions

In this section, we focus on hetero-aggregation in oil-in-water (O/W) emulsions since these are one of the most suitable colloidal systems for utilization within the food industry. Nevertheless, it should be noted that hetero-aggregation can also be induced in water-in-oil (W/O) emulsions containing oppositely charged water droplets [34], or in other types of colloidal suspensions, *e.g.,* air bubbles or biopolymer particles in water.

Hetero-aggregated emulsions are typically formed by mixing together two conventional emulsions. Each of these emulsions contains fat droplets coated by a layer of electrically charged emulsifier molecules, but the type of emulsifier used is different. The two emulsions are then mixed together under conditions where one of them contains negatively charged droplets, and the other contains positively charged droplets, which promotes hetero-aggregation (**Figure 2. 4**). The structure of the hetero-aggregates formed and the subsequent functional performance of the overall emulsion depends strongly on the electrical characteristics of the different fat droplets. One of the most important factors determining the formation of hetero-aggregated emulsions is therefore the nature of the emulsifiers used.

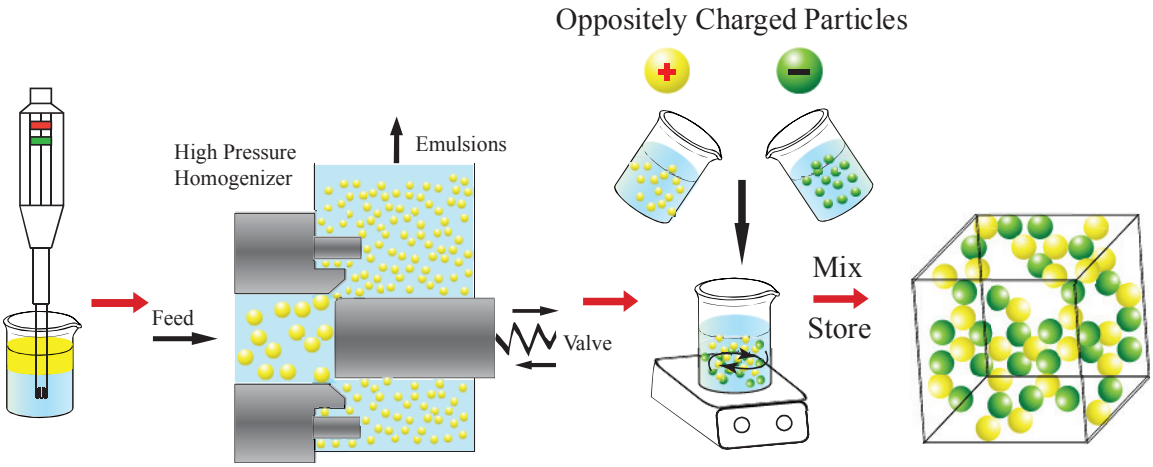

Figure 2.4 A schematic chart of particle-particle hetero-aggregation using the one-step mechanism.

2.4 Emulsifiers

A variety of different types of emulsifiers can be used to prepare oil-in-water emulsions containing electrically charged droplets, such as proteins, polysaccharides, and ionic surfactants (**Figure 2.5**). Each type of emulsifier-system has its own advantages and disadvantages for particular applications. Selection of the most appropriate

emulsifier is one of the most important factors influencing the formation of hetero-aggregated emulsions. In this section, we provide an overview of a number of electrically charged food-grade emulsifiers that can be used.

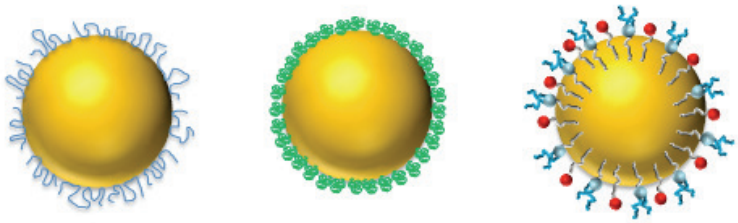

Polysaccharides Globular Protein Surfactant

Figure 2.5 Schematic representation of protein-, polysaccharide- and surfactant coated fat droplets.

2.4.1 Proteins

Protein-based emulsifiers can be isolated from various natural sources, including various animal, plant, and marine products. However, the most commonly used protein-based emulsifiers in the food industry are those derived from bovine milk because of their relatively low cost and ease of isolation, *i.e.,* caseins and whey proteins. Caseins are relatively flexible and disordered proteins that make up about 80% of milk proteins, and include four main fractions: α_{S1}-casein; α_{S2}-casein; β-casein; and κ-casein. Whey proteins are compact globular proteins that make up about 20% of milk proteins, and also include a number of different fractions, such as β-lactoglobulin, α-lactalbumin, bovine serum albumin, lactoferrin and various other minor components [35]

These proteins are amphiphilic molecules that have both non-polar and polar groups on the same molecule, and can therefore adsorb to oil-water interfaces. They normally provide stabilization against droplet aggregation by a combination of electrostatic and steric repulsion [36]. The electrical characteristics of different proteins

are determined by their primary sequence, especially the type, number, and location of ionizable amino acid side groups and other charged groups (such as phosphates) along the polypeptide backbone. Each type of protein can be characterized by its isoelectric point (pI), which is the pH where the net charge on the protein is zero (*i.e.,* the number of positive and negative charges are balanced). Below the pI the electrical charge on the proteins is positive, but above this pH it is negative. The isoelectric points and acid dissociation constant point of some common biopolymers are summarized in Table 2.1.

Types of Emulsifiers							
Proteins (Isoelectric points)				**Polysaccharides** (Acid dissociation constants)			
Casein	*β-Lg*	*Lactoferrin*	*WPI*	*Modified starch*	*Gum Arabic*	*Pectin*	*Chitosan*
4.5	5	8.5	5	2.3	3.5	3.5	6.3-7

Table 2.1 Summary of the isoelectric points and acid dissociation constants (pK_a) of some common food-grade biopolymers that can be used to form electrically charged emulsion droplets: β-Lg = β-lactoglobulin; WPI = whey protein isolate.

When the adsorbed proteins form a relatively thin interfacial coating around the fat droplets, the primary stabilization mechanism is electrostatic repulsion. For this type of system, the stability of the emulsion is particularly sensitive to changes in pH and ionic strength. Droplet aggregation tends to occur when the pH is close to the isoelectric point (low net droplet charge) or at high salt concentrations (strong electrostatic screening). β-lactoglobulin is a commonly used globular protein that forms thin interfacial coatings around fat droplets, and is therefore highly sensitive to solution pH

and ionic strength. On the other hand, when the adsorbed proteins form a relatively thick hydrophilic coating around the fat droplets the stabilization mechanism is a combination of electrostatic and steric repulsion. Emulsions stabilized by this kind of protein are much more resistant to alterations in pH and ionic strength. Lactoferrin is an example of a globular protein that is believed to form thick interfacial coatings around fat droplets due to its relatively high molecular weight, and the fact that it contains hydrophilic carbohydrate side-chains that protrude into the aqueous phase [21, 37]. Experimental studies have shown that lactoferrin-coated fat droplets are highly stable to changes in pH and salt concentration, provided there is sufficient protein present to fully coat the droplet surfaces. If there is insufficient surface coverage, the lactoferrin-coated droplets are prone to aggregation [38]. In addition, lactoferrin-coated droplets seem to be highly sensitive to the type of counter-ions in solution. For example, multivalent anionic species in acetate and phosphate buffers may bind to cationic sites on lactoferrin molecules, thereby reducing their surface charge and altering their physicochemical properties [39].

Another factor that is important for determining the functional performance of globular protein-coated fat droplets in their response to temperature changes. Globular proteins (such as β-lactoglobulin, BSA, and lactoferrin) unfold when they are heated above their thermal denaturation temperature (T_m). These conformational changes expose reactive amino acid groups, such as those containing non-polar or sulfhydryl groups, which promote protein-protein interactions. As a result, fat droplets coated by these proteins may aggregate at elevated temperatures due to increases in the hydrophobic attraction or disulfide bonds between the proteins on different droplets. On

the other hand, there are no major changes in the conformation of caseins when they are heated, and therefore they tend to be more stable to thermal processing.

2.4.2 Polysaccharides

A number of natural and modified polysaccharides are amphiphilic molecules that are capable of stabilizing oil-in-water emulsions, such as gum arabic and modified starch [40]. Modified starch is produced by chemically modifying natural starches so that they gain some non-polar groups. This is normally achieved by covalently attaching non-polar octenyl succinic anhydrides (OSA) side groups to the polar starch backbone. This leads to an amphiphilic biopolymer molecule that can adsorb to oil-water interfaces and stabilize fat droplets against aggregation [41, 42]. The non-polar OSA groups tend to penetrate into the oil droplets, while the polar starch molecules protrude into the surrounding aqueous phase [43]. Previous studies have shown that modified starch coated fat droplets are negatively charged over a wide pH range (pH 2 to 9) due to the presence of anionic groups on the OSA side chains [44]. Modified starch molecules form a relatively thick hydrophilic layer at the droplet surfaces and therefore can prevent droplet aggregation through a combination of steric and electrostatic repulsion.

Gum arabic is isolated from the exudate of a shrub (acacia tree) and is surface active due to the presence of polysaccharide and protein moieties on the same molecule[45]. The protein part is believed to be non-polar and anchors the molecule to the fat droplet surface, whereas the polysaccharide part is polar and protrudes into the aqueous phase [46]. Gum arabic is negatively charged form around pH 2 to 9 can therefore be used to create anionic droplets suitable for fabricating hetero-aggregates [44]. The fact that gum arabic forms a thick negatively charged interfacial coating

around fat droplets means that it mainly provides stabilization against aggregation through a combination of steric and electrostatic repulsion. In general, polysaccharides-based emulsifiers tend to be more stable to pH, ionic strength, and thermal treatment than protein-based emulsifiers [47].

2.4.3 Surfactants

There are a number of food-grade surfactants that can also be used to form electrically charged fat droplets in O/W emulsions. These surfactants consist of a hydrophilic head group that protrudes into the aqueous phase, and a hydrophobic tail group that protrudes into the oil phase. Most of the ionic surfactants available for utilization in the food industry are negatively charged, such as DATEM, CITREM and lysolecithin. Nevertheless, lauric arginate is a cationic surfactant that is capable of producing stable positively charged droplets are relatively low pH values ($pH < 7$). Ionic surfactants can be used in isolation, or they can be mixed with non-ionic surfactants to improve emulsion stability.

2.4.4 Emulsifier Exchange

A potential problem with using two different kinds of fat droplets stabilized with different emulsifiers is the exchange of emulsifiers between them. When one mixes droplets coated by different emulsifiers together then the emulsifier from one droplet may exchange with the emulsifier from a different droplet. As a result the electrical charge on the two kinds of droplets will change, becoming more similar. If complete mixing of the emulsifiers occurs at the droplet interfaces, then all the droplets will eventually have the same charge, which may prevent hetero-aggregation from occurring.

Emulsifier exchange may limit the types of emulsifiers that can be used to form hetero-aggregated systems. Polymeric emulsifiers tend to be more resistant to exchange than small molecule surfactants, particularly if they can be cross-linked at the interface (*e.g.,* by thermal, chemical or enzymatic treatment).

2.5 Preparation of Hetero-aggregated Emulsions

In general, hetero-aggregation can be induced in O/W emulsions using two different approaches based on electrostatic attraction. First, aggregation can be promoted by mixing an emulsion containing positive droplets with one containing negative droplets (**Figure 2.4**). Second, aggregation can be promoted by mixing an emulsion containing charged droplets, with a solution containing oppositely charged polymers (**Figure 2.5**). In this manuscript, we will only focus on particle-particle aggregation. Various kinds of oppositely charged particles can be used to induce particle-particle hetero-aggregation in a system, including fat droplets, air bubbles, starch granules, and various biological cells. Most previous studies have been carried out using oppositely charged fat droplets and therefore we will focus on this system. In this case, hetero-aggregation is induced by mixing an oil-in-water emulsion containing positively charged droplets with another one containing negatively charged droplets. This process can be carried out using either a one-step or two-step method depending on the charge characteristics of the fat droplets:

- *One-step method:* The two emulsions are directly mixed together under conditions where the two types of droplets have opposite charges so that hetero-aggregation occurs immediately.

- *Two-step method:* The two emulsions are mixed together under conditions where the two types of droplets have similar charges, and then the solution conditions (pH) are altered so that the droplet charges become opposite and then hetero-aggregation occurs.

The nature of the hetero-aggregates formed and the resulting physicochemical properties of the mixed system depend on a number of factors, including the total particle concentration, the positive-to-negative particle ratio, the size of the two types of particles, and the mixing method. One of the main purposes of this theis is to carry out systematic studies of heteroaggregation in food-grade oil-in-water emulsions.

2.6 Characterization of Emulsions

Droplet characteristics (such as particle size and charge) influence the stability rheology, and optical properties of emulsions. It is therefore important to have analytical techniques to measure these properties.

2.6.1 Particle size

The particle size is usually reported as either the volume-weighted ($d_{4,3}= \sum d_i n_i^4 / \sum d_i n_i^3$) or surface-weighted mean diameter ($d_{3,2} = \sum d_i n_i^3 / \sum d_i n_i^2$), where n_i is the number of droplets of diameter d_i. The mean particle diameter of emulsion droplets depends on emulsifier type and formation method. The particle size distribution (PSD) defines the fraction of particles in different size ranges. The particle size distribution is usually measured using light scattering or microscopy methods.

2.6.2 Particle Charge

Electrical charge in food emulsions is usually generated by ionized molecules in the interfacial layer surrounding the lipid droplets. The electrical charge on a droplet is usually characterized in different ways: surface charge density (σ), the electrical surface potential (ψ_0), and the zeta-potential (ζ)[31]. Surface charge density is defined as the electric charge per unit area of surface. The relation between surface charge and surface potential can be explained using the Gouy-Chapman theory using the Grahame equation:

$$\sigma = \sqrt{8C_0 \epsilon \epsilon_0 K_B T} \sin h \left(\frac{ze\psi_0}{2K_B T}\right) \qquad (2.9)$$

[48]. The zeta-potential (ζ) is the net surface charge of colloidal particles suspended in a medium. The electrical charge is largely determined by the nature of emulsifier used to stabilized the droplets. Proteins can be positively charged, negatively charged, or neutral depending on pH, whereas polysaccharides charge dependson the charge of ionizable groups on their structure, such as carboxyl or sulfate groups [36]. Therefore, it is important to characterize the electrical charge of emulsifiers prior to the establishment of heteroaggregation. This is usually done using particle electrophoresis methods based on light scattering.

2.6.3 Rheological Properties

Rheological properties of emulsions are mainly determined by the particle concentration, interfacial interactions and viscosity of the surrounding solution. In heteroaggregated systems, extensively aggregated structures are formed and their rheology can be approximated by the following equation:

$$\frac{\eta}{\eta_0} = \left(1 - \frac{\phi}{\phi_c \phi_i}\right)^{-[\eta]\phi_c/\phi_i} \quad (2.10)$$

where η_0 is the shear viscosity of the continuous phase, $[\eta]$ is the intrinsic viscosity (= 2.5), ϕ is the disperse phase volume fraction, ϕ_c is the actual volume fraction of particles. Typically, this value is taken to be approximately equal to that of random close packing of spheres, $\phi_c \approx 0.63$. ϕ_i is independent of the aggregates size. For random close packing of hard spheres $\phi_i = 0.63$ [49]. This equation can be used to predict how to modulate the viscosity of hetero-aggregates. So the equation indicates that the viscosity of emulsions increases as the particle concentration increases [50, 51].

2.6.4 Optical Properties

Visual appearance is the first impression of foods that consumers use to judge the quality, safety and desirability of a product [52]. In general, the scattering pattern of emulsions can be classified by the ratio of particle size to the wavelength of light. For nanoemulsions ($r/\lambda<0.1$), the light is evenly scattered in all directions and they appear transparent. For conventional emulsions ($r/\lambda\approx1$), strong diffusion occurs and the emulsions appear opaque. For high ratios ($r/\lambda>10$), the light is reflect inward and the emulsiosn again appear transparent if $r \gg \lambda$ [65].

The optical properties of emulsions associate with particle size, concentration and refractive index. The appearance of emulsions can be determine by instrumental analysis or naked eye observation. Optical properties can be expressed as L*a*b* value (or CIELAB) which can be quantitatively calculated. L* represents the lightness where L*=0 indicate black and L* = diffuse white; a* indicates the color between red/ magenta (+) and green (-) while b* means the position of color between yellow (+) and blue (-). For

emulsion systems, the appearance depends on particle size, particle concentration and refractive index contrast [53].

2.6.5 Stability

Stability can be defined as the capability of emulsions to keep their physical stability over time. Creaming, flocculation, coalescence, partial coalescence, phase inversion and Ostwald ripening are examples of physical instability. In general, food emulsions are thermodynamically unfavorable systems due to the different density of the two immiscible liquids, and the unfavorable contact between oil and water. Due to their thermodynamic instability, emulsions will always breakdown over time. They can be made kinetically stable by using certain kinds of stabilizers, such as emulsifiers, thickening agents, or weighting agents.

The instability of emulsions due to gravitational separation is referred to as creaming (upwards) or sedimentation (downwards). These changes result "droplet rich" opaque cream layers and "droplet depleted" watery sediment layers. The rate of separation can be calculated by Stokes' law:

$$\nu_{Stokes} = -\frac{2gr^2(\rho_2 - \rho_1)}{9\eta_1} \qquad (2.11)$$

in which *r* is the particle radius; ρ_2 is the density of disperse phase and ρ_1 is the density of continuous phase; η_1 is the viscosity of continuous phase; g is the gravity force.

Flocculation and coalescence are the main reasons of droplet aggregation in emulsions. The flocculation is the process of association of neighboring droplets but each one remains as an individual particle. In the diluted systems, flocculation accelerates gravitational separation due to an increase in particle size [54], but in concentrated

systems it retard separations due to network formation [55, 56]. Coalescence is the process where two or more particles merge into one larger particle due to the breakage of the thin film between them.

According to the **equation 2.11**, the stability of emulsions exhibits a dependence on the characteristics of emulsions droplets (radius and density) and continuous phase (viscosity and density). Thus, emulsions with large mean particle size such as the conventional emulsions ($d_{43} \approx 0.2\mu m$) are less stable to the separation than the nano-emulsions ($d_{32} \approx 0.02\mu m$) and the large difference in density can also accelerate the separation of emulsion system which indicates that the density matching can be an effective mean to stabilize the emulsion system. The addition of thickening agents like pectin can increase the viscosity of continuous phase, thereby inhibiting creaming.

2.7 Potential Biological Fate of Hetero-aggregated Emulsions

Emulsions are often used to encapsulate and deliver bioactive components within the food industry, such as ω-3 fatty acids, carotenoids, flavonoids, and phytosterols [42]. It is therefore important to understand how hetero-aggregated emulsions behave within the complex environment of the human gastrointestinal tract so as to ensure they release any encapsulated components at the appropriate site. In this section, we briefly review the influence of the different stages of the human gastrointestinal tract (mouth, stomach, small intestine) on the properties of hetero-aggregated emulsions.

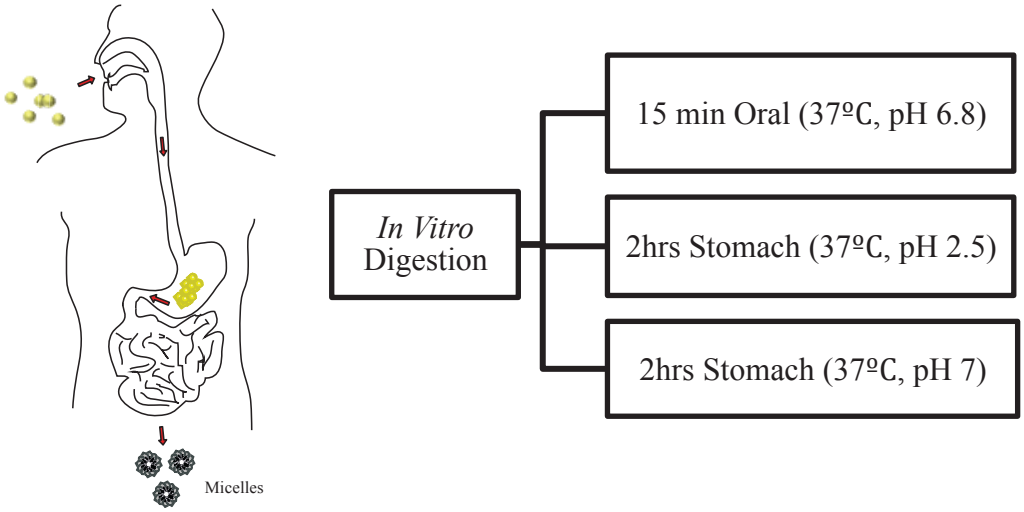

Figure 2.6 The behavior of emulsions in oral-gastric-intestinal tract

2.7.1 Oral phase

The mouth is the first environment that an emulsion experiences after consumption. After ingestion, an emulsion may experience changes in temperature, pH, and ionic strength, as well as being exposed to complex fluid flows, biological fluids (saliva), and biological surfaces (tongue, teeth, and cheeks) [57]. These changes can alter the structural and physicochemical properties of ingested emulsions. For example, changes in pH and ionic strength will alter the electrostatic repulsion between the different charged droplets, which may cause dissociation or rearrangements in the structures of hetero-aggregates. In addition, the anionic polymers within mucin may interact with the cationic droplets within an emulsion, which could also alter the structural organization of the droplets [58]. Fat droplets stabilized by modified starch may also be influenced due to the activity of amylases within the mouth [51].

2.7.2 Gastric phase

After passage through the mouth, emulsions rapidly move through the esophagus and enter the stomach where they are exposed to a highly acidic environment, which contains various biological entities, such as mucin, proteases (pepsin), lipases (gastric lipase), minerals and salts [59]. In the fasting state, the gastric fluids typically have a pH values between about 1 and 3 but this can increase appreciably when a food enters the stomach [59]. The low pH may cause denaturation of globular proteins (*e.g.* whey proteins) that may be used to stabilize fat droplets in hetero-aggregated emulsions. Proteases can hydrolyze proteins absorbed to fat droplet surfaces surface and allow gastric lipase the pH of to the emulsified lipid phase [58, 60]. Moreover, mineral ions within the gastric fluids can reduce the electrostatic forces (attractive and repulsive) between the fat droplets in hetero-aggregated emulsions, which may alter their structural organization. The mobility of the stomach generates a complex fluid flow profile that can also change the structure of aggregated droplets, and therefore the digestion process [61].

2.7.3 Small Intestine Phase

After passing through the stomach, the digesta enters the small intestine, which consists of duodenum, jejunum, and ileum regions. The small intestinal fluids contain a variety of components that may alter the structural organization and digestion of hetero-aggregated emulsions, including sodium bicarbonate, salts, bile, and digestive enzymes. The secretion of bicarbonate increases the pH to around 5-7, which will lead to changes in the surface charge of the fat droplets in emulsions [58, 62]. The presence of various types of mineral ions (*e.g.,* Na^{+}, Ca^{2+}) will influence the electrostatic interactions between hetero-aggregates. The presence of surface active molecules in the bile (such as

bile salts and phospholipids) may change the interfacial composition due to competitive absorption with protein molecules [63, 64]. The adsorption of lipase/co-lipase complex to the droplet surfaces will initiate lipid digestion leading to the formation of free fatty acids and monoacylglycerols, which combine with bile acids and phospholipids to form mixed micelles.

2.8 Practical Applications

Hetero-aggregates formed by electrostatic attraction of oppositely charged emulsion droplets can be used to form novel functional materials suitable for utilization within the food, cosmetics, and pharmaceutical industries.

In relatively dilute systems, hetero-aggregation tends to increase gravitational separation because of the increase in particle size. In many applications this would be undesirable since it will lead to rapid phase separation. However, increased gravitational separation may be useful for certain applications, such as purification. One type of charged particle could be removed from a system by mixing it with oppositely charged particles. Unlike centrifugation or filtration, hetero-aggregation can separate particles with low energy and equipment costs [15, 16]. Hetero-aggregation can also be utilized in DNA technology such as encapsulate and release of DNA from electrostatically assembled materials [17]. Electrostatically driven assemble is also promising application in coating industry. For instance, ceramics are required to have environmentally (pH, thermal and chemical) stable properties, therefore some agents need to be added into the ceramic suspension to enhance the strength and ease the process. With oppositely charge, different particles or microgels containing functional ingredients such as polyeletrolyte

coated alumina can anchor on ceramic surface and aid to improve the performance of ceramic body[65].

In the food area, the rheological control is main application of hetero-aggregation. With the formation of hetero-aggregates, the system can provide desirable high viscous flow with viscoelastic properties. Mostly, human is prone to choose creamy and smooth food indicating high energy density food such as butter, cream wipe and other dressing sauce. The common feature of these products is high fat content with relatively high viscosity and easy to cause obesity. Therefore, hetero-aggregation can be a potential approach to precisely control rheological properties through particle density (particle concentration and fat content) and environmental conditions (pH, ionic strength and thermal treatment), and with low fat content, the hetero-aggregates may mimic similar texture of high fat emulsions. Therefore, high viscous food products such as salad dressing, sauce and soups could be an ideal food matrix to utilize hetero-aggregation technique to produce reduces fat food.

The other advantage of hetero-aggregates is to encapsulate more than one kind of oil soluble component in emulsion system without affecting each other. For example, positively charged emulsion can encapsulate a bioactive lipophilic component while the other functional is trapped in negative charged emulsions. These two oppositely charged emulsion droplets could be mixed together and form microclusters which can be applied in target delivery system. For example, this structure can be used to encapsulate probiotics and deliver to targeted place[66, 67]. In addition, this structure shows fairly similar lipid digestibility and releasing rate suggesting that the successful delivery of bioactive lipid compound to the small intestine without prolonged digestion.

The potential disadvantage of hetero-aggregates is high suspicious to separation caused by the gravitation and result failure in appearance and structure. However, in concentrated system, uniformed appearance can be obtained by the formation of semi-solid structure, so the gravity is not the limitation for the stability of microclusters. The other solution can be the addition of thickener or gelling agents.

CHAPTER 3

MODULATION OF BULK PHYSICOCHEMICAL PROPERTIES OF EMULSIONS BY HETERO-AGGREGATION OF OPPOSITELY CHARGED PROTEIN-COATED LIPID DROPLETS

3.1 Introduction

There has been growing interest in the utilization of structural design principles to create novel or improved functional attributes in food systems, *e.g.,* rheology, optical properties, stability, flavor profile, or nutritional aspects [68-72]. This structural design approach involves utilizing a basic understanding of the building blocks (*e.g.,* water, proteins, carbohydrates, lipids, and minerals), the forces (*e.g.,* molecular and colloidal interactions), and the construction principles (*e.g.,* self-assembly, directed-assembly, and phase disruption) to create specific structures within foods that are known to lead to desirable functional attributes [73]. The structures formed may be in the nanometer, micrometer, or millimeter scales depending on the size and number of building blocks utilized. For example, microemulsions consisting of self-assembled surfactants are nanometer-scale structures that can be used to encapsulate, protect and deliver lipophilic functional food components [74, 75]. Multilayer emulsions consisting of lipid droplets coated by nanolaminated interfacial layers are typically micrometer-scale structures that can be used for similar purposes [76, 77].

In this study, we examine the possibility of using controlled hetero-aggregation of oppositely charged lipid droplets to create microclusters that could have desirable functional properties in foods. In principle, microclusters with different particle characteristics (*e.g.,* particle size, shape, charge, and deformability) can be prepared by

controlling the characteristics of the two (or more) types of lipid droplets used to prepare them (*e.g.,* size and z-potential), as well as the preparation conditions (*e.g.,* droplet concentrations, pH, ionic strength, and stirring conditions). By controlling the characteristics of the microclusters formed it may be possible to create different functional attributes in foods, such as stability, texture, and release characteristics.

A number of experimental and theoretical studies have previously been carried out on the phenomenon of hetero-aggregation, *i.e.,* the aggregation of two or more different kinds of particles [10, 11, 27, 78-81]. The different kinds of particles may aggregate due to differences in their sizes, charges, hydrophobicities or other properties. Practically, hetero-aggregation forms the basis of many important industrial processes, including flotation, waste-water treatment, pharmaceutical preparation, food production, and paper making [11, 82]. A great deal of research has been carried out in this area to establish the conditions whether hetero-aggregation occurs, and to ascertain the nature of the microclusters formed. In dilute systems, relatively small microclusters with different compositions and structures can be formed depending on the nature of the positive and negative particles used [83]. In concentrated systems, clusters of positively and negatively charged particles that extend throughout the entire volume of the system are formed, leading to the creation of soft solids with gel like characteristics [24, 84].

Most previous studies on hetero-aggregation have been carried out using non-food grade particles that are unsuitable for utilization within the food industry. The purpose of the current study was therefore to examine whether functional microclusters could be formed from food-grade particles using the hetero-aggregation approach. For this reason, microclusters were prepared by mixing two emulsions together that

contained lipid droplets with different electrical characteristics, *i.e.,* charge *versus* pH profiles. The electrical characteristics of the two kinds of lipid droplets were varied by using two globular proteins with different isoelectric points: β-lactoglobulin (b-Lg) with pI ≈ 5; lactoferrin (LF) with pI ≈ 8. These proteins are positively charged below their pI and negatively charged above it. Hence, it should be possible to distinguish three different regimes in the charge *versus* pH profiles in a mixed system: (i) $pH < pI_{b\text{-}Lg}$: both proteins are positively charged; (ii) $pI_{b\text{-}Lg} < pH < pI_{LF}$: one protein is negative and the other is positive; (iii) $pH > pI_{LF}$ both proteins are negatively charged. Microclusters should be formed in Regime (ii) due to electrostatic attraction between the oppositely charged lipid droplets. These microclusters may provide a useful means of controlling the physicochemical and functional properties of colloidal food systems, leading to products with improved or novel characteristics.

3.2 Experimental Methods

3.2.1 Materials

Corn oil was purchased from a commercial food supplier (Mazola, ACH Food Companies, Inc., Memphis, TN) and stored at 4 °C until use. Food grade lactoferrin (LOT # 10408282) was supplied by DMV International (Delhi, NY), and the manufacturer reported that it contained 97.7% protein and 0.12% ash. Purified β-lactoglobulin powder (LOT # JE-002-8-415, Le Sueur, MN) was supplied by Davisco Foods International (BioPURE β-lactoglobulin, Eden Prairie, MN). The manufacturer reported the composition of this powder to be 97.4% total protein, 92.5% *β*-lactoglobulin (*β-Lg*), and 2.4% Ash. Monobasic phosphate and dibasic phosphate were purchased from

Sigma-Aldrich (Sigma Chemical Co., St. Louis, Mo) or Fisher Scientific (Pittsburgh, PA). All solvents and reagents were of analytical grade. For confocal microscopy work, a non-polar fluorescent dye (Bodipy 493/503) was purchased from Invitrogen (Carlsbad, CA) and a protein fluorescent dye (Rhodamine B) was purchased from Sigma-Aldrich (St Louis, MO). All other chemicals used in this research were purchased from Sigma-Aldrich (St Louis, MO). Double distilled water was used to make all solutions.

3.2.2 Emulsion Preparation

Single-protein Emulsions: Aqueous emulsifier solutions were prepared by dispersing either β-Lg powder or LF powder into double distilled water, and then stirring for at least 3 h at room temperature to ensure complete dispersion. The pH of the protein solutions was then adjusted to 7.0 using 1M NaOH or 1M HCl. Oil-in-water emulsions containing a single protein type were prepared by blending 10 g of corn oil and 90 g of aqueous protein solution for 2 min using a hand blender (M133/1281-0, 2 speed, Biospec Products Inc., ESGC, Switzerland) and then recirculating them four-times through a two-stage homogenizer (LAB 1000, APV-Gaulin, Wilmington, MA) at a first-stage pressure of 5,400 psi and a second-stage pressure of 600 psi. The emulsions were then stored for 24 hours prior to utilization. Preliminary experiments established that 0.5% β-Lg and 3% LF were suitable levels to form single-protein emulsions with relatively small droplet diameters ($d \approx 0.14$ mm) (see **Section 4.1**), and so these levels were used to form the mixed-protein emulsions.

Mixed-protein Emulsions: Initially, two 10 wt% oil-in-water emulsions stabilized by either 0.5% β-Lg or 3% LF were prepared in distilled water. These two single-protein emulsions had similar initial droplet diameters ($d \approx 0.14$ mm). For each single-protein

emulsion, a series of samples was prepared by adjusting them to different pH values (pH 3, 4, 5, 6, 7, 8, 9) using either 1M NaOH or 1M HCl. These emulsions were then stored overnight at room temperature. At the same pH (3 ,4, 5, 6, 7, 8, or 9), mixed emulsions were prepared by combining different volume ratios of 10 wt% O/W emulsions containing β-Lg-coated or LF-coated droplets (*β-Lg* : LF= 0:100, 10:90, 20:80, 30:70, 40:60, 50:50, 60:40, 70:30, 80:20, 90:10, 100:0). The mixed emulsions were then stirred for 1-2 h and the particle size distribution and charge were measured. Some emulsion samples were allowed to stand overnight at ambient temperature without stirring, and then there appearance and textural characteristics were assessed.

3.2.3 Droplet Charge Measurements

The ζ-potential of emulsions was determined using a particle electrophoresis instrument (Zetasizer Nano ZS series, Malvern Instruments, Worcestershire, UK). The ζ-potential is determined by measuring the direction and velocity of droplet movement in a well-defined electric field. Mixed emulsions were diluted to a droplet concentration of approximately 0.001 wt% using pH-adjusted water to avoid multiple scattering effects. The pH of the water used was adjusted to the same pH as the initial emulsion sample. After loading the samples into the instrument they were equilibrated for about 120 s before particle charge data was collected over 20 continuous readings.

3.2.4 Particle Size Analysis

The particle size distribution of the emulsions was measured using a laser diffraction particle size analyzer (Mastersizer 2000, Malvern Instruments, Ltd., Worcestershire, UK). This instrument measures the angular dependence of the intensity

of light (λ=632.8 nm) scattered from a stirred diluted emulsion. The particle size distribution is then calculated using Mie theory to obtain an optimal analysis of this light energy distribution. To avoid multiple scattering effects the emulsions were diluted to a droplet concentration of approximately 0.005wt% using pH-adjusted water at the same pH as the sample. The emulsions were stirred continuously throughout the measurements to ensure the samples were homogenous. A refractive index ratio of 1.08 was used by the instrument to calculate the particle size distributions. Measurements are reported as the volume–surface mean diameter: $d_{3,2}=\sum d_i n_i^3/\sum d_i n_i^2$, where n_i is the number of droplets of diameter d_i.

3.2.5 General Appearance and Texture

The general appearance and texture of the mixed emulsion samples was determined by simple visible observation and digital photography. The emulsions were placed into glass test tubes and stored for 24 hours at ambient temperature without stirring. Some of the samples were stable to creaming, while some showed evidence of phase separation. The extent of creaming was quantified by a creaming index: CI = 100 × H_S/H_E, where H_S is the height of the serum layer and H_E is the height of the emulsion. The texture of the mixed emulsions was determined by gently inverting the test tubes and observing their flow. The texture of each sample was characterized as low viscosity (LV), high viscosity (HV), or gelled (G).

3.2.6 Microstructure Analysis

The microstructure of the mixed emulsions was observed by confocal scanning fluorescence microscopy. In this set of experiments, the lipid droplets in the β-Lg

emulsions were dyed with Bodipy 493, while the protein phase in the LF emulsions was stained with Rhodamine B. For the β-Lg emulsions, Bodipy 493 dye (0.1 mg/mL) was added to corn oil, and this mixture was covered and stirred overnight to ensure the dye was completely dissolved in the oil. A 10% (w/w) corn oil emulsion stabilized by 0.5% β-Lg was then prepared with the dyed oil using the same procedure described previously. To avoiding fluorescence quenching, alumina foil was used to cover and protect the dyed solutions in all procedures. For the LF emulsions, Rhodamine B was dissolved in distilled water at a concentration of 0.05% (w/v). This solution was then added to a 3% filtered LF solution at a concentration of 5μl/gram and then a LF emulsion was prepared as described previously. Bodipy493 was excited with a 488 nm laser and detected at 515 nm. Rhodamine B was excited with a 543 nm laser and detected at 605 nm. The pinhole setting was small (35 mm), and the image was magnified by a factor of 4× using the digital zoom feature. All pictures were taken using a 10× eyepiece with a 60× objective lens (oil immersion).

3.2.7 Statistical Analysis

All experiments were carried out in either duplicate or triplicate using freshly prepared samples. Results are reported as the calculated means and standard deviations.

3.3 Results & Discussion

3.3.1 Formation of Protein-Coated Droplets

The purpose of the initial experiments was to characterize the properties of the two kinds of protein-coated lipid droplets used to assemble the microclusters. Our initial objective was to establish the optimum amount of protein emulsifier required to produce

stable 10 wt% oil-in-water emulsions with relatively small droplet sizes. We therefore measured the dependence of the mean droplet diameter on initial protein concentration for emulsions prepared by homogenizing oil and aqueous phases together using fixed homogenization conditions (**Figure 3.1**). For both protein types, there was initially a steep decrease in mean droplet diameter with increasing protein concentration followed by a leveling off at higher protein concentrations. The final mean droplet diameter was fairly similar for both b-lactoglobulin and lactoferrin: d_{32} = 0.14 mm. However, the initial decrease in mean droplet diameter with increasing protein concentration occurred more rapidly for b-lactoglobulin than for lactoferrin: 0.5% b-Lg was required to reach the region where the mean droplet diameter did not decrease further, while over 3% LF was required (**Figure 3.1**). These results suggest that the b-lactoglobulin molecules were able to coat the surfaces of the oil droplets within the homogenizer more rapidly than the lactoferrin molecules, thereby preventing re-coalescence more effectively [85-87]. At sufficiently high protein concentrations, there would be enough emulsifier present to cover all of the droplet surfaces formed and to prevent re-coalescence [88]. Under these conditions, the mean droplet diameter is governed mainly by the homogenizer, rather than by the emulsifier properties [85, 86]. This accounts for the observation that the mean particle diameter in the emulsions containing b-lactoglobulin and lactoferrin were fairly similar (d_{32} = 0.14 mm) at sufficiently high protein concentrations (**Figure 3.1**).

When there is insufficient protein present to cover all the droplet surfaces formed within the homogenizer, then the mean droplet diameter is determined mainly by the emulsifier properties, rather than by the homogenization conditions [88, 89]. Under

emulsifier-limiting conditions, the relationship between mean droplet diameter and emulsifier concentration is given by the following relationship [29]:

$$d_{32} = \frac{6\varphi\Gamma_S}{C_a} \tag{3.1}$$

For a fixed disperse phase volume fraction (f), this equation shows that the minimum mean droplet diameter (d_{32}) that can be produced decreases as the emulsifier concentration (C_a) increases, by an amount that depends on the surface load (G_S) of the emulsifier. The surface load is the mass of emulsifier adsorbed per unit surface area of oil-water interface, which is usually expressed in mg m^{-2} [90]. The molecular weight of lactoferrin (≈ 80 kg mol^{-1}) is considerably higher than that of b-lactoglobulin (≈18 kg mol^{-1}), and therefore one would expect LF would have a higher surface load. In other words, it would take a higher mass of LF molecules to completely cover the droplet surfaces than b-Lg. Indeed, it has been reported that the surface load of LF (3%) and b-Lg (1%) are around 4.5 and 1.5 mg m^{-2} at pH 7 [91-93]. Consequently, in the region where surfactant concentration is limiting, one would expect the droplets to be bigger for LF than for b-lg at the same total surfactant concentration (Equation 3.1).

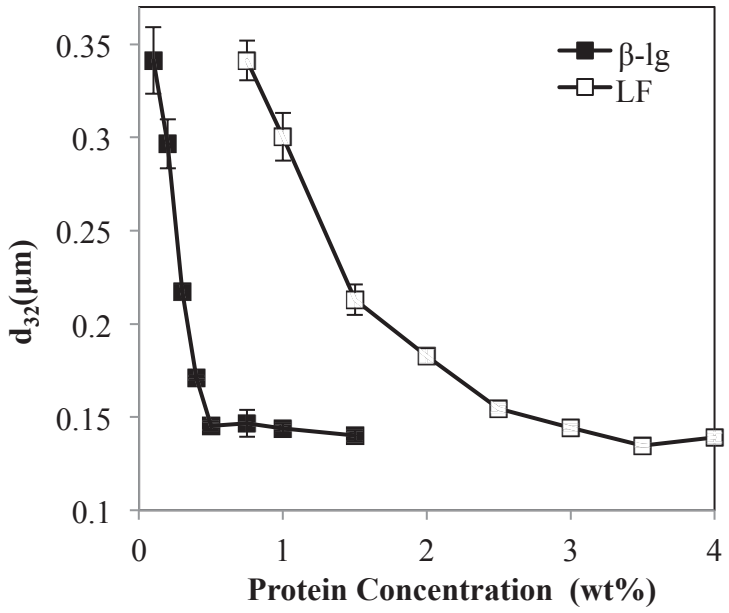

Figure 3.1 Dependence of mean particle diameter (d_{32}) on initial protein concentration (β-Lg or LF) in the aqueous phase of 10 wt% oil-in-water emulsions prepared by highpressure homogenization.

In the remainder of the study, we prepared single-protein emulsions using either 0.5% b-lg or 3% LF as the emulsifier so as to obtain relatively small droplet diameters that were similar for both systems, without having a lot of free emulsifier present in the surrounding aqueous phase. Any free protein in the aqueous phase could interact with protein adsorbed to the droplet surfaces through electrostatic interactions, *e.g.,* free LF could adsorb to b-lg-coated droplets or *vice versa*. In future studies, it would be useful to examine the role of any non-adsorbed protein on the properties of emulsions containing mixed proteins.

3.3.2 Properties of Protein-Coated Droplets in Single Emulsions

The purpose of these experiments was to characterize the influence of pH on the electrical characteristics and physical stability of the two types of single protein-coated lipid droplets. 10 wt% oil-in-water emulsions were prepared that were stabilized by

either b-lactoglobulin (0.5%) or lactoferrin (3%), and then their z-potentials, mean particle diameters, and creaming stabilities were measured as a function of pH.

For both emulsions, the droplet charge went from negative at high pH values to positive at low pH values, but the points of zero charge were different. The point of zero charge was around pH 5.1 for the β-Lg-coated droplets and around pH 8.6 for the LF-coated droplets (**Figure 3.2a**). These differences can be attributed to the differences in the isoelectric points (pI) of the two proteins: pI ≈ 5 for β-Lg; pI ≈ 8.5 for LF [91-93]. At the pI, the negative and positive charges on a protein counter-balance each other so their net charge is zero.

There were distinct differences in the stability of the oil droplets to aggregation when the pH was changed. For the β-Lg-coated droplets, there was evidence of considerable droplet aggregation in the emulsions around pH 4 to 6 (**Figure 3.2b**) and evidence of creaming, *i.e.,* separation of the emulsion into an optically opaque "cream" layer on the top and a clear "serum" layer at the bottom (data not shown). This kind of behavior has previously been attributed to the fact that this pH range is close to the pI of the adsorbed proteins so that the electrical charge on the droplets was not strong enough to generate an electrostatic repulsion that could overcome the attractive van der Waals interactions [94-97]. Interestingly, the LF-coated droplets were relatively stable to droplet aggregation (**Figure 3.2b**) and creaming (data not shown) across the entire pH range studied, even at pH values where their net charge was close to zero, *i.e.,* pH 8 and 9 (**Figure 3.2a**). There are a number of possible explanations for the observed difference between the pH stabilities of the droplets coated by the two different protein types. LF has a higher molecular weight than β-Lg, and therefore presumably forms thicker

interfacial layers that increase the range of the steric repulsion between the droplets, leading to improved stability [23]. In addition, LF is a glycoprotein that has sugar side groups that extend into the aqueous phase [98, 99], and therefore also increase the steric repulsion between the droplets. In addition, there may be other molecular differences between the proteins that impact the colloidal interactions in the system, such as their degree of unfolding after adsorption ("surface denaturation"), their surface hydrophobicity, or the distribution of charged groups on their surfaces. Recent work in our laboratory has shown that some droplet aggregation may occur in LF-stabilized emulsions when the aqueous phase contains a buffer rather than only distilled water, which may be due to ion binding effects [100, 101]. It is clear that further research is required to identify the molecular origin of the influence of pH and specific ions on the aggregation stability of LF-coated oil droplets.

(a)

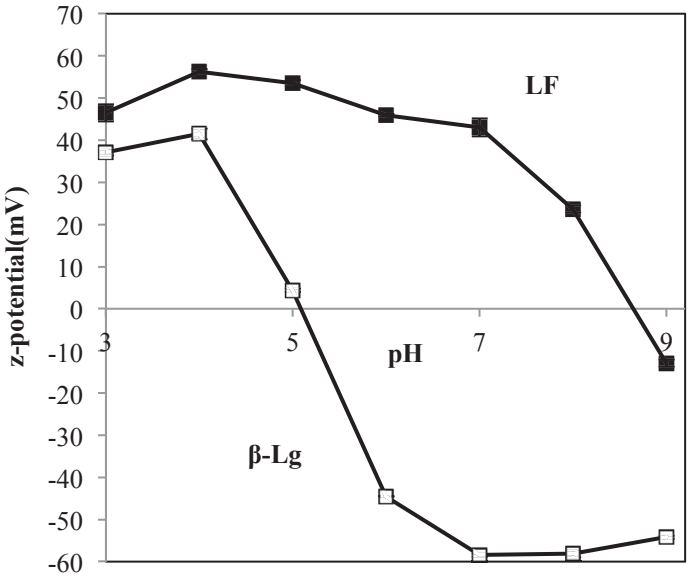

(b)

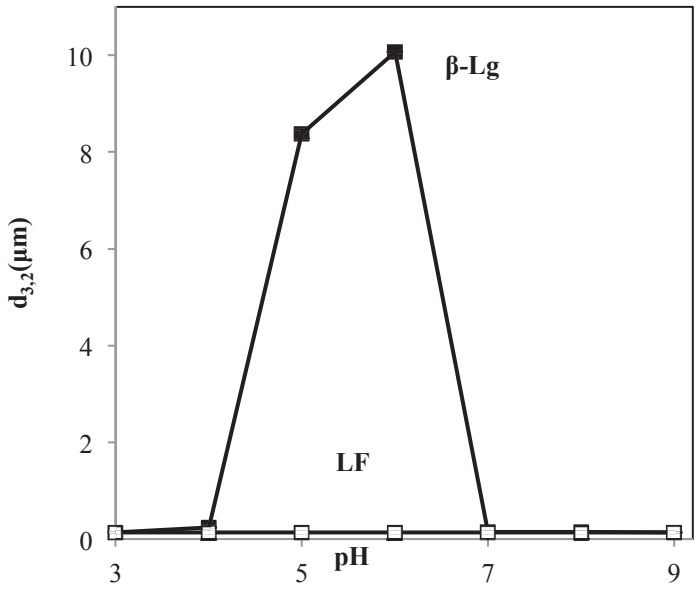

Figure 3.2 (a). Dependence of the droplet charge (z-potential) on pH for diluted 10 wt% oil-in-water emulsions initially stabilized by either 0.5% β-Lg or 3% LF. (b). Dependence of mean particle diameter (d_{32}) on pH for diluted 10 wt% oil-in-water emulsions initially stabilized by either 0.5% β-Lg or 3% LF.

3.3.3 Characteristics of Particles in Mixed Emulsions

The purpose of these experiments was to establish the conditions where clusters could be formed that consisted of mixtures of negative and positive droplets. This was achieved by mixing together different ratios of LF-coated oil droplets and b-Lg-coated oil droplets at various pH values and then measuring the z-potential, mean particle size, creaming stability, microstructure, and observed texture of the resulting mixed systems.

3.3.3.1 Electrical Characteristics

The z-potential of the mixed systems went from highly positive at low pH values to highly negative at high pH values, with the point of zero charge depending on the ratio of b-Lg-to-LF coated droplets in the system (**Figure 3.3**). As the ratio of b-Lg-to-LF coated droplets in the system increased, the point of zero charge decreased (**Figure 3.4**),

which is to be expected since b-Lg has a lower isoelectric point than LF. If one focuses on the z-potential data at a single pH value between the isoelectric points of the two proteins (*e.g.,* pH 6), then one can see that the electrical charge can be made to go from positive to negative by varying the ratio of the positive-to-negative droplets from 0 to 100% (**Figure 3.3**). Similar observations of charge reversal at a single pH value have recently been reported in colloidal dispersions containing mixtures of negative and positive surface-modified solid particles [82]. These results show that it is possible to create emulsions with a variety of different electrical characteristics by mixing together different ratios of charged droplets with different isoelectric points.

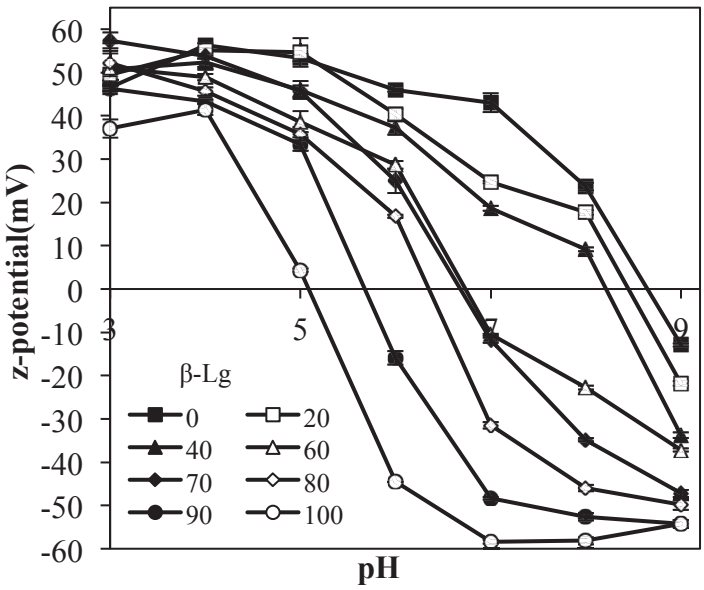

Figure 3.3 Dependence of the droplet charge (z-potential) on pH for diluted 10 wt% oil-inwater emulsions containing different mixtures of β-Lg-coated or LF-coated oil droplets.

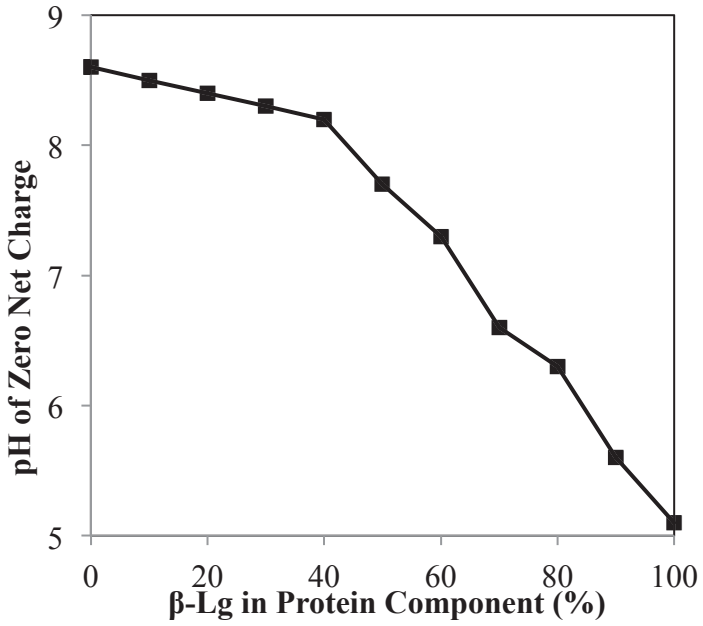

Figure 3.4 Dependence of the point of zero charge (pH where z-potential 1/4 0) on the percentage of β-Lg-coated droplets in mixed emulsions containing different ratios of β-Lg- and LF-coated droplets.

3.3.3.2 Particle Size

We also measured the particle size of the different mixed systems as a function of β-Lg-to-LF-coated droplet ratio and pH using static light scattering (**Figure 3.5**). The samples were diluted with pH-adjusted water prior to analysis to avoid multiple scattering effects, so any observed increases in particle size reflected the formation of aggregates held together by relatively strong attractive forces. In some samples, there may have been some dissociation of aggregates after dilution as indicated by apparent discrepancies between particle size measurements and textural analysis (discussed below).

The mean particle diameter (d32) was found to be highly dependent on particle ratio and pH (Figure 3.5). At low pH values (pH 3 and 4), the particles were relatively small (d32 < 0.22 mm) for all b-Lg-to-LF ratios, indicating that the majority of particles

did not form large clusters. The mean particle diameters of the individual droplets in the two emulsions were both around 0.14 mm, so there may have been some limited cluster formation in this pH region. The lack of more extensive droplet aggregation would be expected since both the b-Lg-coated and LF-coated droplets had a net positive charge in this pH range (Figure 3.2a) and therefore there would have been a strong electrostatic repulsion between them. At intermediate pH values (pH 6 to 8), the measured mean particle diameter was relatively high at most b-Lg-to-LF-coated droplet ratios, indicating that large aggregates were formed. In this pH range, the b-Lg-coated droplets would be negatively charged while the LF-coated oil droplets would be positively charged (Figure 3.2a), and hence the aggregates formed presumably consisted of a mixture of positively and negatively charged droplets held together by electrostatic attraction. Extensive droplet aggregation was also observed at pH 5 in most of the mixed systems even though both the b-Lg-coated and LF-coated droplets had a net positive charge. This phenomenon may be attributed to the fact that the b-Lg-coated droplets were highly aggregated at pH 5 before mixing with the LF-coated droplets because of the weak electrostatic repulsion between them (Figure 3.2b). There was also some droplet aggregation in the emulsions only containing b-Lg-coated droplets at pH 6.

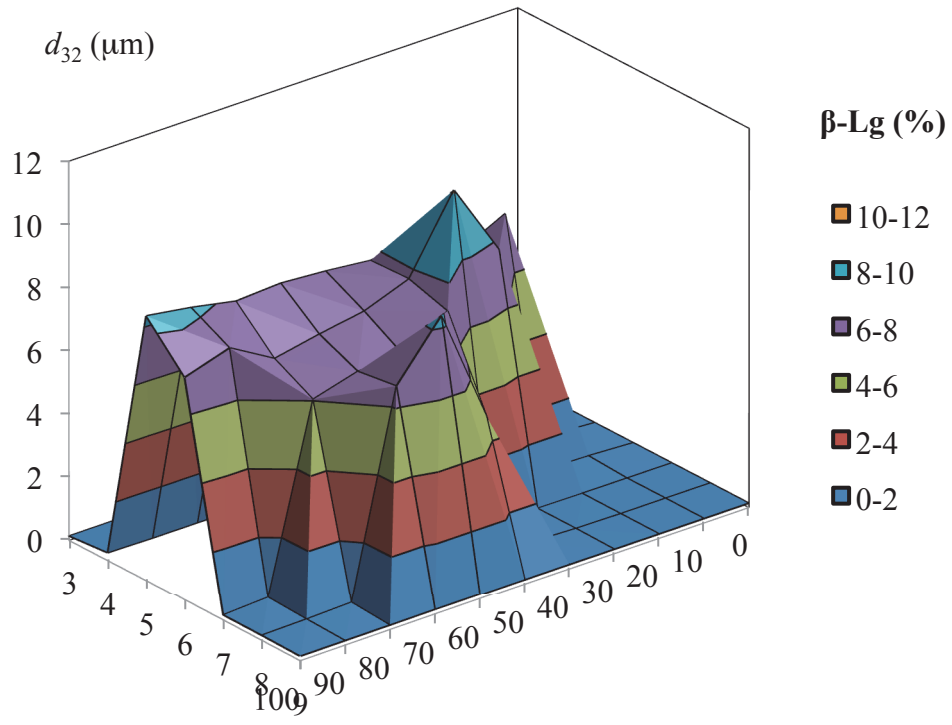

Figure 3.5 Three-dimensional representation of the dependence of mean particle diameter (d_{32}) on the pH and ratio of β-Lg-to-LF-coated oil droplets in mixed emulsions.

Consequently, individual positively charged LF-coated droplets may have interacted with these pre-formed negatively aggregates at this pH rather than with individual negatively charged b-Lg-coated droplets. At high pH values (pH 9), the particles were relatively small (d32 < 0.15 mm) for all b-Lg-to-LF-coated droplet ratios, indicating that microclusters were not formed. This behavior would be expected since both the b-Lg-coated and LF-coated oil droplets had a net negative charge at this pH and so there should be an electrostatic repulsion between them.

3.3.3.3 Macroscopic properties of mixed particle systems

We recorded the creaming stability and textural attributes of the mixed samples by visual observation (**Table 3.1**). Selected examples of photographs of the emulsions at different pH values are shown in **Figure 3.5**. Visual observation of the samples indicated

that some of them were stable to gravitational separation (*i.e.,* they had a uniform milky appearance throughout), whereas others were not (*i.e.,* an opaque cream layer formed at their top and a clear serum layer formed at their bottom). In addition, some of the emulsions were found to cling to the sides of the glass test tubes after they were inverted *e.g.,* the 60:40 and 70:30 β-Lg-to-LF samples at pH 7 (**Figure 3.6**). The samples where this phenomenon occurred tended to exhibit a high degree of droplet aggregation (**Figure 3.5**) and creaming (**Table 3.1**). An increase in the rate of gravitational separation in colloidal dispersions is usually attributed to an increase in particle size due to particle aggregation [29]. Indeed, those systems that were unstable to creaming (**Table 3.1**) also tended to contain large particles (**Figure 3.5**).

pH	**%Volume of *β*-Lg-coated droplets in Mixed Emulsions**										
	100	90	80	70	60	50	40	30	20	10	0
3	0, L	0,L	0,L	0,L	0,L	0,L	0,L	0,L	0,L	0,L	0,L
4	0, L	0,L	0,L	0,L	0,L	0,L	0,L	0,L	0,L	0,L	0,L
5	0,G	44,G	0,G	0,G	0,G	0,G	0,G	0,G	0,G	0,H	0,L
6	0,H	26,G	20,G	16,G	0,G	0,G	0,G	0,G	0,H	0,L	0,L
7	0, L	0,L	0,H	47,G	**22,G**	0,G	**0,H**	0,H	0,L	0,L	0,L
8	0, L	0,L	0,L	0,H	0,G	0,G	0,H	0,L	0,L	0,L	0,L
9	0, L	0,L	0,L	0,L	0,L	0,L	0,L	0,L	0,L	0,L	0,L

Table 3. 1 Influence of pH and mixing ratio on the perceived texture and creaming stability of mixed emulsions containing β-Lg-coated lipid droplets and LF-coated lipid droplets. The first number in each entry is the creaming index (%), while the second letter is the perceived texture: L= Low viscosity; H = High viscosity; G = Gelled. The emulsions that were stable to extensive droplet aggregation exhibited no creaming and had a low viscosity (0,L).

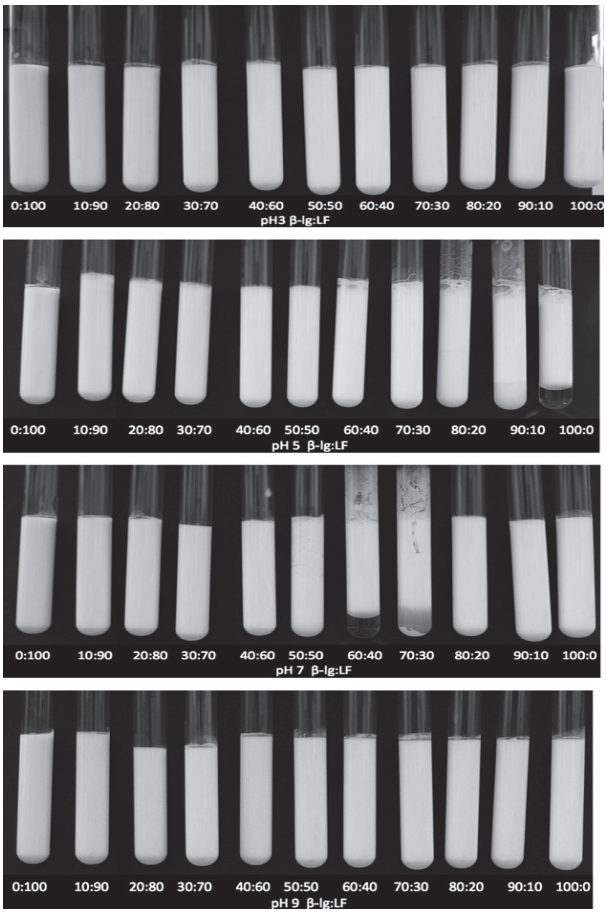

Figure 3.6 Appearance of 10 wt% oil-in-water emulsions containing different ratios of β-Lg-coated and LF-coated oil droplets at pH 3, 5, 7 and 9. Some samples were stable to gravitational separation, whereas others formed a creamed layer. Some samples had gel-like characteristics, whereas others had low or high viscosities.

There were also appreciable differences in the observed textural properties of the emulsions that could not be ascertained by simple visual observation of undisturbed samples (**Table 3.1**). When the test tubes containing the emulsions were inverted some of the samples had a low viscosity (LV) like milk, some of them had a high viscosity (HV) like thick cream, and some of them were gelled (G) like yogurt. Hence, some of the samples were stable to gravitational separation because they did not contain aggregated droplets (*e.g.,* all emulsions at pH 3, 4 and 9), whereas others were stable to creaming because the droplet aggregation was so extensive that a particle network was

formed that presumably inhibited droplet movement (*e.g.,* 40:60 β-Lg:LF emulsions at pH 7). Interestingly, the 40:60 β-Lg:LF emulsions (pH 7) had a relatively high viscosity (**Table 3.1**) indicating that droplet aggregation had occurred, but had a relatively small surface-weighted mean particle diameter (d_{32} < 300 nm) determined by light scattering (**Figure 3.5**). Nevertheless, the full particle size distribution indicated that there was a small population of aggregated particles (data not shown) and the volume-weighted mean particle diameter was relatively large (d_{43} > 3900 nm) indicating that some of the original particles had formed large clusters.

It was possible to prepare gel-like mixed-protein emulsions by mixing together two single-protein emulsions that were liquid. For example, at pH 7 both the pure β-Lg-emulsion and the pure LF-emulsion were fluid, whereas the 50:50 β-Lg:LF emulsion was gel-like. This phenomenon can be attributed to the formation of a particle network of oppositely charged droplets that are strongly attracted to each other. Indeed, recent computer simulations and experiments with colloidal suspensions containing oppositely charged particles have shown that percolating networks of aggregated particles can be formed at certain particle ratios [83, 84], which will determine the rheological properties and stability to gravitational separation of the overall system.

Previous studies have shown that particle gels can be formed by inducing droplet aggregation in emulsions containing protein-coated lipid droplets [87, 94, 102]. Typically, gelation was initiated in these systems by reducing the electrostatic repulsion between similarly charged lipid droplets, *e.g.,* by adding salt or adjusting the pH near to the adsorbed protein's isoelectric point. The main driving force for droplet aggregation in these systems was van der Waals attraction and possibly some hydrophobic attraction.

One would expect a gel formed by inducing strong electrostatic attraction between oppositely charged droplets to have different structural and physicochemical characteristics than a gel formed by screening strong electrostatic repulsion between similarly charged droplets. In future studies, it would be useful to use a combination of microstructural and rheological techniques to systematically examine the differences between these two kinds of particle gel systems. Practically, the formation of mixed particle gels by hetero-aggregation may prove to be a useful method of creating novel textural characteristics in foods.

3.3.3.4 Microstructures of Mixed Particle Systems

Confocal fluorescent microscopy images of selected emulsions indicated that different kinds of microstructures were formed depending on pH and β-Lg-to-LF ratio. For example, images of two mixed emulsions with different β-Lg-to-LF ratios at pH 7 are shown in **Figure 3.7**: 60:40 and 40:60 β-Lg:LF. In this case, the emulsions were mixed together by placing them in test tubes that were stired for 10 min. There was an even distribution of small droplets throughout the mixed emulsion with β-Lg:LF = 40:60, but there was evidence of large clusters containing numerous droplets in the mixed emulsion with β-Lg:LF = 60:40. These differences in microstructure had a major impact on the stability and rheological characteristics of the samples (**Table 3.1**). The mixed emulsion with β-Lg:LF = 40:60 had a high viscosity, was stable to creaming and had an even distribution of droplets (**Figure 3.7**), presumably because a uniform particle network formed throughout the entire sample. On the other hand, the mixed emulsion with β-Lg:LF = 60:40 was gelled and showed visible phase separation, suggesting that the formation of large clusters of droplets led to some compaction of the gel network and

macroscopic phase separation. It should be noted that we could not distinguish the individual LF-coated droplets (stained with Rhodamine B) from the individual β-Lg-coated droplets (dyed with Bodipy 493) in the confocal images, which can be attributed to the fact that the individual droplets were too small (< 200 nm) to resolve by optical microscopy.

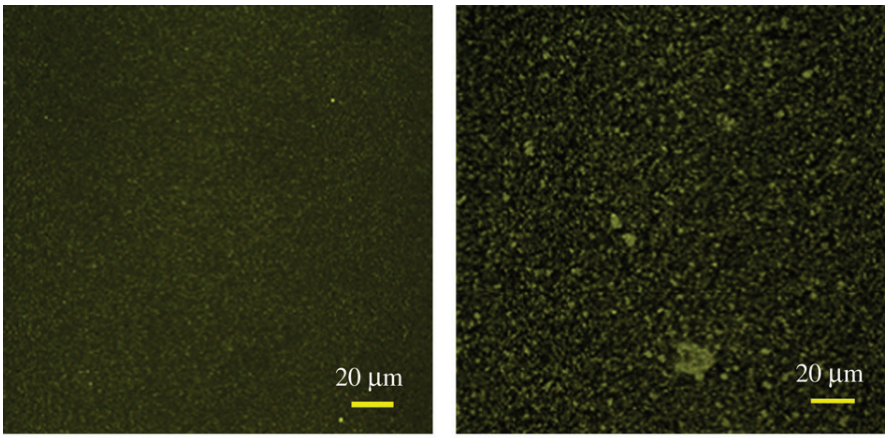

Figure 3.7 Microstructure of 10 wt% oil-in-water emulsions (pH 7) containing different ratios of β-Lg-coated and LF-coated oil droplets. At β-Lg:LF 1/4 40:60, a homogenous microstructure is observed and the sample had a low viscosity and exhibited no creaming. At β-Lg:LF 1/4 60:40, some aggregation is observed in the images and the sample had gel-like characteristics. Mixed samples were prepared by vortexing. The images represent an area of 210 by 210 mm.

Finally, we examined the impact of applying intense high shear stresses to the mixed emulsions on their microstructures by blending them with a high speed mixer. After blending, both emulsions (60:40 and 40:60 β-Lg:LF) showed evidence of extensive droplet coalescence (**Figure 3.8**), since much larger individual droplets were observed in the images than were present in the original emulsions (**Figure 3.7**). Presumably, the adsorbed protein layers surrounding the oil droplets were ripped or torn from the droplet surfaces when the applied shearing forces pulled oppositely charged droplets apart. This

phenomenon may have important practical implications, since it suggests that the emulsions are susceptible to droplet coalescence when sheared.

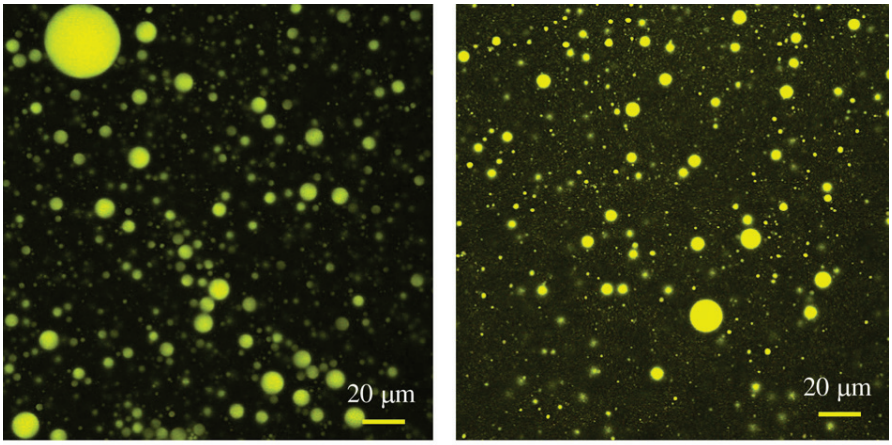

Figure 3.8 Microstructure of 10 wt% oil-in-water emulsions (pH 7) containing different ratios of β-Lg-coated and LF-coated oil droplets. Mixed samples were prepared by high shear mixing. At both β-Lg:LF 1/4 40:60 and 60:40, some droplet coalescence is observed in the images (compare with Fig. 3.7). The images represent an area of 210 by 210 mm

3.4 Conclusions

This study suggests that the rheology and stability of colloidal dispersions consisting of mixtures of negatively and positively charged protein-coated oil droplets can be modulated by varying the ratios of the two types of droplets. The electrical charges on the protein-coated droplets can be made to have opposite signs by altering the pH to values between the isoelectric points of the two emulsions *i.e.,* $pI_{b\text{-}Lg} < pH < pI_{LF}$. Systems that range from low viscosity liquids to gels can be formed at appropriate negative-to-positive droplet ratios. In addition, it may be possible to form microclusters with controlled properties (size and charge) under certain conditions. The utilization of hetero-aggregation to form mixed systems from positive and negative oil droplets may be useful for designing products with desirable or novel functional attributes.

Alternative strategies for creating novel structural and functional properties in food emulsions based on mixtures of oppositely charged proteins also exist. For example, it may be possible to (i) mix positive and negative proteins together prior to homogenization; (ii) add different levels of positive and/or negative proteins to the aqueous phase of an emulsion after formation; (iii) form multiple layers of positive and negative proteins around oil droplets using layer-by-layer electrostatic deposition. These alternative strategies would be interesting areas of future research.

CHAPTER 4

FABRICATION OF FUNCTIONAL MICROCLUSTERS BY HETERO-AGGREGATION OF OPPOSITELY CHARGED PROTEIN-COATED LIPID DROPLETS

4.1 Introduction

Structural design principles can be used to create materials with novel or improved functional attributes, *e.g.,* optical properties, rheology, stability, release characteristics, or biological activity [68-72]. The structural design approach utilizes knowledge of building blocks (*e.g.,* solvents, surfactants, polymers, oils, and minerals), forces (*e.g.,* molecular and colloidal interactions), and construction principles (*e.g.,* self-assembly, directed-assembly, and phase disruption) to create specific structures within materials that are known to lead to desirable functional attributes [73, 103].

A particularly promising approach to creating novel functional materials is to use colloidal particles as building blocks to assemble well-defined nano-scale or microscale structures [9, 103, 104]. Experimental and theoretical studies have shown that a variety of structures can be formed using two or more different types of colloidal particles as building blocks [10, 11, 27, 78-81] . Materials with different structures, physicochemical properties, and functional attributes can be prepared by controlling the characteristics of the colloidal particles (*e.g.,* size, charge, shape, concentration), the environmental conditions (*e.g.* pH, ionic strength, temperature), and the preparation method (*e.g.,* order of addition, mixing conditions).

In this study, we focused on the formation of functional microclusters by controlled hetero-aggregation of oppositely charged particles. In particular, we aimed to

assemble these microclusters entirely from food-grade ingredients (*i.e.,* lipids and proteins) so that they would be suitable for oral ingestion in foods and pharmaceutical products. We hypothesized that microclusters with different functional attributes could be produced by controlling the properties of the initial charged particles and the environmental conditions.

Recently, we studied the influence of hetero-aggregation on the stability and rheology of relatively concentrated (10 wt%) oil-in-water emulsions [105]. These systems were prepared by mixing an emulsion containing β-lactoglobulin-coated lipid droplets with an emulsion containing lactoferrin-coated lipid droplets. These two globular proteins have different electrical charge *versus* pH profiles because of their different isoelectric points: β-lactoglobulin (β-Lg), pI ≈ 5; lactoferrin (LF) pI ≈ 8. We showed that extensive droplet flocculation occurred over a pH range where the two types of lipid droplets had opposite charges, *i.e.,* $pI_{\beta\text{-Lg}} < pH < pI_{LF}$. Droplet flocculation led to creaming instability and/or system gelation. A similar system was used in the current study, except that much more dilute (0.1 wt%) oil-in-water emulsions were used. The utilization of dilute emulsions facilitates our understanding of the nature of the microclusters formed due to hetero-aggregation of oppositely charged protein-coated droplets. In addition, the influence of ionic strength was investigated in this study, so as to elucidate the impact of electrostatic interactions on the formation and properties of microclusters. Finally, we used a recently development mathematical model[25] to interpret microcluster formation in terms of total particle concentration, particle type ratio, and the strength of the attractive interactions between the particles. The knowledge

gained from this study will be useful for the rational design of functional microclusters for utilization in commercial products.

4.2 Experimental Methods

4.2.1 Materials

Corn oil was purchased from a commercial food supplier (Mazola, ACH Food Companies, Inc., Memphis, TN) and stored at 4 °C until use. Lactoferrin powder (LOT #10408282) was supplied by DMV International (Delhi, NY), and the manufacturer reported that it contained 97.7% protein and 0.12% ash. Purified β-lactoglobulin powder (BioPURE, LOT #JE-002-8-415) was supplied by Davisco Foods International (Eden Prairie, MN). The manufacturer reported the composition of this powder to be 97.4% total protein, 92.5% β-lactoglobulin (β-Lg), and 2.4% Ash. Monobasic phosphate and dibasic phosphate were purchased from Sigma-Aldrich (Sigma Chemical Co., St. Louis, MO) or Fisher Scientific (Pittsburgh, PA). All solvents and reagents were of analytical grade. For confocal microscopy work, a non-polar fluorescent dye (Bodipy 493/503) was purchased from Invitrogen (Carlsbad, CA) and a protein fluorescent dye (Rhodamine B) was purchased from Sigma-Aldrich (St Louis, MO). All other chemicals used in this research were purchased from Sigma-Aldrich (St Louis, MO). Double distilled water was used to make all solutions.

4.2.2 Formation of Single-protein Emulsions

Aqueous emulsifier solutions were prepared by dispersing either β-Lg powder or LF powder into double distilled water, and then stirring for at least 3 h at room temperature to ensure complete dispersion. The pH of the protein solutions was then

adjusted to 7.0 using 1M NaOH or 1M HCl. Oil-in-water emulsions containing a single protein type were prepared by blending 10 g of corn oil and 100 g of aqueous protein solution for 2 min using a hand blender (M133/1281-0, 2 speed, Biospec Products Inc., ESGC, Switzerland) and then recirculating them four-times through a two-stage homogenizer (LAB 1000, APV-Gaulin, Wilmington, MA) at a first-stage pressure of 5,400 psi and a second-stage pressure of 600 psi. The β-Lg emulsion was then heated to 90 ℃ for 30 min to cross-link the adsorbed proteins, so as to prevent any competitive adsorption effects. All emulsions were then stored for 24 hours prior to utilization. Preliminary experiments established that 0.5% β-Lg and 3% LF were suitable levels to form single-protein emulsions with relatively small droplet diameters ($d \approx 0.14$ μm), and so these levels were used to form the mixed-protein emulsions.

4.2.3 Formation of Mixed-protein Emulsions

Initially, two 10 wt% oil-in-water emulsions stabilized by either 0.5% β-Lg or 3% LF were prepared in distilled water. These two single-protein emulsions had similar initial droplet diameters ($d \approx 0.14$ μm). These emulsions were then diluted to 1 wt % oil using distilled water, and the pH was adjusted to 7.0 using either 1M NaOH or 1M HCl. Mixed emulsions containing 0.0-0.1 wt% β-Lg droplets (pH 7.0) and 0.1–0.0 wt% LF droplets (pH 7.0) were prepared by mixing different ratios of the two emulsions together, stirring for 10 min, then allowing them to stand for 24 h prior to analysis. After this time, some of the emulsions separated into a thin white creamed layer on top of a clear or slightly turbid serum layer, and so all samples were gently stirred prior to analysis to ensure they were homogeneous.

4.2.4 Influence of Ionic Strength on Emulsion Stability

A 0.2% oil-in-water emulsion containing mixed protein-coated lipid droplets was formed by mixing different mass ratios (0 to100%) of 0.2% oil-in-water emulsions containing either β-Lg-coated droplets or LF-coated droplets. A series of systems with different salt concentrations was prepared by mixing 50 mL aliquots of these mixed emulsions with 50 ml aliquots of various sodium chloride solutions (0, 50, 100, 200, 400, and 800 mM) at pH7.0. The final emulsions contained 0.1% oil and 0 to 400 mM NaCl.

4.2.4.1 Particle Charge Measurements

The ζ-potential of emulsions was determined using a particle electrophoresis instrument (Zetasizer Nano ZS series, Malvern Instruments, Worcestershire, UK). The ζ-potential is determined by measuring the direction and velocity of droplet movement in a well-defined electric field. Mixed emulsions were diluted to a droplet concentration of approximately 0.001 wt% using pH-adjusted water to avoid multiple scattering effects. The pH of the water used was adjusted to the same pH as the initial emulsion sample. After loading the samples into the instrument they were equilibrated for about 120 s before particle charge data was collected over 20 continuous readings. In mixed systems, the signal detected by the instrument is primarily from the particles that scatter light most strongly. In our experiments, emulsion droplets and clusters would be expected to scatter light much more efficiently than non-adsorbed protein molecules, and should therefore dominate the overall signal.

4.2.4.2 Particle Size Analysis

The particle size distribution of the emulsions was measured using a laser diffraction particle size analyzer (Mastersizer 2000, Malvern Instruments, Ltd.,

Worcestershire, UK). This instrument measures the angular dependence of the intensity of light (λ = 632.8 nm) scattered from a stirred diluted emulsion. The particle size distribution is then calculated using Mie theory to obtain an optimal analysis of this light energy distribution. To avoid multiple scattering effects the emulsions were diluted to a droplet concentration of approximately 0.005 wt% using pH-adjusted water at the same pH as the sample. The emulsions were stirred continuously throughout the measurements to ensure the samples were homogenous. Measurements are reported as the volume-length mean diameter: $d_{4,3}=\sum d_i n_i^4/\sum d_i n_i^3$, where n_i is the number of droplets of diameter d_i. It should be noted that particle size measurements made by static light scattering on highly flocculated emulsions should be treated with caution. First, the theory (Mie theory) used to interpret light scattering data assumes that the scattering particles are homogeneous spheres with well-defined refractive indices. In practice, microclusters are non-spherical and non-homogeneous particles, with ill-defined refractive indices. Second, the process of dilution and stirring may have altered the dimensions and structural organization of the microclusters. Consequently, the reported particle sizes should only be treated as a rough estimate of particle dimensions rather than accurate values.

4.2.4.3 Microstructure Analysis

The microstructure of the mixed emulsions was observed by confocal scanning fluorescence microscopy. In this set of experiments, the protein phase in the β-Lg emulsions was stained with Rhodamine B, while the lipid droplets in the LF emulsions were dyed with Bodipy 493. For the β-Lg emulsions, Rhodamine B was dissolved in distilled water at a concentration of 0.05% (w/v) [33]. This dye solution was then added

to a β-Lg emulsion at a level of 5µl/gram protein. For the LF emulsions, Bodipy 493 dye (0.1 mg/mL) was added to corn oil, and this mixture was covered and stirred overnight to ensure the dye was completely dissolved in the oil. A 0.1 wt% corn oil emulsion stabilized by LF was then prepared with the dyed oil using the same procedure as described previously. To avoiding fluorescence quenching, alumina foil was used to cover and protect the dyed solutions in all procedures. Bodipy493 was excited with a 488 nm laser and detected at 515 nm. Rhodamine B was excited with a 543 nm laser and detected at 605 nm. The pinhole setting was small (35 mm), and the image was magnified by digital zoom feature. All pictures were taken using a 10× eyepiece with a 60× objective lens (oil immersion).

The microstructure of selected samples was also analyzed using Transmission Electron Microscopy (TEM). Mixed emulsion samples were diluted 1:10 with distilled water. Diluted samples were applied to glow-discharge treated carbon films on grids for 30 s to enable particle adsorption to the grid surfaces. The remaining liquid was then drained from the grid and a drop of 2% aqueous uranyl acetate solution (pH 4) was added for 15 s to stain them. This solution was removed from the grid by touching it with filter paper, and then the grid was allowed to air dry. Grids were imaged on a transmission electron microscope (JEOL JEM-100S) with a SIA 7C digital camera (Vitaly Feingold 2773 Heath Lane,Duluth GA, 30096). It should be noted that the sample preparation procedure required for TEM may cause some change in the structure of the microclusters formed. However, all samples were prepared in the same way and therefore we were able to compare TEM images on different treatments under similar conditions.

4.2.5 Statistical Analysis

All experiments were carried out in either duplicate or triplicate using freshly prepared samples. Results are reported as the calculated means and standard deviations.

4.3 Theory of Cluster Formation

In this section, a brief description of a simple theoretical approach to describe cluster formation in colloidal dispersions containing a mixture of two different kinds of particles that are attracted to each other is given.

4.3.1 Statistical Model of Cluster Formation

A statistical thermodynamic approach has recently been used to model the formation of clusters in colloidal suspensions containing a mixture of two types of equal-sized particles (A and B) due to hetero-aggregation[25]. This theory relates the average cluster size (*i.e.,* the number of particles per cluster) to the overall particle concentration, the ratio of the two types of particles, and the strength of the attraction between different particle types. It is assumed that the interactions between similar particle types (*i.e.,* A-A or B-B) can be described by a hard shell model, while the interactions between different particle types (*i.e.,* A-B) can be described by a "sticky" hard shell model. The details of this approach are given in the paper by Dickinson [25], and so we only provide the final equations here. The cluster size (S) is given by the following equation:

$$S = \frac{\left[x_A(1+\phi_B\lambda_{AB})^2 + x_B(1+\phi_A\lambda_{AB})^2\right]}{\left[1-\phi_A\phi_B\lambda_{AB}^2\right]^2} \tag{4.1}$$

Here, x_A and x_B are the mole fractions of type A and type B particles, ϕ_A and ϕ_B are the volume fractions, and λ_{AB} is the interaction coefficient:

$$\lambda_{AB} = \frac{K_1}{\tau_{AB} + K_2} \tag{4.2}$$

Where:

$$K_1 = \frac{1}{(1-\phi)} + \frac{3\phi}{2(1-\phi)^2} \qquad K_2 = \frac{\phi}{2(1-\phi)}$$

Here ϕ is the total volume fraction of particles present ($\phi_A + \phi_B$), and $1/\tau_{AB}$ provides a measure of the "stickiness" of the attractive interaction between the different particle types: the larger $1/\tau_{AB}$, the stronger the attraction between different particle types. For a sticky hard shell system, the stickiness parameter can be calculated from the colloidal interaction potential (U_{AB}) between the particles:

$$\frac{1}{\tau_{AB}} = \frac{12}{d^3}\int_d^\infty x^2 \left\{ \exp\left[\frac{U_{AB}(x)}{kT}\right] - 1 \right\} dx \tag{4.3}$$

Here, d is the particle diameter, x is the center-to-center particle separation, k is Boltzman's constant, and T is the absolute temperature. A convenient form for the attractive interaction potential is the Yukawa model [25]:

$$U_{AB}(x) = -\varepsilon \frac{d}{x} \exp\left(\kappa\left[1 - \frac{x}{d}\right]\right) \tag{4.4}$$

Where ε is a measure of the magnitude of the attraction and $1/\kappa$ is a measure of the range of the interaction. The Yukawa potential has proven to be a useful means of calculating the stickiness parameter in terms of the interactions between colloidal particles [25]. It should be noted that the above model is based on the assumption that the system is in thermodynamic equilibrium, but in practice there will be kinetic energy barriers that lead to the formation of metastable structures. A more sophisticated

theoretical approach is required to more accurately model this kind of behavior, such as those based on computer simulations[10, 24, 27]. Even so, the qualitative predictions made using the above model should still provide some useful insights into the main factors that impact cluster formation.

4.3.2 Colloidal Interactions - DLVO Theory

One limitation of the Yukawa potential is that it does not take into account specific colloidal interactions, such as van der Waals or electrostatic interactions, which means that it is difficult to directly account for factors that modulate these interactions, such as pH or ionic strength. To a first approximation, the colloidal interactions between a pair of spherical particles can be described using the DLVO theory [23, 24]:

$$U(h) = U_V(h) + U_E(h) \tag{4.5}$$

where $U(h)$, $U_V(h)$, and $U_E(h)$ are the overall, van der Waals, and electrostatic interaction potentials at a surface-to-surface separation of h. Expressions for the interactions between two spherical particles of similar size but different charge are available in the literature[23, 24]:

$$U_V(h) = -\frac{Ar}{12h} \tag{4.6}$$

$$U_E(h) = \frac{\pi\varepsilon_0\varepsilon_R r}{2}\left(\psi_A^2 + \psi_B^2\right)\times\left[\frac{2\psi_1\psi_2}{\psi_A^2 + \psi_B^2}\ln\left(\frac{1+e^{-\kappa' h}}{1-e^{-\kappa' h}}\right) + \ln(1-e^{-2\kappa' h})\right] \tag{4.7}$$

where r is the droplet radius, A is the Hamaker function, ϵ_0 is the permittivity of free space, ϵ_R is the relative dielectric constant of the aqueous phase, Ψ is the surface potential of the particles (in V), and $1/\kappa'$ is the Debye screening length (m), and the subscripts A and B refer to the two different kinds of droplets. The surface-to-surface

separation can easily be related to the center-to-center separation: $h = x - d$. For aqueous solutions at room temperatures, $1/\kappa' \approx 0.304/\sqrt{I}$ nm, where I is the ionic strength expressed in moles per liter. The van der Waals attraction is always attractive, but the electrostatic may be attractive or repulsive depending on the relative signs of the two droplet charges: opposite (attractive); similar (repulsive).

It should be highlighted that this is a very simple model that ignores many factors that will be important in reality: the presence of an adsorbed layer; retardation of van der Waals interactions; depletion interactions; hydrophobic interactions; multiple particle effects. Nevertheless, this model does provide some useful qualitative insights into the influence of particle charge and ionic strength on the attractive and repulsive interactions in mixed emulsions.

Initially, we attempted to use the DLVO interaction potential (Equation 4.5) to calculate the stickiness parameter using Equation 4.3, but found that we could not obtain physically realistic results, which was attributed to the fact that the van der Waals interaction tends to infinity at close separations. For this reason, we calculated the interaction potentials using the DLVO theory for systems with different ionic strengths, and then found the values of ε and κ that gave the best fit of these potentials to the Yukawa theory. To do this we calculated the value of the DLVO potential at a separation of 1 nm and used this as the magnitude of the attractive potential (ε) in the Yukawa potential. A separation of 1 nm was used since this is approximately equal to the dimensions of a globular protein adsorbed to an oil-water interface. We then found the value of the κ parameter that gave the best fit between the DLVO and Yukawa potentials. The resulting ε and κ values were then used to calculate the stickiness

parameter in Equation 3 from the Yukawa potential. An example of this approach is provided in a later section.

4.4 Results & Discussion

4.4.1 Particle Characteristics in Mixed Emulsions

Our initial objective was to establish the influence of particle ratio on the formation of microclusters in emulsions containing mixtures of negative and positive lipid droplets. This was achieved by mixing together different mass ratios of 0.1 wt% LF-coated oil droplets and 0.1 wt% β-Lg-coated oil droplets at pH 7.0 (where the two droplets have opposite charges) and then measuring the ζ-potential, mean particle size, and microstructure of the resulting systems.

The droplets stabilized by only β-Lg were highly negatively charged (≈ - 64 mV), while those stabilized by only LF were highly positively charged (≈ + 32 mV). The droplets in the two emulsions have opposite charges because pH 7 is between the isoelectric point of β-Lg (pI ≈ 5) and LF (pI ≈ 8). The ζ-potential of the mixed systems went from highly negative to highly positive as the fraction of LF-coated droplets increased, with the point of zero charge being around 70% LF (**Figure 4.1**). The fact that the point of zero charge was appreciably > 50% is probably because there was a higher charge magnitude on the negative β-Lg-coated droplets than on the positive LF-coated droplets, and so a greater number of the positive droplets were required to reach charge neutralization. Similar observations of charge reversal at a single pH value have recently been reported in colloidal dispersions containing mixtures of negative and positive surface-modified solid particles [82]. Our results show that it is possible to

create microclusters with a variety of different electrical characteristics by mixing together different ratios of charged droplets with different isoelectric points.

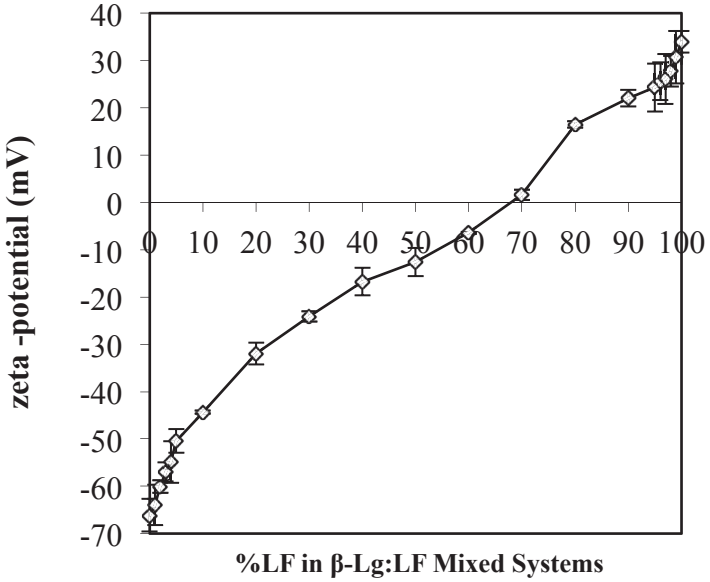

Figure 4.1 Dependence of the droplet charge (ζ-potential) at pH 7.0 on particle ratio for 0.1 wt% oil-in-water emulsions containing different mass ratios of β-Lg-coated or LF-coated oil droplets.

We also measured the mean particle diameter (d_{43}) of the mixed systems as a function of particle ratio using static light scattering (**Figure 4.2a**). The mean particle diameters of emulsions containing only LF-coated droplets ($d_{43} \approx 0.14$ μm) or only β-Lg-coated droplets ($d_{43} \approx 0.14$ μm) were relatively small, indicating that they were stable to droplet aggregation. It was possible to discern three major regimes as the percentage of LF-coated droplets in the system increased: (i) from 0 to 30% LF - d_{43} was relatively small ($d < 500$ nm); (ii) from 30 to 70% LF - d_{43} was relatively large ($d > 1000$ nm); (iii) from 70 to 100% LF - d_{43} was relatively small (< 500 nm). The particle size distribution measurements indicated that the mixed emulsions contained a single broad peak at low and high LF concentrations (Regimes (i) and (iii)), with the majority of particles being <

1000 nm in diameter (**Figure 4.2b**). On the other hand, at intermediate LF concentrations (Regime (ii)) there was evidence of many particles with diameters > 1000 nm, particularly at 40% LF. This result suggests that extensive droplet aggregation occurred at intermediate particle ratios, but that only relatively small microclusters were formed at relatively low and high particle ratios. We postulate that the major driving force for droplet aggregation is electrostatic attraction between oppositely charged protein-coated lipid droplets. Calculations of the strength of the colloidal interactions between the two types of emulsion droplets using Equations 1 to 3 indicate that there was a strong net attraction that would be expected to promote aggregation (see later section).

The sizes of the microclusters formed in this work are in good agreement with recent computer simulations of the aggregates resulting from interactions of oppositely charged particles [24]. At low and high particle ratios, relatively small clusters containing both positively and negatively charged particles are formed, and there are many free individual particles of the charge type that dominates. At intermediate particle ratios, relatively large clusters are formed, and there are few free individual particles.

One would expect that a change in the size of the particles in a dilute colloidal dispersion would influence its stability to gravitational separation. We therefore measured the creaming stability of mixed emulsions containing different ratios of LF-coated droplets to β-Lg-coated droplets. At relatively low (< 30% LF) and high (>70% LF) particle ratios the emulsions were relatively stable to creaming after 24 hours storage at ambient temperature. On the other hand, at intermediate (30% < LF < 70%) particle ratios the emulsions were highly unstable to creaming, with a thin layer of droplets forming on top of a transparent aqueous phase (**Figure 4.2c**). The formation of

microclusters at intermediate particle ratios can clearly been seen in TEM images of samples containing 0%, 40% or 100% LF-coated lipid droplets (**Figure 4.2d**). It is interesting to note that the individual droplets within the microclusters in the 40% LF: 60% β-Lg system appeared to be appreciably larger than in the individual droplets in the emulsions containing only LF-coated droplets or β-Lg-coated droplets. We postulate that some droplet coalescence may have occurred within the microclusters because of the strong attraction between the oppositely charged droplets. Enhance coalescence of protein-coated lipid droplets within highly flocculated systems has been reported previously.[106, 107].

(a)

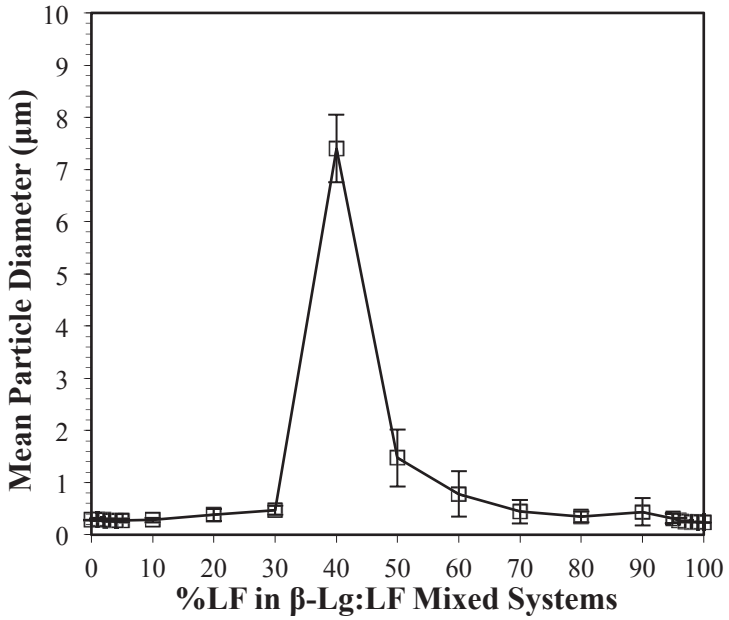

(b)

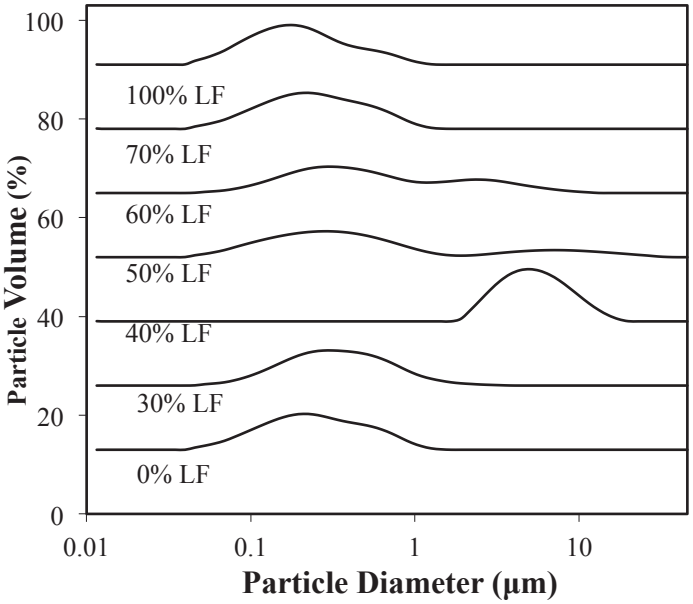

(c)

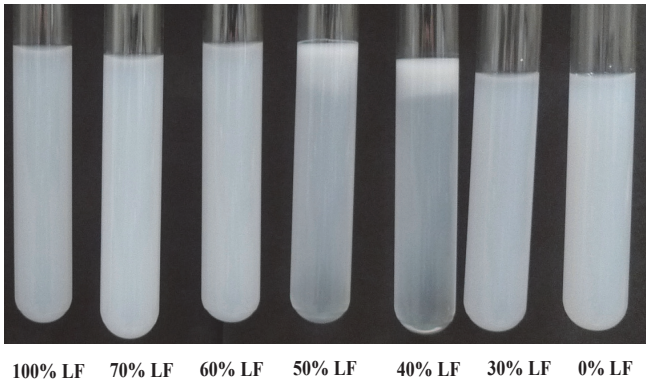

(d)

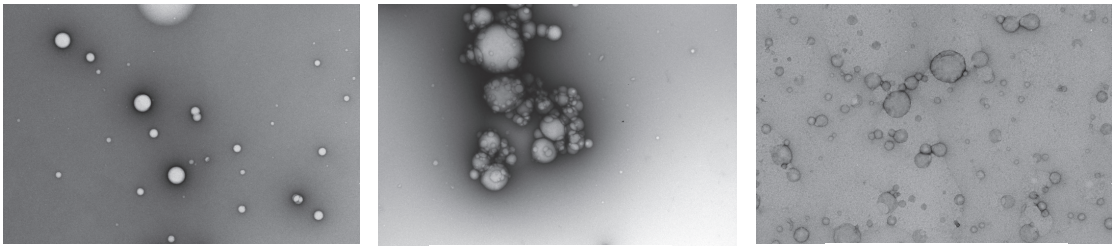

Figure 4.2 (a) Dependence of mean particle diameter (d_{43}) at pH 7.0 on particle ratio for 0.1 wt% oil-in-water emulsions containing different mass ratios of b-Lg-coated

or LF-coated oil droplets. (b) Particle size distributions of 0.1 wt% oil-in-water emulsions containing different mass ratios of b-Lg-coated or LF-coated oil droplets (pH 7). (c) Creaming stability of emulsions containing different mass ratios of LF- and β-Lg-coated lipid droplets after 24 hour storage at ambient temperature. (d) TEM images of emulsions containing different mass ratios of LF- and β-Lg -coated lipid droplets after 24 hour storage at ambient temperature (pH 7, 0 mM NaCl). The scale bars (bottom right corner of each image) represent 200 nm. Each image shown represents an area of approximately 2830 nm long and 1880 nm high.

4.4.2 Influence of Ionic Strength on Cluster Formation

The major force holding together oppositely charged particles in microclusters is postulated to be electrostatic attraction. Consequently, we examined the influence of the presence of salt on microcluster formation and characteristics, since increasing the ionic strength is known to reduce the magnitude and range of electrostatic interactions [29, 108]. Practically, knowledge of the influence of ionic strength on the properties of microclusters is important because many commercial products contain appreciably levels of salt.

The ζ-potential of the β-Lg-coated droplets gradually decreased as the salt concentration was increased (**Figure 4.3**), which can be attributed to electrostatic screening effects, *i.e.,* the accumulation of counter-ions (Na^+) in the vicinity of the lipid droplet surfaces [29, 94, 109]. Interestingly, the ζ-potential on the LF-coated droplets decreased steeply as the salt concentration increased, so that the electrical charge was already close to zero at 25 mM NaCl (**Figure 4.3**). This effect is larger than would be expected from simple electrostatic screening effects, which suggests that there may have been some strong binding of anionic counter-ions (*e.g.,* Cl^-) to cationic patches on the LF-coated lipid droplets. The charge on the microclusters in the mixed emulsion (40% LF: 60% β-Lg) remained close to zero across the entire range of salt concentrations

studied. We also measured the electrical characteristics of mixed emulsions containing either an excess of cationic lactoferrin (96% LF: 4% β-Lg) or an excess of anionic β-lactoglobulin (4% LF: 96% β-Lg). In these systems, one could expect each microcluster to consist of one or a small number of one type of particle (*e.g.,* cationic droplets) surrounded by a larger number of the other type of particle (*e.g.,* anionic droplets), or *vice versa*. The emulsions containing 96% LF behaved similarly to those containing 100% LF, while the emulsions containing 96% β-Lg behaved similarly to those containing 100% β-Lg (**Figure 4.4**). These results suggest that the properties of colloidal dispersions containing a large excess of one type of particle was dominated by that type of particle. Nevertheless, it should be noted that at 0 mM NaCl, the mean particle size was considerably higher in the emulsion containing 96% β-Lg than in the one containing 100% β-Lg, which suggested that the addition of a small amount of LF-coated droplets had promoted some cluster formation.

The dependence of the mean particle diameters and particle size distributions on salt concentration was highly dependent on the particle ratio for the mixed-emulsions (**Figures 4.4** and **4.5**). The β-Lg coated lipid droplets (0% LF) were stable to droplet aggregation at relatively low salt concentrations but exhibited extensive droplets aggregation at ≥ 100 mM NaCl (**Figures 4.4 and 4.5a**). This effect can be attributed to the ability of salts to screen the electrostatic repulsion between droplets [29, 94, 109]. Theoretical predictions of the colloidal interactions between the different kinds of droplets in the system (β-Lg-β-Lg; LF-LF; β-Lg-LF) were made using DLVO theory (Equations 5 to 7). These predictions were made based on the measured initial droplet

diameters ($d \approx 0.14$ μm) and droplet charge potentials at different salt concentrations (**Figure 4.3**).

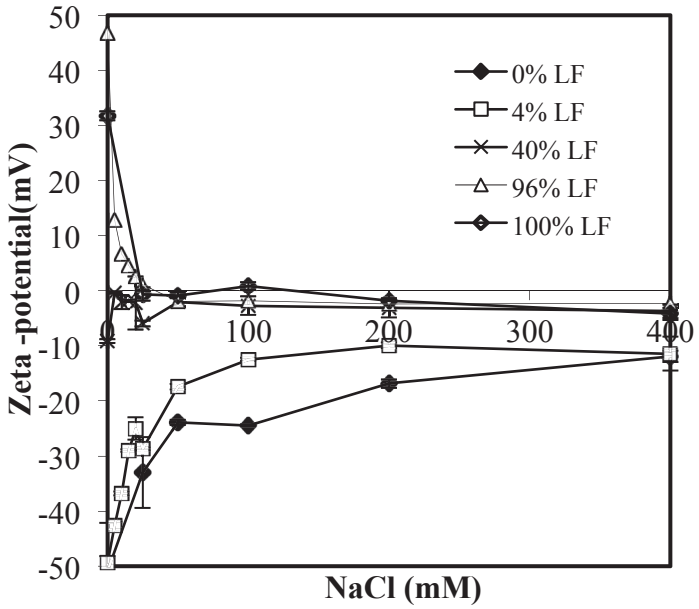

Figure 4.3 Influence of NaCl concentration on the droplet charge (ζ-potential) of 0.1 wt% oil-in-water emulsions containing different ratios of β-Lg-coated or LF-coated oil droplets at pH 7.0.

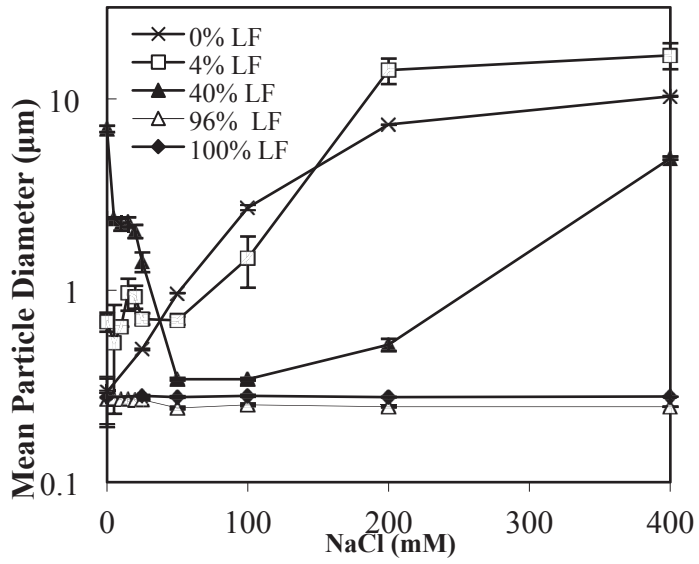

Figure 4.4 Influence of NaCl concentration on the mean particle diameter (d_{43}) of 0.1 wt% oil-in-water emulsions containing different ratios of β-Lg-coated or LF-coated oil droplets at pH 7.0.

These calculations show that the repulsive energy barrier should decrease appreciably as the ionic strength increases for the β-Lg coated droplets (**Figure 4.5a**). At relatively low ionic strengths, the repulsive force (electrostatic) was sufficiently strong to overcome the attractive force (van der Waals). At higher ionic strengths, the electrostatic force is weakened so that it is no longer sufficiently strong to prevent the droplets from aggregation. Fairly similar behavior was observed for mixed emulsions containing 4 % LF-coated droplets and 96% β-Lg-coated droplets (**Figure 4.4**), indicating that their behavior was dominated by the properties of the dominant particle type. Surprisingly, LF-coated lipid droplets (100% LF) were stable to droplet aggregation across the entire salt concentration range studied (**Figures 4.4 and 4.5b**), even though their droplet charge was relatively low (**Figure 4.5**). Theoretical predictions of their colloidal interactions based on DLVO theory (**Figure 3.14**) suggest that they should be highly unstable to droplet aggregation at even low salt concentrations, since there is no energy barrier to prevent the droplets from coming into close proximity. Our experimental data and theoretical predictions suggest that the protein layer formed by LF must have generated a stronger steric repulsion between the droplets than the protein layer formed by β-Lg [92, 93]. LF has a higher molecular weight than β-Lg and therefore should form thicker interfacial layers. In addition, LF is a glycoprotein with hydrophilic carbohydrate groups that will protrude into the surrounding aqueous phase thereby forming thicker layers [100, 110]. Similar behavior was observed for mixed emulsions containing 96 % LF-coated droplets and 4% β-Lg-coated droplets (**Figure 4.4**), again indicating that their behavior was dominated by the properties of the dominant particle type.

(a)

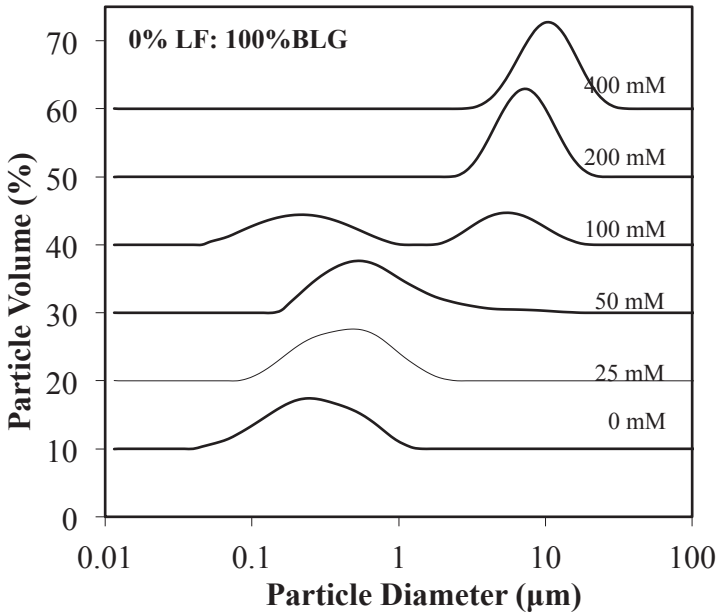
0% LF: 100%BLG
400 mM
200 mM
100 mM
50 mM
25 mM
0 mM
Particle Volume (%)
Particle Diameter (µm)
0
10
20
30
40
50
60
70
0.01
0.1
1
10
100

(b)

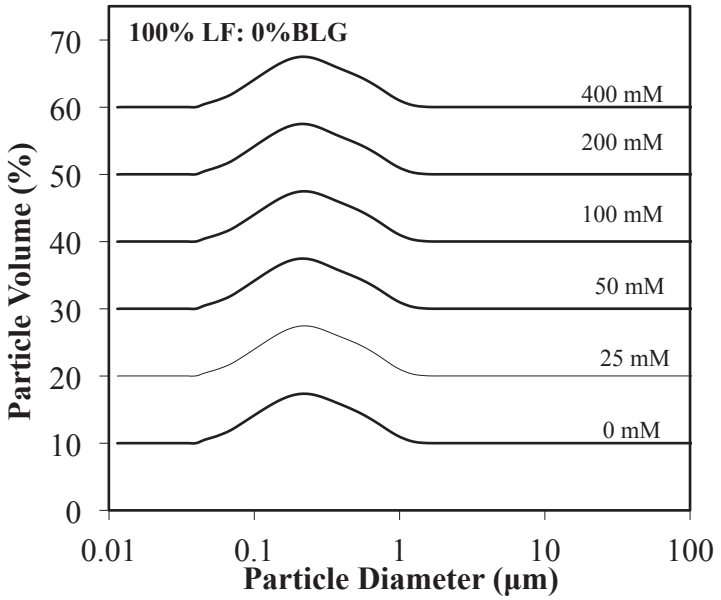
100% LF: 0%BLG
400 mM
200 mM
100 mM
50 mM
25 mM
0 mM
Particle Volume (%)
Particle Diameter (µm)
0
10
20
30
40
50
60
70
0.01
0.1
1
10
100

(c)

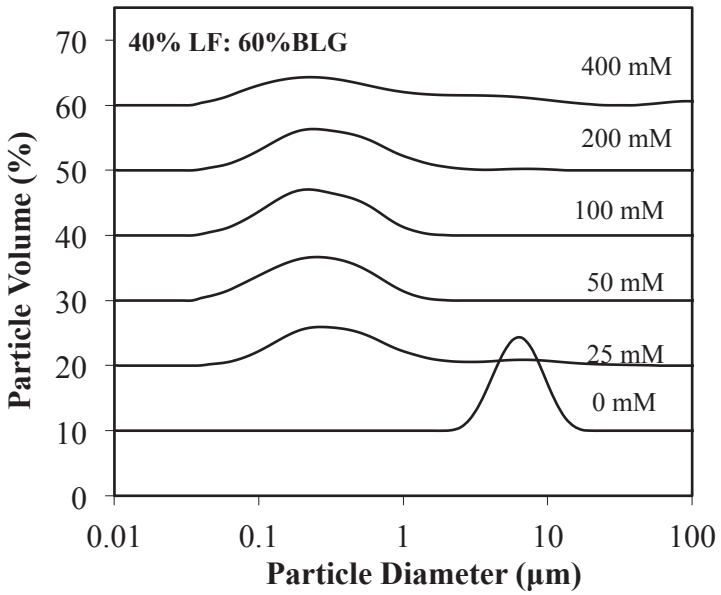

Figure 4.5 Influence of NaCl concentration on the particle size distributions of 0.1 wt% oil-in-water emulsions containing different ratios of β-Lg-coated or LF-coated oil droplets (pH 7). (a) 0% LF: 100% β-Lg; (b) 100% LF: 0% β-Lg; (c) 40% LF: 60% β-Lg.

The influence of salt concentration on the stability of emulsions containing 40% LF- and 60% β-Lg-coated droplets was quite different from emulsions containing only one type of protein-coated droplet (**Figure 4.4** and **4.5c**). In the absence of salt, the measured particle diameter was relatively large because of the formation of microclusters due to strong attraction between the oppositely charged protein-coated droplets. The mean particle diameter decreased steeply when the NaCl concentration was increased from 0 to 50 mM, which suggested that the large microclusters had partially dissociated. This effect can be attributed to a reduction in the strength of the attractive forces operating between the oppositely charged particles with increasing salt concentration. Indeed, theoretical predictions of the colloidal interactions between the different kinds of particles indicate that the attraction between them becomes weaker as the ionic strength

increases (**Figure 4.5c**). The mean particle diameter remained relatively small (d < 500 nm) from 50 to 100 mM NaCl, but then increased appreciably at higher salt concentrations, with a mean particle diameter of around 5 μm being observed at 400 mM NaCl (**Figure 4.4**). We hypothesize that the increase in particle diameter at high salt concentrations was due to flocculation of the β-Lg-coated droplets, as was observed in the emulsion containing only this type of droplet (**Figure 4.4**).

Additional information about the influence of salt on the microstructure of emulsions with different particle ratios and salt concentrations were obtained using confocal fluorescent microscopy (**Figure 4.6**). β-Lg-coated droplets were dyed red (Rhodamine) and LF-coated droplets were dyed green (Bodipy 493). The confocal microscopy images indicated that emulsions containing only β-Lg-coated droplets were stable to droplet aggregation at low salt concentrations (≤ 50 mM), but that extensive aggregation occurred at higher levels **(Figure 4.6)**. On the other hand, emulsions containing only LF-coated droplets were stable to aggregation at all NaCl concentrations studied. The mixed emulsions (40% LF: 60% β-Lg) exhibited a more complex dependence of their aggregation behavior on salt concentration. The majority of droplets appeared to be highly aggregated at low salt concentrations. At intermediate salt concentrations, the size and number of clusters formed decreased, which can be attributed to the reduction in the electrostatic attraction between the droplets at high ionic strengths. At high salt concentrations, there was evidence of extensive droplet aggregation again.

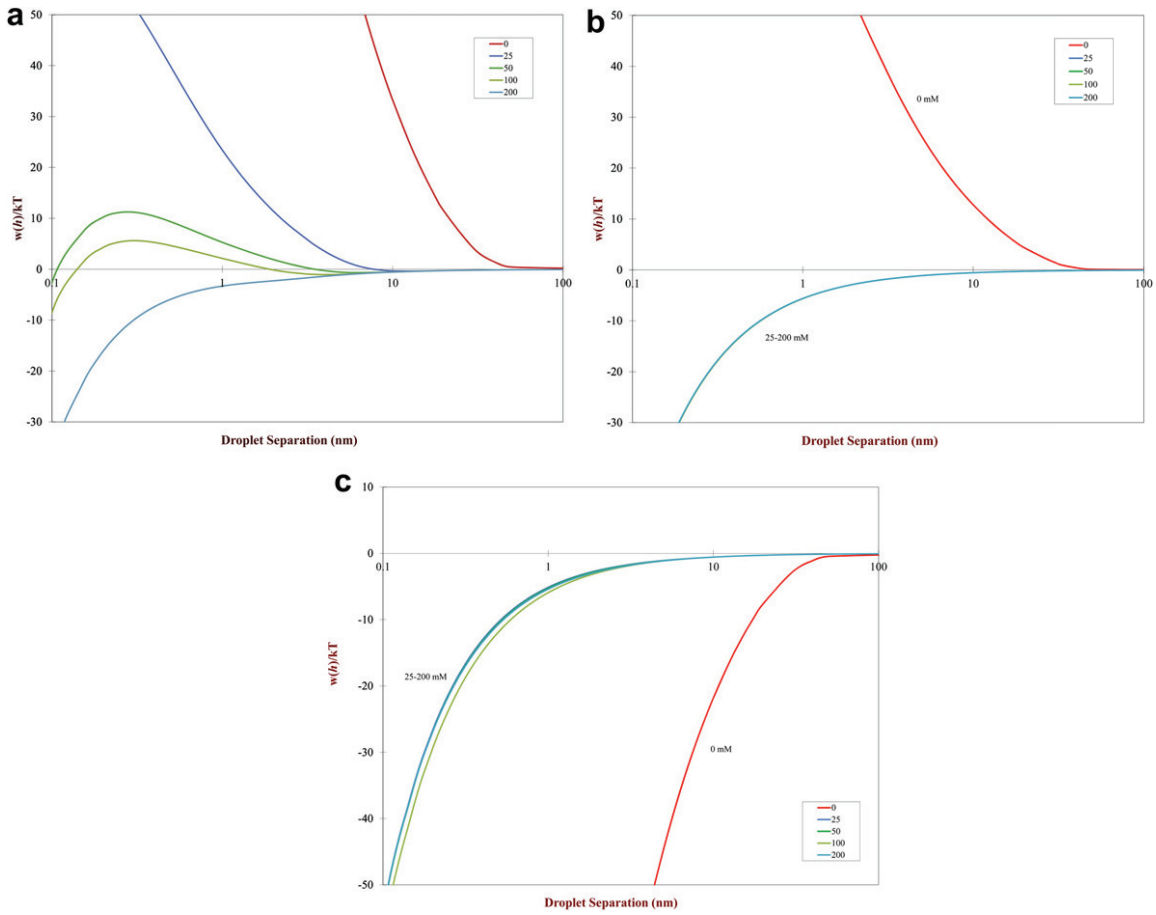

Figure 4. 6 Theoretical calculations of the influence of salt on the colloidal interactions between the droplets in mixed oil-in-water emulsions: (a) β-Lg-β-Lg; (b) LF-LF; (c) β-Lg-LF.

As mentioned earlier, changes in the size of the particles in a dilute colloidal dispersion should influence its stability to gravitational separation. We therefore measured the effect of salt on the creaming stability of the emulsions (**Figure 4.7**). We observed that appreciable creaming had occurred after 24 hour storage at relatively low (< 50 mM NaCl) and high (> 200 mM) NaCl concentrations in the mixed emulsions (40% LF: 60% β-Lg), but that they were stable to creaming at intermediate salt concentrations (25 to 200 mM NaCl). The microstructure and creaming stability results therefore supported the light scattering data.

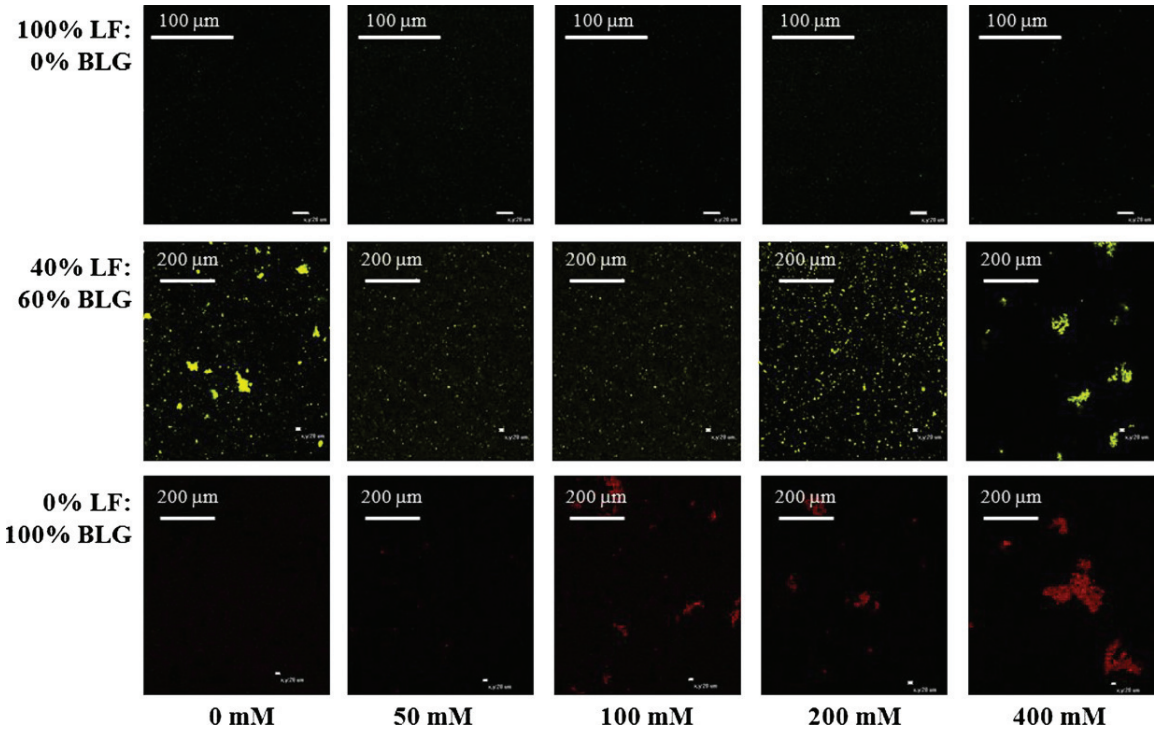

Figure 4.7 Confocal microscopy images of emulsions containing different mass ratios of LF and β-Lg after 24 hour storage at ambient temperature.

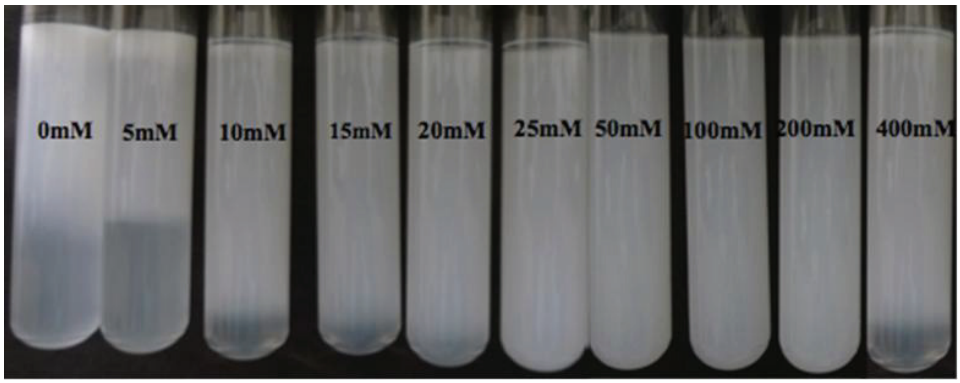

Figure 4. 8 Dependence of creaming stability at pH 7.0 on salt concentration for 0.1 wt% oil-in-water emulsions containing 40% LF-coated and 60% β-Lg-coated lipid droplets.

4.4.3 Theoretical prediction of cluster formation

Finally, we used the statistical thermodynamic model described earlier to predict the influence of particle ratio and stickiness on the formation of clusters in mixed emulsion systems. **Figure 4.8** shows the predicted influence of particle ratio on the

cluster size (*S*) for a number of different attractive potentials (ε) used in the Yukawa model (Equation 4.5). These predictions suggest that the size of the clusters formed should increase as the fraction of Type A particles in the system increases from 0 to 50%, and then decrease upon a further increase from 50 to 100%. In general, these predictions support our experimental observations that the largest clusters were formed at intermediate particle ratios, *i.e.* 30 to 70% (**Figure 4.6a**). As expected, the predictions also show that the cluster size should increase as the strength of the attraction (the stickiness parameter) increases. Based on fitting the Yukawa model to our DLVO predictions for the mixed system (**Figure 4.6c**), we found that the stickiness parameter decreased with increasing salt concentrations: $1/\tau_{AB} \approx \infty$, 1400, 34, 39, 10, and 9.7 for 0, 25, 50, 100, 200 and 400 mM NaCl. The theoretical predictions therefore support the experimental observation that the clusters in the mixed systems dissociated at intermediate salt concentrations due to weakening of the attractive interactions between oppositely charged particles.

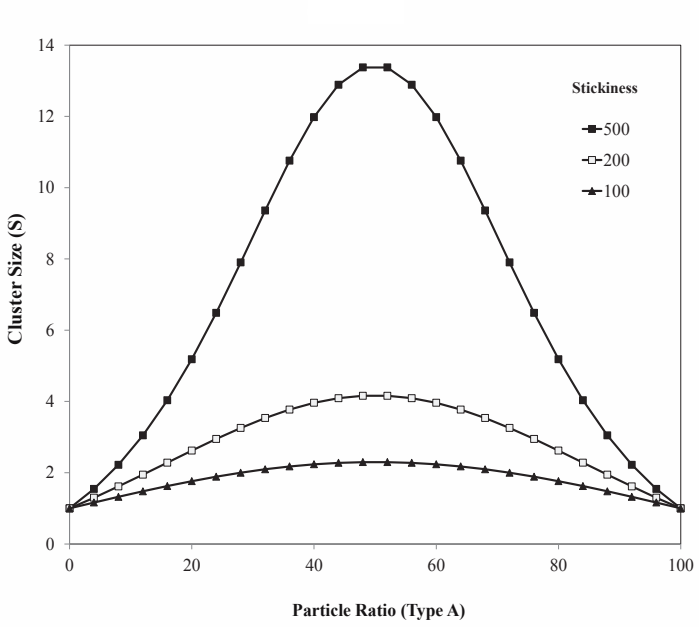

Figure 4. 9 Theoretical calculations of the influence of particle ratio and stickiness parameter (attractive force) on cluster formation due to hetero-aggregation in mixed colloidal dispersions.

4.5 Conclusions

This study suggests that the formation and structure of microclusters in colloidal dispersions consisting of mixtures of negatively and positively charged protein-coated lipid droplets can be modulated by varying the particle ratio and ionic strength. The largest particle clusters were formed at intermediate particle ratios and at low ionic strengths, which was in qualitative agreement with predictions made using a simple statistical thermodynamic model. The mixed systems exhibited an interesting dependence of aggregation stability on salt concentration. The cluster size initially decreased with increasing salt because of a weakening of the electrostatic attraction between β-Lg-coated and LF-coated droplets, but then it increased with a further increase in ionic strength due to a weakening of the electrostatic repulsion between β-Lg-coated droplets. LF-coated droplets appeared to be highly stable to salt-induced

aggregation, possibly due to the fact that the LF formed a relatively thick steric barrier around the droplets. Overall, this study provides valuable insights into the formation and properties of microclusters through hetero-aggregation. These microclusters may be useful functional components in commercial products, for example for controlled delivery or for texture modification.

CHAPTER 5

FABRICATION OF VISCOUS AND PASTE-LIKE MATERIALS BY CONTROLLED HETERO-AGGREGATION OF OPPOSITELY CHARGED LIPID DROPLETS

5.1 Introduction

In many developed countries there has been a rise in the percentage of the population that is either overweight or obese, which is linked to chronic diseases such as heart disease, diabetes, and cancer [111, 112]. A variety of approaches are needed to tackle this problem, including education about diet and exercise, encouragement of healthier lifestyles, and increased availability of affordable and desirable reduced calorie foods. There are considerable challenges to the formulation of foods with reduced calorie contents that still maintain their desirable physicochemical and sensory attributes. For this reason consumers often choose high calorie products that taste good over low calorie alternatives that are healthier but have less desirable organoleptic properties.

For this reason, the food industry is adopting the principles of colloid science and soft matter physics to design foods with novel functional properties by controlling the characteristics and structural organization of the building blocks they contain [72, 73, 103, 113, 114], such as lipids (*e.g.,* triacylglycerols, surfactants, and phospholipids), biopolymers (*e.g.,* proteins and polysaccharides) and colloidal particles (*e.g.,* lipid droplets, fat crystals and air bubbles). In particular, there has been a focus on using structural design principles to create high quality foods with reduced calorie contents. These foods should have similar desirable sensory attributes (appearance, flavor, texture, mouthfeel, and satiety) and physical stability (shelf life) as conventional products, but

should have lower calorie contents. Fat has the highest calories per unit mass of any of the major food components, and therefore it has been a primary target for reducing the overall calorie content of foods. The development of reduced fat foods has proven to be a considerable challenge to the food industry because of the multiple roles that lipid droplets play in determining the overall sensory and physicochemical properties of food products: they influence appearance due to their ability to scatter light [115, 116]; they alter flavor due to their ability to act as an organic solvent for non-polar aroma and taste molecules [117, 118]; they alter texture due to their influence on rheology [119]; they alter perceived mouthfeel due to their interactions with saliva and oral surfaces within the mouth [120, 121]; they contribute to feelings of fullness within and between meals (satiety/satiation) [122].

In this study, we investigate a promising approach of creating reduced fat foods based on controlled *hetero-aggregation* of oppositely charged lipid particles [20, 113]. This approach can be used to create emulsion-based products that are highly viscous or gel-like at much lower fat contents than in conventional (non-aggregated) emulsions. Previously, novel textural attributes have been created by mixing oil-in-water emulsions stabilized by a protein (β-lactoglobulin) with oil-in-water emulsions stabilized by a polysaccharide (gum arabic) under acidic (pH 4.2) conditions [113]. At this pH, the protein-coated lipid droplets were positively charged while the polysaccharide-coated lipid droplets were negatively charged, and hence there was an electrostatic attraction between them. This led to the formation of an aggregated network of lipid droplets that gave the resulting material formed semi-solid rheological properties. In recent studies, we have shown that material rheology and stability can be controlled in systems

containing mixtures of oppositely charged protein-coated lipid droplets by manipulating the positive-to-negative particle ratio, pH, and ionic strength [20]. The properties and behavior of food systems created using this hetero-aggregation approach can be guided by the theoretical and experimental knowledge generated for other types of colloidal dispersion [10, 27].

In the present study, we focused on the formation of semi-solid (paste-like) colloidal dispersions fabricated by controlled hetero-aggregation of oppositely charged protein-coated lipid droplets. These systems were prepared by mixing an emulsion containing β-lactoglobulin-coated lipid droplets with an emulsion containing lactoferrin-coated lipid droplets. These two globular proteins have different electrical charge *versus* pH profiles because of their different isoelectric points: β-lactoglobulin (β-Lg), pI ≈ 5; lactoferrin (LF) pI ≈ 8. Previously, we have shown that particle aggregation occurs when the two types of lipid droplets are oppositely charged (*i.e.* $pI_{\beta\text{-Lg}} < pH < pI_{LF}$) [20]. For applications within the food industry it is important that these materials are fabricated entirely from food-grade ingredients (*i.e.,* lipids and proteins) so that they are suitable for oral ingestion. We hypothesized that the rheological properties of these structures could be tailored by systematically controlling sample composition and preparation conditions. The knowledge gained from this study could be useful for the rational design of fat reduced foods for utilization in commercial products.

5.2. Experimental Methods

5.2.1 Materials

Corn oil was purchased from a commercial food supplier (Mazola, ACH Food Companies, Inc., Memphis, TN). Lactoferrin powder (LOT #10408282) was supplied by DMV International (Delhi, NY), and the manufacturer reported that it contained 97.7% protein and 0.12% ash. Purified *β*-lactoglobulin powder (BioPURE, LOT #JE-002-8-415) was supplied by Davisco Foods International (Eden Prairie, MN). The manufacturer reported the composition of this powder to be 97.4% total protein, 92.5% *β*-lactoglobulin (*β*-Lg), and 2.4% Ash. All solvents and reagents were of analytical grade. Double distilled water was used to make all solutions.

5.2.2 Formation of Single-protein Emulsions

Aqueous emulsifier solutions were prepared by dispersing either β-Lg powder or LF powder into double distilled water, and then stirring for at least 3 h at room temperature to ensure complete dispersion. The pH of the protein solutions was then adjusted to 7.0 using 1M NaOH or 1M HCl. Oil-in-water emulsions containing a single protein type were prepared by blending 20 g of corn oil and 80 g of aqueous protein solution for 2 min using a hand blender (M133/1281-0, 2 speed, Biospec Products Inc., ESGC, Switzerland) and then recirculating them four-times through a two-stage homogenizer (LAB 1000, APV-Gaulin, Wilmington, MA) at a first-stage pressure of 5,400 psi and a second-stage pressure of 600 psi. The β-Lg emulsion was then heated to 90 °C for 30 min to cross-link the adsorbed proteins, so as to prevent any competitive adsorption effects, *i.e.,* exchange of proteins between lipid droplets in different types of

emulsion. The LF emulsions were not heated because they are unstable to thermal treatment when heated above the thermal denaturation temperature of the proteins [101]. All emulsions were then stored for 24 hours prior to utilization. Preliminary experiments reported elsewhere established that 0.5% β-Lg and 3% LF were suitable levels to form single-protein emulsions with relatively small droplet diameters ($d_{43} \approx 0.35$ μm) [20], and so these levels were used to form the mixed-protein emulsions.

5.2.3 Formation of Mixed-protein Emulsions

Initially, two single-protein emulsions stabilized by either 0.5% β-Lg or 3% LF were prepared in distilled water as described in Section 2.1. A series of mixed emulsions containing 0 to 20 wt% *β*-Lg droplets (pH 7.0) and 20 to 0 wt% LF droplets (pH 7.0) were prepared by mixing different ratios of the two emulsions together, stirring for 10 min, then allowing them to stand for 24 h prior to analysis. The resulting mixed emulsions therefore contained different mass ratios of positive-to-negative droplets (0 to 100%). For convenience, we designated the particle ratios in mixed emulsions in terms of the percentage of lactoferrin droplets they contained, *e.g.,* "40%LF emulsion" means an emulsion with 40% lactoferrin-coated droplets and 60% β-Lg-coated droplets.

5.2.4 Influence of pH and Ionic Strength on the Formation of Mixed Systems

pH: For each type of single emulsion, a series of samples was prepared with different pH values using either 1M NaOH or 1M HCl to adjust the pH of the initial samples. A mixed emulsion (40%LF) was then formed by mixing 40% of LF-emulsion with 60% of β-Lg-emulsion (mass percentage), stirring for 10 min, and then allowing them to stand overnight at ambient temperature prior to analysis.

Ionic strength: A 20% oil-in-water emulsion containing mixed protein-coated lipid droplets (40%LF) was formed by mixing 40% of LF-emulsion with 60% of β-Lg-emulsion (pH 7). A series of samples with different ionic strengths was then prepared by adding different amounts of crystalline sodium chloride to the emulsions and stirring to obtain final emulsions containing 0 to 400 mM NaCl. All samples were stored overnight at ambient temperature before analysis.

5.2.5 Rheological Properties

The rheological behavior of samples was measured using a dynamic shear rheometer (Kinexus Rotational Rheometer, Malvern Instruments, Malvern, U.K). A cup and bob geometry consisting of a rotating inner cylinder (diameter 25 mm) and a static outer cylinder (diameter 27.5mm) was used in viscosity and oscillation measurements. The samples were loaded into the rheometer measurement cell and allowed to equilibrate at 25°C for 5 min before beginning all experiments.

Viscosity measurements: Samples underwent a constant shearing treatment (1 s^{-1} for 10 min) prior to analysis to remove history effects. Viscosity (η) measurements were then carried out at different shear rates (0.01 to 10 s^{-1}).

Shear modulus measurements: Initially, we determined the range of the linear viscoelastic region (LVR) in an oscillation measurement (frequency = 0.1 Hz) by subjecting the samples to a range of shear strains (0.001~100%) test. These measurements indicated that there was no appreciable change in the shear modulus below 3% strain, and therefore a value of 1% was used in subsequent studies. The storage modulus (G') and loss modulus (G") were recorded by the instrument software. The influence of frequency on the shear modulus of mixed samples was assessed by

varying the oscillation frequency (0.01~10 Hz) of the inner cylinder (strain = 1%). A temperature cycle (30 to 90 to 30 °C at 5 °C min^{-1}) was used to determine the influence of heating and cooling on the rheological properties of the samples (frequency = 1 Hz, strain = 1%). A thin layer of oil (octanol) was placed on top of the samples to avoid water evaporation during the heat-cool cycle. The influence of a pre-shear treatment (1 s^{-1} for 10 min) on the rheological properties of selected samples was also assessed.

5.2.6 Particle Size and Charge Analysis

The particle size distribution of the emulsions was measured using a laser diffraction particle size analyzer (Mastersizer 2000, Malvern Instruments, Ltd., Worcestershire, UK). To avoid multiple scattering effects the emulsions were diluted to a droplet concentration of approximately 0.005 wt% using pH-adjusted water at the same pH as the sample. The emulsions were stirred continuously throughout the measurements to ensure the samples were homogenous. Measurements are reported as the volume-weighted mean diameter: $d_{4,3}=\sum d_i n_i^4/\sum d_i n_i^3$, where n_i is the number of droplets of diameter d_i. It should be noted that particle size measurements made by static light scattering on highly flocculated emulsions should be treated with caution. First, the theory (Mie theory) used to interpret light scattering data assumes that the scattering particles are homogeneous spheres with well-defined refractive indices. In practice, flocs are non-spherical and non-homogeneous particles, with ill-defined refractive indices. Second, the process of dilution and stirring may have altered the dimensions and structural organization of the flocs. Consequently, the reported particle sizes should only be treated as an indication of strong droplet association rather than a measure of the actual size of any aggregates present in the original non-diluted samples.

The ζ-potential of emulsions was determined using a particle electrophoresis instrument (Zetasizer Nano ZS series, Malvern Instruments, Worcestershire, UK). Emulsions were diluted to a droplet concentration of approximately 0.001 wt% using pH-adjusted water to avoid multiple scattering effects. The pH of the water used was adjusted to the same pH as the initial emulsion sample. After loading the samples into the instrument they were equilibrated for about 120 s before particle charge data was collected over 20 continuous readings.

5.2.7 Microstructure Analysis

The microstructure of selected samples was analyzed using Transmission Electron Microscopy (TEM). Mixed emulsion samples were diluted 1:10 with distilled water. Diluted samples were applied to glow-discharge treated carbon films on grids for 30 s to enable particle adsorption to the grid surfaces. The remaining liquid was then drained from the grid and a drop of 2% aqueous uranyl acetate solution (pH 4) was added for 15 s to stain them. This solution was removed from the grid by touching it with filter paper, and then the grid was allowed to air dry. Grids were imaged on a transmission electron microscope (JEOL JEM-100S) with a SIA 7C digital camera (Vitaly Feingold 2773 Heath Lane,Duluth GA, 30096). It should be noted that the sample preparation procedure required for TEM may cause some change in the structure of the flocs formed. However, all samples were prepared in the same way and therefore we were able to compare TEM images on different treatments under similar conditions.

5.2.8 Statistical Analysis

All experiments were carried out in either duplicate or triplicate using freshly prepared samples. Results are reported as the calculated means and standard deviations.

5.3 Results & Discussion

Initially, we measured the mean particle diameter and electrical characteristics of the two single-protein emulsions used to fabricate the mixed emulsions. The emulsion containing β-lactoglobulin-coated lipid droplets had a ζ-potential of -51 mV and a mean particle diameter (d_{43}) of 0.35 μm, while the one containing lactoferrin-coated lipid droplets had a ζ-potential of + 32 mV and d_{43} of 0.35 μm (pH 7). These measurements confirmed that the two single-protein emulsions contained lipid droplets that had similar dimensions but opposite charges at neutral pH.

5.3.1 Influence of Particle Ratio on Emulsion Rheology and Stability

Our initial objective was to understand the influence of positive-to-negative particle ratio on the rheology and stability of mixed emulsions containing both negatively and positively charged lipid droplets. This was achieved by mixing different mass ratios of 20 wt% LF emulsion and 20 wt% β-Lg emulsion together at pH 7.0 and then measuring their rheological properties, particle sizes, and appearances (**Figure 5.1**).

(a)

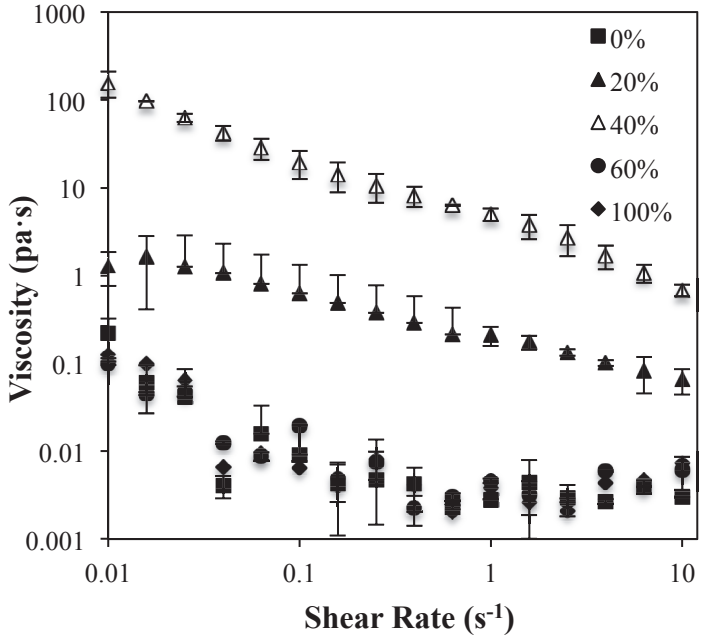
1000
100
10
1
0.1
0.01
0.001
0.01
0.1
1
10
Viscosity (pa·s)
Shear Rate (s-1)
0%
20%
40%
60%
100%

(b)

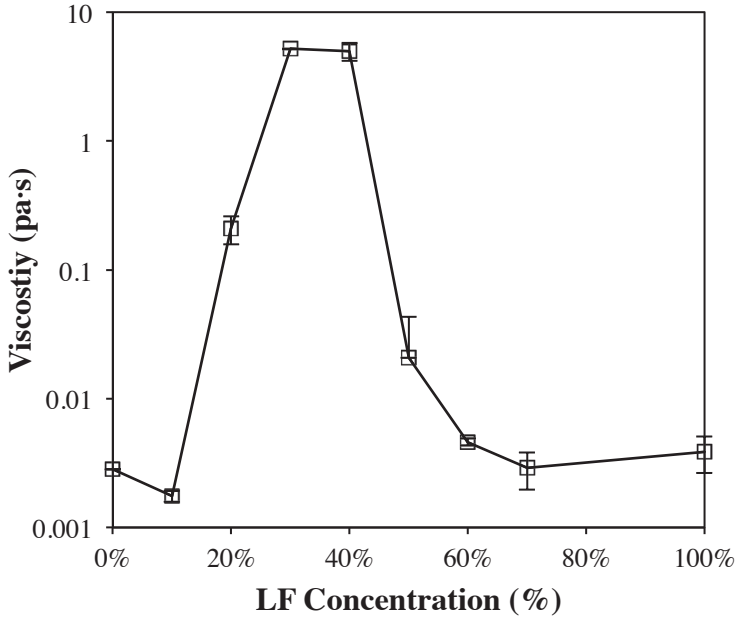
10
1
0.1
0.01
0.001
0%
20%
40%
60%
80%
100%
Viscostiy (pa·s)
LF Concentration (%)

(c)

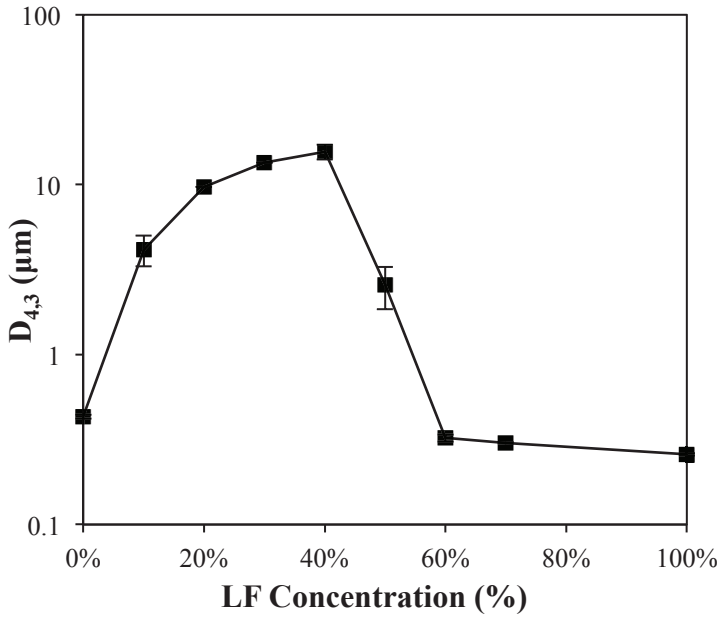

(d)

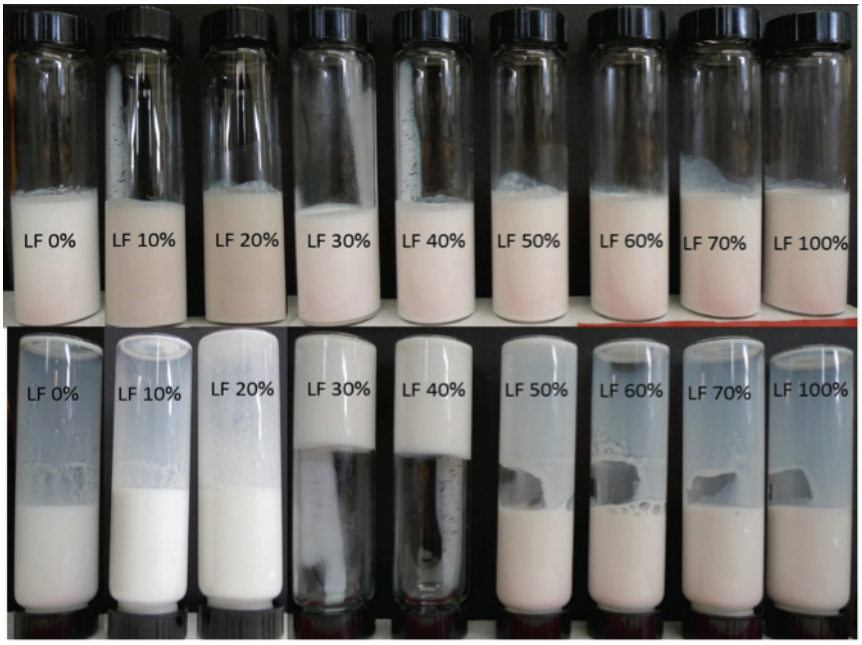

Figure 5.1 (a) Dependence of mean viscosity with change shear rate (0.01~10 s^{-1}) at pH 7.0 on particle ratio for 20% wt% oil-in-water emulsions containing different mass ratios of β-Lg-coated or LF-coated oil droplets. (b) Dependence of mean viscosity at shear rate (10 s^{-1}) at pH 7.0 on particle ratio for 20% wt% oil-in-water emulsions containing different mass ratios of β-Lg-coated or LF-coated oil droplt s． (c). Dependence of mean particle diameter (d_{43}) at pH 7.0 on particle ratio for 20 wt% oil-in-

water emulsions containing different mass ratios of β-Lg-coated or LF-coated oil droplets. (d) Dependence of creaming stability at pH 7.0 for 20 wt% oil-in-water emulsions containing (0~100%) LF-coated and (0~100%) β-Lg-coated lipid droplets.

Apparent viscosity-shear rate profiles for emulsions with different particle ratios are shown in **Figure 5.1a** for selected samples. The magnitude of the viscosity and its dependence on shear rate depended strongly on particle ratio. The 20%LF and 30%LF samples had much higher viscosities than the other samples and exhibited distinct non-Newtonian (shear-thinning) flow profiles, *i.e.* the apparent viscosity decreased appreciably with increasing shear rate. The origin of this shear thinning behavior is likely to be the progressive breakdown of the aggregated structure in the samples as the shear rate was increased. The dependence of the apparent viscosity on particle ratio at a constant shear rate (10 s^{-1}) is shown in **Figure 5.1b**. The emulsions containing only β-Lg-coated droplets (0%LF) and only LF-coated droplets (100%LF) had relatively low viscosities, indicating that there was little particle flocculation in these systems. However, there was a large increase in the apparent viscosity of the emulsions at intermediate particle ratios, with the 30%LF and 40%LF samples having viscosities that were two to three orders of magnitude greater than the single-protein emulsions. Interestingly, the highest viscosity was not observed in the samples containing 50% positively charged and 50% negatively charged droplets, as predicted from theoretical calculations made using a statistical thermodynamics approach [25]. There are a number of possible reasons for this: (i) the mixed emulsions were not at thermodynamic equilibrium; (ii) the two different types of droplet had different charge magnitudes; (iii) non-adsorbed proteins may have played a role.

Information about the tendency of the particles in the emulsions to associate with each other was obtained by measuring their mean particle diameters (**Figure 5.1c**). The emulsions containing only β-Lg-coated droplets (0%LF) and only LF-coated droplets (100%LF) had relatively low mean particle sizes, which suggested that they were relatively stable to flocculation. These emulsions contained only one kind of particle that had relatively high charge magnitudes (either positive or negative), which meant that there would be a strong electrostatic repulsion preventing the droplets from aggregating [94, 123]. At intermediate particle ratios (20%LF to 50%LF) there was a large increase in mean particle diameter, indicating that oppositely charge droplets associated with each other through electrostatic attraction and formed large aggregates that were resistant to breakdown in the light scattering instrument. The reason that large aggregates were not detected in the 60%LF and 80%LF samples may have been because individual negatively charged β-Lg-coated droplet were surrounded by a layer of LF-coated droplets that limited further aggregate growth. This kind of structure has been reported in molecular modeling simulations of aggregation in mixed colloidal dispersions [10, 27]. The formation of a strong particle network in the emulsions at intermediate particle concentrations was demonstrated by storing them in test tubes for 24 hours and then inverting them (**Figure 5.1d**). The emulsions containing low or high particle ratios were fluid-like and flowed to the bottom of the inverted tubes, but the ones containing intermediate particle ratios (30%LF and 40%LF) exhibited solid-like characteristics and remained at the top of the inverted tubes.

5.3.2 Influence of pH on Structure Formation and Rheology

The main driving force for particle aggregation in mixed emulsions at neutral pH has been attributed to electrostatic attraction between the oppositely charged lipid droplets [20]. We therefore examined the influence of pH on emulsion structure and rheology since the electrical characteristics of protein-coated lipid droplets change appreciably with pH [20, 39, 123].

The rheology, aggregation stability, and appearance of the emulsions clearly depended on the pH of the aqueous phase (**Figure 5.2a**). The apparent viscosity (**Figure 5.1b**) and mean particle size (**Figure 5.2c**) of emulsions containing only β-Lg-coated droplets (0%LF) were relatively small at low ($pH \leq 4$) and high ($pH \geq 6$) pH values, which can be attributed to the fact that the droplets were not strongly aggregated because of the relatively large electrostatic repulsion between them [94]. On the other hand, these emulsions had a high apparent viscosity and particle size at pH 5, which has previously been attributed to extensive droplet flocculation occurring when the pH is close to the isoelectric point of the β-Lg-coated droplets [94, 123]. These findings were supported by visual observations of emulsion appearance when they were inverted. The emulsions at pH 5 formed a solid-like material that remained in the top of the test tubes when they were inverted, whereas the other emulsions flowed to the bottom (**data not shown**). The apparent viscosity (**Figure 5.2b**) and particle size (**Figure 5.2c**) of emulsions containing only LF-coated droplets (100%LF) remained relatively low at all pH values studied, which can be attributed to a combination of electrostatic and steric repulsion between the droplets preventing droplet aggregation [39]. Lactoferrin is a relatively large globular protein with some carbohydrate moieties attached to its surface,

and hence it may generate a relatively strong steric repulsion between protein-coated lipid droplets that prevents aggregation near the isoelectric point. The rheological and particle size data was again supported by visual observations of the emulsions: all the emulsions remained fluid and flowed to the bottom of the test tubes when they were inverted (**data not shown**).

The rheology of the mixed emulsions (40%LF) was highly dependent on pH (**Figures 5.2a and 5.2b**). The viscosity of the mixed emulsions was small at relatively low ($pH \leq 4$) and high ($pH = 9$) pH values, but was high at intermediate pH values ($5 \leq pH \leq 8$). This effect can be attributed to the fact that the droplets will only tend to form strongly aggregated structures when they have opposite charges. The isoelectric points of LF-coated droplets and β-Lg coated droplets have been reported to be around pH 8 and pH 5 respectively [20, 39], and hence the emulsions will only have opposite charges in this intermediate pH range . The tendency for strong aggregates and a particle network to be formed in this intermediate pH range was supported by the particle size measurements and visual observation of inverted samples. Extensive particle aggregation was observed at intermediate pH values, but not at relatively low and high pH values (**Figure 5.1c**), while the emulsion at pH 7 remained at the top of the test tubes when they were inverted (**data not shown**).

As mentioned in the previous section, attractive electrostatic interactions between oppositely charged lipid droplets have been attributed to be the major forces holding particles together in the mixed systems. Consequently, we examined the influence of ionic strength on the stability of the emulsions, since increasing ionic strength is known

to reduce the magnitude and range of electrostatic interactions [108]. The ionic strength was altered by adding different levels of a monovalent salt (NaCl) to the emulsions.

(a)

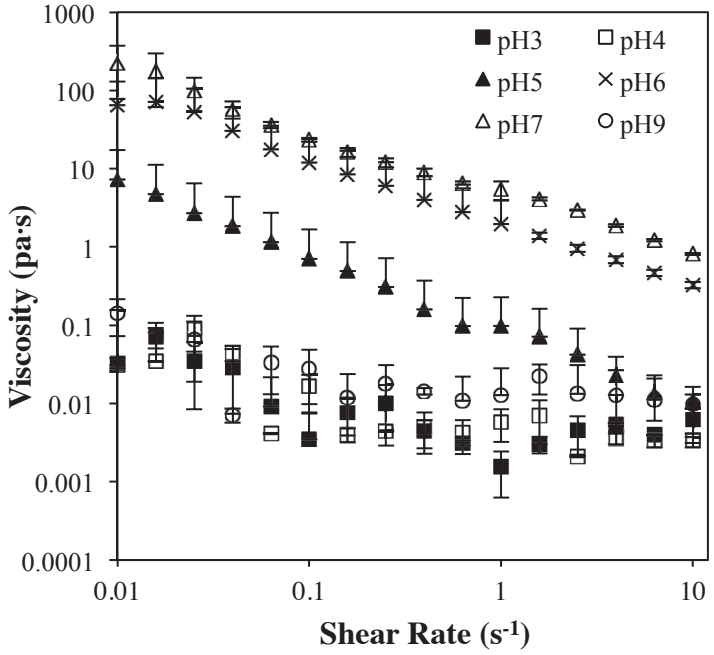

(b)

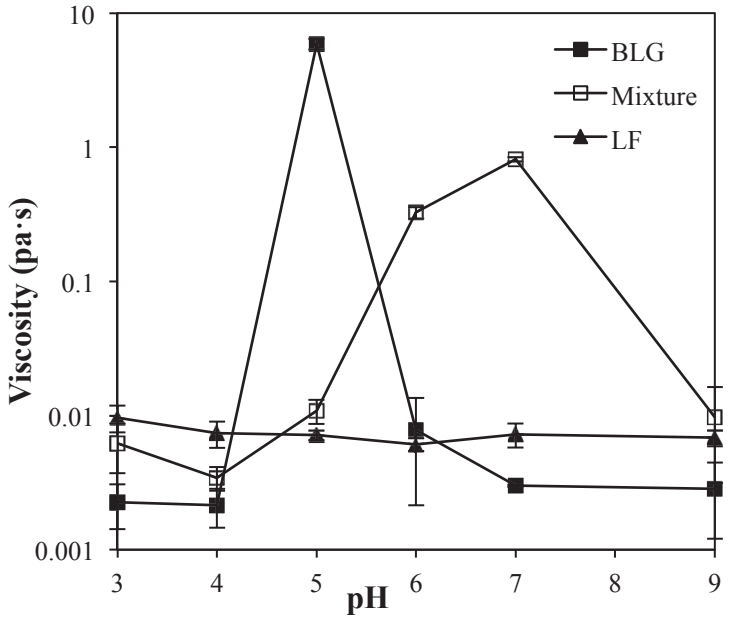

(c)

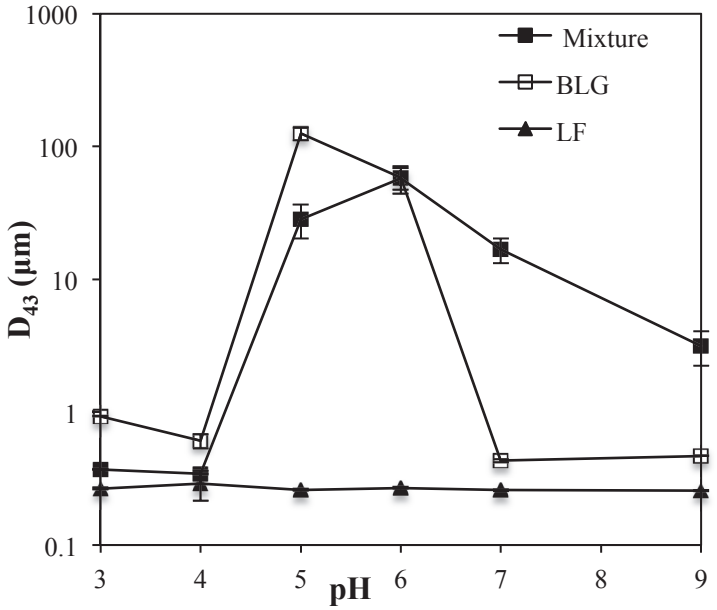

Figure 5.2 (a). Influence of pH on apparent viscosity (10 s−1) of 20 wt.% oil-in-water emulsions (pH 7): 0% LF ("β-Lg"), 40% LF ("Mixture") and 100% LF ("LF"). (b) Influence of pH on apparent viscosity-shear rate profiles of 20 wt.% oil-in-water emulsions containing a mass ratio of 40% LF-coated oil droplets and 60% β-Lg -coated oil droplets (i.e. 40% LF emulsions). (c) Influence of pH on mean particle diameter (d_{43}) of 20 wt.% oil-in-water emulsions (pH 7): 0% LF ("β-Lg"), 40% LF ("Mixture") and 100% LF ("LF").

5.3.3 Influence of Ionic Strength on Structure Formation and Rheology

The rheology, particle size, and microstructure of mixed emulsions containing different salt concentrations were characterized using dynamic shear rheometry (**Figure 5.3a**), light scattering (**Figure 5.3b**), and transmission electron microscopy (**Figure 5.3c**). Both the apparent viscosity and the mean particle diameter (d_{43}) of emulsions containing only β-Lg-coated droplets (0%LF) were relatively small at low ionic strengths (NaCl ≤ 25 mM), increased steeply at intermediate ionic strengths (25 mM ≤ NaCl ≤ 100 mM), and reached relatively high and constant values at high ionic strengths (NaCl ≥ 100 mM) (**Figures 5.3a and 5.3b**). The large increases in apparent viscosity and particle size with

increasing salt concentration can be attributed to the ability of counter-ions (Na^+) to screen the electrostatic repulsion between negatively charged β-Lg-coated droplets [94]. In contrast, the apparent viscosity and mean particle diameter of emulsions containing only LF-coated droplets (100%LF) remained relatively low at all salt concentrations (**Figures 5.3a** and **5.3b**). This suggests that the LF-coated droplets were primarily stabilized by steric repulsion rather than electrostatic repulsion. This can be attributed to the fact that lactoferrin is a relatively large molecule that has hydrophilic carbohydrate groups that protrude into the aqueous phase thereby forming a thick interfacial layer [39].

(a)

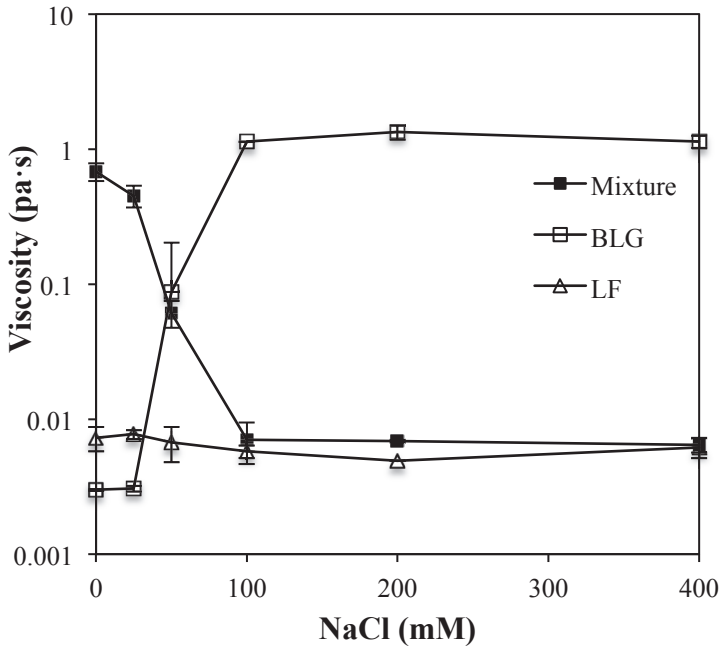

(b)

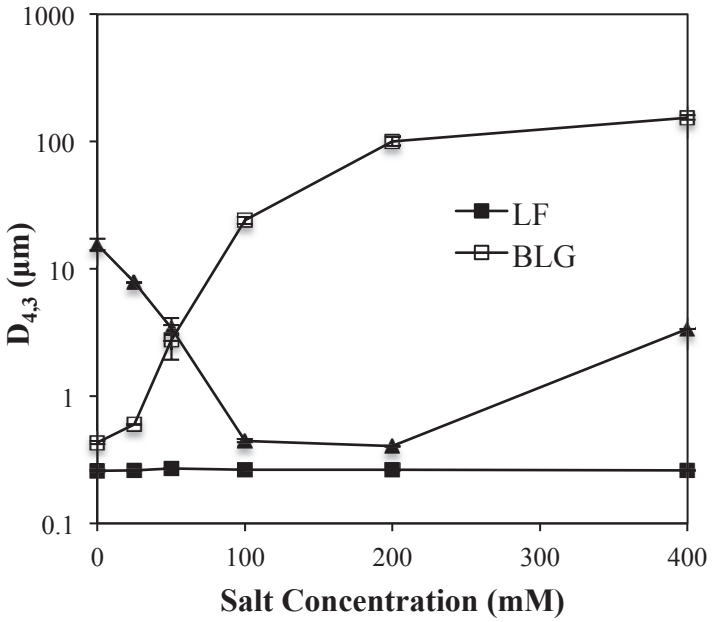

(c)

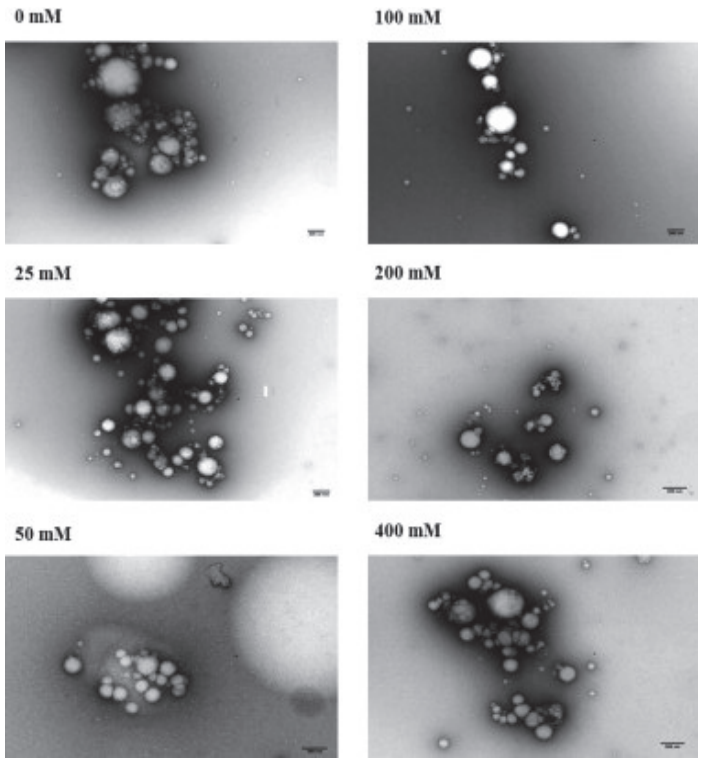

Figure 5.3 (a) Influence of salt concentration on the apparent viscosity of 20 wt.% oil-in-water emulsions (pH 7): 0% LF ("β-Lg"), 40% LF ("Mixture") and 100% LF("LF"). (b) Influence of salt concentration on the mean particle diameter (d_{43}) of

20 wt.% oil-in-water emulsions (pH 7): 0% LF ("β-Lg"), 40% LF ("Mixture") and 100% LF ("LF"). (c) Influence of salt concentration onTEM images of 20 wt.% oil-in-water emulsions containing a mass ratio of 40% LF-coated oil droplets and 60% β-Lg-coated oil droplets (i.e., 40% LF emulsion). (d) The scale bars (bottom right corner of each image) represent 200 nm. Each image shown represents an area of approximately 2830 nm long and 1880 nm high.

The influence of salt on the rheology and particle size of the mixed emulsions (40% LF) was quite different from that of the other two emulsions. In the absence of added salt the mixed emulsions were highly viscous and contained relatively large particles (**Figures 5.3a and 5.3b**). The apparent viscosity decreased steeply when the salt concentration was increased from 0 to 50 mM NaCl, and then reached a relatively constant value at higher ionic strengths. The mean particle diameter also decreased when the salt concentration was increased from 0 to 50 mM NaCl, but then it increased when the salt content was increased from 200 to 400 mM NaCl. The light scattering measurements were supported by TEM measurements, which showed that the samples were highly aggregated at low ionic strength, became less aggregated at intermediate ionic strength, and then became more aggregated again at higher ionic strength (**Figure 5.3c**). Visual observations of the mixed emulsions showed that the samples containing 0 and 25 mM NaCl formed gels that remained at the top of the tubes after inversion, whereas the samples containing high salt concentrations all flowed to the bottom after inversion (**data not shown**). We hypothesize that the change in particle aggregation and rheology in the system is due to the influence of salt on the magnitude of electrostatic attractive and repulsive interactions. At low ionic strength, aggregates containing anionic β-Lg-coated droplets and cationic LF-coated droplets are formed due to strong electrostatic attraction between oppositely charged particles. As the salt concentration is increased these aggregates are disrupted because of a decrease in the electrostatic

attraction between oppositely charged droplets. At higher ionic strengths, the β-Lg-coated droplets may aggregate due to a decrease in the electrostatic repulsion between similarly charged droplets. The reason that we did not see an appreciable increase in the apparent viscosity of the mixed emulsions at the highest ionic strength (400 mM NaCl) maybe because only 50% of the particles in this system were β-Lg-coated droplets. It was not possible to distinguish the different kinds of particles within the aggregates from the TEM images. Selective staining of the particles would be an interesting means of identifying the nature of the particles within the aggregates in future studies.

5.3.4 Viscoelastic Properties of Mixed Emulsions

The mixed emulsions were capable of forming paste-like structures under certain conditions, and so we used measurements of the complex shear modulus to characterize their viscoelastic behavior. Mixed emulsion (40%LF) samples were placed in the measurement cell (without pre-shear) for 10 minutes, and then the storage modulus (G') and loss modulus (G'') were measured as a function of applied shear frequency (**Figure 5.4**). In the frequency range studied (0.1 to 10 Hz), the storage modulus was always appreciably higher than the loss modulus ($G'>G''$) indicating that the structures formed had predominantly elastic-like characteristics. The samples became more rigid (increasing G') with increasing frequency suggesting that there was a characteristic relaxation time associated with rearrangement of the gel structure.

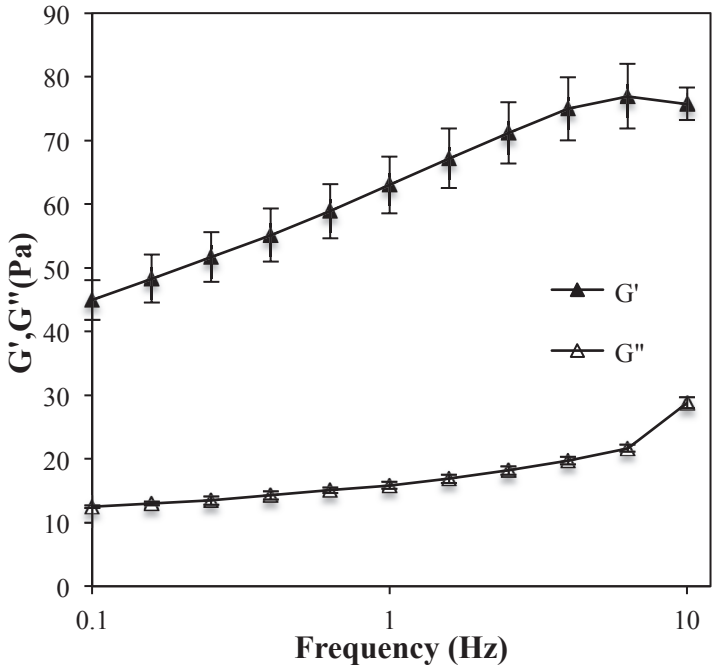

Figure 5.4 The influence of oscillation frequency on the storage modulus (G′) and loss modulus (G″) of 20% wt.% oil-in-water emulsions containing 40% LF-coated oil droplets and 60% β -Lg-coated oil droplets (pH 7, 0 mM NaCl, strain = 1%). Measurements were made prior to a pre-shear treatment.

The influence of the pre-shear treatment on the shear modulus of selected samples was also examined. Mixed emulsions were placed in the measurement cell of the rheometer and either pre-sheared (1 s^{-1}) or held without shear for 10 minutes prior to measurement. There was a large decrease in both the storage and loss modulus after pre-shearing (**Figure 5.5**), which indicated that the particle networks formed in the mixed emulsions were irreversibly disrupted on the time-scale of our experiments. This may have important implications for commercial applications of mixed emulsions formed by hetero-aggregation.

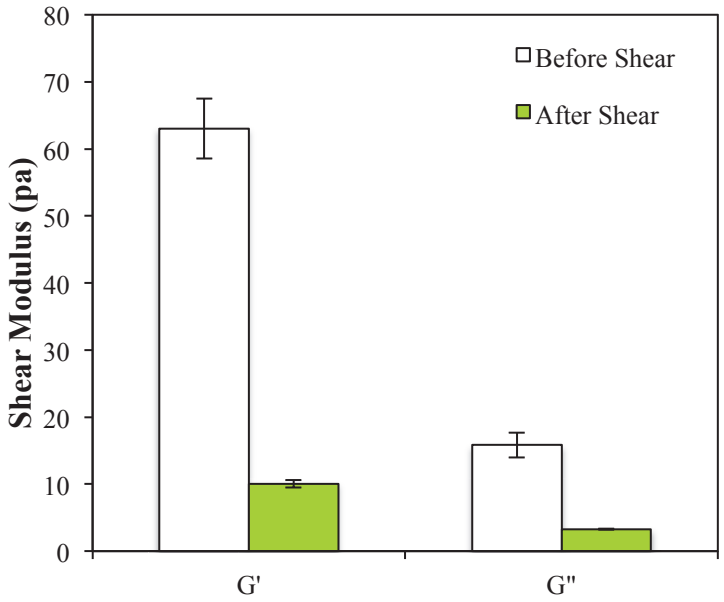

Figure 5.5 Influence of pre-shear treatment (1 s^{-1} for 10 min) on the storage modulus (G′) and loss modulus (G″) of 20 wt.% oil-in-water emulsions containing 40% LF-coated oil droplets and 60% β -Lg-coated oil droplets (pH 7, 0 mM NaCl, strain = 1%).

Finally, we measured the temperature dependence of the mixed emulsions (40%LF) by incubating then at 30 ºC for 10 min (without pre-shear), heating them from 30 to 90 ºC (1 ºC/min), holding them at 90 ºC for 5 minutes, and then cooling them from 90 to 30 ºC (1 ºC/min) (**Figure 5.6**). The emulsions were heated in the absence of salt (0 mM NaCl), which meant that electrostatic repulsive/attractive interactions should be relatively strong. There was a small increase in the shear modulus of the single emulsions (0%LF or 100%LF) after heating to 90 ºC (**Figure 5.6b**). On the other hand, there was a large increase in the shear modulus of the mixed emulsions (40%LF) after heating above about 60-70 ºC (**Figure 5.6a**). The increase in shear modulus can be attributed to increased particle aggregation in the system resulting from thermal denaturation of the globular proteins (β-lactoglobulin or lactoferrin) adsorbed to the droplet surfaces, which leads to an increased hydrophobic attraction between the droplets

[97, 123]. Previous studies have shown that both β-lactoglobulin-coated [97, 123] and LF-coated lipid droplets [39] aggregate when the emulsions are heated above the thermal denaturation temperature of the proteins. Lactoferrin has been reported to have two thermal denaturation temperatures around 61 and 93 ºC [124], whereas β-lactoglobulin has been reported to have a single thermal denaturation temperature around 78 ºC [125]. Our experiments indicate that it is possible to increase the shear modulus of the mixed systems by over two orders of magnitude by heating them above the thermal denaturation temperature of the adsorbed proteins. Consequently, it may be possible to form food materials with novel textural properties by applying a thermal treatment to them.

(a)

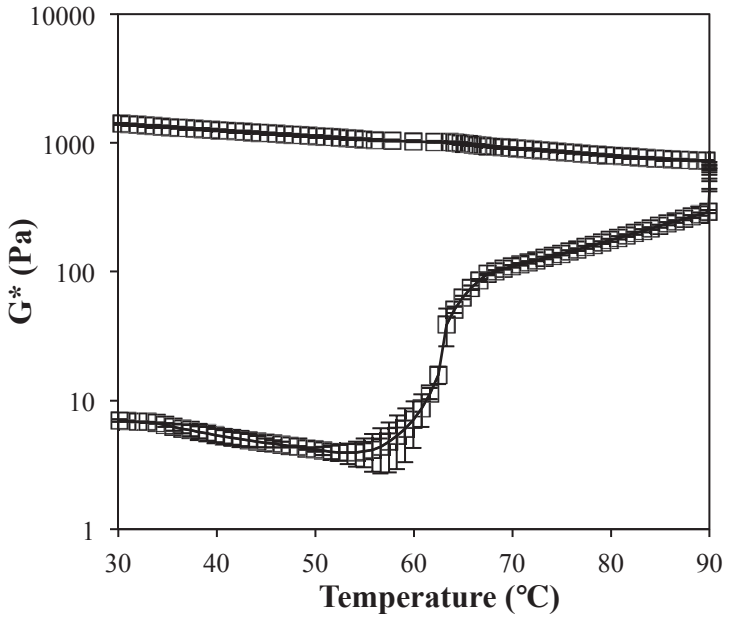

(b)

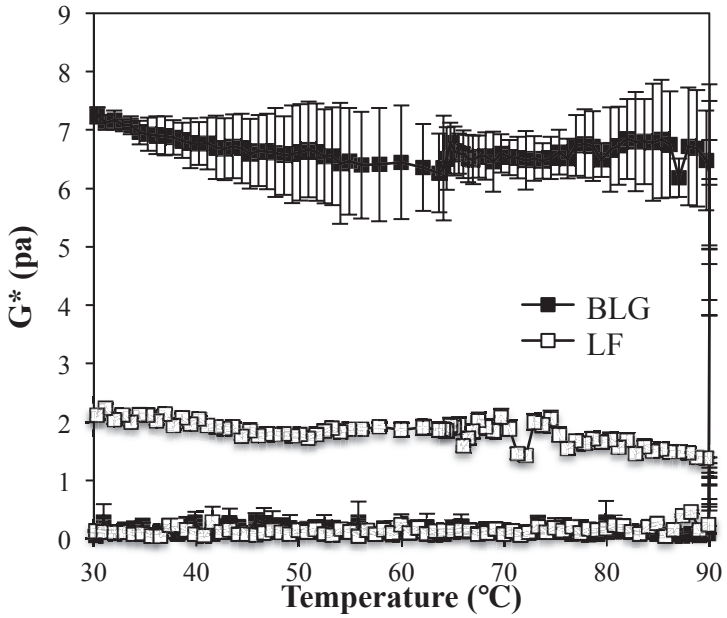

Figure 5. 6 (a) Influence of thermal treatment on the complex modulus (G*) of 20 wt.% oil-in-water emulsions containing 40% LF-coated oil droplets and 60% β-Lg-coated oil droplets (pH 7, 0 mM NaCl, strain = 1%). (b) Influence of thermal treatment on complex modulus (G*) of 20 wt.% oil-in-water emulsions containing either LF-coated oil droplets ("LF") or β-Lg-coated oil droplets ("β-Lg") (pH 7, 0 mM NaCl, strain = 1%).

5.4 Conclusions

This study has shown that the rheological properties of colloidal dispersions consisting of mixtures of negatively and positively charged protein-coated lipid droplets can be modulated by varying the particle ratio, pH, ionic strength, and temperature. The highest viscosity and largest gel strength were formed at intermediate particle ratios, neutral pH, and low ionic strengths. The mixed systems exhibited an interesting dependence of aggregation stability on pH and salt concentration. At low or high pH value, aggregates were disassociated because the charges on the different lipid droplets were no longer opposite in sign. The cluster size and viscosity initially decreased with increasing salt because of a weakening of the electrostatic attraction between β-Lg-

coated and LF-coated droplets, but then it increased with a further increase in ionic strength due to a weakening of the electrostatic repulsion between β-Lg-coated droplets. LF-coated droplets appeared to be highly stable to pH and salt-induced aggregation, possibly due to the fact that the LF formed a relatively thick steric barrier around the droplets. The shear modulus of mixed emulsions increased appreciably after thermal treatment, which was attributed to an increased hydrophobic attraction between the droplets brought about by thermal denaturation of the adsorbed proteins. Overall, this study provides valuable insights into the formation and rheological properties of highly viscous and paste-like structures by controlled hetero-aggregation of oppositely charged particles. These materials may be useful functional components in commercial products, for example reduced-fat foods, cosmetics, or personal care products.

CHAPTER 6

FABRICATION OF REDUCED FAT PRODUCTS BY CONTROLLED HETERO-AGGREGATION OF OPPOSITELY CHARGED LIPID DROPLETS

6.1 Introduction

Obesity is a major health problem in many developing and developed countries because it is associated with increased risk of diseases, such as heart disease, diabetes, stroke, and cancer [112, 126]. The prevalence of obesity has been attributed to the widespread availability of inexpensive calorie-dense foods, and an increase in more sedentary lifestyles. One approach to tackling obesity is to create satisfying, convenient, and affordable food products with reduced calorie contents. Fats are the major food component with the highest calorie density, and therefore there has been considerable emphasis on producing reduced fat foods. Nevertheless, the development of reduced fat products has proved to be a great challenge because removing some or all of the fat changes the physicochemical properties and sensory perception of foods [117]. If reduced fat food products have undesirable sensory attributes then consumers may not purchase them even though they may be healthier than their full-fat analogs.

In this article, we are primarily concerned with the influence of fat on the properties of emulsified foods, such as sauces, dressings, desserts, and beverages [49]. One of the main challenges to reducing the fat content of emulsified foods is that they play many different roles in determining their overall properties [127]. Reducing the fat droplet concentration in an emulsion tends to decrease its viscosity, decrease its creaming stability, reduce its lightness, and alter its flavor profile [49, 128, 129]. There is therefore a need to understand the complex roles that fat droplets play in determining

food quality, and in developing new strategies to create reduced fat foods with desirable physicochemical and sensory attributes.

In this study, we examined the possibility of using controlled hetero-aggregation of oppositely charged lipid droplets to produce reduced fat emulsions with similar textures and appearances as high fat products. Recently, we have showed that materials with novel textural attributes could be created by mixing anionic β-lactoglobulin (β-Lg) coated lipid droplets with cationic lactoferrin coated lipid droplets [20, 21]. In particular, highly viscous or gel-like mixed-particle emulsions could be prepared by mixing two low viscosity single-particle emulsions with the same fat content. In the current study, we examined the influence of fat content on the formation and properties of mixed-particle emulsions formed by hetero-aggregation. The knowledge gained from this study could be helpful for designing reduced fat food emulsions.

6.2 Experimental Methods

6.2.1 Materials

Corn oil was purchased from a commercial food supplier (Mazola, ACH Food Companies, Inc., Memphis, TN) and stored at 4 °C until use. Lactoferrin powder (LOT #10404498) was supplied by Friesland-Campinanin (Delhi, NY), which the manufacturer reported contained 97.7% protein and 0.12% ash. Purified β-lactoglobulin powder (BioPURE, LOT #JE-001-0-415) was supplied by Davisco Foods International (Eden Prairie, MN), which the manufacturer reported contained 97.4% total protein, 92.5% *β*-lactoglobulin (*β*-Lg), and 2.4% Ash. All solvents and reagents were of analytical grade. Double distilled water was used to make all solutions.

6.2.2 Formation of Single-particle Emulsions

Aqueous emulsifier solutions were prepared by dispersing either β-Lg powder or LF powder into double distilled water, and then stirring for at least 3 h at room temperature to ensure complete dispersion. The pH of the protein solutions was then adjusted to 7.0 using either 1M NaOH or 1M HCl. For each protein type, oil-in-water emulsions with different oil contents (5%, 7.5%, 10%, 20%, 40%) were prepared by blending appropriate amounts of corn oil and aqueous protein solution for 2 min using a hand blender (M133/1281-0, 2 speed, Biospec Products Inc., ESGC, Switzerland) and then recirculating them four-times through a two-stage homogenizer (LAB 1000, APV-Gaulin, Wilmington, MA) at a first-stage pressure of 5,400 psi and a second-stage pressure of 600 psi. The β-Lg emulsion was then heated to 90 °C for 30 min to cross-link the adsorbed proteins, so as to prevent any competitive adsorption effects. All emulsions were then stored for 24 hours prior to utilization. Preliminary experiments established that a β-Lg-to-oil ratio of 0.5:10 and a LF-to-oil ratio of 3:10 were suitable to form single-protein emulsions with relatively small droplet diameters (d_{43} < 0.5 μm) [20].

6.2.3 Formation of Mixed-particle Emulsions

Initially, two series of oil-in-water emulsions (pH 7.0) were prepared with the same protein-to-oil ratio, but different fat contents (5-40 wt%) and protein types (0.25-2% β-Lg or 1.5-12% LF). These emulsions were then stored overnight at room temperature. A series of mixed emulsions containing 0 to 40 wt% β-Lg-coated oil droplets (pH 7.0) and 40 to 0 wt% LF-coated oil droplets (pH 7.0) were prepared by mixing different mass ratios of the two emulsions together, stirring for 10 min, and then allowing them to stand for 24 h prior to analysis. The resulting mixed emulsions

therefore contained different mass ratios of positive-to-negative droplets (0 to 100%).

6.2.4 Particle Charge and Size Measurements

The ζ-potential of emulsions was determined using a particle electrophoresis instrument (Zetasizer Nano ZS series, Malvern Instruments, Worcestershire, UK). The ζ-potential is determined by measuring the direction and velocity of droplet movement in a well-defined electric field. Emulsions were diluted to a droplet concentration of approximately 0.001 wt% using pH-adjusted water to avoid multiple scattering effects. The pH of the water used to carry out the dilution was adjusted to the same pH as the emulsion sample. After loading the samples into the instrument they were equilibrated for about 120 s before particle charge data was collected over 20 continuous readings.

The particle size distribution of the emulsions was measured using a laser diffraction particle size analyzer (Mastersizer 2000, Malvern Instruments, Ltd., Worcestershire, UK). This instrument measures the angular dependence of the intensity of light ($\lambda = 632.8$ nm) scattered from a stirred diluted emulsion. The particle size distribution is then calculated using Mie theory to obtain an optimal analysis of this light energy distribution. To avoid multiple scattering effects the emulsions were diluted to a droplet concentration of approximately 0.005 wt% using pH-adjusted water at the same pH as the sample. The emulsions were stirred continuously throughout the measurements to ensure the samples were homogenous. Measurements are reported as the volume-length mean diameter: $d_{4,3}=\sum d_i n_i^4 / \sum d_i n_i^3$, where n_i is the number of droplets of diameter d_i. It should be noted that particle size measurements made by static light scattering on highly flocculated emulsions should be treated with caution. First, the theory (Mie theory) used to interpret light scattering data assumes that the scattering particles are

homogeneous spheres with well-defined refractive indices. In practice, microclusters are non-spherical and inhomogeneous particles, with ill-defined refractive indices. Second, the process of dilution and stirring may have altered the dimensions and structural organization of the microclusters. Consequently, the reported particle sizes should only be treated as a qualitative indication of changes in particle dimensions rather than accurate values.

6.2.5 Rheological Properties

The rheological behavior of samples was measured using a dynamic shear rheometer (Kinexus Rotational Rheometer, Malvern, U.K.). A cup and bob geometry consisting of a rotating inner cylinder (diameter 25 mm) and static outer cylinder (diameter 27.5 mm) was used in viscosity and oscillation measurements. The samples were loaded into the rheometer measurement cell and allowed to equilibrate at 25 ºC for 5 min before beginning all experiments.

Viscosity measurements: Samples underwent a constant shearing treatment (1 s^{-1} for 10 min) prior to analysis to remove history effects. Viscosity (η) measurements were then carried out at different shear rates (0.01 to 10 s^{-1}).

Shear modulus measurements: Initially, we determined the range of the linear viscoelastic region (LVR) in an oscillation measurement (frequency = 0.1 Hz) by subjecting the samples to a range of shear strains (0.001~100%). These measurements indicated that there was no appreciable change in the shear modulus below 3% strain, and therefore a value of 1% was used in subsequent studies. The storage modulus (G') and loss modulus (G'') were recorded by the instrument software.

6.2.6 Microstructure Analysis

The microstructure of selected samples was analyzed using Transmission Electron Microscopy (TEM). Mixed emulsion samples were diluted 1:10 with distilled water. Diluted samples were applied to glow-discharge treated carbon films on grids for 30 s to enable particle adsorption to the grid surfaces. The remaining liquid was then drained from the grid and a drop of 2% aqueous uranyl acetate solution (pH 4) was added for 15 s to stain them. This solution was removed from the grid by touching it with filter paper, and then the grid was allowed to air dry. Grids were imaged on a transmission electron microscope (JEOL JEM-100S) with a SIA 7C digital camera (Vitaly Feingold 2773 Heath Lane, Duluth GA, 30096).

6.2.7 Colourimetry

In this non-destructive approach, the colour of mixture was analyzed by measuring colour for different fat content mixed emulsion. The tristimulus colour coordinates (L∗a∗b∗) of the nanoemulsions were measured using ColorFlex EZ (ColorFlex EZ, Hunter Lab, Virginia, US). The three coordinates of LAB represent the lightness of the color (L* = 0 yields black and L* = 100 indicates diffuse white; specular white may be higher), its position between red/magenta and green (a*, negative values indicate green while positive values indicate magenta) and its position between yellow and blue (b*, negative values indicate blue and positive values indicate yellow). Samples were placed into a transparent flat-faced plate and covered by white cape, and then the colour was recorded. All measurements were repeated three times.

6.2.8 Statistical Analysis

All experiments were carried out in either duplicate or triplicate using freshly prepared samples. Results are reported as the calculated means and standard deviations.

6.3 Results and Discussion

Initially, the mean particle diameter and electrical characteristics of the two single-particle emulsions were analyzed. Emulsions containing β-lactoglobulin-coated lipid droplets had similar charges (ζ = -42 ± 2 mV) and mean particle diameters (d_{43} = 0.35 ± 0.04 μm), irrespective of initial droplet concentration (**Figure 6.1a**). Similarly, emulsions containing lactoferrin-coated lipid droplets had similar ζ-potential values (ζ = +26 ± 2 mV) and diameters (d_{43} = 0.32 ± 0.04 μm), irrespective of initial droplet content (**Figure 6.1b**). These experiments indicated that the two single-particle emulsions contained lipid droplets with similar dimensions but opposite charges at neutral pH.

6.3.1 Influence of Oil Content on Microcluster Formation

Our initial objective was to establish the influence of oil content on the formation of microclusters in mixed-particle emulsions containing negatively charged and positively charged lipid droplets. This was achieved by preparing a series of emulsions with different oil contents (5 to 40%) but the same mass ratio of β-lg to LF (60%-to-40%) coated droplets, and then measuring their mean particle diameters (**Figure 6.1a**) and charges (**Figure 6.1b**). This mass ratio was selected since we have previously shown that the greatest degree of droplet flocculation occurs in mixed systems containing 60% β-lg-coated droplets and 40% LF-coated droplets [20].

(a)

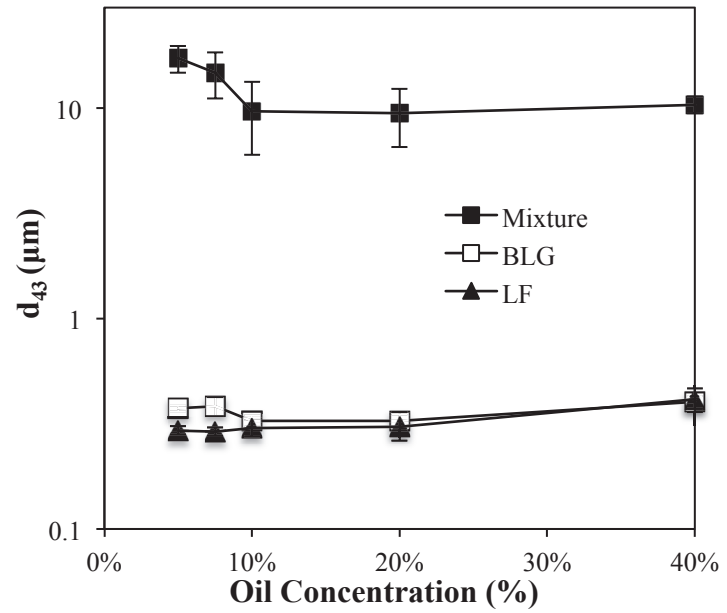

(b)

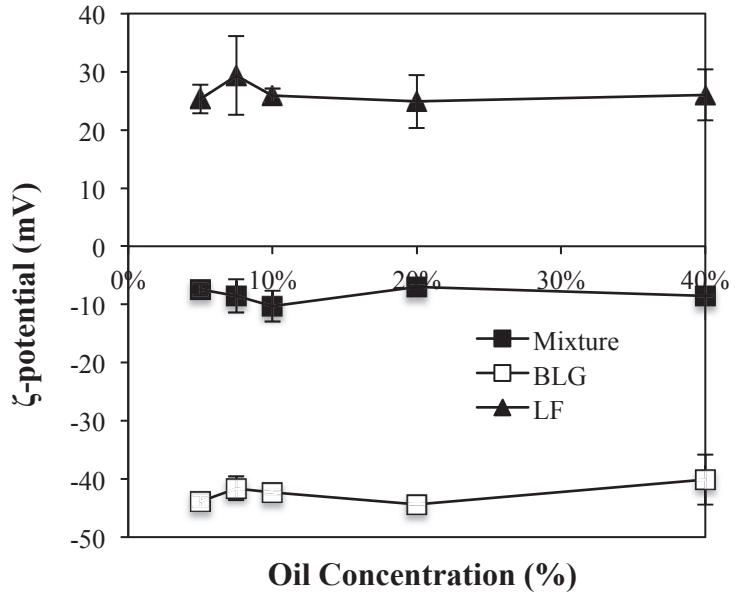

Figure 6.1 (a). Influence of oil concentration on the mean particle diameter of oil-in-water emulsion (pH 7) containing β-lactoglobulin (β-Lg)-coated droplets, lactoferrin (LF)-coated droplets, or a mixture of 40% LF-coated droplets and 60% β-Lg-coated droplets (mixture). (b). Influence of oil concentration on the net particle charge in oil-in-water emulsion (pH 7) containing β-Lg-coated droplets, LF-coated droplets, or a mixture of 40% LF-coated droplets and 60% β-Lg -coated droplets (mixture).

Emulsions containing only β-lg-coated droplets ($d_{43} \approx 0.35\mu m$) and only LF-coated droplets ($d_{43} \approx 0.32\ \mu m$) had relatively small particle sizes, which suggested that they were relatively stable to flocculation (**Figure 6.1a**). This effect can be attributed to the fact that emulsions containing lipid droplets that all have the same net charge will have an electrostatic repulsion acting between them, which prevents the droplets from coming close enough together to aggregate. In this case, the β-lg coated droplets had a charge of about -42 mV while the LF coated droplets had a charge of about +26 mV (**Figure 6.1b**), and so there should have been a relatively strong electrostatic repulsion operating in both single-particle emulsions. On the other hand, the mixed-particle emulsions had relatively large particle diameters ($d_{43} \approx 10$ - $20\ \mu m$), which were relatively independent of oil droplet concentration (**Figure 6.1a**). The presence of large particles in the emulsions is evidence of microcluster formation due to hetero-aggregation of the oppositely charged lipid droplets. Indeed, transmission electron microscopy (TEM) images of the mixed-particle emulsions indicated that they contained flocs with dimensions around 10 μm (**Figure 6.2**). The net charge on the microclusters formed was slightly negative (- 8 mV) (**Figure 6.1b**), which indicates that the overall charge was dominated by the anionic β-lg coated droplets, rather than the cationic LF-coated droplets. The β-lg coated droplets were present at a lower percentage (40%) than the LF-coated droplets (60%), but they had a higher charge magnitude (-42 mV compared to + 26 mV).

Previous studies have found that the human tongue can only sense soft particles as individual entities when their dimensions exceed a threshold value of around 80 μm [130]. This suggests that microclusters formed by hetero-aggregation of oppositely

charged protein-coated droplets would not be detected as individual particles by the tongue, and therefore have a smooth textural perception. Nevertheless, further work is required to study the sensory properties of mixed-particle systems compared to single-particle systems to test this hypothesis.

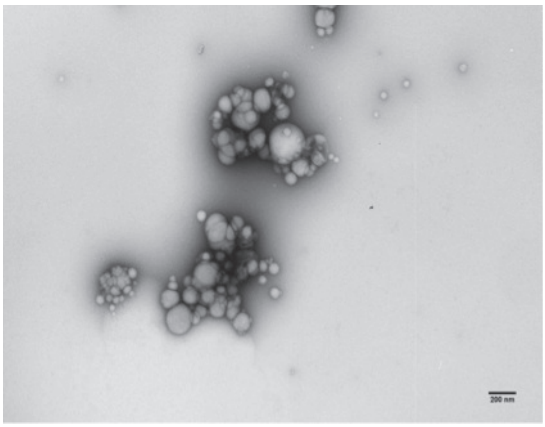

Figure 6.2 TEM images of 20 wt% oil-in-water emulsions containing a mass ratio of 40% LF-coated oil droplets and 60% β-Lg-coated oil droplets. The scale bars (bottom right corner of each image) represent 200nm. The image shown represents an area of approximately 2830nm long and 1880 nm high.

6.3.2 Influence of Oil Concentration on Emulsion Rheology

In this series of experiments we examined the influence of oil droplet concentration on the rheology of single-particle (100% LF or 100% β-Lg) and mixed-particle (40% LF and 60% β-Lg) emulsions. The shear stress *versus* shear strain profiles for selected mixed-particle emulsions with different fat contents are shown in **Figure 6.3**. The rheology profiles clearly indicate that the concentrated mixed-particle emulsions were non-ideal plastic materials with paste-like properties: they do not flow below a critical shear stress (the "yield stress"), but do flow when the shear stress exceeds this value. The yield stresses were estimated to be around 0.05, 0.9 and 28 Pa, for the 10, 20 and 40% fat samples, respectively (**Figure 6.3**). We could not determine yield stresses

for mixed-particle emulsions with lower fat contents. These results suggest that mixed-particle emulsions contained a network of droplets held together by attractive electrostatic interactions. At sufficiently high fat contents, the aggregated particle network spanned the entire volume of the system, which generated elastic-like rheological properties [131]. Presumably, this particle network was deformed and disrupted when the shear stresses applied were sufficiently high compared to the attractive forces holding the droplets together, which led to fluid-like behavior.

(a)

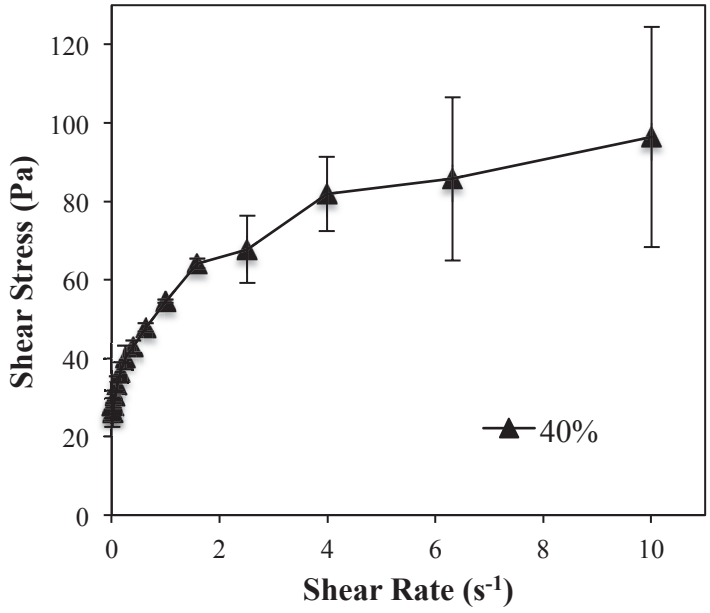

(b)

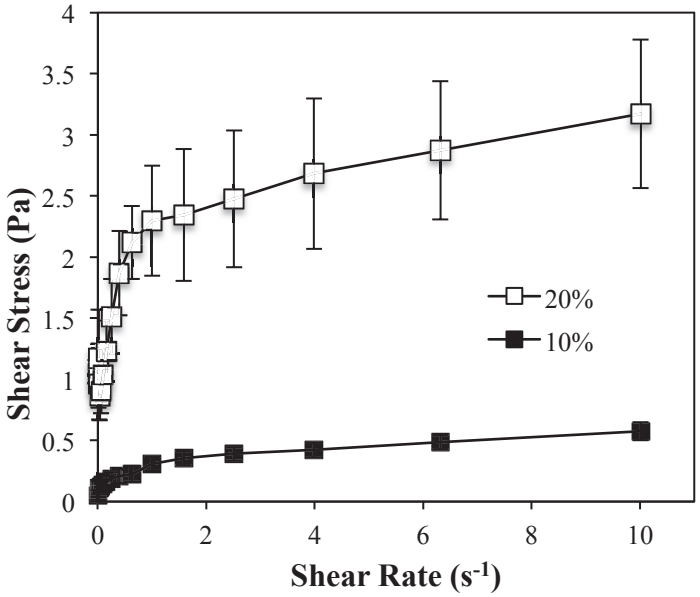

Figure 6.3 Relationship between applied shear stress and measured shear rate for oil-in-water emulsions (pH 7) containing a mixture of 40% LF-caoted droplets and 60% β-Lg-caoted droplets: (A) 40% total fat and (B) 10% or 20% total fat.

The apparent shear viscosity *versus* shear rate profiles of mixed-particle emulsions with different fat contents are shown in **Figure 6.4**. The magnitude of the shear viscosity and its dependence on shear rate were strongly influenced by fat content. The 10%, 20%, and 40% fat content samples had much higher viscosities than the other samples and exhibited distinct non-Newtonian (shear-thinning) flow behavior, *i.e.,* the viscosity decreased appreciably with increasing shear rate. Shear thinning is likely to be caused by progressive deformation and disruption of the microclusters formed by droplet hetero-aggregation as the shear rate was increased [131]. On the other hand, the emulsions with low fat contents (5% and 7.5%) had relatively low viscosities that were not highly dependent on applied shear rate.

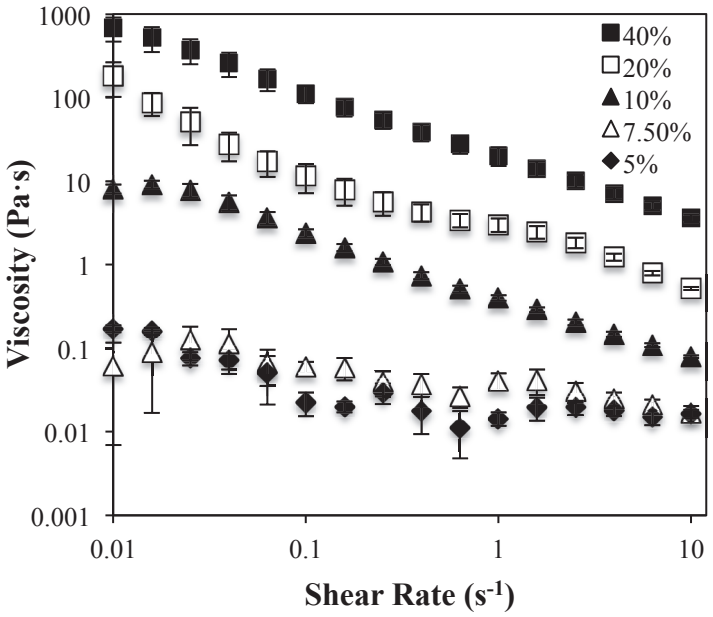

Figure 6.4 Influence of applied shear rate and total fat content on the apparent shear viscosity of oil-in-water emulsions (pH 7) containing a mass ratio of 40% LF-coated droplets and 60% β-Lg-coated droplets

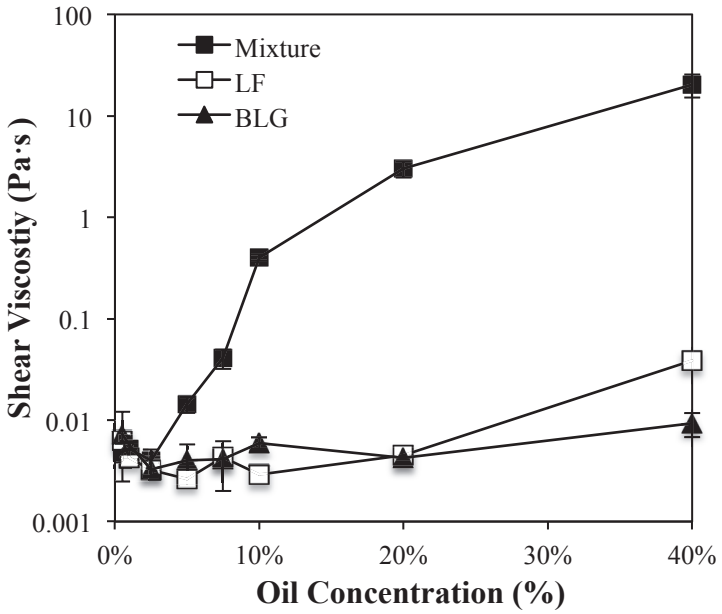

Figure 6.5 Influence of oil concentration on the apparent shear viscosity of oi-in-water emulsions (pH 7) containing β-Lg-coated droplets, LF-coated droplets or a mixture of 40% LF-coated droplets and 60% β-Lg-coated droplets (mixture).

The dependence of the apparent shear viscosity on droplet concentration for the

single-particle and mixed-particle emulsions at a constant shear rate (1 s^{-1}) was measured (**Figure 6.5)**. The viscosity of the single-particle emulsions was relatively low for all fat contents studied. For example, even in the most concentrated emulsions (40% oil) containing only β-Lg-coated droplets or only LF-coated droplets the viscosities were less than 0.1 Pa s, indicating that there was little droplet flocculation in these systems. Conversely, the mixed-particle emulsions had relatively high viscosities for fat contents ranging from 5 to 40%, with the viscosity increasing with increasing droplet concentration. Indeed, the mixed-particle emulsion containing 7.5% fat had a higher viscosity than either of the single-particle emulsions containing 40% fat (**Figure 6.5**). The physicochemical basis for the influence of microcluster formation on the rheology of mixed-particle emulsions is discussed in Section 6.3.6. Our results suggest that controlled droplet hetero-aggregation may prove to be a useful means of producing highly viscous or paste-like products with reduced fat content.

6.3.3 Viscoelastic Properties of Mixed-particle Emulsions

The mixed-particle emulsions formed paste-like structures at relatively high fat contents (≥ 10%) and so we used measurements of their complex shear modulus at low strains to characterize their viscoelastic behavior. Initially, we determined the linear viscoelastic region of the samples by measuring the shear modulus *versus* applied strain at a fixed frequency (0.1 Hz). The shear modulus remained relatively constant from 0.03 to 3% strain, but then decreased appreciably at higher strains. We therefore used a constant strain of 1 % for the subsequent measurements.

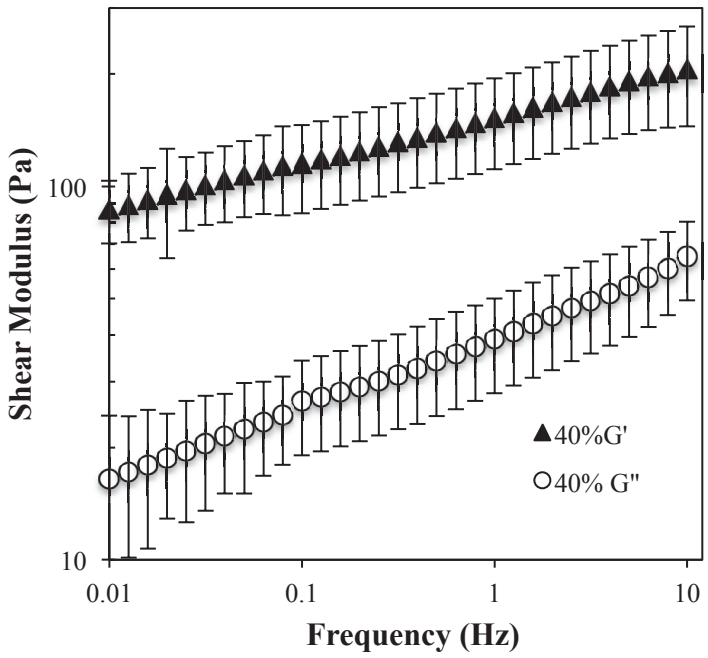

Figure 6.6 Influence of oscillation frequency on the shear modulus of 40% oil-in-water emulsions (pH 7) containing a mixture of 40% LF-coated droplets and 60% β-Lg-coated droplets.

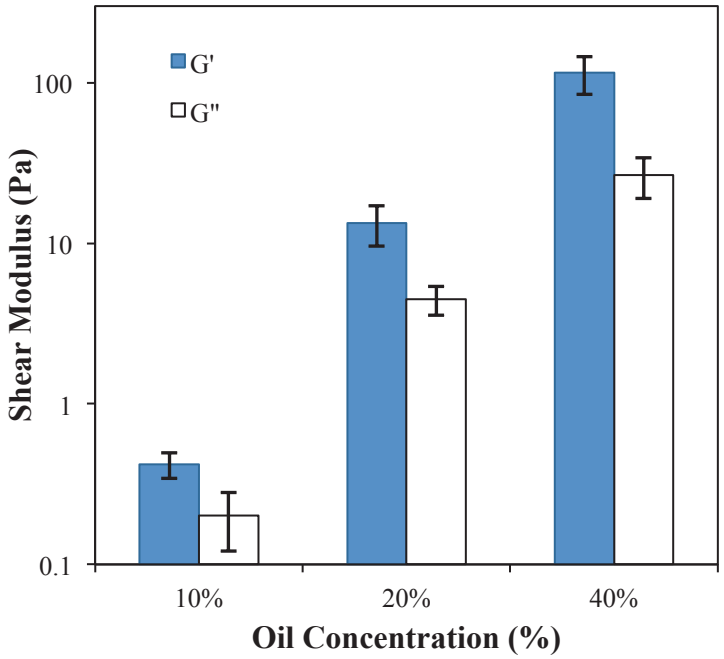

Figure 6.7 Influence of oil concentration on the shear modulus of oil-in-water emulsions (pH 7) containing 40% LF-coated droplets and 60% β-Lg-coated droplets. Measurements were made at a strain of 1% and frequency of 0.1Hz.

Selected mixed emulsions (10, 20 and 40% oil) were placed in the measurement cell for 10 minutes to reach thermal equilibrium, and then their storage modulus (G') and loss modulus (G'') were measured as a function of applied shear frequency. Data for the mixed-particle emulsion containing 40% fat is shown in **Figure 6.6**. In the frequency range studied (0.1 to 10 Hz), the storage modulus was always appreciably higher than the loss modulus ($G'>G''$) indicating that the structures formed had predominantly elastic-like characteristics. The emulsion became more rigid (increasing G') with increasing frequency suggesting that there was a characteristic relaxation time associated with rearrangement of the particles in the gel network. The influence of fat content on the storage and loss modulus of the mixed-particle emulsions is reported in **Figure 6.7** at a fixed frequency and strain (0.1 Hz, 1%)**.** The storage modulus was larger than the loss modulus for all samples studied, indicating that they were predominantly elastic-like. The magnitude of the storage and loss moduli increased with increasing fat content, which can be attributed to the formation of a network of droplets held together by attractive electrostatic interactions. As the fat content increases, the number of attractive particle-particle interactions per unit volume increases, which will lead to an increase in the gel strength [131].

6.3.4 Influence of Oil Concentration on Emulsion Appearance

Fat droplets play an important role in determining the optical properties of emulsion-based products because of their ability to scatter light waves [132]. We therefore measured the influence of droplet concentration on the overall color (L^*, a^*, b^*) values of the single-particle and mixed-particle emulsions (**Figure 6.8**). L^* values are a measure of lightness (higher value indicates a lighter color), a^* values are a

measure of redness/greenness, and, b^* values are a measure of yellowness/blueness. The overall color intensity ("chroma") of the emulsions was calculated from these values: $C^* = [(a^*)^2 + (b^*)^2]^{1/2}$. We found that the lightness and chroma of the single-particle and mixed-particle emulsions were fairly similar, and did not depend strongly on fat content from 5 to 40 wt% oil. These results suggest that changing the fat content within this range does not have a major impact on the visual appearance of the products (provided creaming does not occur). Our data is in agreement with experimental and theoretical studies of the influence of droplet concentration on the color of oil-in-water emulsions [53, 133, 134].

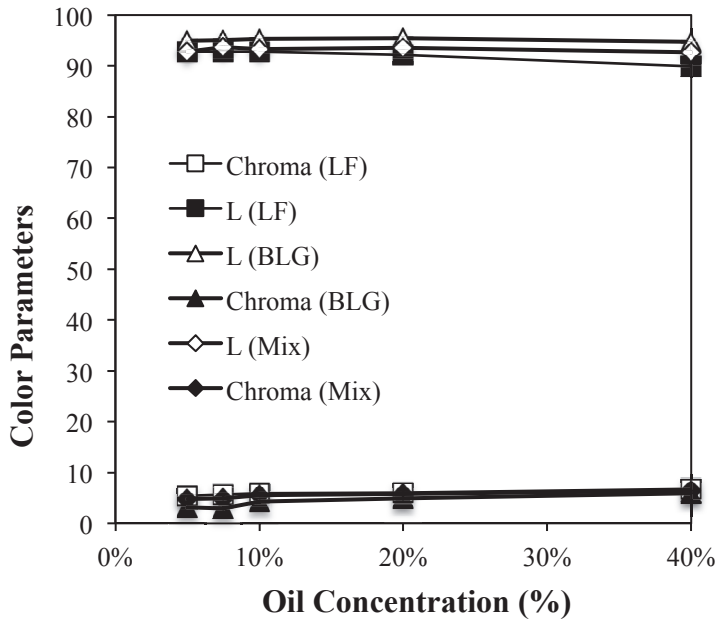

Figure 6.8 Influence of oil concentration on the color parameter (lightness and chroma) of oil-in-water emulsion (pH 7) containing β-Lg-coated droplets, LF-coated droplets, or a mixture of 40% LF-coated droplets and 60% β-Lg-coated droplets (mixture). Pictures were recorded 24h after storage (upper pictures), and then after these samples were inverted (lower pictures).

6.4.5 Creaming Stability of Microcluster Suspensions

Visual observations of the mixed-particle samples after 24 hours storage

indicated that creaming occurred in the samples with the lower fat contents (≤ 20 wt%), but not in the sample with the highest fat content (40 wt%)(**Figure 6.9**). When the samples were inverted after 24 hours storage, the ones with relatively low fat contents (≤ 20 wt%) flowed to the bottom of the tubes, whereas the ones with the highest fat content (40 wt%) remained at the top. The observed creaming instability can be attributed to the increase in particle size that occurs when droplets become aggregated, which increases the gravitational force acting on the particles, thereby leading to more rapid creaming [49]. At low droplet concentrations, there were insufficient particles present to form a three-dimensional network throughout the entire volume of the material and so the microclusters were free to move upwards, but at high droplet concentrations a space-filling particle network was formed that inhibited droplet movement. The fact that the mixed-particle systems with low and intermediate fat contents could flow to the bottom of the tubes after inversion suggests that the gels formed were relatively weak. Indeed, visual observations of the samples suggested they had a texture similar to yogurt. The single-particle samples were all stable to phase separation during storage (data not shown), which can be attributed to their relatively small droplet sizes. They also all flowed to the bottom of the tubes after inversion, which indicated that they were fluid-like. The physicochemical basis for the influence of microcluster formation on the creaming stability of the mixed-particle emulsions is discussed in the following section.

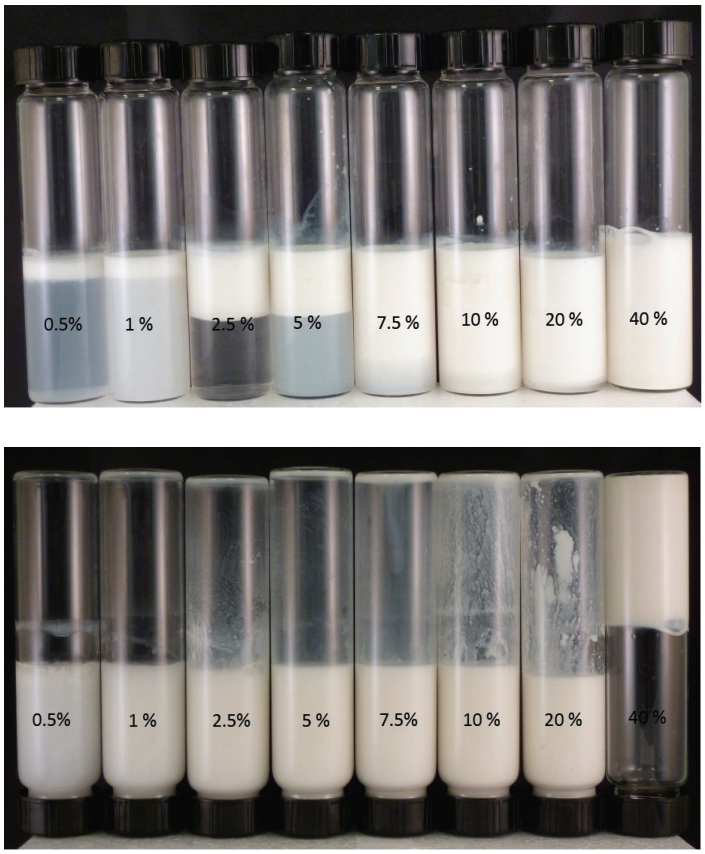

Figure 6.9 Influence of oil concentration on the visible appearance of oil-in-water emulsions (pH 7) containing 40% LF-coated droplets and 60% β-Lg-coated droplets. Pictures were recorded 24h after storage (upper pictures), and then after these samples were inverted (lower pictures).

6.4 Creaming and Viscosity of Microcluster Suspensions

In this section, we use simple mathematical models to account for the influence of microcluster formation on the creaming stability and viscosity of mixed-particle emulsions containing microclusters.

6.4.1 Creaming Stability of Microcluster Suspensions

The creaming rate of an isolated rigid spherical particle in an ideal liquid is given by Stoke's law [49]:

$$U = -\frac{2gr^2(\rho_2 - \rho_1)}{9\eta_1} \tag{6.1}$$

Where U is the creaming velocity, η is the shear viscosity, r is the particle radius, g is the acceleration due to gravity, ρ is the density, and the subscripts *1* and *2* refer to the continuous and dispersed phases, respectively. The creaming rate of a flocculated emulsion depends on the size, concentration, and structure of the flocs. If one assumes that the flocs are spherical then Stoke's Law can be used to predict the creaming velocity, except the characteristics of the individual droplets are replaced by those of the flocs:

$$U_{floc} = -\frac{2gr_{floc}^2(\rho_{floc} - \rho_1)}{9\eta_1} \tag{6.2}$$

The radius (r_{floc}) and density (ρ_{floc}) of flocs depend on the number of droplets per floc (n) and the internal packing of the droplets within the flocs (ϕ_i = [volume of droplets within floc]/[volume of floc]). If it is assumed that the droplets are evenly arranged within the flocs then:

$$r_{floc} = r \cdot \sqrt[3]{\frac{n}{\phi_i}} \tag{6.3}$$

where, ϕ_i is independent of the floc size. For random close packing of hard spheres $\phi_i = 0.63$ [49]. This equation indicates that the floc size should increase as the number of droplets within it increases or the packing density decreases. If it is assumed that the droplets form fractal aggregates with a fractal dimension of D then the floc size is related to the internal packing of the droplets within the floc by [135]:

$$r_{floc} = r \cdot \phi_i^{1/(D-3)} \tag{6.4}$$

This equation indicates that the size of a fractal floc increases as the fractal dimension decreases because the packing of the droplets within the flocs becomes more open. For a constant fractal dimension, the internal packing of the droplets within the flocs decreases as the floc size increases (since $D < 3$).

The density of the flocs can be calculated from knowledge of the packing of the droplets within them:

$$\rho_{floc} = \phi_i \rho_2 + (1 - \phi_i)\rho_1 \tag{6.5}$$

Flocculation increases the effective size of the particles within the emulsion (which enhances creaming), while decreasing the density contrast between the particles and the surrounding fluid (which retards creaming). The overall influence of flocculation on the creaming velocity can be conveniently characterized by a creaming instability ratio: U_{floc}/U. For dilute emulsions this ratio can be calculated using Stoke's law (Equations 1 and 2) and the density of the flocs (**Equation 6.5**):

$$\frac{U_{floc}}{U} = \frac{r_{floc}^2 \phi_i}{r^2} \tag{6.6}$$

As expected this equation predicts that the creaming rate should increase as the size of the flocs increases or as the droplets become more densely packed within the flocs. For a fractal floc the creaming instability ratio is related to the fractal dimension:

$$\frac{U_{floc}}{U} = \left(\frac{r_{floc}}{r}\right)^{D-1} \tag{6.7}$$

Since D ranges between 1 and 3 flocculation should always cause an increase in creaming velocity in dilute emulsions containing fractal flocs.

In a concentrated non-flocculated suspension the creaming velocity is reduced because of hydrodynamic interactions between the particles and can be described by a semi-empirical equation:

$$U_{\phi} = U\left(1 - \frac{\phi}{\phi_c}\right)^{k\phi_c} \tag{6.8}$$

where, ϕ is the disperse phase volume fraction, and ϕ_c and k are parameters that depend on the nature of the spherical particles. Normally, ϕ_c is related to the disperse phase volume fraction at which the spherical particles become close packed. This equation predicts that the creaming velocity decreases as the droplet concentration increases, until creaming is completely inhibited once a certain disperse phase volume fraction (ϕ_c) has been exceeded. Typically, this value is taken to be approximately equal to that of random close packing of spheres, *i.e.,* $\phi_c \approx 0.63$. To a first approximation, the creaming velocity of a concentrated suspension containing spherical flocs can be described by the same equation by replacing U with U_{floc} and ϕ with ϕ_{floc} ($=\phi/\phi_i$):

$$U_{\phi} = U_{floc}\left(1 - \frac{\phi}{\phi_c\phi_i}\right)^{k\phi_c} \tag{6.9}$$

This equation indicates that the creaming velocity should decrease as the particle size increases (through U_{floc}), as the droplet concentration increases (through ϕ), or as the packing of the droplets within the microclusters decreases (through ϕ_i). The above equations explain why we observed faster creaming in the dilute mixed-particle emulsions containing microclusters (large r) than in the dilute single-particle emulsions containing individual droplets (small r), and why creaming was not observed in the mixed-particle emulsions at higher droplet concentrations, where $\phi/\phi_i \approx \phi_c$ (**Figure 6.9**)

6.4.2 Rheology of Microcluster Suspensions

The concentration dependence of the apparent viscosity (η) of non-flocculated emulsions can be described over a wide range of droplet concentrations using the following semi-empirical equation [136]:

$$\frac{\eta}{\eta_1} = \left(1 - \frac{\phi}{\phi_c}\right)^{-[\eta]\phi_c} \tag{6.10}$$

where, [η] is the intrinsic viscosity (= 2.5) and ϕ_c is a parameter related to the disperse phase volume fraction at which the spherical particles become close packed, *i.e.,* $\phi_c \approx 0.63$. This equation describes the experimental observation that the viscosity of a single-particle emulsion increases dramatically when the droplets become close packed (*i.e.,* $\phi \sim \phi_c$).

The apparent viscosity of a flocculated emulsion depends on the concentration, size and structure of the flocs. In the case where the floc structure is unaltered by the application of shear forces, the apparent viscosity of a concentrated suspension containing spherical flocs can be described by Equation 10 by replacing ϕ with ϕ_{floc} ($=\phi/\phi_i$):

$$\frac{\eta}{\eta_1} = \left(1 - \frac{\phi}{\phi_c\phi_i}\right)^{-[\eta]\phi_c/\phi_i} \tag{6.11}$$

This equation predicts that the rapid increase in apparent viscosity of a flocculated should occur at a lower droplet volume fraction than for a non-flocculated emulsion, by an amount that increases as the openness of the droplet packing within the flocs increases. This phenomenon would therefore account for the fact that the mixed-

particle emulsions containing microclusters ($\phi_i < 0.63$) had higher viscosities than the single-particle emulsions containing individual droplets ($\phi_i = 1$).

6.5 Conclusions

This study investigated the influence of fat content on the rheological and optical characteristics of colloidal dispersions containing mixtures of negatively and positively charged protein-coated lipid droplets. The shear viscosity of mixed-particle emulsions was much higher than single-particle emulsions of the same fat content, which was attributed to the formation of microclusters containing positive and negative droplets held together by electrostatic attraction. The effective volume fraction of these microclusters is higher than that of the individual droplets from which they are comprised, due to the solvent trapped inside them. The mixed-particle emulsions exhibited strong shear thinning behavior, which was attributed to microcluster deformation and disruption. The apparent shear viscosity of mixed-particle emulsions increased with increasing fat content, and eventually paste-like materials were formed at high droplet concentrations. It was possible to formulate mixed-particle emulsions with relatively low fat contents (7.5%) that had similar viscosities to single-particle emulsions with high fat contents (40%). The appearance of mixed-particle and single-particle emulsions was fairly similar, and did not depend strongly on fat content from 5 to 40%. Overall, this study provides valuable insights into the properties of highly viscous and paste-like materials formed by controlled hetero-aggregation of oppositely charged particles. These materials may be useful functional components in commercial products, for example reduced-fat foods, cosmetics, or personal care products.

CHAPTER 7

MODULATION OF EMULSION RHEOLOGY THROUGH ELECTROSTATIC HETERO-AGGREGATION OF OPPOSITELY CHARGED LIPID DROPLETS: INFLUENCE OF PARTICLE SIZE AND EMULSIFIER CONTENT

7.1 Introduction

There is growing interest in the utilization of soft matter physics principles to fabricate commercial materials with novel physicochemical and functional properties, *e.g.,* foods, cosmetics, and pharmaceuticals [72, 73]. Recent studies have reported that controlled hetero-aggregation of oppositely charged lipid droplets can be used to manipulate the characteristics of emulsion-based products [20, 21, 113]. These studies have shown that products with high viscosities or paste-like characteristics can be prepared by mixing an emulsion containing positive droplets with another one containing negative droplets. The oppositely charged droplets interact with each other through electrostatic attraction leading to the formation of microclusters. At sufficiently high particle concentrations, a three-dimensional network of aggregated droplets extends throughout the volume of the material leading to elastic-like behavior. The microstructure and rheological properties of these mixed systems has been shown to depend on total particle concentration, on the ratio of positive-to-negative particles, and on aqueous phase properties that modulate electrostatic interactions, such as pH and ionic strength [20, 21]. The novel materials produced by controlled hetero-aggregation of lipid droplets may be useful for a range of commercial applications, such as pharmaceuticals, foods, and cosmetics. For example, this principle can be used to produce reduced-fat food products with similar textures as high-fat products [105].

In this article, we focus on the influence of particle size on microcluster formation and rheology of mixed emulsions created by electrostatic hetero-aggregation of oppositely charged lipid droplets. We also examine the influence of initial protein content on the formation and properties of these systems, since free protein may bind to any charged sites on lipid droplet surfaces and alter their ability to interact with other droplets. The knowledge gained from this study will facilitate the rational design of emulsion-based products where highly viscous or gel-like characteristics are required at low particle concentrations.

7.2 Experimental Methods

7.2.1 Materials

Corn oil was purchased from a commercial food supplier (Mazola, ACH Food Companies, Inc., Memphis, TN) and stored at 4 °C until use. Lactoferrin powder (LOT #10404498) was supplied by Friesland-Campinanin (Delhi, NY) and was reported to contain 97.7% protein and 0.12% ash. β-lactoglobulin powder (BioPURE, LOT #JE-001-0-415) was supplied by Davisco Foods International (Eden Prairie, MN) and was reported to contain 97.4% total protein, 92.5% β-lactoglobulin (β-Lg), and 2.4% ash. Glacial acetic acid, sodium acetate, and Bradford assay agents were purchased from Sigma-Aldrich (Sigma Chemical Co., St. Louis, MO) or Fisher Scientific (Pittsburgh, PA). All other chemicals were purchased from Sigma-Aldrich (St Louis, MO). Double distilled water was used to prepare all solutions.

7.2.2 Emulsion Preparation

7.2.2.1 Formation of Single-protein Emulsions

Aqueous emulsifier solutions were prepared by dispersing either β-Lg powder or LF powder into acetic acid buffer (pH 6, 10 mM), and then stirring for at least 3 h at room temperature to ensure complete dispersion. The pH of the protein solutions was then adjusted to 6.0 using 1M NaOH or HCl. Oil-in-water emulsions containing a single protein type were prepared by blending 20 g of corn oil and 80 g of aqueous protein solution for 2 min using a hand blender (M133/1281-0, 2 speed, Biospec Products Inc., ESGC, Switzerland) and then recirculating them four-times through a two-stage homogenizer (LAB 1000, APV-Gaulin, Wilmington, MA) at a first-stage/second-stage pressure of 5,400/600 psi (to produce small droplets) and 400/10 psi (to produce large droplets). β-Lg emulsions were then heated to 90 ºC for 30 min to cross-link the adsorbed proteins, so as to prevent any competitive adsorption effects with the lactoferrin mixed systems. All emulsions were then stored for 24 hours prior to utilization.

Preliminary experiments established that a β-Lg-to-oil mass ratio of 0.05-to-1 and a LF-to-oil mass ratio of 0.3-to-1 were suitable to form single-protein emulsions with relatively little free protein [20]. Based on this knowledge, two different levels of protein were used to prepare 20 wt% oil-in-water emulsions with different non-adsorbed protein contents: (i) 1% β-Lg and 6% LF; (ii) 0.1% β-Lg and 0.6% LF. 1.0% β-Lg and 6% LF are suitable for producing emulsions with relatively small droplet diameters ($d_{43} \approx 0.35$ μm) with little free protein. Hence, when droplets containing relatively large droplets are produced at low homogenization pressures using this amount they will contain an appreciable amount of protein that is not directly adsorbed at the oil-water interface.

7.2.2.2 Formation of Mixed-protein Emulsions

Mixed emulsions containing 0 to 20 wt% β-Lg-coated droplets (pH 6.0) and 20 to 0 wt% LF-coated droplets (pH 6.0) were prepared by mixing different ratios of the two single-protein 20 wt% oil-in-water emulsions together, stirring for 10 min, and then allowing them to stand for 24 h prior to analysis. After this time, some of emulsions separated into a thin white creamed layer on top of a clear or slightly turbid serum layer, and so all samples were gently stirred prior to analysis to ensure they were homogeneous.

We prepared a series of mixed emulsion samples containing droplets with different sizes and charges: (i) Small Cationic – Small Anionic, S(+):S(-); (ii) Large Cationic – Small Anionic, L(+):S(-); (iii) Small Cationic – Large Anionic, S(+):L(-); and, (iv) Large Cationic – Large Anionic, L(+):L(-). For most experiments, the small anionic and cationic droplets were produced by homogenizing at high pressure using 1.0% β-Lg and 6.0% LF (respectively), while the large anionic and cationic droplets were produced by homogenizing at low pressure using 0.1% β-Lg and 0.6% LF. However, in some experiments we also produced anionic and cationic emulsions with high levels of additional protein by homogenizing at low pressure using 1.0% β-Lg and 6.0% LF.

7.2.3 Emulsion Characterization

7.2.3.1 Particle Charge Measurements

The ζ-potential of emulsions was determined using a particle electrophoresis instrument (Zetasizer Nano ZS, Malvern Instruments, Worcestershire, UK). The ζ-potential of any particles in the system was measured after 200-fold dilution with an acetic acid buffer solution (pH = 6.0). After loading the samples into the instrument they

were equilibrated for about 120 s before particle charge data were collected over 20 continuous readings.

7.2.3.2 Particle Size Analysis

The particle size distribution of emulsions was measured using a laser diffraction particle size analyzer (Mastersizer 2000, Malvern Instruments, Ltd., Worcestershire, UK). To avoid multiple scattering effects the emulsions were diluted approximately 200-fold using pH-adjusted acetic acid buffer (pH = 6.0). The emulsions were stirred continuously throughout the measurements to ensure they were homogenous. Measurements are reported as the volume-length mean diameter: $d_{43}=\sum d_i n_i^4 / \sum d_i n_i^3$, where n_i is the number of droplets of diameter d_i.

7.2.3.3 Rheological Properties

The rheological behavior of samples was measured using a dynamic shear rheometer (Kinexus Rotational Rheometer, Malvern, U.K.). A cup and bob geometry consisting of a rotating inner cylinder (diameter 25 mm) and static outer cylinder (diameter 27.5 mm) was used in viscosity. The samples were loaded into the rheometer measurement cell and allowed to equilibrate at 25 ºC for 5 min before beginning all experiments. Samples underwent a constant shearing treatment (1 s^{-1} for 10 min) prior to analysis to remove history effects. The shear stress of the emulsions was then measured over a range of shear rates (0.01 to 10 s^{-1}), and the apparent viscosity was calculated from this data.

7.2.3.4. Microstructure Analysis

The microstructure of the mixed emulsions was assessed by optical microscopy. Mixed emulsions were diluted 30-fold and then gently agitated in a glass test tube before

analysis to ensure that they were homogeneous and that the particles could be easily distinguished from one another. A drop of diluted sample was then placed on a microscope slide and covered by a cover slip, and then the microstructure was determined using optical microscopy (Nikon microscope Eclipse E400, Nikon Corporation, Japan). Images were acquired using a CCD camera (CCD-300-RC, DAGE-MTI, Michigan City, IN) connected to digital image processing software (Micro Video Instruments, Inc., Avon, MA) installed on a computer. All microscopic examinations were carried out on the same day as the ζ-potential and particle size measurements.

7.2.4 Statistical Analysis

All experiments were carried out in either duplicate or triplicate using newly prepared samples. Results are reported as the calculated means and standard deviations.

7.3 Results and Discussion

7.3.1 Characteristics of Single-protein emulsions

Initially, the mean diameters and electrical characteristics of the particles in the single-protein 20 wt% oil-in-water emulsions (pH 6) were analyzed. Small anionic droplets [S(-)] were produced using a relatively high emulsifier concentration (1% β-Lg) and homogenization pressure, whereas large anionic droplets [L(-)] were produced using a relatively low emulsifier concentration (0.1% β-Lg) and homogenization pressure. Similarly, small cationic droplets [S(+)] were produced using a relatively high emulsifier concentration (6% LF) and homogenization pressure, whereas large cationic droplets [L(+)] were produced using a relatively low emulsifier concentration (0.6% LF) and homogenization pressure. The β-lactoglobulin-coated lipid droplets [L(-) and S(-)] had

ζ-potentials of ≈ -19 and -30 mV and mean particle diameters (d_{43}) of ≈ 3.0 and 0.3 μm, respectively. The LF-coated lipid droplets [L(+) and S(+)] had ζ-potentials of ≈ +10 and +11 mV and d_{43} of ≈ 3.5 and 0.3 μm, respectively. The two emulsions had opposite charges because pH 6 is between the isoelectric point of β-Lg (pI ≈ 5) and LF (pI ≈ 8). The magnitude of the charge on the β-Lg-coated droplets was appreciably different for droplets with different sizes, whereas that of the LF-coated droplets was not. The physicochemical origin of the dependence of droplet charge on particle size for the β-Lg-coated droplets is currently unknown. Overall, these experiments showed that we were able to prepare single-protein emulsions containing lipid droplets that were either cationic or anionic and either small or large by varying emulsifier type, concentration, and homogenization conditions.

7.3.2 Influence of Particle Size on Hetero-aggregation in Mixed Emulsions

The objective of these experiments was to establish the influence of initial droplet size on the aggregation behavior of emulsions containing mixtures of negative and positive lipid droplets. The mixed emulsions were formed by combining different ratios of cationic and anionic single-protein emulsions. The ζ-potential of all the mixed emulsions went from negative to positive as the percentage of positive (LF-coated) lipid droplets increased, although the points of zero charge depended somewhat on droplet size (**Figure 7.1**). Part of this difference can be attributed to the dependence of the initial charge of the negative (β-Lg-coated) droplets on their size: ζ ≈ -19 and -30 mV for large and small droplets, respectively. Consequently, a smaller amount of large anionic droplets was needed to neutralize the charge on a fixed amount of cationic droplets, than small anionic droplets. In addition, the organization of the droplets within the clusters

formed by hetero-aggregation may have depended on droplet size [24], which would alter the net charge characteristics of the composite particles. Our results show that it is possible to create clusters with different electrical characteristics by mixing together different ratios of lipid droplets with different particle sizes and charges.

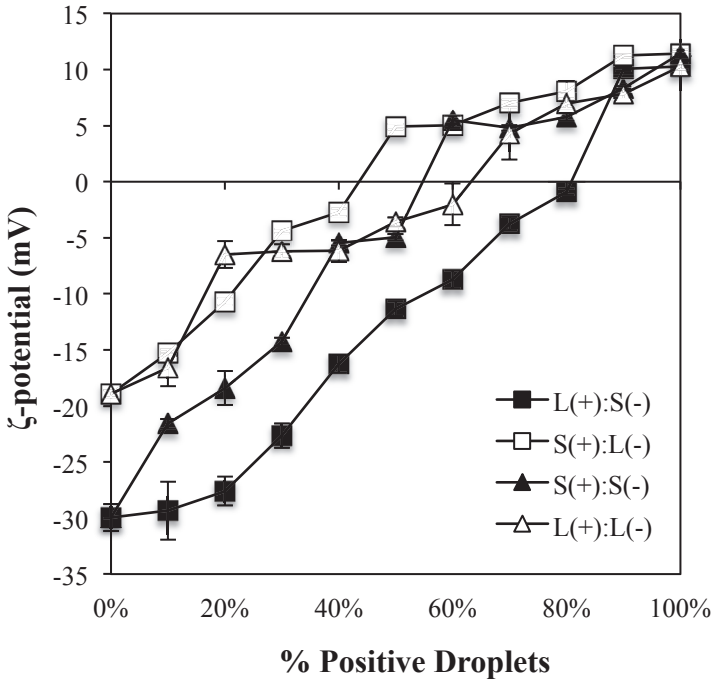

Figure 7.1 Dependence of particle charge (ζ-potential) on the ratio of positive-to-negative droplets in mixed emulsions prepared by mixing LF-coated lipid droplets with β-Lg-caoted lipid droplets (pH6). Key: L=large droplets; S= small droplets; += cationic droplets; -+ anionic droplets.

We also measured the mean diameter (d_{43}) of the particles present within the mixed systems as a function of particle ratio using static light scattering (**Figure 7.2**). Initially, we compare the behavior of mixed emulsions with similar droplet sizes (either both small or both large), but different charges (one positive and one negative). There was not a large change in the mean particle size when mixed emulsions were prepared by mixing large positive and large negative droplets together (**Figure 7.2a**). A maximum mean particle diameter of around 6.4 μm was reached at 40% positive/60% negative

droplets, which indicated that any clusters formed were relatively small (about twice as big as the original lipid droplets). Conversely, there was a large increase in the mean particle size when mixed emulsions were prepared by mixing small positive and small negative droplets together (**Figure 7.2a**). A maximum mean particle diameter was also observed at 40% positive/60% negative droplets, but the mean particle diameter was over 60 μm (*i.e.,* over 100 times the diameter of the original lipid droplets). These results suggest that small droplets are much more effective at forming clusters through hetero-aggregation than large droplets.

The mixed emulsions containing droplets with different sizes and different charges also showed appreciable aggregation at intermediate positive-to-negative particle ratios, but the maximum amount of aggregation occurred at different particle ratios (**Figure 7.2b**). A maximum particle size was obtained at 40% positive/60% negative droplets for the system containing small positive and large negative droplets [S(+):L(-)], but the maximum size was obtained at 60% positive/40% negative droplets for the system containing large positive and small negative droplets [L(+):S(-)]. These results clearly show that the aggregation stability of mixed emulsions depends on both the size and charge of the lipid droplets. All the mixed emulsions containing small droplets (either positive or negative) exhibited extensive droplet aggregation, but the mixed emulsions containing only large droplets did not, which suggests that small droplets are essential for forming a network of aggregated particles. Theoretical and experimental studies of suspensions of oppositely charged particles have shown that the nature of the clusters formed by hetero-aggregation depend on the relative concentrations, sizes, and charges of the different particles [24, 84], which support the findings of our study.

(a)

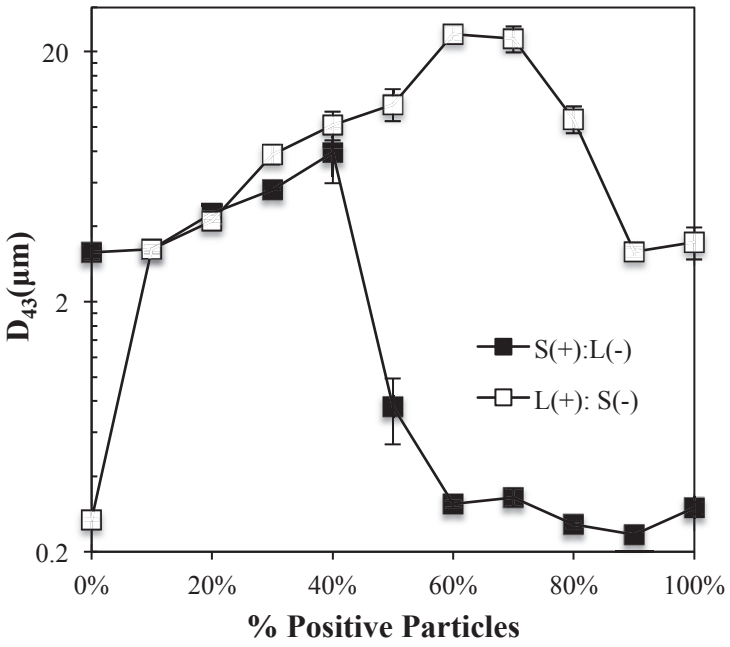
20
2
0.2
D_{43}(µm)
S(+):L(-)
L(+): S(-)
0%
20%
40%
60%
80%
100%
% Positive Particles

(b)

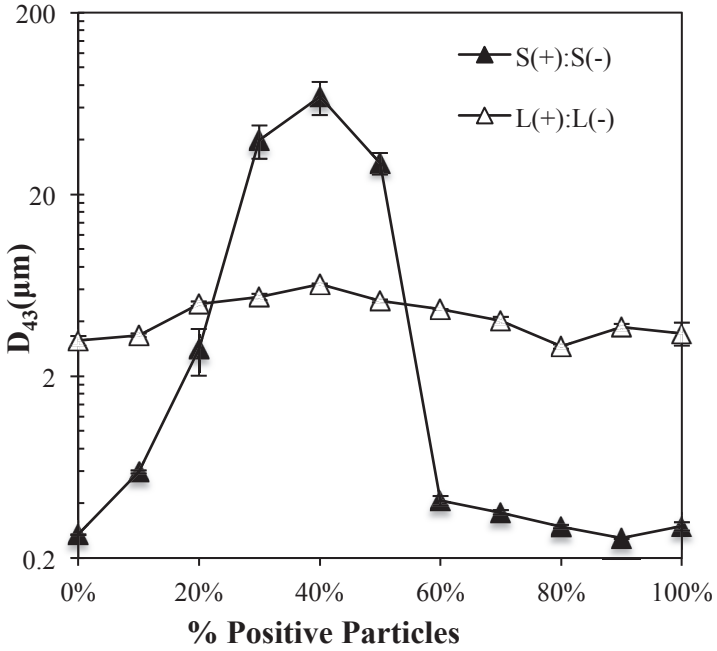
200
20
2
0.2
D_{43}(µm)
S(+):S(-)
L(+):L(-)
0%
20%
40%
60%
80%
100%
% Positive Particles

Figure 7.2 Dependence of mean particle diameter on the ratio of postitive-to-negative droplets in mixed emulsions prepared by mixing LF-coated lipid droplets with β-Lg-coated lipid droplets (pH 6). The mixed emulsions contain droplets with similar sizes, but different charges. Key: L=large droplets; S=small droplets; +=cationic droplets; - + anionic droplets

7.3.3 Influence of Particle Size on Rheology of Mixed Emulsions

The rheological properties of emulsions containing aggregated particles depend on the structural organization and interactions of the particles in the system [105, 137]. Consequently, we examined the influence of particle ratio, charge, and size on the rheology of mixed emulsions. Mixed emulsions were prepared by blending anionic droplets and cationic droplets at a particle ratio where the maximum amount of aggregation was observed (**Figure 7.2**): 40% positive/60% negative droplets for S(+):S(-), L(+):L(-) and S(+):L(-); 60% positive/40% negative droplets for L(+):S(-).

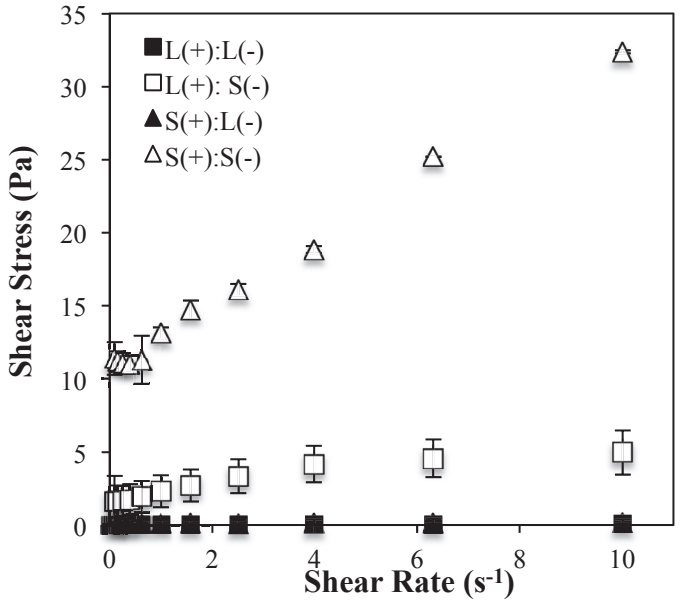

Figure 7.3 Dependence of rheological flow curves (shear stress *versus* shear rate) on the size and charge of the droplets in mixed emulsions prepared by blending LF-coated lipid droplets with β-Lg-coated lipid droplets (pH 6). Key: L= large droplets; S= small droplets; + = cationic droplets,; - = anionic droplets.

The rheological flow profiles (shear stress *versus* shear rate) of mixed emulsions containing different droplet sizes and charges were measured (**Figure 7.3)**, and their apparent viscosities calculated (**Figure 7.4**). Emulsions containing large cationic and large anionic droplets were fluid-like and had relatively low apparent viscosities. On the other hand, emulsions containing small cationic and small anionic droplets were paste-like, *i.e.,* they did not flow until a critical yield stress was exceeded (≈ 10 Pa), but then they flowed at higher applied stresses with a high apparent viscosity. Emulsions containing large cationic droplets and small anionic droplets [L(+):S(-)] also exhibited some paste-like characteristics, but the yield stress (2 Pa) was considerably lower than that for the mixed system containing only small droplets. Emulsions containing small cationic droplets and large anionic droplets [S(+):L(-)] were fluid-like, but their viscosity was appreciably higher than that of emulsions containing only large droplets. These results indicated that systems with very different rheological characteristics could be produced by mixing droplets with different sizes and charges.

The influence of positive-to-negative droplet ratio on the apparent viscosity at a constant shear rate (10 s^{-1}) is shown in **Figure 7.5**. There was a large increase in the apparent viscosity at intermediate particle ratios for the mixed emulsions containing small anionic and small cationic droplets, but only a slight increase in viscosity for the emulsions containing large anionic and large cationic droplets (**Figure 7.5a**). There was also an appreciable increase in the apparent viscosity at intermediate particle ratios for the mixed emulsions containing large cationic and small anionic droplets [L(+):S(-)], but only a slight increase for the emulsions containing small cationic and large anionic droplets [S(+):L(-)] (**Figure 7.5b**). The rheology measurements are therefore in good

agreement with the particle size measurements, indicating that systems where extensive droplet aggregation occurred (high d_{43}) had high viscosities or paste-like properties. This effect can be attributed the increase in effective particle concentration that occurs when droplets aggregate in emulsions [137].

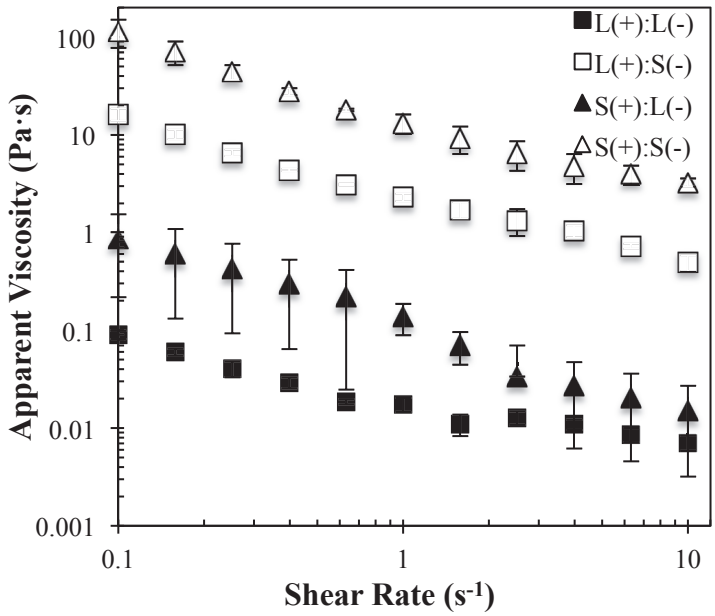

Figure 7.4 Dependence of the apparent viscosities on shear rate for mixed emulsions containing droplets with different sizes and charges prepared by blending LF-coated lipid droplets with β-Lg-coated lipid droplets (pH 6). Key: L= large droplets; S= small droplets; + = cationic droplets; - = anionic droplets.

(a)

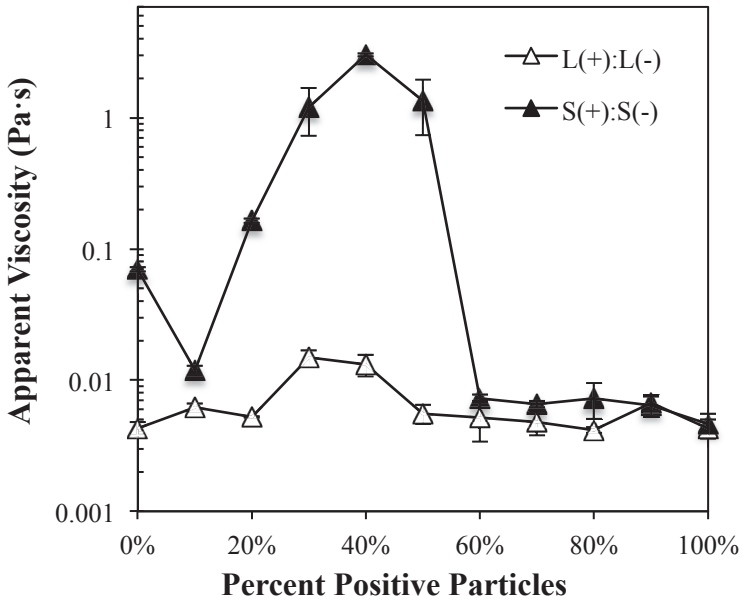

(b)

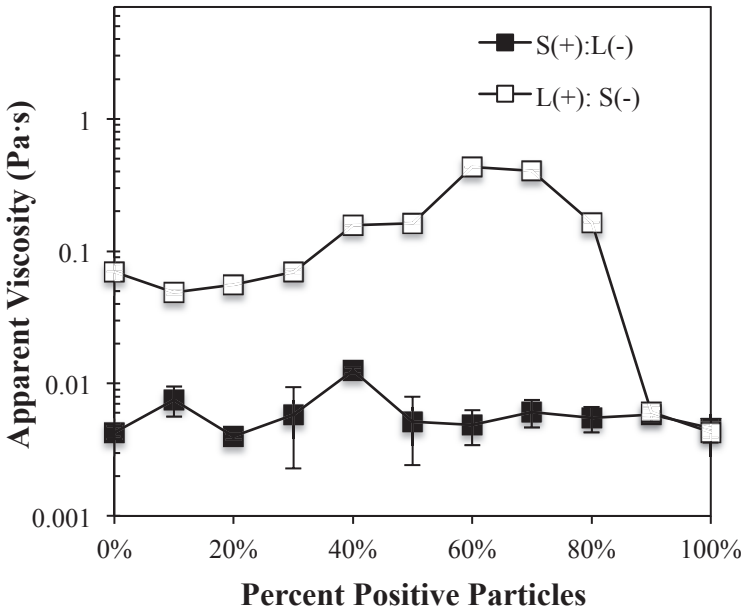

Figure 7.5 Dependence of apparent viscosity on the ratio of positive-to-negative droplets in mixed emulsions prepared by mixing LF-coated lipid droplets with β-Lg-coated lipid droplets (pH 6). The mixed emulsions contain droplets with similar size, but different charges. Key: L= large droplets; S= small droplets; + = cationic droplets; -=anionic droplets.

7.3.4 Influence of Protein Content on Hetero-aggregation

A significant fraction of the emulsifier used to form an oil-in-water emulsion may remain in the aqueous phase after homogenization, depending on the initial emulsifier concentration, the emulsifier surface load, and the surface area of droplets produced [29]. We therefore examined the influence of initial protein content on the formation of aggregates in the mixed emulsions. As in the previous section, mixed emulsions were prepared by blending anionic droplets and cationic droplets at a particle ratio where the maximum amount of aggregation was observed: 40% positive/60% negative droplets for S(+):S(-), L(+):L(-) and S(+):L(-); 60% positive/40% negative droplets for L(+):S(-).

Single-protein 20 wt% oil-in-water emulsions containing large droplets but different free protein contents were prepared by using different initial levels of emulsifier to form the anionic droplets (1.0 or 0.1% β-Lg) and cationic droplets (6 or 0.6% LF). The mean droplet diameters of all these emulsions were fairly similar: d_{43} = 3.0 and 2.7 μm for the droplets prepared using 1.0 and 0.1% β-Lg, and 3.5 and 3.1 μm for the droplets prepared using 6.0 and 0.6% LF. Since the mean droplet sizes (and therefore the surface areas) were similar there should have been a higher concentration of free proteins or weakly adsorbed proteins in the emulsions prepared with the higher amounts of initial protein. The electrical characteristics of the droplets in the single-protein emulsions depended somewhat on initial protein content: ζ-potential = -33.4 and -18.9 mV for droplets prepared using 1.0 and 0.1% β-Lg, and + 12.1 and + 10.3 mV for droplets prepared using 6.0 and 0.6% LF. These differences in electrical characteristics may have been due to changes in interfacial composition caused by additional protein, or due to non-adsorbed protein contributing to the electrophoretic signal used to calculate the ζ-

potential. Nevertheless, the β-Lg-coated and LF–coated oil droplets still had opposite charges at this pH. Single-protein 20 wt% oil-in-water emulsions containing small anionic or cationic droplets were formed at constant protein contents (1.0% for β-Lg and 6.0% for LF). Mixed emulsions were then formed by blending emulsions containing anionic droplets (small or large) with those containing cationic droplets (small or large).

Measurements of the net charge, mean particle diameter, and apparent viscosity (at 10 s^{-1}) of mixed emulsions containing different particle sizes and charges indicated that additional protein had an appreciable influence on their physicochemical properties (**Figure 7.6)**. The magnitude and sign of the electrical charge in the mixed systems depended on the initial level of protein present (**Figure 7.6a)**. For example, the particles in the mixed emulsion containing large cationic and small anionic droplets [L(+):S(-)] were negatively charged at low protein content but positively charged at high protein content. The additional protein in this case was cationic LF, which may have adsorbed to the surfaces of the β-Lg-coated droplets making them less negative or even positive.

The degree of particle aggregation (**Figure 7.6b**) and the increase in viscosity (**Figure 7.6c**) were appreciably lower for the mixed emulsions containing high protein contents than those containing low protein contents. Optical microscopy images of the mixed emulsions also showed that there was less flocculation in the emulsions containing the higher protein contents (**Figure 7.7**). We propose that there was a competition between droplet-droplet and droplet-protein interactions in these mixed systems. Droplet-droplet interactions dominate at low protein levels, whereas droplet-protein interactions dominate at high protein levels. For example, anionic proteins may bind to the surfaces of cationic droplets, thereby reducing the tendency of the cationic droplets to

aggregate with anionic droplets. These results clearly show that the amount of free protein present in the mixed emulsions has a major impact on their physicochemical properties, and so this parameter should be controlled when utilizing hetero-aggregation to create novel structures and textures.

(a)

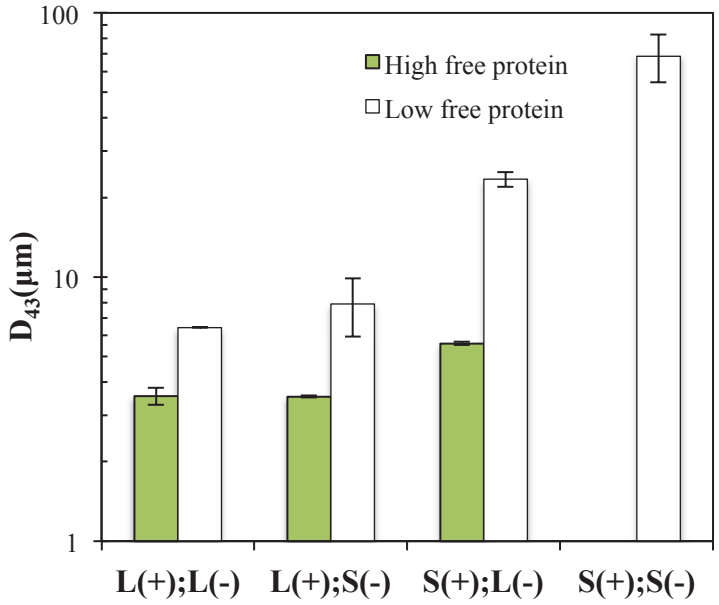

(b)

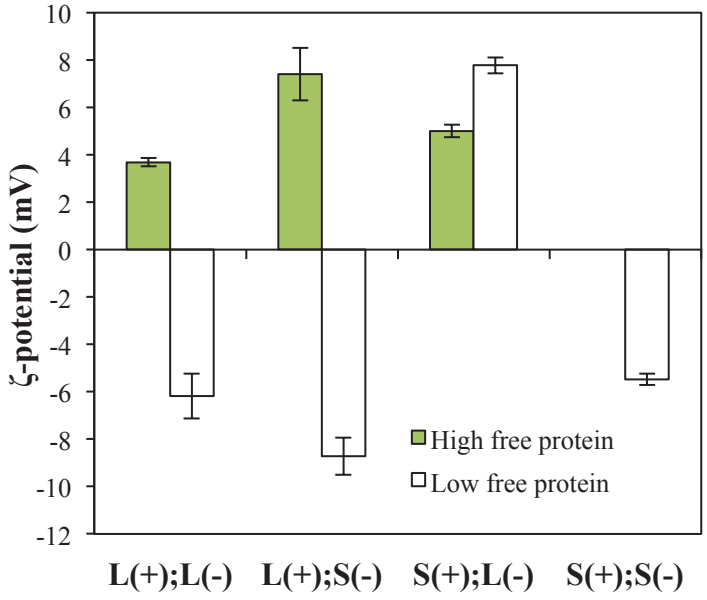

(c)

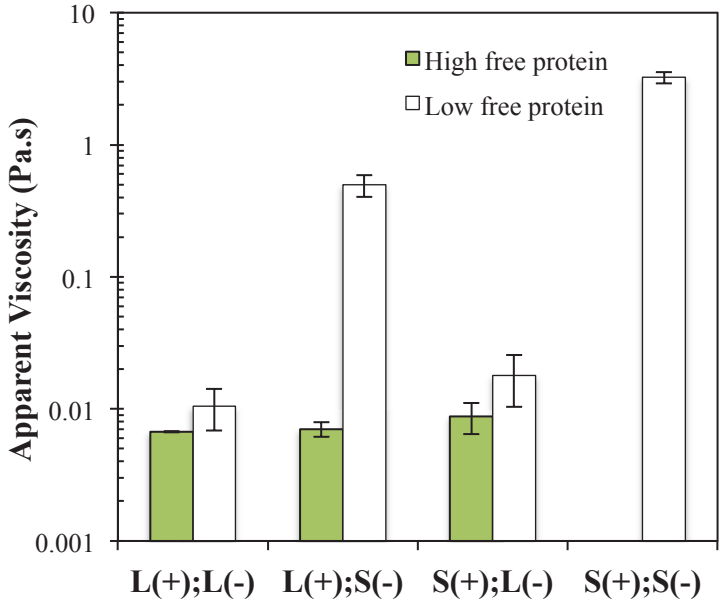

Figure 7.6 Influence of free protein content on (a) electrical charge, (b) mean particle size and (c) apparent viscosity of mixed emulsions prepared by blending LF-coated lipid droplets with β-Lg-coated lipid droplets (pH 6). Key: L= large droplets; S = small droplets; + = cationic droplets; - = anionic droplets.

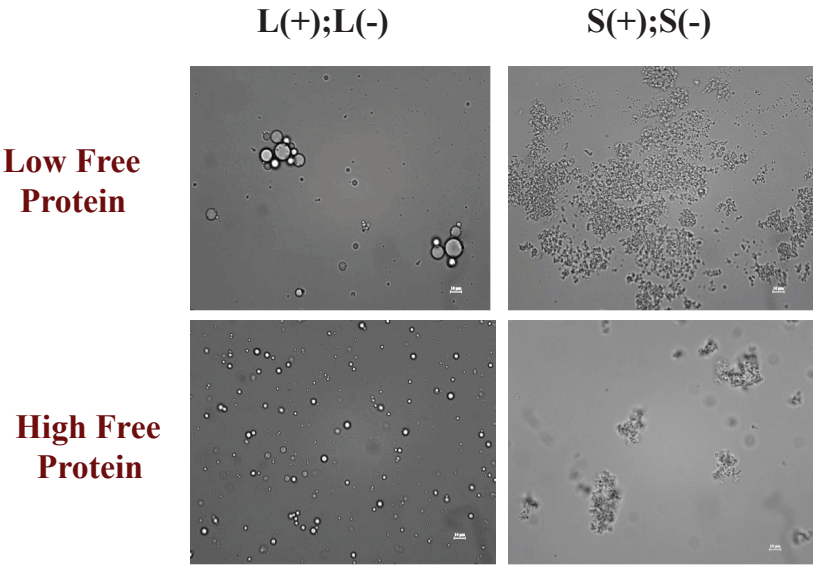

Figure 7.7 Microstructure of mixed emulsions prepared by blending LF-coated lipid droplets with β-Lg-coated lipid droplets (pH 6). Key: L= large droplets; S = small droplets; + = cationic droplets; - = anionic droplets.

7.4 Conclusions

This study has shown that the rheological properties of colloidal dispersions consisting of mixtures of negatively and positively charged protein-coated lipid droplets can be modulated by varying particle size, positive-to-negative particle ratio, and free protein content. Highly viscous or paste-like materials can be formed in mixed emulsions containing only small droplets at intermediate particle ratios, but not in mixed emulsions containing only large droplets. This effect can be attributed to the better ability of small droplets to form a three-dimensional network of aggregated particles that extends throughout the volume of the system. The presence of additional proteins in the mixed emulsions decreased the tendency for droplet aggregation to occur, which was attributed to a competition between droplet-protein and droplet-droplet electrostatic interactions. Overall, this study provides valuable insights into the formation and rheological properties of highly viscous or paste-like materials by controlled hetero-aggregation of oppositely charged particles. These materials may be useful functional components in commercial products such as reduced-fat foods, cosmetics, pharmaceuticals, or personal care products.

CHAPTER 8

INFLUENCE OF ELECTROSTATIC HETERO-AGGREGATION OF LIPID DROPLETS ON THEIR STABILITY AND DIGESTIBILITY UNDER SIMULATED GASTROINTESTINAL CONDITIONS

8.1 Introduction

There is considerable interest in the utilization of structural design principles to create colloidal foods with improved nutritional profiles, by controlling lipid digestibility within the gastrointestinal tract [71, 72], by encapsulating, protecting and delivering lipophilic bioactive agents through the diet [138, 139], and by reducing the caloric density of high calorie foods [73]. Structural design principles have been utilized to create novel functional attributes in foods by controlling the spatial organization of their ingredients to form structures such as particles, fibers, tubes, sheets, and coatings . Recent studies have shown that novel properties can be created using food-grade ingredients by controlled hetero-aggregation of oppositely charged lipid droplets [21, 140]. The microstructure and rheological properties of these systems can be manipulated by controlling the total lipid content, the ratio of positive-to-negative particles, the particle size, and the environmental conditions (*e.g.,* pH, ionic strength, and temperature). This approach may therefore have potential application in the food industry to create products with novel textural characteristics or reduced fat contents (since highly viscous products can be formed at lower fat contents than in the absence of hetero-aggregation).

Previously, we induced hetero-aggregation by mixing an emulsion contain cationic protein-coated lipid droplets with one containing anionic protein-coated droplets[20, 21]. This was achieved by using two globular proteins with different

isoelectric points (pI) to stabilize the lipid droplets: β-lactogobulin (pI ≈ 5) and lactoferrin (pI ≈ 8). At pH values between the isoelectric points of the two proteins, the lipid droplets have opposite charges and therefore tend to aggregate through electrostatic attraction. The purpose of the current study was to examine the influence of hetero-aggregation on the potential biological fate of ingested emulsions, since this might influence the rate of lipid digestibility and/or the release of any encapsulated bioactive components. Indeed, a number of studies have shown that droplet aggregation under simulated or actual gastrointestinal tract (GIT) conditions may influence the biological fate of ingested emulsions[61, 141]. Previous research has examined the stability and digestion of lipid droplets coated with either β-lactoglobulin[142-144] or lactoferrin[58, 100, 145]. However, there have been no previous studies on the influence of hetero-aggregation of protein-coated lipid droplets on their behavior under GIT conditions.

In this study, we focused on the influence of hetero-aggregation on the stability and digestibility of lipid droplets within a simulated gastrointestinal tract. We hypothesized that the electrostatic attraction between oppositely charged protein-coated lipid droplets would affect the aggregation stability, rheological properties, and digestibility of emulsions under model GIT conditions. We also compared the results obtained using a full GIT model that simulates the oral, gastric and small intestinal stages, with a simple GIT model that only simulates the small intestinal stage. This was done since simple GIT models are often used as an initial screening tool for identifying the major factors that influence the behavior of lipids under GIT conditions[64]. The knowledge gained from this study should be useful for creating emulsion-based functional food products designed to improve human health and wellness.

8.2 Experimental Methods

8.2.1 Materials

Corn oil was purchased from a commercial food supplier (Mazola, ACH Food Companies, Inc., Memphis, TN) and stored at 4 °C until use. Lactoferrin powder (LOT #10404498) was supplied by FrieslandCampinanin (Delhi, NY), and the manufacturer reported that it contained 97.7% protein and 0.12% ash. Purified β-lactoglobulin powder (BioPURE, LOT #JE-001-0-415) was supplied by Davisco Foods International (Eden Prairie, MN). The manufacturer reported the composition of this powder to be 97.4% total protein, 92.5% β-lactoglobulin (β-Lg), and 2.4% Ash. All other chemicals used in this research were purchased from Sigma-Aldrich (St Louis, MO). Double distilled water was used to make all solutions.

8.2.2 Formation of Single-protein Emulsions

Aqueous emulsifier solutions were prepared by dispersing either β-Lg powder or LF powder into distilled water, and then stirring for at least 3 h at room temperature to ensure complete dispersion. The pH of the protein solutions was then adjusted to 7.0 using 1M NaOH or HCl. Oil-in-water emulsions containing a single protein type were prepared by blending 10 g of corn oil and 90 g of aqueous protein solution for 2 min using a hand blender (M133/1281-0, 2 speed, Biospec Products Inc., ESGC, Switzerland) and then recirculating them four-times through a high pressure homogenizer (Microfluidizer M-110 L processor, Microfluidics Inc., Newton, MA) operating at 90 MPa. The β-Lg emulsion was then heated to 90 ℃ for 30 min to cross-link the adsorbed proteins, so as to prevent any competitive adsorption effects. All emulsions were then

stored for 24 hours prior to utilization. Preliminary experiments established that 1% β-Lg and 3% LF were suitable levels to form single-protein emulsions with relatively small droplet diameters ($d_{43} \approx$ 0.35 μm), and so these levels were used to form the mixed-protein emulsions.

8.2.3 Formation of Mixed-protein Emulsions

Initially, two 10 wt% oil-in-water emulsions stabilized by either 0.5% β-Lg or 3% LF were prepared in distilled water, and then adjusted to pH 7.0. These two single-protein emulsions had similar initial droplet diameters ($d_{43} \approx$ 0.35 μm). Mixed emulsions were then prepared by mixing 40 wt% of the β-Lg emulsion with 60 wt% of the LF emulsion, stirring for 10 min, then allowing them to stand for 24 h prior to analysis. This particle ratio was selected based on our previous results, which showed that the maximum amount of droplet aggregation occurred under these conditions [REF].

8.2.4 Simulated Gastrointestinal Tract

Each emulsion sample was passed through a full simulated GIT model that consisted of a mouth, gastric phase and small intestine phase, or a simple simulated GIT model that only consisted of the small intestine phase. Measurements of the microstructure, particle size distribution, and particle charge were measured at each stage (Section 2.5).

Oral stage: Artificial saliva (pH 6.8) containing 3 % mucin was prepared according to the composition shown in **Table 1.** As starch was not present in any of our emulsions, we did not include salivary amylases in the artificial saliva. The *in vitro* oral model consisted of a conical flask (125 mL) containing simulated saliva maintained at

37 °C with continuous shaking at 100 rev min^{-1} for 15 min in a temperature controlled air incubator (Innova Incubator Shaker, Model 4080, New Brunswick Scientific, New Jersey, USA) to mimic the conditions in the mouth. Each emulsion was mixed with artificial saliva (ratio 1:1 w/w). The resulting mixture contained 5% (w/w) oil and was taken for characterization at the end of the incubation period.

Chemical name	**Chemical formula**	**Concentration (g/L)**
Sodium chloride	$NaCl$	1.594
Ammonium nitrate	NH_4NO_3	0.328
Potassium phosphate	KH_2PO_4	0.636
Potassium chloride	KCl	0.202
Potassium citrate	$K_3C_6H_5O_7.H_2O$	0.308
Uric acid sodium salt	$C_5H_3N_4O_3 .Na$	0.021
Urea	H_2NCONH_2	0.198
Lactic acid sodium salt	$C_3H_5O_3Na$	0.146
Porcine gastric mucin (Type II)		30
Water	H_2O	Remainder

Table 8.1 Chemical composition of artificial saliva using to simulate oral conditions [146, 147].

Gastric stage: Simulated gastric fluid (SGF) was prepared by adding 2 g NaCl, 7 mL HCl, and 3.2 g of pepsin (from porcine gastric mucosa) to a flask and then diluting with distilled water to a volume of 1 L, and finally adjusting to pH 1.2 using 1.0 M HCl (United States Pharmacopeial Convention, 2000). Samples taken from the oral stage were mixed with SGF (ratio 1:1 w/w) so the final mixture contained 2.5% (w/w) oil.

This mixture was then adjusted to pH 2.5 using 1 M NaOH and incubated at 37 °C for 2 h. Samples were taken for characterization at the end of the incubation period.

Small intestinal stage: Samples obtained from the simulated gastric model were incubated for 2 h at 37 °C in a simulated small intestinal fluid (SIF) containing 2.5 mL pancreatic lipase (4.8 mg mL^{-1}), 4 mL bile extract solution (5 mg mL^{-1}) and 1 mL calcium chloride solution (750 mM), and the free fatty acids (FFA) released were monitored by determining the amount of 0.25 M NaOH needed to maintain a constant pH of 7.0 within the reaction chamber using an automatic titration unit. The pH-stat used (Metrohm USA, Inc.) was controlled by dedicated software (Tiamo 1.2.1 software, Metrohm GA, Switzerland). All additives were dissolved in double distilled water (pH 7.0) before use. Lipase addition and initialization of the titration program were carrier out only after the addition of all other pre-dissolved ingredients and careful balancing of the pH to 7.0. Samples were taken for physicochemical and structural characterization at the end of the 2 h digestion period. The volume of NaOH added to the emulsion was recorded and used to calculate the concentration of free fatty acids generated by lipolysis.

The amount of free fatty acids released was calculated using the following equations:

$$V_{max}=2\times\left[\frac{m_{oil}}{MW_{oil}}\times\frac{1000}{C_{NaOH}}\right]$$

$$\%\text{FFA Released}=\frac{V_{Exp}}{V_{Max}}\times 100\%$$

Here, m_{oil} is the total mass of oil present in the reaction vessel (g), MW_{oil} is the molecular weight of the oil (g per mol), C_{NaOH} is the concentration of sodium hydroxide

in the titration burette (mol per 1000 cm^3), and V_{Max} is the volume of NaOH titrated into the reaction vessel to neutralize the FFA released assuming that all the triacylglycerols are converted into two free fatty acids. Finally, V_{Exp} is the actual volume of NaOH titrated into the reaction vessel to neutralize the FFA released during the experiment.

8.2.5 Particle size, Charge and Rheological Measurements

Particle size measurement: The particle size distribution of the emulsions was measured using a laser diffraction particle size analyzer (Mastersizer 2000, Malvern Instruments, Ltd., Worcestershire, UK). To avoid multiple scattering effects the emulsions were diluted to a droplet concentration of approximately 0.005 wt% using pH-adjusted water at the same pH as the sample. The emulsions were stirred continuously throughout the measurements to ensure the samples were homogenous. Measurements are reported as the volume-weighted mean diameter: $d_{4,3}=\sum d_i n_i^4/\sum d_i n_i^3$, where n_i is the number of droplets of diameter d_i. We note that particle size measurements made by static light scattering on highly flocculated emulsions should be treated with caution. First, the theory (Mie theory) used to interpret light scattering data assumes that the scattering particles are homogeneous spheres with well-defined refractive indices. In practice, flocs are non-spherical and non-homogeneous particles, with ill-defined refractive indices. Second, the process of dilution and stirring may have altered the dimensions and structural organization of the flocs. Consequently, the reported particle sizes should only be treated as an indication of strong droplet association rather than a measure of the actual size of any aggregates present in the original non-diluted samples.

Particle charge measurements*:* The ζ-potential of emulsions was determined using a particle electrophoresis instrument (Zetasizer Nano ZS series, Malvern

Instruments, Worcestershire, UK). Emulsions were diluted to a droplet concentration of approximately 0.001 wt% using pH-adjusted water to avoid multiple scattering effects. The pH of the water used was adjusted to the same pH as the initial emulsion sample. After loading the samples into the instrument they were equilibrated for about 120 s before particle charge data was collected over 20 continuous readings.

***Rheological properties**:* The rheological behavior of samples was measured using a dynamic shear rheometer (Kinexus Rotational Rheometer, Malvern, U.K.). A cup and bob geometry consisting of a rotating inner cylinder (diameter 25 mm) and static outer cylinder (diameter 27.5 mm) was used. The samples were loaded into the rheometer measurement cell and allowed to equilibrate at 25 ºC for 5 min before beginning all experiments. Samples underwent a constant shearing treatment (1 s^{-1} for 10 min) prior to analysis to remove history effects. The shear stress of the emulsions was then measured over a range of shear rates (0.01 to 50 s^{-1}), and the apparent viscosity was calculated from this data.

8.2.6 Emulsion Microstructure

Confocal imaging of emulsion microstructures was carried out with a 60× oil immersion objective lens using a Nikon confocal microscope (C1 Digital Eclipse) at ambient temperature. Samples were imaged at various stages of digestion: (i) immediately after preparation, (ii) after 15min incubation at pH 6.8 in simulated saliva (iii) after 2 h incubation at pH 2.5 in SGF, and (iv) after 2 h incubation at pH 7 in SI. Emulsion samples were stained with the fluorescent dye Nile red (0.1 wt% dissolved in 100% ethanol). The fluorescent dye was excited by an argon 476 nm laser and emitted light was collected between 555-620nm.

8.3 Results and Discussion

8.3.1 Influence of Initial Emulsion Composition and Microstructure on Behavior within a Model GIT

8.3.1.1 Initial Emulsions

Initially, the single-protein emulsions contained relatively small droplets (d_{43} < 0.4 μm) after preparation at pH 7 (**Figure 8.1a and 8.2**), which suggested they were stable to droplet aggregation under these conditions. As expected, the β-Lg-coated droplets were highly negatively charged because they were above their isoelectric point, whereas the LF-coated droplets were highly positively charged because they were below their isoelectric point (**Figure 8.1b**). On the other hand, the mixed emulsions contained relatively large particles (d_{43} ≈ 13 μm) (**Figure 8.1a**), suggesting that the oppositely charged lipid droplets were attracted to each other and formed microclusters. The particle size distribution measurements (**Figure 8.2a**) and confocal microscopy images (**Figure 8.2**) suggested that the microclusters were fairly uniform in size, ranging from around 3 to 30 μm. The microclusters formed in the mixed emulsions had a slight negative charge, which suggests that the anionic β-Lg-coated droplets may have been preferentially located at their outer edges. These measurements indicated that there were appreciable differences between the microstructural and electrical properties of the initial emulsions, which we hypothesize would alter their subsequent fate within the GIT model.

(a)

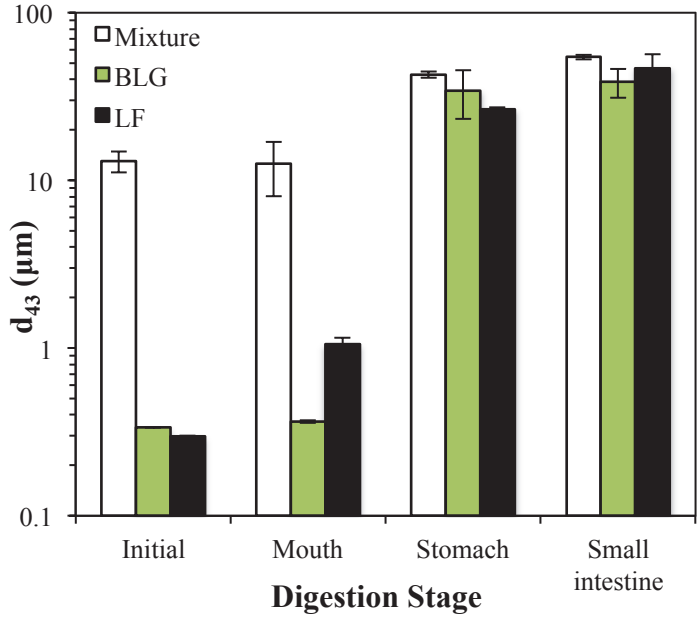

(b)

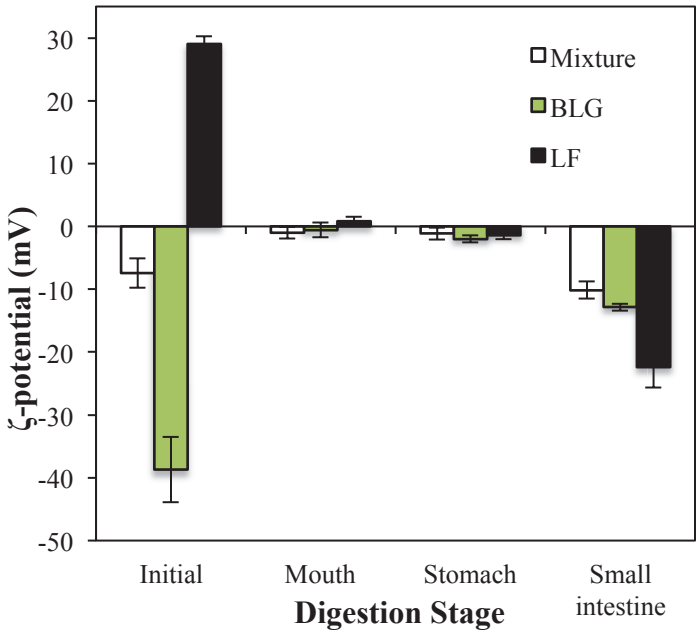

Figure 8.1 Influence of initial emulsion type on (a) the mean particle diameter (d_{43}), and (b) the droplet charge, measured at various stages in an *in vitro* gastrointestinal tract model. The emulsions initially contained β-Lg-coated droplets, LF-coated droplets, or a mixture of the two.

(a)

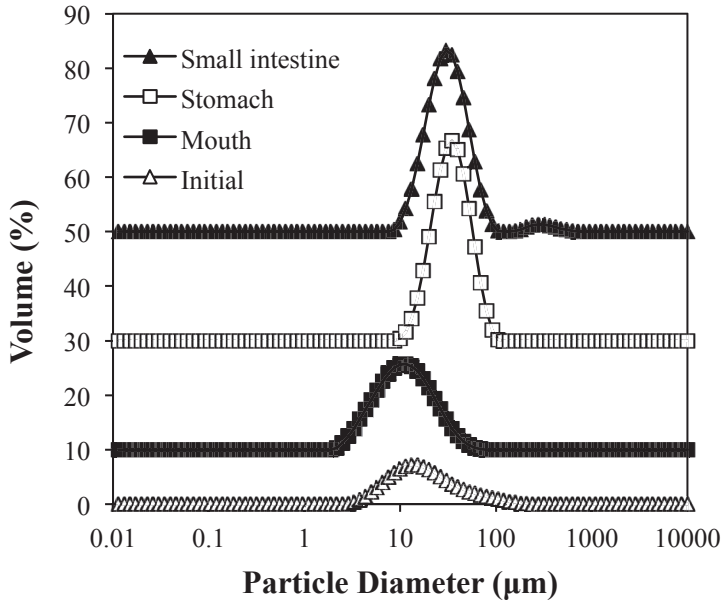
Small intestine
Stomach
Mouth
Initial
Volume (%)
Particle Diameter (µm)
0
10
20
30
40
50
60
70
80
90
0.01
0.1
1
10
100
1000
10000

(b)

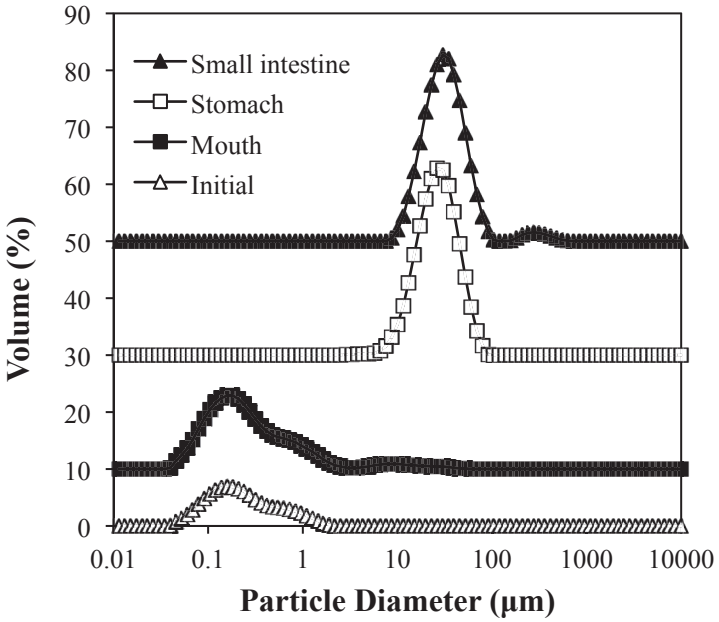
Small intestine
Stomach
Mouth
Initial
Volume (%)
Particle Diameter (µm)
0
10
20
30
40
50
60
70
80
90
0.01
0.1
1
10
100
1000
10000

(c)

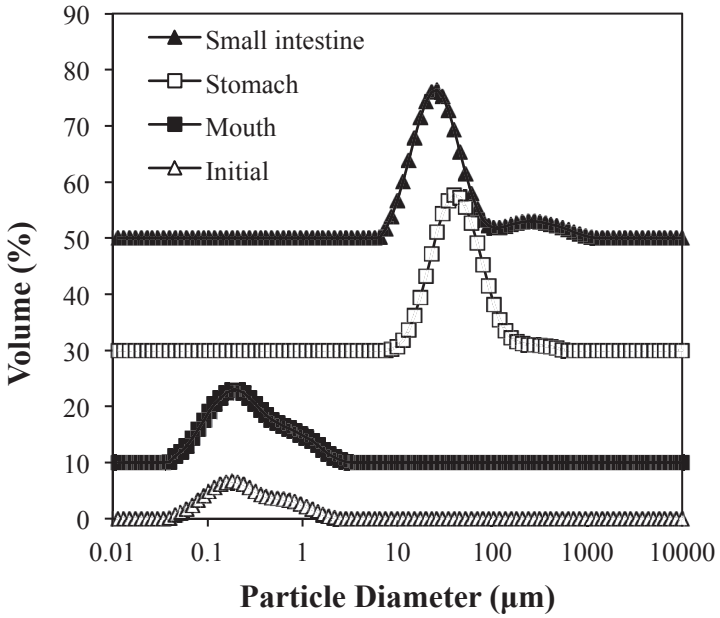

Figure 8.2 Influence of initial emulsion type on the particle size distribution measured at various stages in an in vitro gastrointestinal tract model : (a) mixed emulsions; (b) LF emulsion; (c) β-Lg emulsion.

8.3.1.2 Response to Oral Conditions

There were appreciable alternations in the microstructures and electrical properties of the emulsions after they were incubated in artificial saliva. There was a pronounced decrease in the magnitude of the electrical charge on the particles in all the emulsions: from +29 to + 0.6 mV for the LF emulsion; from -39 to -0.6 mV for the β-Lg emulsion; and, from -7 to -1 mV for the mixed system (**Figure 8.1b**). This decrease in droplet charge may have originated from a number of physicochemical phenomena associated with specific components in the saliva: (i) electrostatic screening by mineral ions; (ii) binding of multivalent counter-ions to droplet surfaces; (iii) adsorption of polyelectrolytes (mucin) to the droplet surfaces. Interestingly, the large reduction in the magnitude of the ζ-potential did not promote droplet aggregation in the β-Lg-emulsions

or any further aggregation in the mixed emulsions (**Figure 8.1a**), which might have been expected due to the reduction in electrostatic repulsion between the particles. It is possible that some of the mucin molecules formed a coating around the lipid droplets, thereby generating a steric repulsion that prevented aggregation. Alternatively, any aggregates formed may have dissociated during the particle size measurements due to dilution and stirring. There was an appreciable increase in the mean particle diameter of the emulsions containing LF-coated lipid droplets after incubation in simulated oral conditions (**Figure 8.1a**). This effect may have been because of bridging flocculation caused by binding of anionic mucin molecules to the cationic lipid droplets. These structures would be more difficult to breakdown within the light scattering instrument, which is possibly why the particle sizing data indicated that they were larger. Previous research has also found that lactoferrin-coated lipid droplets undergo extensive aggregation when mixed with artificial saliva, which was attributed to electrostatic screening and bridging effects by salts and polyelectrolytes (mucin) in the saliva.

8.3.1.3 Response to Gastric Conditions

There were major changes in the particle sizes and microstructures of all the emulsions after they were incubated in simulated gastric fluid (SGF). There was a large increase in mean particle diameter (**Figure 8.1a**), larger particles were observed in the particle size distribution (**Figure 8.2**), and there was evidence of extensive flocculation in the confocal microscopy images (**Figure 8.2**). Droplet aggregation within the gastric stage can be attributed to the combined effects of various active constituents within the SGF: acids, salts, and pepsin. The pH is reduced from around neutral in the oral stage to highly acidic in the gastric stage, which will influence the electrical characteristics of the

various proteins in the system. The lactoferrin should remain highly positively charged as the pH is reduced, whereas the β-lactoglobulin should go from negative, to neutral, to positive as the pH is altered from above to below its isoelectric point. At pH values below the isoelectric point of β-lactoglobulin (pI ≈ 5), both the proteins should have similar positive charges and should therefore not be strongly attracted to each other. Previous studies have shown that protein-coated droplets may undergo irreversible aggregation when they are passed through their isoelectric points, due to the reduction in electrical charge[148]. Some of the droplet aggregation in the systems containing β-lactoglobulin may therefore be attributed to this effect. There are also appreciable amounts of dissolved ions in the gastric fluid arising from the NaCl present in the SGF and the various salts added in the oral phase. Salt ions are known to promote droplet flocculation in protein-stabilized emulsions due to their ability to screen electrostatic interactions or bind to droplet surfaces causing charge neutralization or bridging effects[31]. Some of the droplet aggregation observed may therefore be due to the increase in ionic strength of the aqueous phase surrounding the lipid droplets. Finally, SGF contains pepsin, which is an enzyme capable of catalyzing the hydrolysis of proteins under acidic conditions[149]. The hydrolysis of the adsorbed or free proteins in the emulsions may have altered their stability to droplet aggregation [141]. For example, the peptides that remain at the interface may be unable to provide sufficient electrostatic and/or steric repulsions. As a result, emulsions are highly susceptible to flocculation and coalescence. Previous researchers have also reported that extensive droplet aggregation occurs when protein-stabilized emulsions are exposed to simulated gastric conditions[145, 147].

8.3.1.4 Response to Small Intestine Conditions

Finally, we compared the behavior of the three different emulsions after incubation under small intestine conditions. For all three systems, the mean particle diameter was relatively high (**Figure 8.1a**), there was evidence of large particles in the particle size distributions (**Figure 8.2**), and extensive droplet aggregation was observed in the confocal microscopy images (**Figure 8.2**). The microscopy images indicate that there were smaller amounts of lipid droplets present in the small intestine than in the stomach, which is due to dilution and digestion of the droplets. The confocal images also suggest that some droplet coalescence had occurred, since the size of the individual droplets in the small intestine appears to be larger than in the gastric stage. Coalescence may have been a result of protein and lipid hydrolysis during digestion reducing the resistance of the interfacial membranes to rupture. The electrical charge on the particles after the small intestine phase was much more negative than after the gastric stage, which is probably due to adsorption of anionic species to the surfaces of non-digested fat and/or due to the presence of anionic species generated by the digestion process (such as mixed micelles and vesicles). Bile salts, phospholipids and free fatty acids are all negatively charged at neutral pH and may therefore have contributed to the formation of anionic colloidal particles. Surprisingly the negative charge was greatest in the emulsions that initially contained only lactoferrin, which should be positively charged at this pH. One would expect that the proteins would be fully or partly digested at the end of the small intestine phase. Although it is still possible that protein type influenced the nature of the colloidal structures formed in the small intestine fluid after digestion.

8.3.2 Influence of Initial Emulsion Composition and Microstructure on Lipid Digestion

The rate of digestion of the emulsions during the small intestine stage was monitored using a pH-stat method, *i.e.,* by measuring the amount of alkali solution that had to be added to maintain a neutral pH [150]. In systems containing both lipids and proteins the pH may change due to lipid hydrolysis (producing fatty acids) or protein hydrolysis (producing amino acids and peptides). We therefore measured the amount of alkali solution that had to be added to the digestion reaction chamber for the three emulsions and for corresponding protein solutions that contained the same type and amount of proteins as the emulsions. The amount of free fatty acids released was then calculated by subtracting the data for the emulsion from the data for the corresponding protein solution, assuming that the protein was digested similarly in both systems. In practice, some globular proteins are digested at somewhat different rates when they are present in solution or at oil-water interfaces[63, 151].

For all three protein solutions (β-Lg, LF, and mixed), there was an appreciable increase in the amount of alkaline solution added to the samples during digestion (**Figure 8.3**), which can be attributed to protein hydrolysis. Bile extracts similar to the ones used in this study are known to have protease activity[145], and there may also be some residual protease (pepsin) remaining in the samples from the gastric stage. The total amount of alkali added to the samples was fairly similar for all three proteins, which suggests that they were all digested by a similar amount. We also found that the amount of alkali added to the three different emulsions during digestion was fairly similar (**Figure 8.4a**), which suggests the lipids were also digested at a similar rate. Indeed, we

observed no major differences in the rate or extent of lipid digestion in mixed emulsions or single-protein emulsions (**Figure 8.4b**). These experiments suggest that the initial microstructure of the emulsions had little impact on their subsequent digestion in the small intestine. Presumably, this occurs since the original structure of the emulsions was progressively destroyed as they passed through the GIT. For example, there were changes in the structural organization of the lipid droplets in the system, their particle sizes, and their interfacial compositions (**Figure 8.1 to 8.2**), which may be attributed to interactions with the various components in the intestinal fluids they encounter. It should be noted that none of the emulsions was completely digested at the end of the small intestine stage, which we attribute to the relatively high amount of fat (2.5 wt%) that was present during the lipid digestion stage. In reality, the human body would respond to a high fat meal by producing more lipase to digest the lipids and more bile salts and phospholipids to solubilize the digestion products (free fatty acids and monoacylglycerols) produced.

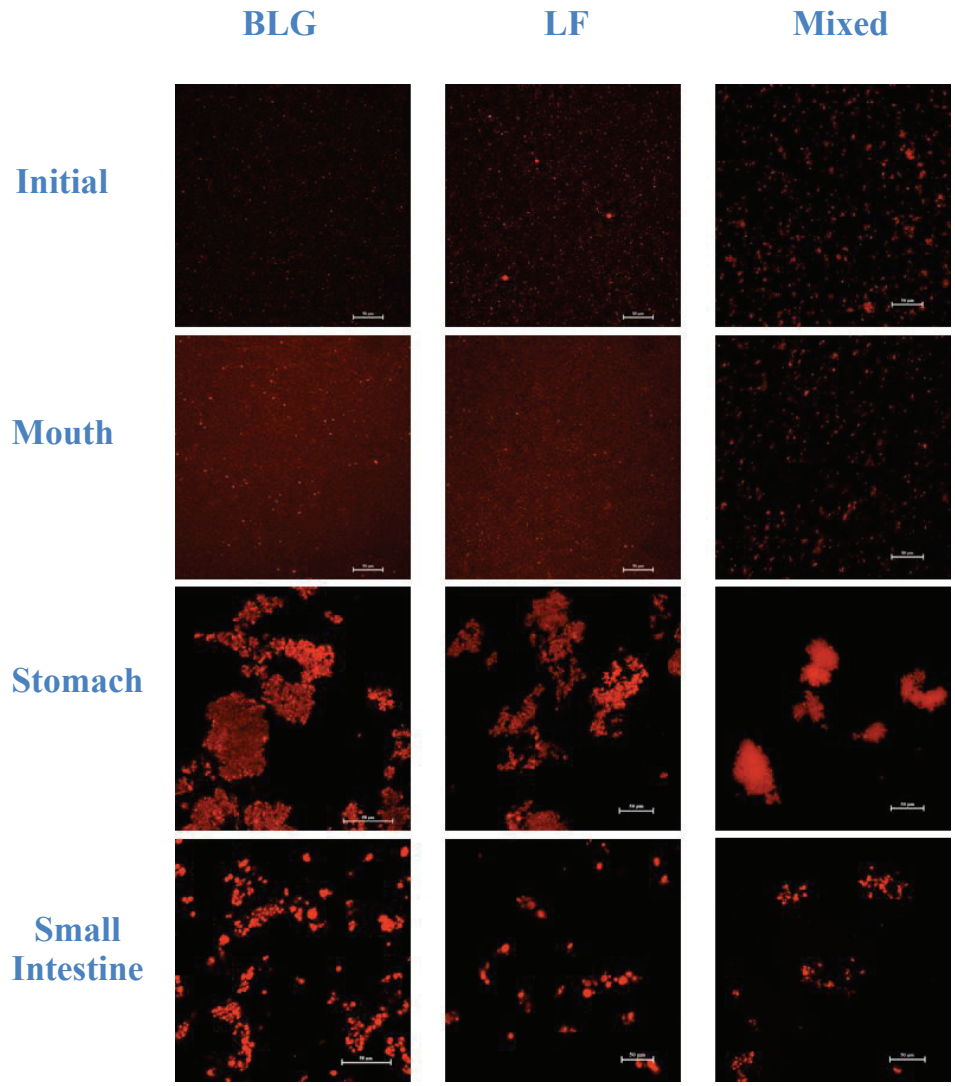

Figure 8.3 Influence of initial emulsion type on the microstructure measured by confocal fluorescence microscopy at various stages in an *in vitro* gastrointestinal tract model. The emulsions studied were mixed, LF and β-Lg stabilized emulsions, respectively. The fat phase was stained red, and the scale bars are 50μm.

(a)

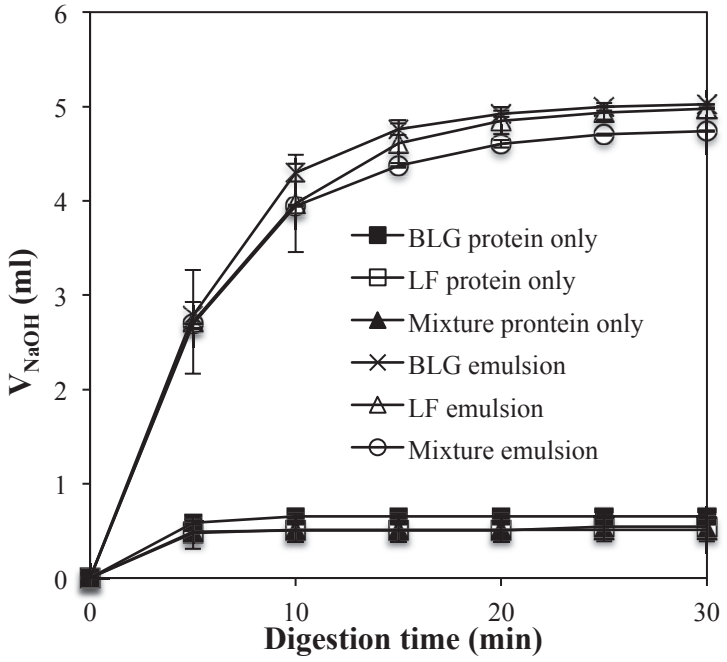

(b)

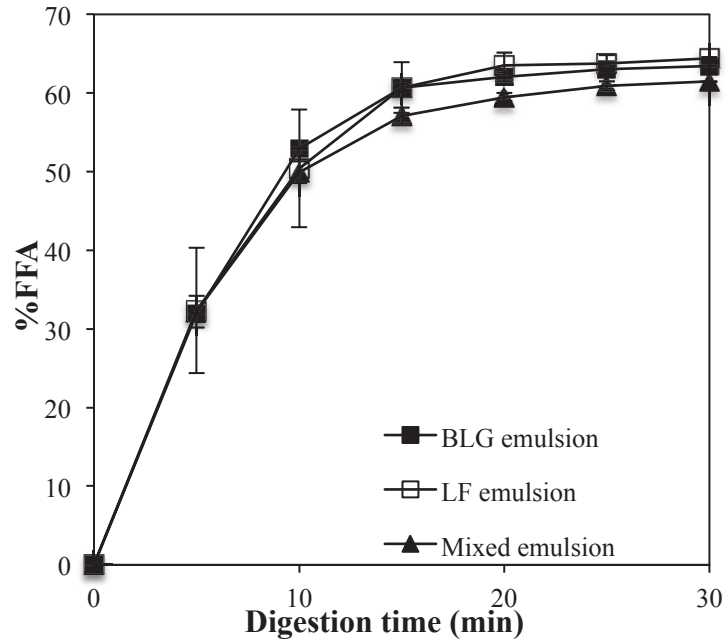

Figure 8.4 (a) Volume of NaOH solution titrated into the digestion vessel to maintin the pH at 7.0 for emulsions and protein solutions. The emulsions contained different kinds of protein-coated oil droplets (β-Lg, LF or mixed). The aqueous solutions had the same type and concentration of protein as the corresponding emulsions. (b)

Calculated free fatty acids release due to lipid digestion for emulsions containing different kinds of protein-coated droplets (β-Lg, LF or mixed).

8.3.3 Influence of Initial Emulsion Composition Rheological Properties in Simulated GIT Conditions

The rheological properties of ingested foods may influence their behavior within the gastrointestinal tract. The mixed emulsions initially had much higher viscosities than the two single-protein emulsions, and so we examined the influence of passage through the GIT on their rheological properties.

The dependence of the apparent viscosity on the shear rate of the mixed emulsions in different stages of the simulated GIT is shown in **Figure 8.5a**. In general, the viscosity of the mixed emulsions decreased as they passed through each stage of the GIT model: initial > oral > gastric > small intestine. The main reason for this decrease is the progressive dilution of the emulsions with the various intestinal fluids, since a decrease in droplet concentration is known to cause a reduction in emulsion viscosity[31]. This dilution effect appears to be larger than any increase in viscosity due to the presence of biopolymers (such as mucin in the mouth) or increased aggregation (*e.g.,* in the stomach). For the mixed emulsions, there was an appreciable decrease in apparent viscosity with increasing shear rate, particularly in the initial samples. This shear thinning behavior can be attributed to progressive disruption of flocculated droplets with increasing applied shear force[131]. Shear thinning behavior was also observed in the samples collected from the single-protein emulsions (data not shown).

The apparent viscosities of the mixed emulsions were compared with those of the single-protein emulsions at different stages of the GIT at a constant applied shear rate of 10 s^{-1} (**Figure 8.5b**). In general, there was a decrease in viscosity as the emulsions passed

through each stage of the GIT model for all three emulsions, which can be attributed to the dilution effect mentioned earlier. The only exceptions to this trend were the LF emulsion and β-Lg emulsion where the viscosities were either similar are higher in the gastric stage than in the oral stage. This effect may be attributed to the extensive droplet flocculation that was observed in the simulated gastric fluids, since flocculation is known to increase viscosity[131]. The mixed emulsions had much higher viscosities than the single-protein emulsions in the oral stage, but fairly similar viscosities in the gastric and small intestinal stages (**Figure 8.6**). This behavior can be attributed to the fact that the mixed emulsion was highly aggregated in the oral phase, but the other single-protein emulsions were not, and that all the emulsions were highly aggregated in the SGF and SIF. This effect may have important implications for the design of functional foods that have highly viscous ("creamy") textures in the mouth, but that behave like conventional emulsions within the stomach and small intestine.

(a)

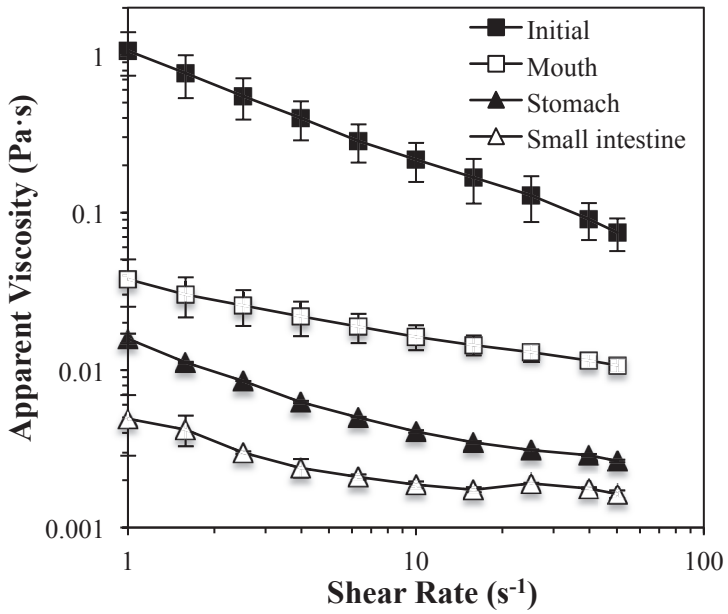

(b)

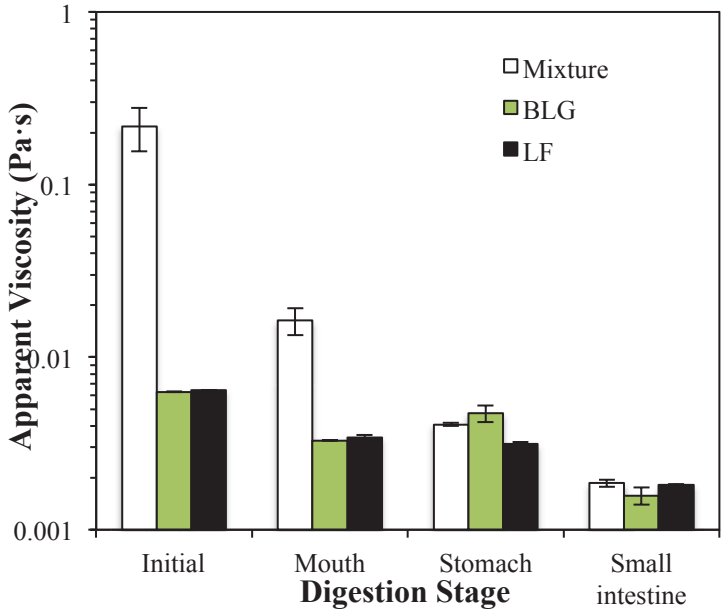

Figure 8.5 (a) Apparent shear viscosity *versus* shear rate profiles of mixed emulsions at various stages in an *in vitro* gastrointestinal tract model. (b) Influence of initial emulsion type on apparent shear viscosity (at $10s^{-1}$) of emulsions at different stages in an *in vitro* gastrointestinal tract model. The emulsions initially contained β-Lg-coated droplets, or a mixture of the two.

(a)

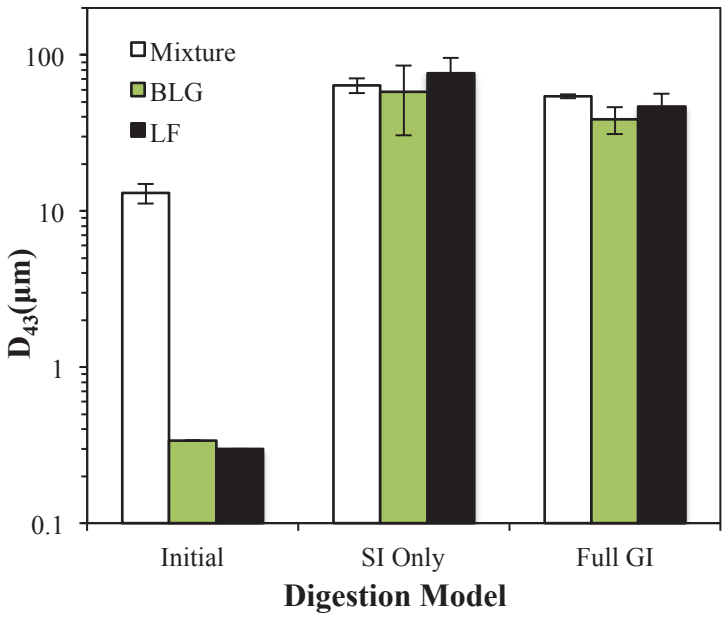

(b)

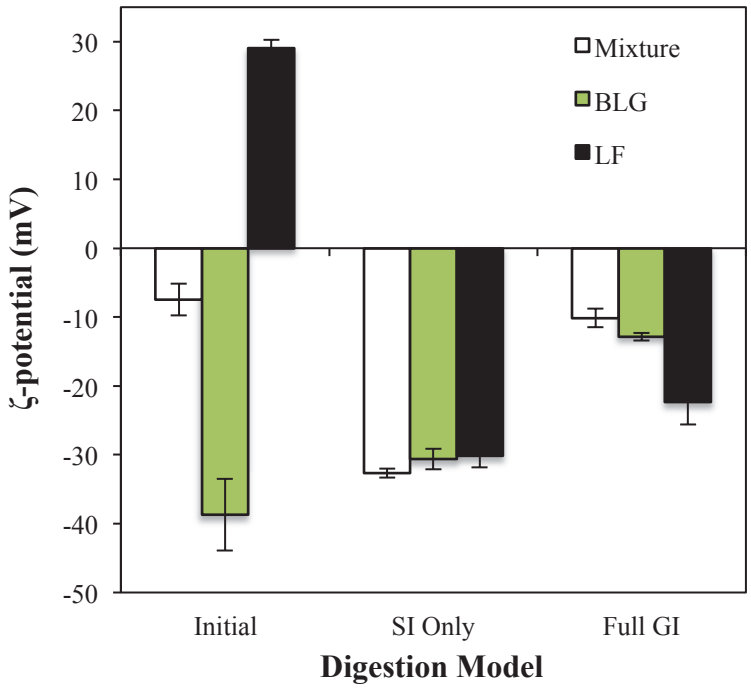

Figure 8. 6 (a) Influence of initial emulsion type on the mean particle diameter (d_{43}) measured after passage through two different *in vitro* gastrointestinal tract models: (i) full GI model (oral, gastric and small intestine); (ii) small intestine only. (b) Influence of initial emulsion type on the droplet charge measured after passage through two different *in vitro* gastrointestinal tract models; (i) full GI model (oral, gastric and small intestine); (ii) small intestine only.

8.3.4 Comparison of full and simplified *in vitro* digestion models

Finally, we compared the results obtained with a full simulated GIT model that included oral, gastric and small intestine stages, with a simplified GIT model that only included the small intestine stage. We did this because the simplified GIT model is often used in screening studies designed to determine the influence of emulsion composition and structure on lipid digestion [REF – Li 2011].

The particle sizes, charges and microstructures of the three emulsions after being passed through the simple and full GIT models were compared. We observed little

difference in the mean particle size or microstructure of the three emulsions using either GIT model (**Figure 8.6a and 8.7**). Nevertheless, we did observe some differences in the electrical characteristics of the particles (**Figure 8.6b**). The emulsions that had been through the simple model all had fairly similar high negative charges (-30 to -32 mV), whereas the emulsions that had been through the full model had lower negative charges that were more dependent on initial emulsion type (-10 to -22 mV). This suggests that there were some components within the artificial saliva or the gastric fluids that contributed to the electrical characteristics of the particles present after digestion in the small intestine. Some of the ionic components within the intestinal fluids may have become incorporated into the particles formed after the small intestine stage, *e.g.,* mineral ions, biopolymers (*e.g.,* mucin), or enzymes (*e.g.,* pepsin). Alternatively, the difference in the electrical characteristics of the particles may have been due to digestion of some or all of the proteins by pepsin leading to the generation of different electrical species in the system.

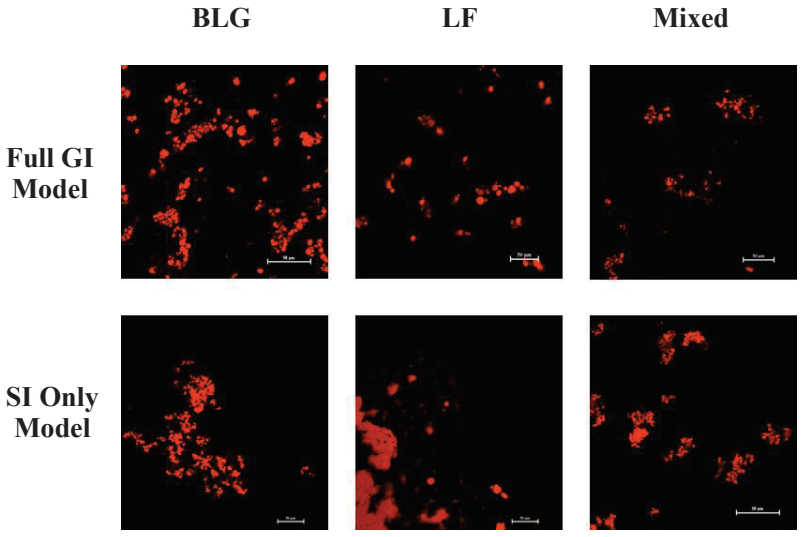

Figure 8.7 Influence of initial emulsion type on the microstructure measured by confocal fluorescence microscopy after passage through two different in vitro

gastrointestinal tract model: (i) full GI model (oral, gastric and small intestine); (ii) small intestine only. The fat phase was stained red, and the scale bars are 50 μm long.

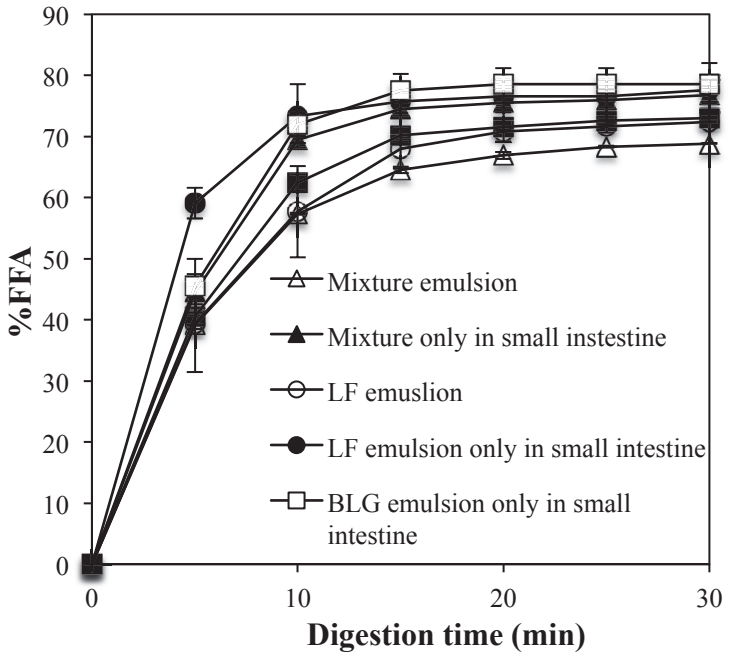

Figure 8.8 Influence of initial emulsion type on the calculated release of free fatty acids after passage through two different in vitro gastrointestinal tract models: (i) full GI model (oral, gastric and small intestine); (ii) small intestine only.

We also observed some differences in the rate of lipid digestion in the three emulsions when they were subjected to either the simple or full GIT models (**Figure 8.8**). For all three emulsions, the rate and extent of lipid digestion was somewhat less for the full model, than for the simple model. This suggests that there were some changes in the structural organization or interfacial composition of the emulsions as a result of passage through the oral and gastric stages that altered their susceptibility to digestion. Having said this, the pH-stat measurements indicated that all the samples were digested at a fairly similar rate and extent. In other words, there were some slight quantitative differences between the two methods, but the results obtained were qualitatively fairly

similar. This suggests that the simple digestion model may be appropriate for studying the digestion of protein-stabilized emulsions.

8.4 Conclusions

The purpose of this study was to examine the influence of hetero-aggregation on the behavior of protein-coated lipid droplets within simulated gastrointestinal conditions. Initially, we hypothesized that differences in the microstructural and rheological properties of the original emulsions would influence their behavior in the GIT model. We found that the mixed emulsions, containing a mixture of anionic and cationic protein-coated lipid droplets, were initially much more viscous than single-protein emulsions with similar fat contents. The mixed emulsions remained much more viscous than the single-protein emulsions in simulated mouth conditions, but the electrical characteristics, aggregation state and viscosity of all the emulsions were fairly similar in the stomach and small intestine stages. As a result, all of the emulsions were hydrolyzed at a similar rate and to a similar extent by intestinal enzymes. Overall, our results suggest that the initial microstructural organization of protein-stabilized emulsions does not have a major impact on their subsequent digestion under simulated small intestinal conditions. This information is important for the design of functional foods that have desirable physicochemical and sensory characteristics, but that are also digested appropriately in the gastrointestinal tract.

CHAPTER 9

MODIFICATION OF EMULSION PROPERTIES BY HETERO-AGGREGATION OF OPPOSITELY CHARGED STARCH-COATED AND PROTEIN-COATED FAT DROPLETS

9.1 Introduction

The high hedonic rating of many commercial food products is related to their relatively high fat contents, *e.g.,* mayonnaises, sauces, dressings, and desserts [152, 153]. However, fat has a higher caloric value and a weaker satiety/satiation effect (on a per weight basis) than other major food nutrients [154, 155], which may lead to passive overconsumption and an increase in overweight and obesity [156]. The development of reduced fat foods is therefore a major goal of many food scientists [157, 158]. Unfortunately, it is difficult to remove fats from fatty foods without adversely affecting their desirable quality attributes. Fats play an important role in determining the appearance, texture, and flavor of foods, and when they are removed many of the desirable qualities are lost [129]. The food industry is therefore searching for effective strategies to reduce the fat content of foods, without adversely altering the desirable quality attributes. Various fat-reduction strategies have been developed, including the use of indigestible fats, reduced calorie fats, thickening agents, and colloidal particles [127].

One approach that we have recently studied in our laboratory is the utilization of *hetero-aggregation* of oppositely charged fat droplets to create highly viscous or paste like materials with reduced fat contents [20, 21, 159, 160]. Hetero-aggregation is defined as the aggregation of dissimilar particles, which may differ in their size, shape,

charge, chemical composition, or other properties [10, 11]. This approach has been widely used in non-food science applications for a variety of reasons, such as controlling the rheological properties of ceramics [12], creating ion exchange columns [13], removing colloidal particles from solutions [14], and encapsulating and targeting biomolecules [15-18]. Our previous studies have shown that hetero-aggregates can be formed from food ingredients by mixing two emulsions together containing oppositely charged protein-coated fat droplets [20, 21]. Previously, we used lactoferrin (LF) and β-lactoglobulin (β-Lg) at neutral pH to create droplets with different charges, since LF has an isoelectric point around 8 and is therefore positive, whereas β-Lg has an isoelectric point around 5 and is therefore negative [20]. However, LF and β-Lg are highly purified proteins that are too expensive for widespread use as functional ingredients in many foods. It is therefore important to identify alternative emulsifiers that are more suitable for commercial application in the food industry. Previous researchers have shown that novel textural attributes could be created in model foods by mixing an emulsion containing β-lactoglobulin-coated fat droplets with one containing gum arabic-coated fat droplets under acidic (pH 4.2) conditions [113]. In this study, we investigated the possibility of using whey protein isolate (WPI) and modified starch (MS) as two food-grade emulsifiers with different electrical characteristics to induce hetero-aggregation in mixed emulsions.

Whey protein isolate is a mixture of surface-active globular proteins normally isolated from diary milk, such as β-lactoglobulin, α-lactalbumin and bovine serum albumin [35]. WPI-coated droplets are positively charged below the isoelectric point of the adsorbed globular proteins (pI ≈ 5), but negatively charged above this value [94].

Modified starch is formed by covalently attaching non-polar (octenyl succinic anhydride) groups to hydrophilic starch molecules to form an amphiphilic molecule that can adsorb to oil-water interfaces and stabilize emulsions [41, 42]. MS-coated fat droplets have been shown to be negatively charged over a wide pH range due to the presence of anionic groups on the MS backbone [44]. At pH values below the isoelectric point of WPI, one would expect hetero-aggregation to occur between the anionic MS-coated droplets and the cationic WPI-coated droplets. We hypothesized that these economical food-grade emulsifiers may be suitable for producing novel desirable characteristics in reduced-fat products through the hetero-aggregation process.

9.2 Experimental Methods

9.2.1 Materials

Corn oil was purchased from a commercial food supplier (Mazola, ACH Food Companies, Inc., Memphis, TN). Powdered whey protein isolate (97.7 wt% protein) was supplied by Davisco Foods Intl. (Eden Prairie, MN, U.S.A.). Powdered OSA-modified starch (PURITY GUM^{TM} Ultra) was supplied by the National Starch LLC (Bridgewater, N.J., U.S.A.). Glacial acetic acid, sodium acetate, and sodium azide were purchased from Sigma-Aldrich (Sigma Chemical Co., St. Louis, MO) or Fisher Scientific (Pittsburgh, PA). All other chemicals were purchased from Sigma-Aldrich (St Louis, MO). Double distilled water was used to prepare all solutions.

9.2.2 Emulsion Preparation

Preparation of Single-droplet Type Emulsions: Aqueous emulsifier solutions were prepared by dispersing either WPI (1 wt%) or MS (4 wt%) powder into acetic acid

buffer (10 mM, 0.02% sodium azide, pH 7) and then stirring for 3 hours at room temperature to ensure complete dispersion. These emulsifier levels were selected based on previous studies that have shown that emulsions with relatively small droplet diameters can be produced [44]. The pH of aqueous emulsifier solutions was then adjusted to pH 3.5 using 1M NaOH or 1M HCl. Oil-in-water emulsions were prepared by homogenizing 20 wt% oil phase with 80 wt% aqueous phase at ambient temperature. Coarse emulsions were formed using a hand blender (M133/1281-0, 2 speed, Biospec Products Inc., ESGC, Switzerland) for 2 min at level 2. These emulsions were then passed four-times through a two-stage homogenizer (LAB 1000, APV-Gaulin, Wilmington, MA) at a first-stage pressure of 5,400 psi and a second-stage pressure of 600 psi. All emulsions were stored for 24 hours prior to utilization. The diameters of the WPI- and MS-stabilized emulsions produced were similar: $d_{43} \approx 0.37$ μm.

Preparation of Mixed-droplet Type Emulsions: Initially, two series of emulsions stabilized by either 1% WPI or 4% MS were prepared in acetic acid buffer. Mixed emulsions containing WPI (0 to 10 wt%, pH 3.5) and MS (10 to 0 wt%, pH 3.5) were prepared by mixing two single emulsions together, stirring for 10 min, and then storing them for 24 h before analysis. After these steps, the mixed emulsions contained different mass ratios of negative-to-positive particles, *i.e.,* MS-coated-to-WPI-coated oil droplets. For convenience, we used the notation"70% MS" to refer to mixtures containing 70 wt% MS-stabilized emulsion and 30% wt% WPI-stabilized emulsion.

9.2.3 Influence of pH on Emulsion Stability

The influence of pH on the electrical charge, stability, and rheology of WPI-emulsions, MS-emulsions, and mixed-emulsions (70% MS) were examined. Emulsions

were adjusted to a particular pH value (pH 2.5-6.5) using either 1M HCl or 1M NaOH, and then stored overnight prior to analysis.

9.2.4 Particle Characterization

Particle Size: The particle size distribution of the emulsions was measured using a laser diffraction particle size analyzer (Mastersizer 2000, Malvern Instruments, Ltd., Worcestershire, UK). To avoid multiple scattering effects the emulsions were diluted to a droplet concentration of approximately 0.005 wt% using pH-adjusted water at the same pH as the sample. The emulsions were stirred continuously throughout the measurements to ensure they were homogenous. Measurements are reported as the volume-weighted mean diameter: $d_{4,3}=\sum d_i n_i^4/\sum d_i n_i^3$, where n_i is the number of droplets of diameter d_i.

It should be noted that particle size measurements made by static light scattering on highly flocculated emulsions should be treated with caution. First, the theory (Mie theory) used to interpret light scattering data assumes that the scattering particles are homogeneous spheres with well-defined refractive indices. In practice, flocs are non-spherical and non-homogeneous particles, with ill-defined refractive indices. Second, the process of dilution and stirring may have altered the dimensions and structural organization of the flocs. Consequently, the reported particle sizes should only be treated as an indication of strong droplet association rather than a measure of the actual size of any aggregates present in the original non-diluted samples.

Particle Charge: The ζ-potential of the particles in the emulsions was determined using a particle electrophoresis instrument (Zetasizer Nano ZS series, Malvern Instruments, Worcestershire, UK). Emulsions were diluted to a droplet concentration of approximately 0.001 wt% using pH-adjusted water to avoid multiple scattering effects.

After loading the samples into the instrument they were equilibrated for about 120 s before particle charge data was collected over 20 continuous readings.

9.2.5 Rheological Properties

The rheological behavior of samples was characterized using a dynamic shear rheometer (Kinexus Rotational Rheometer, Malvern, U.K.). A cup and bob geometry consisting of a rotating inner cylinder (diameter 25 mm) and static outer cylinder (diameter 27.5 mm) was used in viscosity and oscillation measurements. The samples were loaded into the rheometer measurement cell and allowed to equilibrate at 25 ºC for 5 min before beginning all experiments. Samples underwent a constant shearing treatment (1 s^{-1} for 10 min) prior to analysis to remove history effects. The shear stress of the emulsions was then measured over a range of shear rates (1 to 100 s^{-1}), and the apparent viscosity was calculated from this data.

9.2.6 Microstructure Analysis

The microstructures of the emulsions were observed using confocal scanning fluorescence microscopy. The oil droplets in the MS emulsions were dyed with Bodipy 493, while the protein phase in the WPI emulsions was stained with Rhodamine B. For the MS emulsions, Bodipy 493 dye (0.1 mg/mL) was added to corn oil, and this mixture was covered and stirred overnight to ensure the dye was completely dissolved in the oil. A 20 wt% corn oil-oil-water emulsion stabilized by 4% MS was then prepared with the dyed oil using the same procedure described previously. To avoiding fluorescence quenching, alumina foil was used to cover and protect the dye solutions in all procedures. For the WPI emulsions, Rhodamine B was dissolved in distilled water at a concentration

of 0.05% (w/v). This solution was then added to a 1% WPI solution at a concentration of 5 μl/gram and then a WPI emulsion was prepared as described previously. Bodipy493 was excited with a 488 nm laser and detected at 515 nm. Rhodamine B was excited with a 543 nm laser and detected at 605 nm. The pinhole setting was small (35 mm), and the image was magnified by a factor of 4× using the digital zoom feature. All pictures were taken using a 10× eyepiece with a 60× objective lens (oil immersion).

9.2.7 Statistical Analysis

All experiments were carried out in either duplicate or triplicate using freshly prepared samples. Results are reported as the calculated means and standard deviations.

9.3 Results and Discussion

9.3.1 Properties of Single-droplet Type Emulsions

Initially, we measured the particle diameter and electrical characteristics of the two single-droplet type emulsions. At pH 3.5, emulsions containing MS-coated fat droplets had a mean particle diameter (d_{43}) of 0.37 μm and a ζ-potential of -1.8 mV. The negative charge on the MS-coated lipid droplets can be attributed to the presence of carboxyl groups ($-COO^-$) on the OSA-modified starch molecules [161]. The WPI-coated fat droplets had a mean particle diameter (d_{43}) of 0.37 μm and a ζ-potential of + 62 mV. The positive charge on the WPI-coated lipid droplets can be attributed to the fact that the acidic pH used was well below the isoelectric point of the adsorbed proteins (pI ≈ 5) [44]. The relatively small size of the particles in these emulsions can be attributed to the fact that the repulsive forces acting between the droplets outweighed the attractive forces, thereby inhibiting aggregation. In the case of the WPI-coated droplets, the most

important repulsive force is electrostatic repulsion due to their high positive charge, but in the case of MS-coated droplets it is steric repulsion due to the presence of a relatively thick hydrophilic adsorbed layer [29]. Overall, these results show that the WPI- and MS-stabilized emulsions contained droplets that had similar dimensions but opposite charges at pH 3.5.

9.3.2 Influence of Particle Ratio on Particle Properties in Mixed Emulsions

The initial objective was to understand the influence of the ratio of negative-to-positive particles on hetero-aggregation in mixed emulsions containing MS-coated and WPI-coated droplets. These mixed emulsions were formed by mixing together two 5 wt% oil-in-water emulsions stabilized by either MS or WPI at different mass ratios.

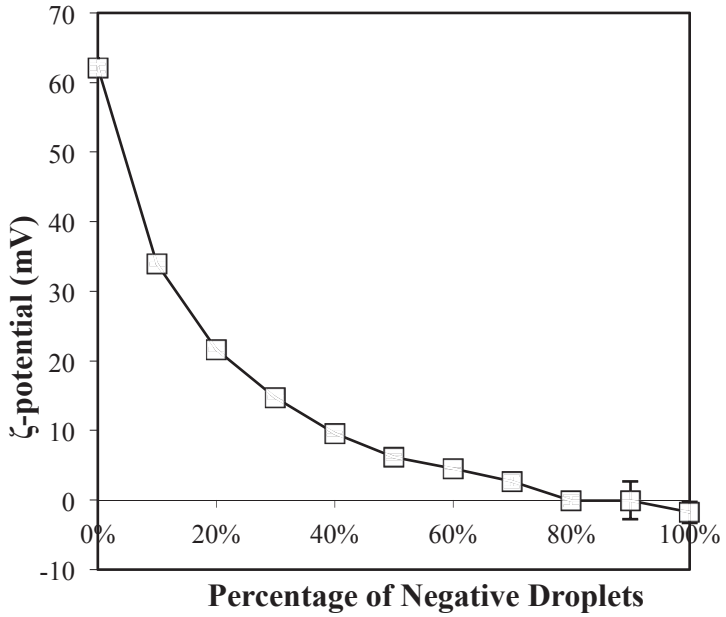

Figure 9.1 Change in electrical characteristics of the particles in mixed emulsions containing cationic WPI-coated droplets and anionic MS-coated droplets (pH 3.5).

As expected, the ζ-potential in the mixed systems went from highly positive to slightly negative as the concentration of negatively charged droplets (MS-coated)

increased (**Figure 9.1**). The point of zero charge was around 80% negative droplets, which can be attributed to the fact that the magnitude of the positive charge on the WPI-coated droplets (+ 62 mV) was much higher than that of the negative charge on the MS-coated droplets (-1.8 mV). Hence, a greater number of anionic MS-coated droplets were required to neutralize the cationic WPI-coated droplets. A similar result was found in our previous work on the formation of microclusters in protein-stabilized emulsions containing fat droplets with opposite charges of different magnitude [20, 21].

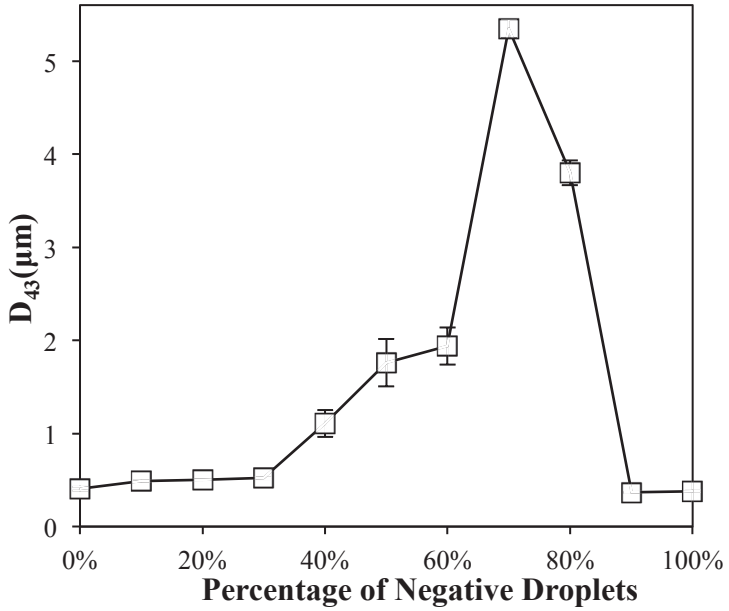

Figure 9.2 Change in mean particle diameter of the particles in mixed emulsions containing cationic WPI-coacted droplets and anionic MS-coated droplets (pH 3.5).

The influence of negative-to-positive particle ratio on the size of the particles in the mixed emulsions was also measured (**Figure 9.2**). The mean particle diameter of the single-droplet type emulsions were both relatively small ($d_{43} \approx 0.37$ μm) at pH 3.5, indicating that they were stable to aggregation under these conditions. The dependence of mean particle diameter on particle ratio can be divided into three regimes: (i) from 0 to 30% MS, the particle size was relatively small ($d_{43} < 0.5$ μm); (ii) from 40% to 80% MS,

the particle size was relatively large (d_{43} > 1 μm); (iii) from 90% to 100% MS, the particle size was again relatively small (d_{43} < 0.5 μm). These measurements suggest that relatively small clusters of droplets were formed at low and high particle ratios, but that large clusters were formed at intermediate values. The largest clusters (d_{43} > 5 μm) were formed at 70% MS-coated droplets and 30% WPI-coated droplets (**Figure 9.2**), which was close to the composition where the net charge on the clusters was zero (**Figure 9.1**).

Confocal fluorescent microscopy images of the single and mixed emulsions also showed extensive droplet aggregation at intermediate particle ratios (**Figure 9.3**). Images of the emulsions containing either MS-coated or WPI-coated droplets indicated that they contained small droplets evenly dispersed throughout the system. On the other hand, images of mixed emulsions (70% MS, 30% WPI) showed that they contained large clusters of droplets. The fact that these clusters appeared yellow in the fluorescent microscopy images suggests that they contained a mixture of different droplets.

The main driving force for fat droplet association in these systems is presumably electrostatic attraction between the oppositely charged droplets. At relatively low particle ratios, one would expect any negatively charged droplets to be surrounded by positively charged droplets resulting in the formation of relatively small clusters (**Figure 9.4**). Similarly, at relatively high particle ratios, one would expect any positively charged droplets to be completely surrounded by negatively charged droplets, again resulting in the formation of small clusters. On the other hand, at intermediate particle ratios one would expect that the clusters could grow quite large due to the possibility of electrostatic attraction between many more droplets (**Figure 9.4**). In addition, there may be further aggregation of clusters whose net charge is close to zero, because there would

be no strong electrostatic repulsion to overcome the van der Waals attraction between them.

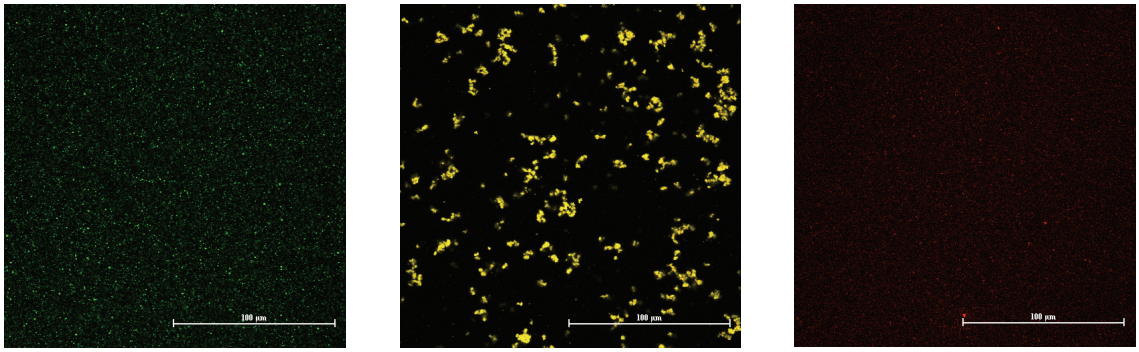

100% MS-coated Droplets **70% MS-&30% WPI-coated droplets** **100% WPI-coated droplets**

Figure 9.3 Change in microstructure of emulsions containing cationic WPI-coated droplets, anionic MS-coated droplets or mixtures of the two types (pH 3.5).

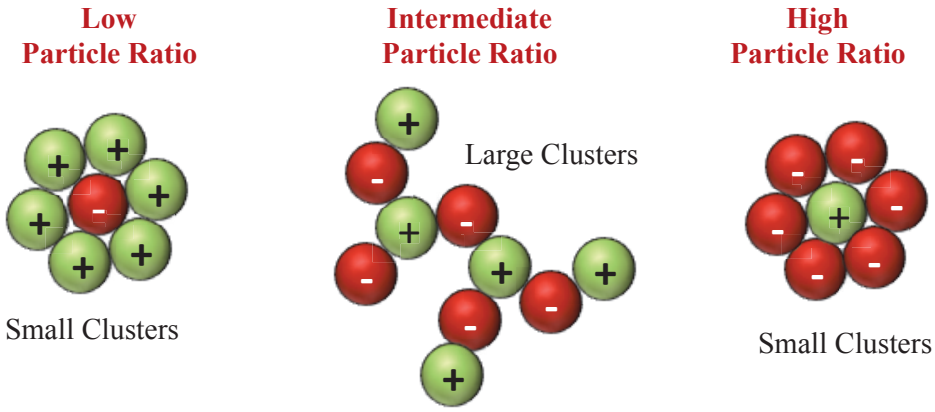

Figure 9.4 Highly schematic representation of proposed structures formed in mixed emulsions containing positively-charged and negatively-charged droplets at different particle ratios.

Statistical thermodynamics models of the aggregation state of particles in mixed colloidal systems suggest that the maximum amount of aggregation should occur in systems containing 50% positively charged and 50% negatively charged particles [25]. There are a number of possible reasons for the different between the theoretical predictions and our experimental measurements: (i) the mixed emulsions were not at

thermodynamic equilibrium; (ii) the two different kinds of droplet had very different charge magnitudes; and, (iii) non-adsorbed biopolymers played a role.

9.3.3 Influence of Particle Ratio on Rheology and Creaming of Mixed Emulsions

The rheology and creaming stability of emulsions is known to depend strongly on the aggregation state of the droplets [29]. We therefore measured the rheological properties and appearance of mixed emulsions with different particle ratios at pH 3.5.

The flow profiles (apparent viscosity *versus* shear rate) of selected mixed emulsions with different particle ratios are shown in **Figure 9.5a**. At low and high particle ratios the mixed emulsions had relatively low apparent shear viscosities (< 0.03 Pa s) that did not change appreciably with shear rate. On the other hand, at intermediate particle ratios (70% and 80% MS) the mixed emulsions had relative high viscosities (> 0.5 Pa s) and showed distinct shear thinning behavior. The origin of this shear thinning flow behavior can be related to the progressive breakdown of the droplet clusters upon application of increasing external shear forces [162]. The influence of particle ratio on the apparent viscosity determined at a constant shear rate (1 s^{-1}) is compared in **Figure 9.5b**. The mixed emulsions containing 70% and 80% MS-coated droplets had the highest apparent viscosities, which correlates to the samples with the highest amount of droplet aggregation in the light scattering measurements (**Figure 9.2**). The apparent viscosity of the mixed emulsions containing 70% MS were over 10-times higher than either of the single-droplet type emulsions.

Visual observations of emulsion appearance after the test tubes containing them were inverted (**Figure 9.5b**) supported the rheology measurements. Mixed emulsions with relatively low and high particle ratios were fluid-like and flowed to the bottom of

the tubes, whereas those with intermediate particle ratios were solid-like and remained at the top of the tubes after inversion.

(a)

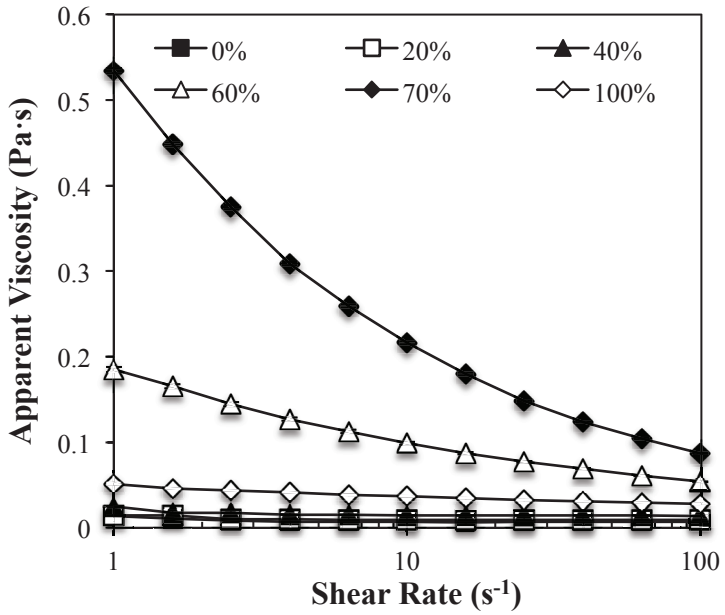

(b)

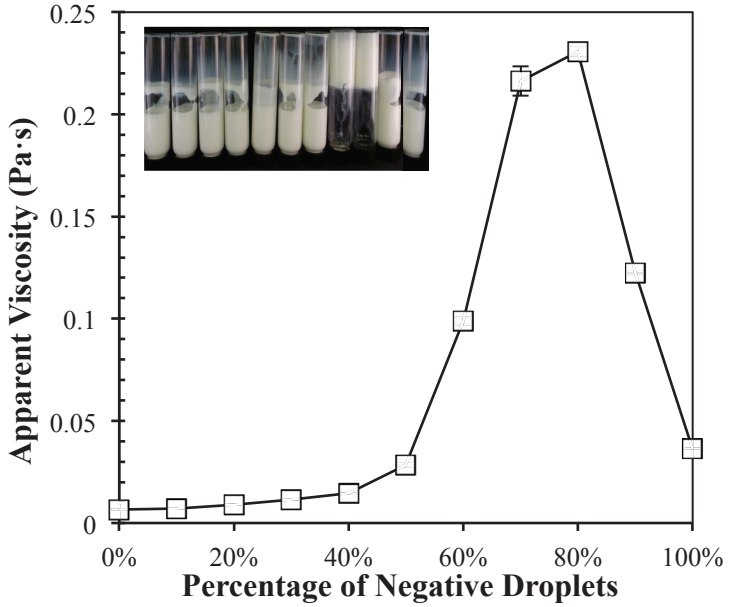

Figure 9.5 (a) Change in apparent viscosity of mixed emulsions containing cationic WPI-coated droplets and anionic MS-coated droplets as a function of applied

shear rate (pH 3.5). (b) Change in apparent viscosity (at 10 s^{-1}) of mixed emulsions containing cationic WPI-coated droplets and anionic MS-coated droplets (pH 3.5).

9.3.4 Influence of pH on Properties of Mixed Emulsions

Finally, we examined the influence of pH on the properties of the mixed emulsions, since changes in pH will modulate the sign and magnitude of the electrical charge on the biopolymer-coated droplets, thereby influencing the nature of any aggregates formed.

As reported previously [44, 163], WPI-coated droplets went from highly positive at low pH to highly negative at high pH (with a point of zero charge around pH 5), while MS-coated droplets were slightly negative across the whole pH range (**Figure 9.6a**). These measurements suggest that the droplets in the mixed emulsions should have opposite charges below about pH 5. The electrical charge of the particles in the mixed emulsions (70% MS, 30% WPI) was between that of the single-droplet type systems, which suggests that droplet aggregation may have occurred and formed clusters with intermediate charges.

As reported previously [44, 163], MS-coated droplets were stable to droplet aggregation across the whole pH range, whereas WPI-coated droplets were only stable at low and high pH values but aggregated around their isoelectric point (pI ≈ 5) (**Figure 9.6b**). The difference in pH-stability between these two emulsifiers can be attributed to their different stabilization mechanisms [29]. MS-coated droplets are primarily stabilized by steric repulsion and are therefore not strongly affected by pH, whereas WPI-coated droplets are primarily stabilized by electrostatic repulsion and therefore tend to aggregate around their isoelectric point [36, 164, 165]. The mean particle sizes were relatively low in the mixed emulsions at the lowest (pH 2.5) and highest (pH 6.5) pH

values studied in this work (**Figure 9.6b**), but were relatively high at intermediate pH values ($3.5 \leq pH \leq 5.5$). The reason that aggregation was not observed at pH 2.5 may have been because the MS-coated droplets lost most of their negative charge and therefore could not interact with the positive WPI-coated droplets (**Figure 9.6a**). Conversely, the reason that aggregation did not occur at pH 6.5 may have been because both the MS- and WPI-coated droplets were strongly negatively charged (**Figure 9.6a**), and therefore there would be an electrostatic repulsion between them preventing aggregation. At intermediate pH values the electrostatic attraction between the droplets was strong enough to promote hetero-aggregation.

The rheological measurements were in close agreement with the light scattering measurements. The viscosity of the MS-stabilized emulsions remained relatively low and constant across the entire pH range, suggesting that there was no droplet aggregation. The viscosity of the WPI-stabilized emulsions was relatively small at low and high pH values, suggesting that the droplets remained non-aggregated, but was very high around the isoelectric point suggesting that extensive droplet aggregation occurred (**Figure 9.6c**). The viscosity of the mixed emulsions was highest at intermediate pH values because of extensive droplet aggregation driven by electrostatic attraction of oppositely charged droplets leading to the formation of large clusters.

The viscosity of non-aggregated MS-stabilized emulsions was considerably higher than that of non-aggregated WPI-stabilized emulsions. It is likely that a fraction of the emulsifiers in these emulsions was not absorbed to the droplet surfaces, but was instead dispersed within the aqueous phase. These free biopolymer molecules will contribute to the aqueous phase viscosity. The MS-stabilized emulsions contained a

higher overall biopolymer concentration than the WPI-stabilized emulsions, and the structure of MS molecules is more open and flexible than that of WPI molecules, which would lead to a higher viscosity enhancement for MS [166].

(a)

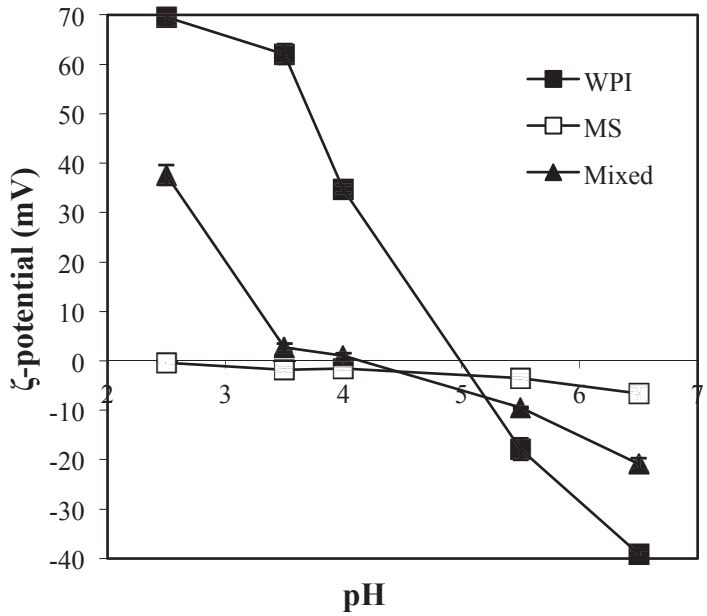

(b)

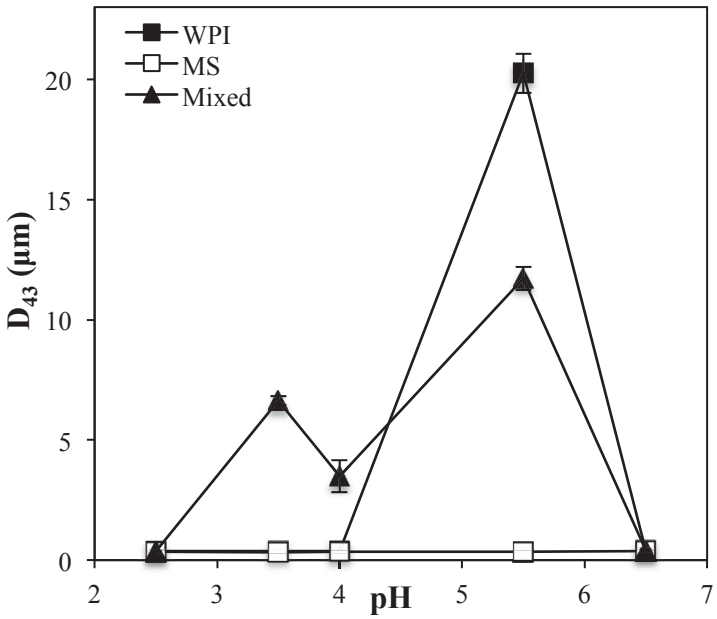

(c)

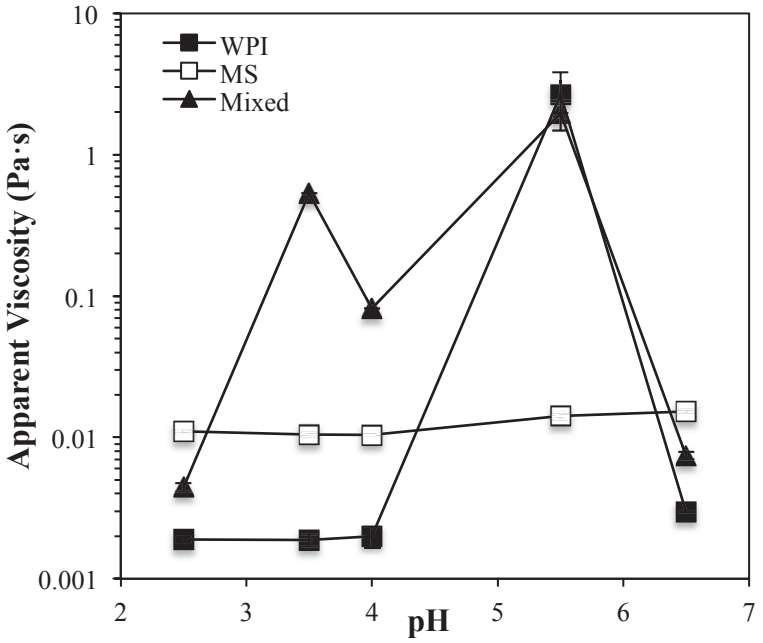

Figure 9.6 (a) In fluence of pH on the electrical characteristics of the particles in emulsions containing WPI-coated droplets, MS-coated droplets or a mixed emulsion (70% MS:30% WPI). (b) Influence of pH on the mean diameter of the particles in emulsions containing WPI-coated droplets, MS-coated droplets or a mixed emulsion (70% MS: 30% WPI). (c) Inflluence of pH on the mean diameter of the particles in emulsions containing WPI-coated droplets, MS-coated droplets or a mixed emulsion (70% MS: 30% WPI).

9.4 Conclusions

This study has shown that the rheological properties of emulsions can be controlled by mixing negative polysaccharide-coated droplets with positive protein-coated droplets to induce droplet aggregation through electrostatic attraction. The rheological characteristics of the mixed emulsions could be modulated by varying the particle ratio and solution pH. At low and high negative-to-positive particle ratios, low viscosity mixed emulsions were obtained because of the small droplet clusters formed, but at intermediate particle ratios highly viscous or paste-like emulsions were produced

due to the formation of large droplet clusters. Overall, this study provides valuable insights into the formation of highly viscous and paste-like food materials by controlled hetero-aggregation of oppositely charged oil droplets. These materials were assembled entirely from commonly used food-ingredients (corn oil, modified starch, and whey protein isolate), and therefore this approach may be useful for economically producing reduced-fat food products.

CHAPTER 10

INTERFACIAL ENGINEERING USED MIXED PROTEIN SYSTEMS: EMULSION-BASED DELIVERY SYSTEMS FOR ENCAPSULATION AND STABILIZATION OF B-CAROTENE

10.1 Introduction

There is increasing interest within the food and beverage industry in the development of colloidal delivery systems to encapsulate, stabilize, and deliver bioactive lipophilic compounds, such as carotenoids, oil-soluble vitamins, flavonoids, phytosterols, and polyunsaturated fats [5, 72, 167]. Oil-in-water emulsions are particularly suitable for incorporating these components into aqueous-based food and beverage products because the bioactive components can simply be solubilized within the oil phase prior to homogenization. One of the most important factors determining the physical and chemical stability of emulsions is the nature of the interfacial layer coating the fat droplets. Traditionally, oil-in-water emulsions are prepared using a single type of emulsifier that adsorbs to the droplet surfaces during homogenization [168]. In this case, the physicochemical stability of the fat droplets can be controlled by selecting emulsifiers that form interfaces with different characteristics, *e.g.,* polarity, thickness, charge, and chemistry [5]. There are a number of different emulsifiers that can be used by the food industry to achieve this goal, including small molecule surfactants, phospholipids, proteins and polysaccharides [29, 168, 169]. Nevertheless, the scope for controlling interfacial properties is limited by the number of emulsifiers commercially available and legally acceptable [21, 60, 170].

There has therefore been considerable interest in improving the functional performance of emulsion-based delivery systems by engineering the properties of the interfacial layer using mixed emulsifier systems [5, 164, 171, 172]. In this article, we focus on the modification of interfacial properties using mixed globular protein systems, since there is increasing interest within the food industry in using natural emulsifiers to stabilize emulsions. In principle, a variety of different interfacial structures can be formed using two different globular proteins as emulsifiers: P_1 and P_2 (**Figure 10.1**). *Mixed-droplet emulsions* consist of two different kinds of protein-coated fat droplets, with each kind being coated by a different globular protein [21, 37, 173]. These emulsions are formed by mixing an emulsion containing [P_1]-coated droplets with another emulsion containing [P_2]-coated droplets. Here we use square brackets to designate a single interfacial layer. *Nanolaminated emulsions* consist of fat droplets coated by multiple layers of protein, with each layer consisting of a single protein type [33, 39, 93]. These emulsions are usually formed by sequential deposition of oppositely charged proteins onto fat droplet surfaces using an electrostatic layer-by-layer (LbL) method [174]. Interfacial layers with different structures can be formed using the same pair of proteins depending on which protein is used to stabilize the initial emulsion formed during homogenization, *e.g.,* [P_1]-[P_2]-coated or [P_2]/-[P_1]-coated droplets. *Mixed-interface emulsions* consist of fat droplets coated by one or more layers of protein, with each layer consisting of a mixture of different kinds of protein, *e.g.,* [P_1/P_2]-coated [175]. These emulsions are usually formed by mixing the two proteins together prior to homogenization, and then homogenizing the oil and mixed protein solution together under conditions where both proteins adsorb to the fat droplet surfaces.

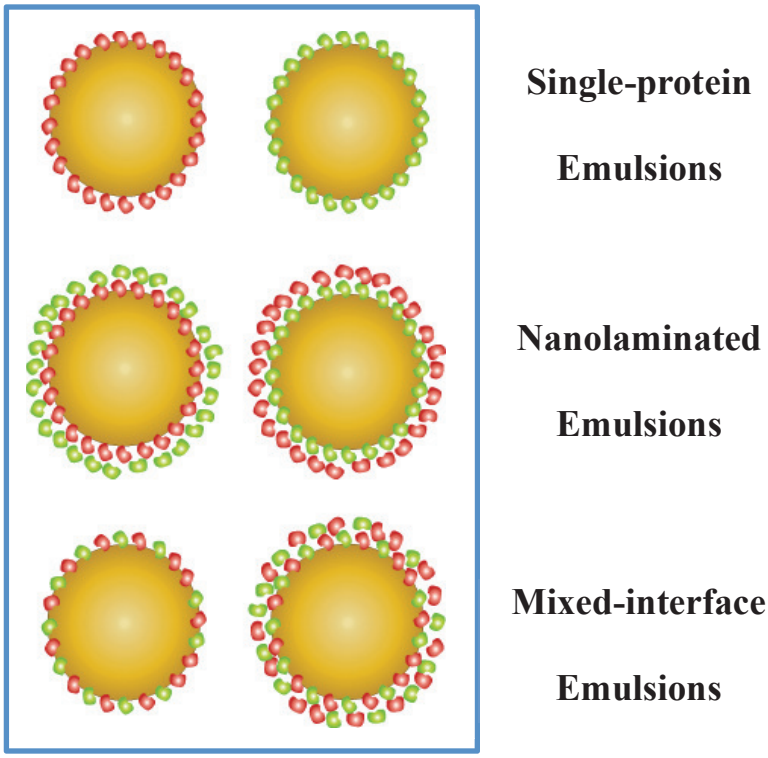

Figure 10.1 A variety of different interfacial structures can be formed using two different proteins, including emulsions stabilized by a single protein layer, nanolaminated protein layers, or mixed interfacial layers.

In the current study, we use two globular proteins to fabricate oil-in-water emulsions with different interfacial compositions and structures: β-lactoglobulin (β-Lg) and lactoferrin (LF). β-Lg is a surface-active globular protein normally isolated from bovine milk that has a molecular weight of 18.4 kDa and an isoelectric point (pI) around pH 5 [72, 176]. Previous studies suggest that β-Lg forms a thin electrically charged coating around fat droplets that opposes droplet aggregation primarily through electrostatic repulsion [37]. LF is a surface-active globular glycoprotein that is naturally present in mammalian secretions such as milk, saliva, tears, semen, and mucous [177]. LF has a molecular weight of 80 kDa and an isoelectric point around pH 8.5 [178]. Previous studies suggest that LF forms a thick electrically charged coating around fat

droplets that opposes droplet aggregation through both steric and electrostatic repulsion [38, 93]. LF and β-Lg tend to form electrostatic complexes over a fairly wide pH range due to the appreciable differences in their isoelectric points, *i.e.,* $5 < pH < 8.5$ [39, 93]. This characteristic enables various kinds of interfacial structures to be assembled from these two globular proteins.

The main purpose of this study was to examine the influence of interfacial composition and structure on the physical stability of emulsions to environmental stresses (pH and salt) and on the chemical degradation of an encapsulated bioactive lipid (β-carotene). β-carotene is a carotenoid that is widely used in foods as a colorant, but is also being increasingly use as a nutraceutical agent due to its pro-vitamin A activity [179, 180]. β-carotene has a conjugated polyunsaturated hydrocarbon chain that makes it particularly prone to auto-oxidation [180-182], which leads to color fading and loss of desirable nutritional attributes [182, 183]. We hypothesized that the nature of the protein interface coating the fat droplets would influence the rate of β-carotene degradation in emulsion-based delivery systems.

10.2 Materials and Methods

10.2.1 Materials

Corn oil was purchased from a commercial food supplier (Mazola, ACH Food Companies, Inc., Memphis, TN) and stored at 4 °C until use. Lactoferrin powder was supplied by FrieslandCampinanin (Delhi, NY), and the manufacturer reported that it contained 97.7% protein and 0.12% ash. β-lactoglobulin powder (BioPURE) was supplied by Davisco Foods International (Eden Prairie, MN). The manufacturer reported

the composition of this powder to be 97.4% total protein, 92.5% β-lactoglobulin, and 2.4% ash. β-carotene (Type I, C9750) was purchased from the Sigma Chemical Company (St. Louis, MO). All other chemicals used in this research were purchased from Sigma-Aldrich (St Louis, MO). Double distilled water was used to make all solutions.

10.2.2 Emulsion Preparation

Preparation of single-protein emulsions: The oil phase was prepared by dispersing crystalline β-carotene (0.25 wt%) in corn oil by sonicating for 1 min sonication, then heating (50-60°C) for 5 min, and then stirring at room temperature for about 1 hour. After this process the β-carotene was fully dissolved within the corn oil, *i.e.,* a clear orange/yellow colored oil was obtained. Aqueous emulsifier solutions were prepared by dispersing either LF (0.75 wt%) or β-Lg (0.75 wt%) powder and 0.01% sodium azide (prevention of bacterial growth) into double distilled water and then stirring for 3 hours at room temperature to ensure complete dispersion. The LF solution had to be filtered to remove a small amount of insoluble particles. Primary emulsions were prepared by homogenizing 5 wt% oil phase with 95 wt% aqueous phase at ambient temperature with the samples being covered by aluminum foil (to avoid light exposure). Coarse emulsions were formed using a high shear mixer (M133/1281-0, 2 speed, Biospec Products Inc., ESGC, Switzerland) for 2 min at level 2. These emulsions were then passed 4 times through a high-pressure microfluidizer (M-110 L processor, Microfluidics Inc., Newton, MA) at 11,000 psi (75.8 MPa).

Preparation of nanolaminated emulsions: Nanolaminated emulsions containing LF- β-Lg -coated droplets were formed by mixing 1.5% LF solution with 10% oil-in-

water emulsions containing β-Lg-coated droplets in a 1:1 ratio at pH 6.5. Nanolaminated emulsions containing β-Lg-LF-coated droplets were formed by mixing 1.5% β-Lg solution with 10% oil-in-water emulsions containing LF-coated droplets in a 1:1 ratio at pH 6.5. At this pH the β-Lg is negatively charged (pH > pI) and the LF is positively charged (pH < pI), which promotes adsorption of the globular proteins in solution to the oppositely charged droplet surfaces. Both the final nanolaminated emulsions produced using this method contained 5 wt% oil phase (β-carotene + corn oil), 0.75 wt% LF, and 0.75 wt% β-Lg.

Preparation of mixed-interface emulsions: Mixed interface emulsions were prepared by blending 5 wt% oil phase (β-carotene + corn oil) with 95% aqueous phase (0.75 wt% LF + 0.75 wt% β-Lg in solution) using a high shear mixer a high shear mixer (M133/1281-0, Biospec Products Inc., ESGC, Switzerland) for 2 min. The coarse emulsions produced were then passed 4 times through a microfluidizer (M-110 L processor, Microfluidics Inc., Newton, MA) at 11,000 psi (75.8 MPa).

After formation all emulsions were stored overnight prior to analysis.

10.2.3 Color Degradation of β-carotene Enriched Emulsions

Color fading of β-carotene emulsions was measured using a non-destructive colorimetric method described previously [184]. Samples were covered with foil to avoid light exposure and stored at 37 °C to accelerate pigment degradation. A colorimeter (ColorFlex EZ, Hunter lab) was used to measure the tristimulus color coordinates (L*, a*, b*) of the emulsions during storage. The total color difference (ΔE^*) was then calculated from these values:

$$\Delta E^* = \sqrt{\left[\left(L^* - L_0^*\right)^2 + \left(a^* - a_0^*\right)^2 + \left(b^* - b_0^*\right)^2\right]} \quad (10.1)$$

Where L^*, a^* and b^* are the measured color coordinates of the emulsions at a certain incubation time, and L_0^*, a_0^* and b_0^* are the initial values at zero time.

10.2.4 Influence of Environmental Stresses on Emulsion Physicochemical Stability

After preparation, emulsions were subjected to a range of environmental stresses:

- *pH*: Emulsions were adjusted to a particular pH value (pH 3 to 9) using either 1M HCl or 1M NaOH solutions, stirred for 10 minute, and then stored overnight.
- *Ionic strength*: A series of systems with different salt concentrations was prepared by mixing 50 mL aliquots of emulsions with 50 mL aliquots of sodium chloride solutions (0 to 600 mM) at pH 6.5. The samples were stirred for 10 min and then stored overnight.
- *Temperature*: Glass test tubes containing 5% oil-in-water emulsions were placed in a water bath set at a particular temperature (from 30 to 90°C) for 30 min, then cooled to room temperature, and then stored overnight.

10.2.5 Particle Characterization

Particle size distributions were determined using dynamic light scattering (Zetasizer Nano ZS series, Malvern Instruments, Worcestershire, U.K.). Emulsion samples were diluted in pH-adjusted double distilled water at a ratio of 1:200 (v/v) and then placed in a capillary test tube that was loaded into the instrument. Particle sizes were reported as the Z-average mean diameter calculated from the measured particle size

distribution.The ζ-potential of the particles in the emulsions was determined using a particle electrophoresis instrument (Zetasizer Nano ZS series, Malvern Instruments, Worcestershire, UK). Emulsions were diluted to a droplet concentration of approximately 0.001 wt% using pH-adjusted water to avoid multiple scattering effects. After loading the samples into the instrument they were equilibrated for about 120 s before particle charge data was collected over 20 continuous readings.

10.2.6 Statistical Analysis

All experiments were carried out three times on newly prepared samples, with two to three measurements being made per sample. Results are reported as averages and standard deviations of these measurements.

10.3 Results and Discussion

10.3.1 Formulation of Primary and Secondary Emulsions

The electrical charges on fat droplets coated by different kinds of interfacial protein layers were measured (**Figure 10. 2a**). At pH 6.5, the ζ-potential was initially +32 mV for the LF-coated droplets and -65 mV for the β-Lg-coated droplets, indicating that these two globular proteins had opposite electrical charges under these conditions. The high stability of the LF-emulsions and β-Lg-emulsions to droplet aggregation can therefore be attributed to strong electrostatic repulsion between the droplets, as well as some steric repulsion in the case of the LF-coated droplets [38]. The electrical charges on the β-Lg-LF- and LF- β-Lg-laminated droplets were intermediate between that of the β-Lg- and LF-coated droplets, suggesting that their interfaces contained a mixture of proteins. Interestingly, the charge did not seem to be dominated by the protein that was

believed to form the outer layer at the interface. The mixed-interface emulsions initially had a high negative charge that was similar to that on the β-Lg-emulsions. This may have occurred due to preferential adsorption of the smaller β-Lg molecules to the droplet surfaces during homogenization, or because the β-Lg molecules tended to be located in the outer layers. After 15 days storage, we noticed an appreciable decrease in the negative charge on the mixed-interface emulsions, which suggests that there was some change in the interfacial composition or structure over time. This may have occurred because LF molecules originally present in the aqueous phase adsorbed to the oil droplet surfaces, which could have been through a competitive adsorption or co-adsorption process. In addition, there may have been some rearrangement in the structural organization of the LF and β-Lg molecules at the droplet surfaces over time, which changed their electrical characteristics

The mean particle diameter (d_{43}) of emulsions with different interfacial characteristics was measured after 0 and 14 days storage at ambient temperature (**Figure 10.2b**). The initial particle size was relatively small (d_{43} < 250 nm) in most of the emulsions, suggesting that they were relatively stable to droplet aggregation. However, the particles in the β-Lg-LF-emulsion (d = 385 nm) were appreciably larger than those in the LF-emulsion (d = 208 nm), which suggests that some droplet aggregation occurred during the preparation of these emulsions. One possible reason is that the β-Lg molecules did not completely saturate the surfaces of the LF-coated droplets, and so some bridging flocculation occurred in this system between positive patches on one droplet and negative patches on another droplet. After 15 days storage, the droplet size either remained fairly similar to the initial values (β-Lg-, β-Lg-LF- and LF- β-Lg-coated

emulsions) or increased appreciably (LF- or mixed interface emulsions), suggesting that some droplet aggregation occurred during storage in these later systems.

It is important to stress that the stability of the laminated emulsions to droplet aggregation was very sensitive to the method used to prepare them. We found that less aggregation occurred when LF-emulsions were mixed with β-Lg solution (or β-Lg-emulsions were mixed with LF solution) at pH 8 and then adjusted to pH 6.5, than if they were directly mixed at pH 6.5. A similar finding was reported for the formation of multilayer emulsions from protein-stabilized droplets and oppositely charged polysaccharides [76].

(a)

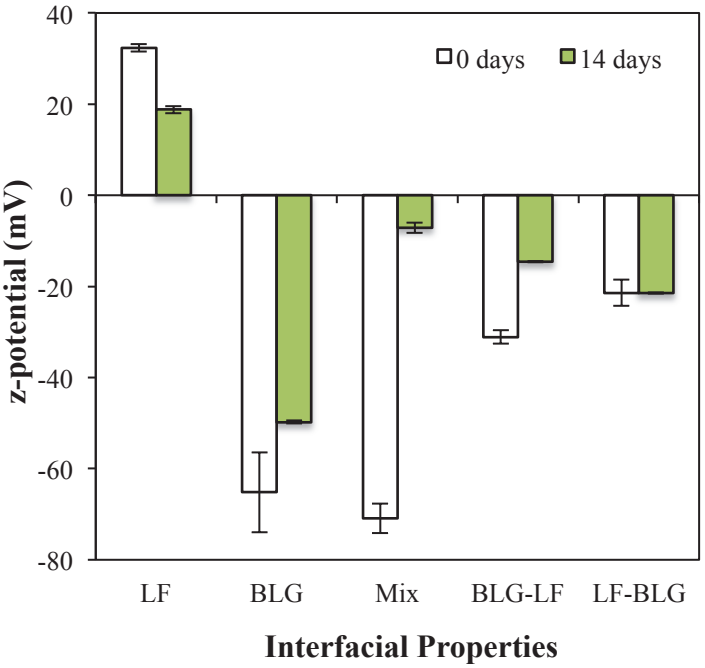

(b)

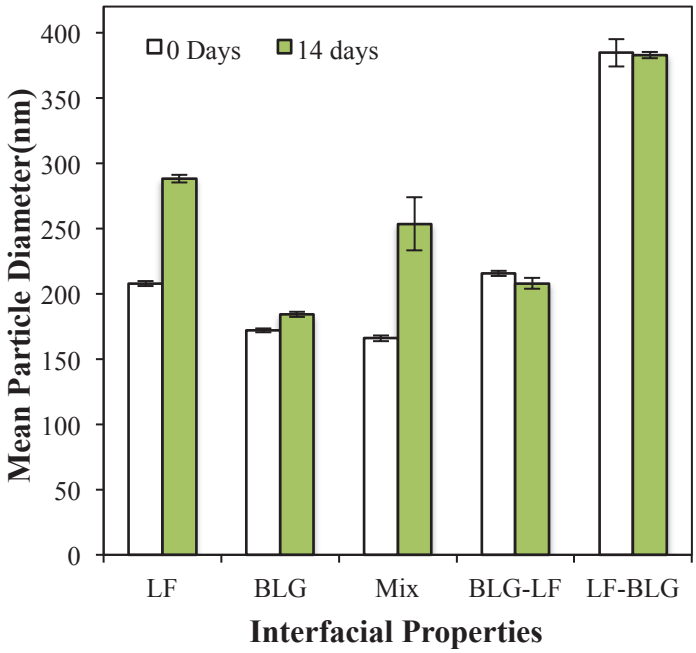

Figure 10.2 (a) zeta-potential of β-carotene enriched emulsions with different interfacial properties measured after 0-14 days storage at 37 °C under oxygen and nitrogen enviornment. (b) Mean particle size of β-carotene enriched emulsions with different interfacial properties measured after 0 and 14 days storage under oxygen and nitrogen enviornment.

10.3.2 Influence of Environmental Stresses on Emulsion Stability

Emulsion-based delivery systems containing β-carotene may be incorporated into food and beverage products that have different pH values and ionic strengths. In addition, ingested delivery systems must pass through the gastrointestinal tract where they are exposed to variations in pH and ionic strength in the mouth, stomach, and small intestine. We therefore examined the influence of pH and ionic strength on the electrical characteristics and stability of the β-carotene enriched emulsions. Emulsion samples were incubated at different pH and ionic strength values for 24 hours and then their physicochemical properties were measured.

10.3.2.1 Influence of pH on β-carotene Enriched Emulsions

The ζ-potential of β-Lg-emulsions went from highly positive to highly negative as the pH was increased from 2 to 9, with a point of zero charge around pH 4.5 (**Figure 10.3a**). This result can be attributed to the fact that the pH moved from below to above the isoelectric point of the β-Lg molecules adsorbed to the droplet surfaces [76, 97, 123]. The charge on the droplets in the LF-emulsions went from highly positive to slightly negative as the pH was increased from 2 to 9, with a point of zero charge around pH 8.5, which can be attributed to the appreciably higher isoelectric point of LF compared to β-Lg [38, 93]. The ζ-potential of all the emulsions containing both β-Lg and LF also went from positive to negative with increasing pH, but the point of zero charge was around pH 5, *i.e.,* slightly higher than that of β-Lg-coated droplets. Surprisingly, the mixed interface, LF- β-Lg-nanolaminated, and β-Lg-LF-nanolaminated emulsions all had fairly similar charge-pH profiles (**Figure 10.3a**). These results suggest that the droplets were coated by a mixture of both LF and β-Lg molecules, and that the β-Lg molecules dominated the overall electrical characteristics of the interfaces. This may have occurred because there were more β-Lg than LF molecules present at the droplet surfaces, or because the β-Lg molecules arranged themselves so that they were preferentially located within the outer protein layer.

The mean particle diameter of the β-Lg-emulsions was relatively small at low pH values (≤ 3) and high pH values (≥ 6) (**Figure 10.3b**), which can be attributed to strong electrostatic repulsion between β-Lg-coated droplets in these pH ranges [123]. On the other hand, the β-Lg-emulsions were unstable to droplet aggregation at intermediate pH values (pH 4 and 5), which can be attributed to the fact that the protein molecules were

near their isoelectric point and so there was little charge on them. Under these conditions, the van der Waals attraction is sufficiently strong to overcome the weak electrostatic repulsion between the droplets thereby leading to aggregation [29]. The size of the particles in the LF-emulsions remained relatively low across the entire pH range studied, indicating that the LF-coated droplets were stable to droplet aggregation. As discussed previously, steric repulsion plays an important role in determining the aggregation stability of LF-coated droplets due to the fact that LF molecules have a relatively high molecular weight and contain hydrophilic carbohydrate side chains that protrude into the aqueous phase [38, 39, 93].

All the emulsions containing a mixture of β-Lg and LF were unstable to droplet aggregation at intermediate pH values (**Figure 10.3b**). This effect can be partly attributed to the relatively low magnitude of the electrical charge on the droplets in this pH range (**Figure 10.3a**), and so the electrostatic repulsion between them would be relatively weak. However, the fact that the LF-coated droplets were stable but the LF- β-Lg-nanolaminated droplets were not, suggests that LF was unable to provide strong steric repulsion when used in combination with β-Lg. This may have occurred because LF did not form a uniform outer layer around the β-Lg-coated droplets. Instead, a mixed interfacial layer may have formed, or there may have been some uncovered patches on the droplet surfaces.

(a)

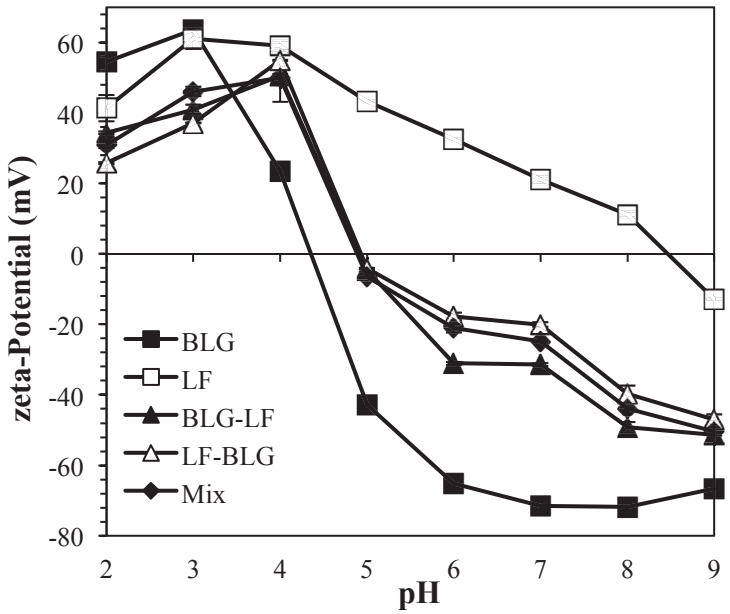

(b)

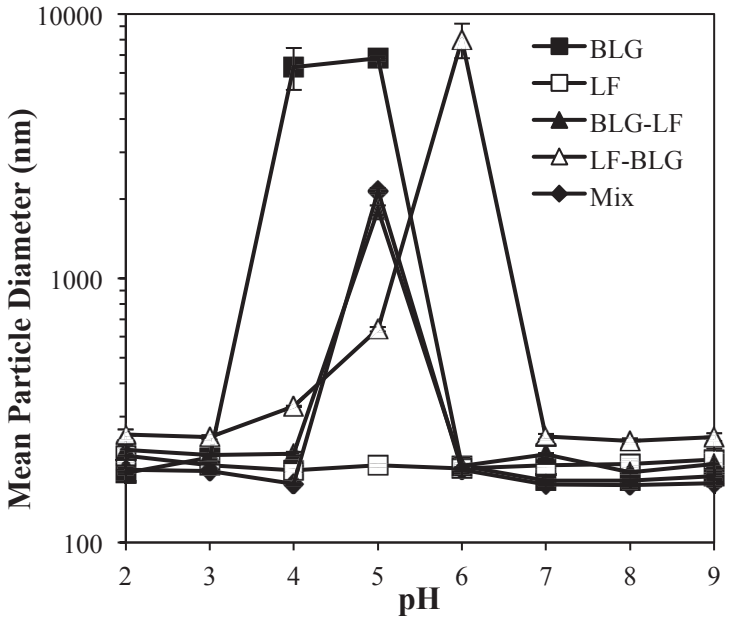

Figure 10.3 (a) Influnece of pH on ζ-potential in β-carotene enriched emulsions with different interfacial properties (5% corn oil, 0.25% β-carotene). (b) Influnece of pH on droplet aggregation in β-carotene enriched emulsions with different interfacial properties (5% corn oil, 0.25% β-carotene).

10.3.2.2 Influence of Salt on β-carotene Enriched Emulsions

The influence of salt addition on the electrical characteristics and aggregation stability of the various emulsion-based delivery systems was measured at pH 6.5 (**Figure 10.4**). The magnitude of the electrical charge on all of the emulsions decreased with increasing salt concentration (**Figure 10.4a**), which can be mainly attributed to electrostatic screening effects [29]. Interestingly, we observed charge reversal in the LF-coated droplets, with the charge going from highly positive to slightly negative with increasing NaCl concentration. This suggests that there may have been some binding of anionic chloride ions (Cl^-) to positively charged groups on the surfaces of the LF molecules.

The β-Lg-emulsions were unstable to salt addition, with the mean particle diameter increasing with increasing NaCl concentration (**Figure 10.4b**). Droplet aggregation was attributed to progressive screening of the electrostatic repulsion between the β-Lg -coated droplets as the salt concentration increased. All of the other emulsions appeared to be stable to salt addition as indicated by the fact that there was no change in mean particle diameter with increasing salt concentration. This effect may have been partly due to the steric repulsion generated by the presence of LF molecules at the droplet surfaces [39].

(a)

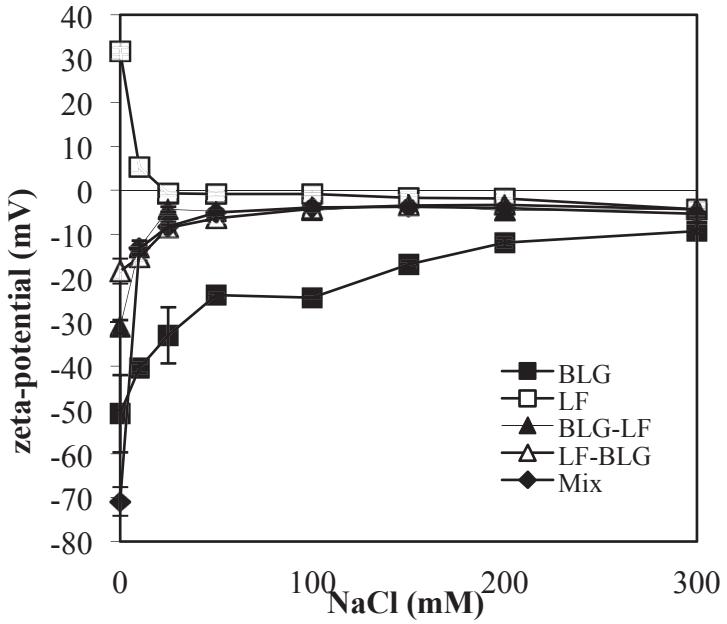

(b)

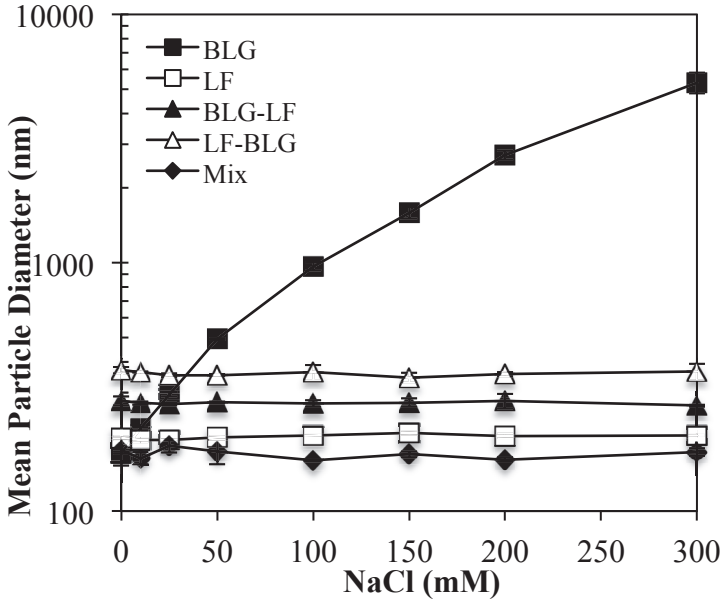

Figure 10.4 (a) Influnence of ionic strength on ζ-potential of β-carotene enriched emulsions with different interfacial properties (5% corn oil, 0.25% β-carotene). (b) Influnece of ionic strength on droplet aggregation of β-carotene enriched emulsions with different interfacial properties (5% corn oil, 0.25% β-carotene).

10.3.2.3 Influence of Thermal Treatment on β-carotene Enriched Emulsions

The effect of thermal treatment on the stability of β-carotene enriched emulsions was determined at pH 6.5 (no salt) by holding samples at temperatures ranging from 30 to 90°C for 30 min. There were some appreciable changes in the electrical characteristics (ζ-potential) of the droplets in some of the emulsions with increasing holding temperature (**Figure 10.5a**), which suggests that there were alterations in the composition and/or structural organization of the droplets interfaces in these systems. For example, the positive charge on the LF-coated droplets increased appreciably when the holding temperature was increased from 60 to 70 ºC, which may have been due to thermal denaturation of this globular protein and subsequent alterations in the organization of the cationic groups in the interface. There was also an appreciable increase in the negative charge on the droplets in both laminated emulsions (LF- β-Lg and β-Lg-LF) with increasing holding temperature. A possible explanation for this effect is that there was a reorganization of the LF and β-Lg molecules at the droplet surfaces due to thermal treatment, *e.g.,* β-Lg molecules may have preferentially moved to the outer surfaces or LF molecules may have desorbed from the droplet surfaces. Further studies are needed to identify the physicochemical basis of these changes in droplet charge with heating.

(a)

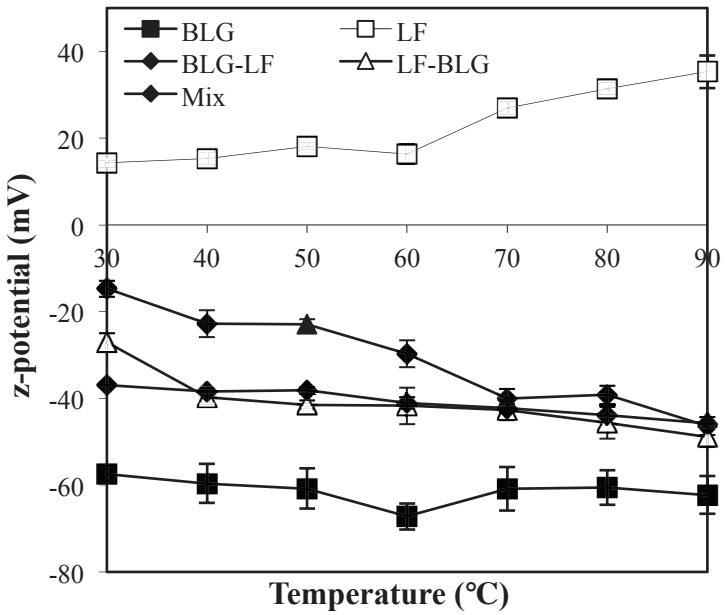

(b)

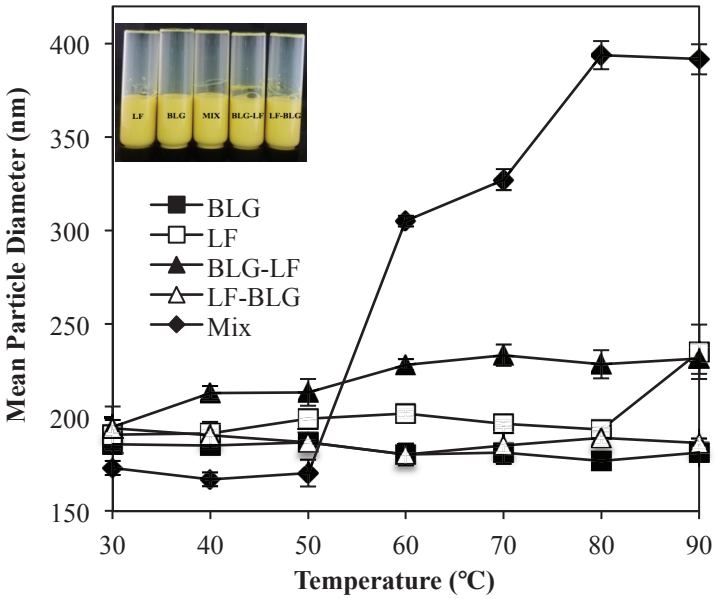

Figure 10.5 (a) Influnece of holding temperature (for 30 minutes) on ζ-potential of β-carotene enriched emulsions with different interfacial properties (5% corn oil, 0.25% β-carotene). (b) Influnece of holding temperature (for 30 minutes) on droplet aggregation of β-carotene enriched emulsions with different interfacial properties (5% corn oil, 0.25% β-carotene).

All single (LF or β-Lg) and laminated (LF-β-Lg or β-Lg-LF) emulsions exhibited good stability to droplet aggregation at all holding temperatures as evidenced by their relatively small particle sizes and ability to flow when the test tubes were inverted (**Figure 10.5b**). However, there was an appreciable increase in the mean particle size of the mixed-interface emulsions held at ≥ 50 °C, suggesting that some droplet aggregation had occurred within these systems. Even so, the mixed-interface emulsions still remained fluid when they were inverted, indicating that droplet aggregation did not cause gelation. These studies show that the initial interfacial composition and structure does have an influence on the thermal stability of the protein-coated lipid droplets. Previous studies have reported that LF-coated lipid droplets aggregated when heated above around 50 °C [38, 39, 101], which was attributed to unfolding of the adsorbed globular proteins leading to an increase in hydrophobic attraction between the droplets. On the other hand, we found that the LF-coated lipid droplets were relatively stable to droplet aggregation at elevated temperatures in the current study (**Figure 10.5b).** This apparent discrepancy may be due to differences in the amount of LF available to cover the droplet surfaces in the different studies. Previous studies have shown that the stability of fat droplets to aggregation is better at high LF-to-fat droplet ratios [39, 185] than at low ratios [38, 39, 101]. Presumably, at higher protein-to-fat ratios the droplets are more stable to aggregation because the LF forms a uniform and thick interfacial layer that generates a strong steric repulsion.

10.3.3 Influence of Interfacial Properties on β-carotene Degradation

β-carotene is a polyunsaturated molecule that it highly susceptible to chemical degradation and therefore tends to lose its orange-red color during storage [180]. We

therefore measured color fading of the β-carotene emulsions using a non-destructive colorimetric method described previously [184]. There was a rapid change in the total color difference of the β-Lg-emulsions during the first day of storage, followed by a more gradual increase afterwards (**Figure 10.6a**). On the other hand, there was only a slight increase in ΔE^* for the other emulsions over time. These results suggested that the presence of LF within the emulsion-based delivery systems was able to retard the chemical degradation of encapsulated β-carotene. This could be due to the ability of lactoferrin molecules to strongly bind iron ions (Fe^{2+} or Fe^{3+}) [186, 187], since transition metals are known to catalyze oxidation reactions [180]. The nature of the interfacial coatings (LF-β-Lg, β-Lg -LF, or LF/ β-Lg) did not appear to have a major impact on the rate of β-carotene degradation, again highlighting the importance of having some LF present in the systems. We also found that ΔE^* was somewhat less for samples that were routinely flushed with nitrogen during storage to lower the oxygen concentration (**Figure 10.6b**), which highlights the role that oxygen plays in color fading rate.

(a)

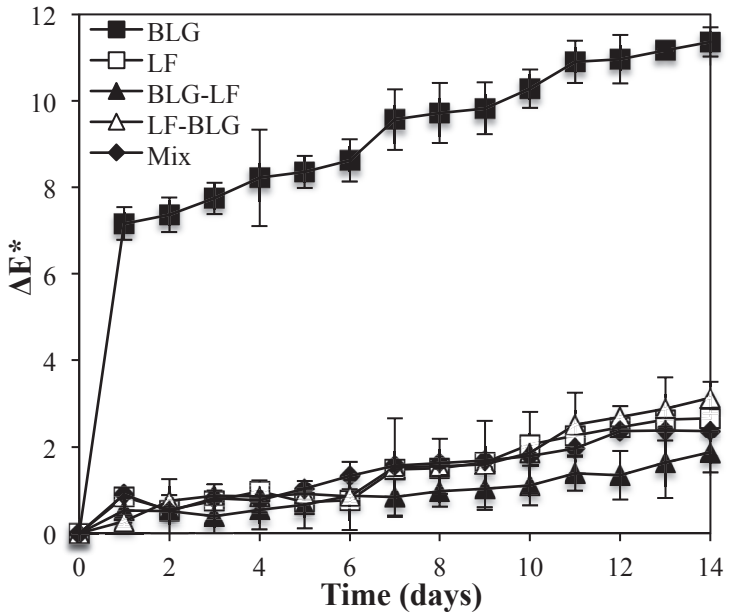

(b)

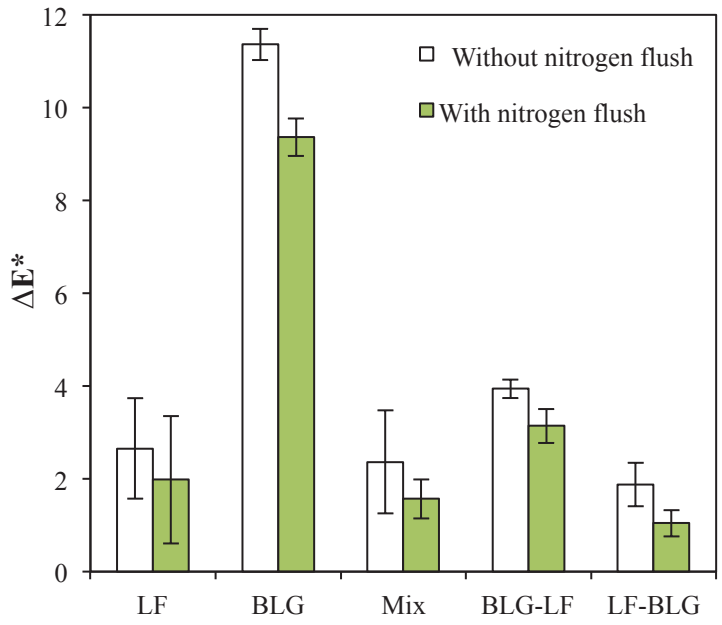

Figure 10.6 (a) Total color change (Δ*E**) of β-carotene enriched emulsions with different interfacial properties during storage at 37 °C. (b) Total color change (Δ*E**) of β-carotene enriched emulsions with different interfacial properties after storage at 37 °C for 14 days with or without nitrogen flushing.

10.4 Conclusions

The results of this study have important implications for the development of effective delivery systems for bioactive lipophilic components. The stability of protein-coated emulsions to droplet aggregation under different pH and ionic strength conditions depended on interfacial properties. Lactoferrin-coated droplets were stable to droplet aggregation when the pH was varied from 2 to 9, whereas those containing β-Lg, β-Lg-LF, LF-β-Lg or LF/β-Lg were all unstable to droplet aggregation at intermediate pH values. LF-coated droplets also had good stability to the presence of NaCl (even though the droplet charge was close to zero) and to elevated temperatures. These results suggest that LF-coated droplets are stabilized primarily by steric repulsion, rather than electrostatic repulsion. The chemical degradation of β-carotene occurred relatively quickly in emulsions containing β-Lg-coated oil droplets, but was much slower in all emulsions containing LF. Metal ions are known to play an important role in promoting the chemical degradation of carotenoids, and therefore the ability of lactoferrin to chelate metal ions would account for LFs ability to delay β-carotene degradation. Alternatively, the LF may have been able to bind to β-carotene and protect it from degradation. Overall, this study suggests that droplets coated by LF alone may be the most suitable for forming physically and chemically stable delivery systems for β-carotene. However, LF is relatively expensive and cationic droplets may cause some problems in commercial products (such as astringent mouthfeel and precipitation with anionic components), and therefore using LF in combination with β-Lg may be desirable for certain applications. Finally, we should mention that a recent study in our laboratory found that the bioaccessibility of β-carotene measured using an *in vitro* method was relatively low for

LF-coated oil droplets[188]. Consequently, it is important to ensure that carotenoids are both protected during storage, and released after ingestion.

CHAPTER 11

CONCLUSIONS

The overall goal of this work was to determine whether hetero-aggregation of biopolymer-coated fat droplets could be used to produce novel textures and reduced fat foods. Initially, two emulsions were prepared containing oppositely charged droplets, and then hetero-aggregation was induced by mixing them together to promote electrostatic attraction. The nature of the hetero-aggregates formed influenced the texture, stability, and appearance of the products.

In this work, lactoferrin (LF) and β-lactoglobulin (β-Lg) were selected as emulsifiers due to their opposite charges at neutral pH ($pI_{\beta\text{-}Lg} < pH < pI_{LF)}$. Results showed that the formation and stability of microclusters created by mixing two oppositely charged protein-coated lipid droplets could be modulated by controlling particle ratio, size, charge, and interactions. The largest microclusters were obtained by mixing LF-coated lipid droplets (3%LF, 10% oil) and β-Lg-coated lipid droplets (0.5% β-Lg, 10%) together at intermediate particle ratio (40% LF : 60% β-Lg). The presence of excess proteins in the aqueous phase can inhibit the formation of large aggregates due to their ability to bind to fat droplet surfaces and neutralize the charge. The aggregation observed in dilute systems (0.1%wt oil) was in reasonable agreement with predictions made using a simple statistical thermodynamic model. However, in concentrated systems, gelled structures were formed due to the ability of the microclusters to form a three-dimensional network.

The rheological properties of suspensions containing mixtures of negatively and positively charged protein-coated lipid droplets exhibited an interesting dependence on

the fat content and environmental stresses. The viscosity of mixed-droplet emulsions is much higher than single-droplet emulsions, which was attributed to the network formation due to electrostatic attraction. Addition, increasing the fat content increased the apparent viscosity of the mixed emulsions and led to shear thinning due to the destruction and deformation of the aggregated structure by mechanical shearing. The rheological properties of concentrated emulsions also depended on environmental conditions such as pH, salt concentration, and temperature. The reduced electrostatic attraction induced by adjusting the pH or increasing the ionic strength led to the a weakened gel structure suggesting disassociation of aggregates. When the temperature was above the thermal denaturation point of the proteins (60 ºC), heating caused an increase in particle size of the microclusters and the gel strength of mixed emulsions due to increased hydrophobic attraction. The optical characteristics of low fat mixed emulsions were similar to high fat single emulsions. This result suggested the potential application of hetero-aggregation in producing reduced fat food products.

It is also important to understand the potential biological fate of microclusters containing oppositely charged fat droplets when developing food systems. An *in vitro* gastrointestinal model was utilized to examine the biophysical stability of microclusters (*e.g.,* charge, size, rheology, and microstructure) under simulated oral, gastric, and intestinal conditions. Our results showed that the mixed emulsions had higher viscosities than the two single emulsions in the mouth, but the electrical characteristics, aggregation state, and viscosity of all the emulsions were fairly similar in the stomach and small intestine stages. As a result, all of the emulsions were hydrolyzed at a similar rate and to a similar extent by intestinal enzymes.

Since the LF and β-Lg are highly purified expensive proteins, we also examined the possibility of using alternative food-grade emulsifiers. Whey protein isolate (WPI: $pI_{WPI} \approx 4.5$) and modified starch (MS: $pKa_{MS} \approx 2.3$) were used as examples of cationic and anionic emulsifiers at pH 3.5. This study showed that highly viscous textures could be formed by mixing negative MS-coated lipid droplets and positive WPI-coated lipid droplets at intermediate particle ratios due to aggregation through electrostatic attraction. The rheological properties of these mixed emulsions could be manipulated by controlling the particle ratio and solution pH.

Finally, the possibility of using mixed proteins to inhibit the chemical degradation of a bioactive agent (β-carotene) was studied. The influence of interfacial composition (β-Lg; LF; β-Lg-LF; LF-β-Lg; or LF/ β-Lg) on the physical and chemical stability of emulsion-based delivery systems containing β-carotene was examined under different environmental stresses, including pH, ionic strength, and temperature. Emulsions were all unstable to aggregation at intermediate pH values except the LF-coated lipid droplets. In addition, the presence of LF improved the stability of emulsions to high salt concentrations and elevated temperatures. LF also retarded the chemical degradation of β-carotene. Therefore LF-coated emulsions were the most suitable form for fabricating physically and chemically stable delivery systems for β-carotene.

In summary, the knowledge obtained from this study is important for the design of delivery systems for lipophilic compounds and for the production of reduced fat food products using hetero-aggregation. It was shown that the performance and physicochemical properties of hetero-aggregates could be modulated by varying

formation conditions. For the future, the sensory evaluation of reduced fat products formed by hetero-aggregation would be important for their practical application.

BIBLIOGRAPHY

1. Thow, A.M., et al., *The effect of fiscal policy on diet, obesity and chronic disease: a systematic review*. Bulletin of the World Health Organization, 2010. **88**(8): p. 609-14.
2. Jacobson, D. and B. Gance-Cleveland, *A systematic review of primary healthcare provider education and training using the Chronic Care Model for Childhood Obesity*. Obesity Reviews, 2011. **12**(501): p. e244-e256.
3. Stanley, W.C., et al., *Dietary Fat and Heart Failure: Moving From Lipotoxicity to Lipoprotection*. Circulation Research, 2012. **110**(5): p. 764-776.
4. Abumrad, N.A., et al., *Moving Beyond "Good Fat, Bad Fat": The Complex Roles of Dietary Lipids in Cellular Function and Health*. Advances in Nutrition, 2012. **3**(1): p. 60-68.
5. McClements, D.J., *Advances in fabrication of emulsions with enhanced functionality using structural design principles*. Current Opinion in Colloid & Interface Science, 2012. **17**(5): p. 235-245.
6. Thurgood, J.E. and S. Martini, *Effects of Three Emulsion Compositions on Taste Thresholds and Intensity Ratings of Five Taste Compounds*. Journal of Sensory Studies, 2010. **25**(6): p. 861-875.
7. Giroux, H.J., V. Perreault, and M. Britten, *Characterization of hydrophobic flavor release profile in oil-in-water emulsions*. Journal of food science, 2007. **72**(2): p. S125-9.
8. Bayarri, S., A.J. Taylor, and J. Hort, *The role of fat in flavor perception: effect of partition and viscosity in model emulsions*. Journal of Agricultural and Food Chemistry, 2006. **54**(23): p. 8862-8.
9. Hsu, M.F., et al., *Self-assembled shells composed of colloidal particles: Fabrication and characterization*. Langmuir, 2005. **21**(7): p. 2963-2970.
10. Lopez-Lopez, J.M., et al., *Stability of binary colloids: kinetic and structural aspects of heteroaggregation processes*. Soft Matter, 2006. **2**(12): p. 1025-1042.
11. Yates, P.D., et al., *Heteroaggregation with nanoparticles: effect of particle size ratio on optimum particle dose*. Colloids and Surfaces a-Physicochemical and Engineering Aspects, 2005. **255**(1-3): p. 85-90.
12. Piechowiak, M.A., et al., *Aggregation kinetics and gel formation in modestly concentrated suspensions of oppositely charged model ceramic colloids: a numerical study*. Physical Chemistry Chemical Physics, 2012. **14**(4): p. 1431-1439.
13. Han, S.J., et al., *Preparation of anionic ion exchange latex particles via heteroaggregation*. Journal of Applied Polymer Science, 2013. **127**(5): p. 3601-3612.
14. Findlay, A.D., D.W. Thompson, and E. Tipping, *The aggregation of silica and haematite particles dispersed in natural water samples*. Colloids and Surfaces a-Physicochemical and Engineering Aspects, 1996. **118**(1-2): p. 97-105.
15. Spruijt, E., et al., *Reversible assembly of oppositely charged hairy colloids in water*. Soft Matter, 2011. **7**(18): p. 8281-8290.

16. Lemmers, M., et al., *Multiresponsive Reversible Gels Based on Charge-Driven Assembly*. Angewandte Chemie-International Edition, 2010. **49**(4): p. 708-711.
17. Ohsugi, A., et al., *Catch and release of DNA in coacervate-dispersed gels*. Macromolecular Rapid Communications, 2006. **27**(15): p. 1242-1246.
18. McParlane, J., et al., *Dual pH-triggered physical gels prepared from mixed dispersions of oppositely charged pH-responsive microgels*. Soft Matter, 2012. **8**(23): p. 6239-6247.
19. Islam, A.M., B.Z. Chowdhry, and M.J. Snowden, *Heteroaggregation in colloidal dispersions*. Advances in Colloid and Interface Science, 1995. **62**(2-3): p. 109-136.
20. Mao, Y.Y. and D.J. McClements, *Modulation of bulk physicochemical properties of emulsions by hetero-aggregation of oppositely charged protein-coated lipid droplets*. Food Hydrocolloids, 2011. **25**(5): p. 1201-1209.
21. Mao, Y.Y. and D.J. McClements, *Fabrication of functional micro-clusters by heteroaggregation of oppositely charged protein-coated lipid droplets*. Food Hydrocolloids, 2012. **27**(1): p. 80-90.
22. Norio Ise, I.S.S., *Structure Formation in Solution: Ionic Polymers and Colloidal Particles*. 1 ed2005, New York: Springer.
23. Guzey, D. and D.J. McClements, *Impact of electrostatic interactions on formation and stability of emulsions containing oil droplets coated by beta-lactoglobulin-pectin complexes*. Journal of Agricultural and Food Chemistry, 2007. **55**(2): p. 475-485.
24. Piechowiak, M.A., et al., *Oppositely Charged Model Ceramic Colloids: Numerical Predictions and Experimental Observations by Confocal Laser Scanning Microscopy*. Langmuir, 2010. **26**(15): p. 12540-12547.
25. Dickinson, E., *Simple statistical thermodynamic model of the heteroaggregation and gelation of dispersions and emulsions*. Journal of colloid and interface science, 2011. **356**(1): p. 196-202.
26. Pawar, A.B. and I. Kretzschmar, *Fabrication, Assembly, and Application of Patchy Particles*. Macromolecular Rapid Communications, 2010. **31**(2): p. 150-168.
27. Lopez-Lopez, J.M., et al., *Electrostatic heteroaggregation regimes in colloidal suspensions*. Advances in colloid and interface science, 2009. **147-148**: p. 186-204.
28. Meakin, P., *The Effects of Reorganization Processes on Two-Dimensional Cluster-Cluster Aggregation*. Journal of colloid and interface science, 1986. **112**(1): p. 187-194.
29. McClements, D.J., *Food Emulsions: Principles, Practice, and Techniques*. 2nd ed. CRC series in contemporary food science.2005, Boca Raton: CRC Press.
30. McClements, D.J. and J. Rao, *Food-Grade Nanoemulsions: Formulation, Fabrication, Properties, Performance, Biological Fate, and Potential Toxicity*. Critical Reviews in Food Science and Nutrition, 2011. **51**(4): p. 285-330.
31. McClements, D.J., *Food Emulsions: Principles, Practices, and Techniques*. 2nd ed, ed. F.M. Clydesdale2005, New York: CRC.
32. Muschiolik, G., *Multiple emulsions for food use*. Current Opinion in Colloid & Interface Science, 2007. **12**(4-5): p. 213-220.

33. Matalanis, A., et al., *Fabrication and characterization of filled hydrogel particles based on sequential segregative and aggregative biopolymer phase separation*. Food Hydrocolloids, 2010. **24**(8): p. 689-701.
34. Iqbal, S., et al., *Structuring of lipid phases using controlled heteroaggregation of protein microspheres in water-in-oil emulsions*. Journal of Food Engineering, 2013. **115**(3): p. 314-321.
35. Hu, M., D.J. McClements, and E.A. Decker, *Lipid oxidation in corn oil-in-water emulsions stabilized by casein, whey protein isolate, and soy protein isolate*. Journal of Agricultural and Food Chemistry, 2003. **51**(6): p. 1696-1700.
36. McClements, D.J., *Protein-stabilized emulsions*. Current Opinion in Colloid & Interface Science, 2004. **9**(5): p. 305-313.
37. Mao, Y. and D. Julian McClements, *Fabrication of reduced fat products by controlled heteroaggregation of oppositely charged lipid droplets*. Journal of food science, 2012. **77**(5): p. E144-52.
38. Tokle, T. and D.J. McClements, *Physicochemical properties of lactoferrin stabilized oil-in-water emulsions: Effects of pH, salt and heating*. Food Hydrocolloids, 2011. **25**(5): p. 976-982.
39. Schmelz, T., et al., *Modulation of physicochemical properties of lipid droplets using beta-lactoglobulin and/or lactoferrin interfacial coatings*. Food Hydrocolloids, 2011. **25**(5): p. 1181-1189.
40. Nakauma, M., et al., *Comparison of sugar beet pectin, soybean soluble polysaccharide, and gum arabic as food emulsifiers. 1. Effect of concentration, pH, and salts on the emulsifying properties*. Food Hydrocolloids, 2008. **22**(7): p. 1254-1267.
41. Trubiano, P.C., *The role of specialty food starches in flavor emulsions*. Flavor Technology, 1995. **610**: p. 199-209.
42. McClements, D.J., E.A. Decker, and J. Weiss, *Emulsion-based delivery systems for lipophilic bioactive components*. Journal of food science, 2007. **72**(8): p. R109-24.
43. Shogren, R.L., et al., *Distribution of octenyl succinate groups in octenyl succinic anhydride modified waxy maize starch*. Abstracts of Papers of the American Chemical Society, 2000. **220**: p. U111-U111.
44. Charoen, R., et al., *Influence of Biopolymer Emulsifier Type on Formation and Stability of Rice Bran Oil-in-Water Emulsions: Whey Protein, Gum Arabic, and Modified Starch*. Journal of food science, 2011. **76**(1): p. E165-E172.
45. Phillips, G.O. and P.A. Williams, *Handbook of hydrocolloids*2000: CRC PressI Llc.
46. McNamee, B.F., E.D. O'Riordan, and M. O'Sullivan, *Emulsification and microencapsulation properties of gum arabic*. Journal of Agricultural and Food Chemistry, 1998. **46**(11): p. 4551-4555.
47. Chanamai, R. and D.J. McClements, *Comparison of gum arabic, modified starch, and whey protein isolate as emulsifiers: Influence of pH, CaCl(2) and temperature*. Journal of food science, 2002. **67**(1): p. 120-125.
48. Hans-Jurgen, B.G., Karleinz; Kappl, Michael, *Physics and Chemistry of Interface*2006, Germany: Wiley-VCH.

49. McClements, D.J., *Food Emulsions: Principles, Practices, and Techniques*, 2005, CRC Press: Boca Raton, Fl.
50. Payet, L. and E.M. Terentjev, *Emulsification and stabilization mechanisms of o/w emulsions in the presence of chitosan*. Langmuir : the ACS journal of surfaces and colloids, 2008. **24**(21): p. 12247-52.
51. Simo, O.K., et al., *Novel strategies for fabricating reduced fat foods: Heteroaggregation of lipid droplets with polysaccharides*. Food Research International, 2012. **48**(2): p. 337-345.
52. Gonzalez-Tomas, L. and E. Costell, *Relation between consumers' perceptions of color and texture of dairy desserts and instrumental measurements using a generalized Procrustes analysis*. Journal of dairy science, 2006. **89**(12): p. 4511-4519.
53. Chantrapornchai, W., F. Clydesdale, and D.J. McClements, *Influence of droplet characteristics on the optical properties of colored oil-in-water emulsions*. Colloids and Surfaces a-Physicochemical and Engineering Aspects, 1999. **155**(2-3): p. 373-382.
54. Dickinson, E., Stainsby G., *Colloids in Food*1982, London: Application Science.
55. Vakarelski, I.U., et al., *Lateral Hydrodynamic Interactions between an Emulsion Droplet and a Flat Surface Evaluated by Frictional Force Microscopy*. Langmuir, 2010. **26**(11): p. 8002-8007.
56. Geigenmuller, U. and P. Mazur, *Many-Body Hydrodynamic Interactions between Spherical Drops in an Emulsion*. Physica A, 1986. **138**(1-2): p. 269-298.
57. Fabian, T.K., et al., *Salivary Defense Proteins: Their Network and Role in Innate and Acquired Oral Immunity*. International Journal of Molecular Sciences, 2012. **13**(4): p. 4295-4320.
58. Sarkar, A., et al., *Behaviour of an oil-in-water emulsion stabilized by beta-lactoglobulin in an in vitro gastric model*. Food Hydrocolloids, 2009. **23**(6): p. 1563-1569.
59. Kalantzi, L., et al., *Characterization of the human upper gastrointestinal contents under conditions simulating bioavailability/bioequivalence studies*. Pharmaceutical research, 2006. **23**(1): p. 165-176.
60. McClements, D.J. and Y. Li, *Structured emulsion-based delivery systems: Controlling the digestion and release of lipophilic food components*. Advances in colloid and interface science, 2010. **159**(2): p. 213-228.
61. Golding, M. and T.J. Wooster, *The influence of emulsion structure and stability on lipid digestion*. Current Opinion in Colloid & Interface Science, 2010. **15**(1-2): p. 90-101.
62. Sarkar, A., D.S. Horne, and H. Singh, *Interactions of milk protein-stabilized oil-in-water emulsions with bile salts in a simulated upper intestinal model*. Food Hydrocolloids, 2010. **24**(2-3): p. 142-151.
63. Mackie, A. and A. Macierzanka, *Colloidal aspects of protein digestion*. Current Opinion in Colloid & Interface Science, 2010. **15**(1-2): p. 102-108.
64. McClements, D.J. and Y. Li, *Review of in vitro digestion models for rapid screening of emulsion-based systems*. Food & Function, 2010. **1**(1): p. 32-59.

65. Greenwood, R., et al., *The use of poly (N-isopropylacrylamide) microgels as a multi-functional processing aid for aqueous alumina suspensions*. Journal of the European Ceramic Society, 2000. **20**(11): p. 1707-1716.
66. Heidebach, T., P. Forst, and U. Kulozik, *Microencapsulation of Probiotic Cells for Food Applications*. Critical Reviews in Food Science and Nutrition, 2012. **52**(4): p. 291-311.
67. Islam, M.A., et al., *Microencapsulation of Live Probiotic Bacteria*. Journal of Microbiology and Biotechnology, 2010. **20**(10): p. 1367-1377.
68. McClements, D.J., *Emulsion Design to Improve the Delivery of Functional Lipophilic Components*. Annual Review of Food Science and Technology, 2010. **1**(1): p. 241-269
69. Aguilera, J.M., *Why food microstructure?* Journal of Food Engineering, 2005. **67**(1-2): p. 3-11.
70. Aguilera, J.M., *Seligman Lecture 2005 - Food product engineering: Building the right structures*. Journal of the Science of Food and Agriculture, 2006. **86**(8): p. 1147-1155.
71. Mcclements, D.J., E.A. Decker, and Y. Park, *Controlling Lipid Bioavailability through Physicochemical and Structural Approaches*. Critical Reviews in Food Science and Nutrition, 2009. **49**(1): p. 48-67.
72. McClements, D.J., et al., *Structural Design Principles for Delivery of Bioactive Components in Nutraceuticals and Functional Foods*. Critical Reviews in Food Science and Nutrition, 2009. **49**(6): p. 577-606.
73. Mezzenga, R., et al., *Understanding foods as soft materials*. Nature Materials, 2005. **4**(10): p. 729-740.
74. Flanagan, J. and H. Singh, *Microemulsions: A potential delivery system for bioactives in food*. Critical Reviews in Food Science and Nutrition, 2006. **46**(3): p. 221-237.
75. Spernath, A. and A. Aserin, *Microemulsions as carriers for drugs and nutraceuticals*. Advances in Colloid and Interface Science, 2006. **128**: p. 47-64.
76. Guzey, D. and D.J. McClements, *Formation, stability and properties of multilayer emulsions for application in the food industry*. Advances in colloid and interface science, 2006. **128**: p. 227-248.
77. McClements, D.J., *Design of Nano-Laminated Coatings to Control Bioavailability of Lipophilic Food Components*. Journal of Food Science, 2010. **75**(1): p. R30-R42.
78. Viota, J.L., et al., *Stability of mixtures of charged silica, silica-alumina, and magnetite colloids*. Journal of Colloid and Interface Science, 2005. **290**(2): p. 419-425.
79. Puertas, A.M., et al., *On the kinetics of heteroaggregation versus electrolyte concentration: comparison between simulation and experiment*. Colloids and Surfaces a-Physicochemical and Engineering Aspects, 1999. **151**(3): p. 473-481.
80. Rasa, M., A.P. Philipse, and J.D. Meeldijk, *Heteroaggregation, repeptization and stability in mixtures of oppositely charged colloids*. Journal of Colloid and Interface Science, 2004. **278**(1): p. 115-125.

81. Furusawa, K. and S. Satou, *The build-up of polyelectrolyte or colloid particle multilayers on latex surfaces*. Colloids and Surfaces a-Physicochemical and Engineering Aspects, 2001. **195**(1-3): p. 143-150.
82. Rollie, S. and K. Sundmacher, *Determination of Cluster Composition in Heteroaggregation of Binary Particle Systems by Flow Cytometry*. Langmuir, 2008. **24**(23): p. 13348-13358.
83. Cerbelaud, M., R. Ferrando, and A. Videcoq, *Simulations of heteroaggregation in a suspension of alumina and silica particles: Effect of dilution*. Journal of Chemical Physics, 2010. **132**(8).
84. Cerbelaud, M., et al., *Self-assembly of oppositely charged particles in dilute ceramic suspensions: predictive role of simulations*. Soft Matter, 2010. **6**(2): p. 370-382.
85. Jafari, S.M., et al., *Re-coalescence of emulsion droplets during high-energy emulsification*. Food Hydrocolloids, 2008. **22**(7): p. 1191-1202.
86. Walstra, P., *Principles of emulsion formation*. Chemical Engineering Science, 1993. **48**: p. 333.
87. Surh, J., *Comparison of Emulsion-stabilizing Property between Sodium Caseinate and Whey Protein Concentrate: Susceptibility to Changes in Protein Concentration and pH*. Food Science and Biotechnology, 2009. **18**(3): p. 610-617.
88. Tcholakova, S., et al., *Interrelation between drop size and protein adsorption at various emulsification conditions*. Langmuir, 2003. **19**(14): p. 5640-5649.
89. Tcholakova, S., N.D. Denkov, and T. Danner, *Role of surfactant type and concentration for the mean drop size during emulsification in turbulent flow*. Langmuir, 2004. **20**(18): p. 7444-7458.
90. Alamed, J., D.J. McClements, and E.A. Decker, *Influence of heat processing and calcium ions on the ability of EDTA to inhibit lipid oxidation in oil-in-water emulsions containing omega-3 fatty acids*. Food Chemistry, 2006. **95**(4): p. 585-590.
91. Ye, A.Q. and H. Singh, *Electrostatic interactions between lactoferrin and beta-lactoglobulin in oil-in-water emulsions*, in *Food Colloids: Self-Assembly and Material Science*, E. Dickinson and M.E. Leser, Editors. 2007. p. 167-175.
92. Ye, A.Q. and H. Singh, *Adsorption behaviour of lactoferrin in oil-in-water emulsions as influenced by interactions with beta-lactoglobulin*. Journal of Colloid and Interface Science, 2006. **295**(1): p. 249-254.
93. Ye, A.Q. and H. Singh, *Formation of multilayers at the interface of oil-in-water emulsion via interactions between lactoferrin and beta-lactoglobulin*. Food Biophysics, 2007. **2**(4): p. 125-132.
94. Demetriades, K., J.N. Coupland, and D.J. McClements, *Physical properties of whey protein stabilized emulsions as related to pH and NaCl*. Journal of Food Science, 1997. **62**(2): p. 342-347.
95. Hunt, J.A. and D.G. Dalgleish, *Effect of Ph on the Stability and Surface-Composition of Emulsions Made with Whey-Protein Isolate*. Journal of Agricultural and Food Chemistry, 1994. **42**(10): p. 2131-2135.

96. Kim, H.J., E.A. Decker, and D.J. McClements, *Impact of protein surface denaturation on droplet flocculation in hexadecane oil-in-water emulsions stabilized by beta-lactoglobulin*. Journal of Agricultural and Food Chemistry, 2002. **50**(24): p. 7131-7137.
97. Kim, H.J., E.A. Decker, and D.J. McClements, *Role of postadsorption conformation changes of beta-lactoglobulin on its ability to stabilize oil droplets against flocculation during heating at neutral pH*. Langmuir, 2002. **18**(20): p. 7577-7583.
98. Baker, E.N. and H.M. Baker, *Molecular structure, binding properties and dynamics of lactoferrin*. Cellular and Molecular Life Sciences, 2005. **62**(22): p. 2531-2539.
99. Baker, E.N. and H.M. Baker, *A structural framework for understanding the multifunctional character of lactoferrin*. Biochimie, 2009. **91**(1): p. 3-10.
100. Lesmes, U., P. Baudot, and D.J. McClements, *Impact of interfacial composition on physical stability and in vitro lipase digestibility of triacylglycerol oil droplets coated with lactoferrin and/or caseinate*. Journal of Agricultural and Food Chemistry, 2010. **58**(13): p. 7962-9.
101. Tokle, T., U. Lesmes, and D.J. McClements, *Impact of Electrostatic Deposition of Anionic Polysaccharides on the Stability of Oil Droplets Coated by Lactoferrin*. Journal of Agricultural and Food Chemistry, 2010. **58**(17): p. 9825-9832.
102. Tangsuphoom, N. and J.N. Coupland, *Effect of pH and ionic strength on the physicochemical properties of coconut milk emulsions*. Journal of Food Science, 2008. **73**(6): p. E274-E280.
103. Ubbink, J., A. Burbidge, and R. Mezzenga, *Food structure and functionality: a soft matter perspective*. Soft Matter, 2008. **4**(8): p. 1569-1581.
104. Dinsmore, A.D., et al., *Colloidosomes: Selectively permeable capsules composed of colloidal particles*. Science, 2002. **298**(5595): p. 1006-1009.
105. Mao, Y. and D.J. McClements, *Modulation of Bulk Physicochemical Properties of Emulsions by Hetero-aggregation of Oppositely Charged Protein-Coated Lipid Droplets*. Food Hydrocolloids, 2011(In press).
106. Ye, A., Y. Hemar, and H. Singh, *Enhancement of coalescence by xanthan addition to oil-in-water emulsions formed with extensively hydrolysed whey proteins*. Food Hydrocolloids, 2004. **18**(5): p. 737-746.
107. Ye, A.Q., Y. Hemar, and H. Singh, *Influence of polysaccharides on the rate of coalescence in oil-in-water emulsions formed with highly hydrolyzed whey proteins*. Journal of Agricultural and Food Chemistry, 2004. **52**(17): p. 5491-5498.
108. Israelachvili, J., *Intermolecular and Surface Forces, Second Edition*1992, London, UK: Academic Press.
109. Demetriades, K. and D.J. McClements, *Flocculation of whey protein stabilized emulsions as influenced by dextran sulfate and electrolyte*. Journal of Food Science, 1999. **64**(2): p. 206-210.
110. Ye, A. and H. Singh, *Electrostatic interactions between lactoferrin and beta-lactoglobulin in oil-in-water emulsions*, in *Food Colloids: Self-Assembly and Material Science*, E. Dickinson and M.E. Leser, Editors. 2007. p. 167-175.

111. Aranceta, J., et al., *Prevention of Overweight and Obesity From A Public Health Perspective*. Nutrition Reviews, 2009. **67**: p. S83 - S88.
112. Vanamala, J., C.C. Tarver, and P.S. Murano, *Obesity-Enhanced Colon Cancer: Functional Food Compounds and their Mechanisms of Action*. Current Cancer Drug Targets, 2008. **8**(7): p. 611-633.
113. Schmitt, C. and E. Kolodziejczyk, *Protein-polysaccharide complexes: From basics to food applications*, in *Gums and Stabilizers for the Food Industry 15*, P.A. Williams and G.O. Phillips, Editors. 2009, Royal Society of Chemistr: Cambridge, U.K. p. 211-222.
114. Ubbink, J. and J. Kruger, *Physical approaches for the delivery of active ingredients in foods*. Trends in Food Science & Technology, 2006. **17**(5): p. 244-254.
115. McClements, D.J., *Theoretical prediction of emulsion color*. Advances in Colloid and Interface Science, 2002. **97**(1-3): p. 63-89.
116. Velikov, K.P. and E. Pelan, *Colloidal delivery systems for micronutrients and nutraceuticals*. Soft Matter, 2008. **4**(10): p. 1964-1980.
117. De Velde, F.V., E.H.A. De Hoog, and R. Ruijschop, *Sensory perception of emulsions: translating science into products*. Agro Food Industry Hi-Tech, 2008. **19**(3): p. 50-52.
118. Guichard, E., *Interactions between flavor compounds and food ingredients and their influence on flavor perception*. Food Reviews International, 2002. **18**(1): p. 49-70.
119. Arancibia, C., et al., *Flavor release and sensory characteristics of o/w emulsions. Influence of composition, microstructure and rheological behavior*. Food Research International, 2011. **44**(6): p. 1632-1641.
120. van Aken, G.A., M.H. Vingerhoeds, and R.A. de Wijk, *Textural perception of liquid emulsions: Role of oil content, oil viscosity and emulsion viscosity*. Food Hydrocolloids, 2011. **25**(4): p. 789-796.
121. Malone, M.E., I.A.M. Appelqvist, and I.T. Norton, *Oral behaviour of food hydrocolloids and emulsions. Part 1. Lubrication and deposition considerations*. Food Hydrocolloids, 2003. **17**(6): p. 763-773.
122. Irvine, P.A., M.B.E. Livingstone, and R.W. Welch, *Strategies for modifying foods to increase satiety, and reduce subsequent intakes*. Agro Food Industry Hi-Tech, 2007. **18**(5): p. 22-24.
123. Demetriades, K. and D.J. McClements, *Influence of pH and heating on physicochemical properties of whey protein-stabilized emulsions containing a nonionic surfactant*. Journal of Agricultural and Food Chemistry, 1998. **46**(10): p. 3936-3942.
124. Bengoechea, C., I. Peinado, and D.J. McClements, *Formation of protein nanoparticles by controlled heat treatment of lactoferrin: Factors affecting particle characteristics*. Food Hydrocolloids, 2011. **25**(5): p. 1354-1360.
125. Jones, O., E.A. Decker, and D.J. McClements, *Thermal analysis of beta-lactoglobulin complexes with pectins or carrageenan for production of stable biopolymer particles*. Food Hydrocolloids, 2010. **24**(2-3): p. 239-248.
126. Aranceta, J., et al., *Prevention of overweight and obesity from a public health perspective*. Nutrition Reviews, 2009. **67**(5): p. S83-S88.

127. Williams, C. and J. Buttriss, eds. *Improving the Fat Content of Foods*. 2006, CRC Press.: Boca Raton, FL.
128. van Vliet, T., et al., *Colloidal aspects of texture perception*. Advances in Colloid and Interface Science, 2009. **150**(1): p. 27-40.
129. McClements, D.J. and K. Demetriades, *An integrated approach to the development of reduced-fat food emulsions*. Critical Reviews in Food Science and Nutrition, 1998. **38**(6): p. 511-536.
130. Engelen, L., et al., *Relating particles and texture perception*. Physiology & Behavior, 2005. **86**(1-2): p. 111-117.
131. Quemada, D. and C. Berli, *Energy of interaction in colloids and its implications in rheological modeling*. Advances in colloid and interface science, 2002. **98**(1): p. 51-85.
132. Chanamai, R. and D.J. McClements, *Comparison of gum arabic, modified starch, and whey protein isolate as emulsifiers: Influence of pH, CaCl2 and temperature*. Journal of Food Science, 2002. **67**(1): p. 120-125.
133. Chantrapornchai, W., F. Clydesdale, and D.J. McClements, *Influence of droplet size and concentration on the color of oil-in-water emulsions*. Journal of Agricultural and Food Chemistry, 1998. **46**(8): p. 2914-2920.
134. Chantrapornchai, W., F. Clydesdale, and D.J. McClements, *Theoretical and experimental study of spectral reflectance and color of concentrated oil-in-water emulsions*. Journal of Colloid and Interface Science, 1999. **218**(1): p. 324-330.
135. Bremer, L.G.B., et al., *FORMATION, PROPERTIES AND FRACTAL STRUCTURE OF PARTICLE GELS*. Advances in Colloid and Interface Science, 1993. **46**: p. 117-128.
136. Liu, S. and J.H. Masliyah, *Rheology of suspensions*, in *"Suspensions: Fundamentals and Applications in the Petroleum Industry"* L.L. Schramm, Editor 1996, American Chemical Society Washington, D.C. .
137. Larson, R.G., *The Structure and Rheology of Complex Fluids*1999, Oxford: Oxford University Press, Oxford, UK.
138. Li, Y., et al., *Modulation of lipid digestibility using structured emulsion-based delivery systems: Comparison of in vivo and in vitro measurements*. Food & function, 2012.
139. McClements, D.J., et al., *Designing food structure to control stability, digestion, release and absorption of lipophilic food components*. Food Biophysics, 2008. **3**(2): p. 219-228.
140. Schmitt, C. and S.L. Turgeon, *Protein/polysaccharide complexes and coacervates in food systems*. Advances in colloid and interface science, 2011. **167**(1-2): p. 63-70.
141. Golding, M., et al., *Impact of gastric structuring on the lipolysis of emulsified lipids*. Soft Matter, 2011. **7**(7): p. 3513-3523.
142. Maldonado-Valderrama, J., et al., *The effect of physiological conditions on the surface structure of proteins: Setting the scene for human digestion of emulsions*. The European Physical Journal E, 2009. **30**(2): p. 165-174.
143. Maldonado-Valderrama, J., et al., *Effect of gastric conditions on Œ≤-lactoglobulin interfacial networks: influence of the oil phase on protein structure*. Langmuir, 2010. **26**(20): p. 15901-15908.

144. Hu, M., et al., *Role of calcium and calcium-binding agents on the lipase digestibility of emulsified lipids using an< i> in vitro</i> digestion model*. Food Hydrocolloids, 2010. **24**(8): p. 719-725.
145. Singh, H. and A. Sarkar, *Behaviour of protein-stabilised emulsions under various physiological conditions*. Advances in colloid and interface science, 2011. **165**(1): p. 47-57.
146. Gal, J.Y., Y. Fovet, and M. Adib-Yadzi, *About a synthetic saliva for in vitro studies*. Talanta, 2001. **53**(6): p. 1103-1115.
147. Sarkar, A., K.K.T. Goh, and H. Singh, *Colloidal stability and interactions of milk-protein-stabilized emulsions in an artificial saliva*. Food Hydrocolloids, 2009. **23**(5): p. 1270-1278.
148. Demetriades, K., J. Coupland, and D. McClements, *Physical properties of whey protein stabilized emulsions as related to pH and NaCl*. Journal of food science, 1997. **62**(2): p. 342-347.
149. Wickham, M., R. Faulks, and C. Mills, *In vitro digestion methods for assessing the effect of food structure on allergen breakdown*. Molecular nutrition & food research, 2009. **53**(8): p. 952-8.
150. Li, Y. and D.J. McClements, *New mathematical model for interpreting pH-stat digestion profiles: impact of lipid droplet characteristics on in vitro digestibility*. Journal of Agricultural and Food Chemistry, 2010. **58**(13): p. 8085-92.
151. Macierzanka, A., et al., *Emulsification alters simulated gastrointestinal proteolysis of beta-casein and beta-lactoglobulin*. Soft Matter, 2009. **5**(3): p. 538-550.
152. Drewnowski, A., *Taste preferences and food intake*. Annual review of nutrition, 1997. **17**: p. 237-53.
153. Drewnowski, A., *Why do we like fat?* Journal of the American Dietetic Association, 1997. **97**(7 Suppl): p. S58-62.
154. Cooling, J. and J. Blundell, *Are high-fat and low-fat consumers distinct phenotypes? Differences in the subjective and behavioural response to energy and nutrient challenges*. European journal of clinical nutrition, 1998. **52**(3): p. 193-201.
155. Blundell, J.E., et al., *Resistance and susceptibility to weight gain: individual variability in response to a high-fat diet*. Physiology & Behavior, 2005. **86**(5): p. 614-22.
156. Micha, R. and D. Mozaffarian, *Saturated Fat and Cardiometabolic Risk Factors, Coronary Heart Disease, Stroke, and Diabetes: a Fresh Look at the Evidence*. Lipids, 2010. **45**(10): p. 893-905.
157. Rogers, M.A., *Novel structuring strategies for unsaturated fats - Meeting the zero-trans, zero-saturated fat challenge: A review*. Food Research International, 2009. **42**(7): p. 747-753.
158. Nehir El, S. and S. Simsek, *Food Technological Applications for Optimal Nutrition: An Overview of Opportunities for the Food Industry*. Comprehensive Reviews in Food Science and Food Safety, 2012. **11**(1): p. 2-12.

159. Mao, Y.Y. and D.J. McClements, *Modulation of emulsion rheology through electrostatic heteroaggregation of oppositely charged lipid droplets: Influence of particle size and emulsifier content*. Journal of colloid and interface science, 2012. **380**: p. 60-66.
160. Mao, Y.Y. and D.J. McClements, *Fabrication of Reduced Fat Products by Controlled Heteroaggregation of Oppositely Charged Lipid Droplets*. Journal of Food Science, 2012. **77**(5): p. E144-E152.
161. Shogren, R.L., et al., *Distribution of octenyl succinate groups in octenyl succinic anhydride modified waxy maize starch*. Starch-Starke, 2000. **52**(6-7): p. 196-204.
162. Kondaraju, S., H. Farhat, and J.S. Lee, *Study of aggregational characteristics of emulsions on their rheological properties using the lattice Boltzmann approach*. Soft Matter, 2012. **8**(5): p. 1374-1384.
163. Qian, C., et al., *Comparison of Biopolymer Emulsifier Performance in Formation and Stabilization of Orange Oil-in-Water Emulsions*. Journal of the American Oil Chemists Society, 2011. **88**(1): p. 47-55.
164. Dickinson, E., *Hydrocolloids at interfaces and the influence on the properties of dispersed systems*. Food Hydrocolloids, 2003. **17**(1): p. 25-39.
165. Dickinson, E., *Flocculation of protein-stabilized oil-in-water emulsions*. Colloids and Surfaces B-Biointerfaces, 2010. **81**(1): p. 130-140.
166. McClements, D.J., *Comments on viscosity enhancement and depletion flocculation by polysaccharides*. Food Hydrocolloids, 2000. **14**(2): p. 173-177.
167. McClements, D.J., *Emulsion Design to Improve the Delivery of Functional Lipophilic Components*. Annual Review of Food Science and Technology, Vol 1, 2010. **1**: p. 241-269.
168. Kralova, I. and J. Sjoblom, *Surfactants Used in Food Industry: A Review*. Journal of Dispersion Science and Technology, 2009. **30**(9): p. 1363-1383.
169. Stauffer, S.E., *Emulsifiers*1999, St Paul, MN: Eagen Press.
170. Shchukina, E.M. and D.G. Shchukin, *Layer-by-layer coated emulsion microparticles as storage and delivery tool*. Current Opinion in Colloid & Interface Science, 2012. **17**(5): p. 281-289.
171. Gunning, P.A., et al., *Molecular interactions in mixed protein plus ionic surfactant interfaces*, in *Food Colloids: Interactions, Microstructure and Processing*, E. Dickinson, Editor 2005. p. 143-151.
172. Dickinson, E., *Mixed biopolymers at interfaces: Competitive adsorption and multilayer structures*. Food Hydrocolloids, 2011. **25**(8): p. 1966-1983.
173. Mao, Y. and D.J. McClements, *Modulation of emulsion rheology through electrostatic heteroaggregation of oppositely charged lipid droplets: Influence of particle size and emulsifier content*. Journal of colloid and interface science, 2012. **380**(1): p. 60-6.
174. Caruso, F. and H. Mohwald, *Protein multilayer formation on colloids through a stepwise self-assembly technique*. Journal of the American Chemical Society, 1999. **121**(25): p. 6039-6046.
175. Tokle, T., E.A. Decker, and D.J. McClements, *Utilization of interfacial engineering to produce novel emulsion properties: Pre-mixed lactoferrin/beta-lactoglobulin protein emulsifiers*. Food Research International, 2012. **49**(1): p. 46-52.

176. Kontopidis, G., C. Holt, and L. Sawyer, *Invited review: beta-lactoglobulin: binding properties, structure, and function*. Journal of dairy science, 2004. **87**(4): p. 785-96.
177. Ward, P.P., E. Paz, and O.M. Conneely, *Multifunctional roles of lactoferrin: a critical overview*. Cellular and Molecular Life Sciences, 2005. **62**(22): p. 2540-2548.
178. Levay, P.F. and M. Viljoen, *Lactoferrin - a General-Review*. Haematologica, 1995. **80**(3): p. 252-267.
179. Abdel-Aal, E.S.M. and M.H. Akhtar, *Recent advances in the analyses of carotenoids and their role in human health*. Current Pharmaceutical Analysis, 2006. **2**(2): p. 195-204.
180. Boon, C.S., et al., *Role of Iron and Hydroperoxides in the Degradation of Lycopene in Oil-in-Water Emulsions*. Journal of Agricultural and Food Chemistry, 2009. **57**(7): p. 2993-2998.
181. Kanner, J., H. Mendel, and P. Budowski, *Pro-Oxidant and Antioxidant Effects of Ascorbic-Acid and Metal-Salts in a Beta-Carotene-Linoleate Model System*. Journal of food science, 1977. **42**(1): p. 60-64.
182. Handelman, G.J., et al., *Characterization of Products Formed during the Autoxidation of Beta-Carotene*. Free Radical Biology and Medicine, 1991. **10**(6): p. 427-437.
183. Sommerburg, O., et al., *beta-carotene cleavage products after oxidation mediated by hypochlorous acid - A model for neutrophil-derived degradation*. Free Radical Biology and Medicine, 2003. **35**(11): p. 1480-1490.
184. Qian, C., et al., *Physical and chemical stability of beta-carotene-enriched nanoemulsions: Influence of pH, ionic strength, temperature, and emulsifier type*. Food Chemistry, 2012. **132**(3): p. 1221-1229.
185. Tokle Tanushree, E.A.D., David Julian McClements, *Utilization of interfacial engineering to produce novel emulsion properties: Pre-mixed lactoferrin/β-lactoglobulin protein emulsifiers*. Food Research International, 2012. **49**(1): p. 7.
186. Sun, Y.E., et al., *Autoxidation of Unsaturated Lipids in Food Emulsion*. Critical Reviews in Food Science and Nutrition, 2011. **51**(5): p. 453-466.
187. Waraho, T., D.J. McClements, and E.A. Decker, *Mechanisms of lipid oxidation in food dispersions*. Trends in Food Science & Technology, 2011. **22**(1): p. 3-13.
188. Tokle, T., Y. Mao, and D.J. McClements, *Potential Biological Fate of Emulsion-Based Delivery Systems: Lipid Particles Nanolaminated with Lactoferrin and beta-lactoglobulin Coatings*. Pharmaceutical research, 2013.